AUGUST 2023

M.Sc in Mechanical Engineering

ABDULRAAOUF OKASH

REPUBLIC OF TÜRKİYE

GAZİANTEP UNIVERSITY

GRADUATE SCHOOL OF NATURAL & APPLIED SCIENCES

PERFORMANCE ANALYSIS OF AN ORGANIC RANKINE CYCLE WITH OPTIMIZATION OF HEAT TRANSFER COMPONENTS

M.SC. THESIS

IN

MECHANICAL ENGINEERING

BY

ABDULRAAOUF OKASH

AUGUST 2023

PERFORMANCE ANALYSIS OF AN ORGANIC RANKINE CYCLE WITH OPTIMIZATION OF HEAT TRANSFER COMPONENTS

M.Sc. Thesis

in

Mechanical Engineering

Gaziantep University

Supervisor

Prof. Dr. Recep YUMRUTAŞ

Co-Supervisor

Doç. Dr. Hüseyin YAĞLI

by

Abdulraaouf OKASH

AUGUST 2023

I hereby declare that all information in this document has been obtained and presented in accordance with academic rules and ethical conduct. I also declare that, as required by these rules and conduct, I have fully cited and referenced all material and results that are not original to this work.

Abdulraaouf OKASH

ABSTRACT

PERFORMANCE ANALYSIS OF AN ORGANIC RANKINE CYCLE WITH OPTIMIZATION OF HEAT TRANSFER COMPONENTS

OKASH, Abdulraaouf
M.Sc. in Mechanical Engineering
Supervisor: Prof. Dr. Recep YUMRUTAŞ
Co-Supervisor: Assoc. Prof. Dr. Hüseyin YAĞLI

August 2023

180 Pages

This study focused on optimizing the performance of an Organic Rankine Cycle (ORC) that comprises four heat exchanger components, namely a preheater, evaporator, and superheater which are all finned tube type, as well as a horizontal shell and tube condenser. The main objective of the study was to achieve an optimal design for heat exchanger components with minimal heat transfer surface area while keeping the pressure drop below 0.2 bar. Through significant design procedures by using the trial and error method, 1244 distinct designs have been reached, and an optimum design has been selected for each heat exchanger component. Upon performance analysis of the ORC based on the optimum designs of heat exchanger components, it has been determined that the selected fluids namely R245fa, R600, R123, R236fa, R142b, and R600a exhibited high performance compared to the ideal case (no pressure drop across the heat exchanger components), with over 98% performance observed across all selected fluids.

Key Words: ORC (Organic Rankine Cycle) 1, Performance 2, Optimization 3, Heat exchanger, pressure drop

ÖZET

ISI DEĞIŞTIRICI BILEŞENLERINE BAĞLI OLARAK BIR ORGANIK RANKINE ÇEVRIMININ PERFORMANS ANALIZI VE OPTIMIZASYONU

OKASH, Abdulraaouf
Yüksek Lisans Tezi, Makine Mühendisliği
Danışman: Prof. Dr. Recep YUMRUTAŞ
İkinci Danışman: Doç. Dr. Hüseyin YAĞLI

Ağutos 2023

180 sayfa

Bu çalışma, tamamen kanatlı boru tipi ısı değiştiricilerden oluşan bir Organik Rankine Çevrimi (ORC) sisteminin performansının optimize edilmesine odaklanmaktadır. Bu sistemin temel bileşenleri, bir ön ısıtıcı, bir buharlaştırıcı, bir kızdırıcı ve bir yatay kabuk ve borulu kondansatör içermektedir.

Çalışmanın temel hedefi, her bir ısı değiştirici bileşeni için en düşük ısı transfer yüzey alanını korurken basınç düşüşünü 0,2 barın altında tutacak en uygun tasarımlar elde etmektir. Deneme yanılma yöntemi kullanılarak gerçekleştirilen önemli tasarım süreçleri sonucunda, toplamda 1244 farklı tasarım seçeneği değerlendirilmiş ve her ısı değiştirici bileşeni için en uygun tasarım seçilmiştir.

ORC sisteminin ısı değiştirici bileşenlerinin en uygun tasarımlarına dayalı yapılan performans analizi sonuçlarına göre, seçilen çalışma akışkanları (R245fa, R600, R123, R236fa, R142b ve R600a) ideal çalışma koşullarına göre yüksek performans sergilemektedir (tüm yüzeylerde basınç düşüşü olmamaktadır). ORC içerisinde çalışılan tüm akışkanlarda %98'in üzerinde verimlilik gözlenmiştir. Bu sonuçlar, ORC sistemi için en iyi çalışma koşullarının ve bileşen tasarımlarının belirlendiğini göstermektedir.

Anahtar Kelimeler: ORC (Organik Rankine Çevrimi) 1, Performans 2 Optimizasyon 3, Isı değiştirici, basınç düşüşü

''Dedicated to my family''

I would like to dedicate this thesis to my beloved family, whose unwavering support, encouragement, and understanding have been the driving force behind my pursuit of higher education. Their love and belief in me have inspired and motivated me throughout this journey. I am grateful for their sacrifices and constant encouragement, which have made this achievement possible. This accomplishment is as much theirs as it is mine, and I will always be grateful for their presence in my life.

ACKNOWLEDGEMENTS

I would like to take this opportunity to express my sincere appreciation to my esteemed supervisor, Prof. Dr. Recep YUMRUTAS, for his invaluable guidance, unwavering support, and encouragement throughout my research journey. His expertise, insightful feedback, and mentorship have been instrumental in shaping my work and achieving my goals. I am deeply grateful for his unwavering dedication and commitment to excellence.

Furthermore, I extend my heartfelt thanks to my Co-supervisor, Assoc. Prof. Dr. Huseyin YAGLI, for his significant contributions to my research project. His thoughtful insights, constructive criticism, and invaluable advice have been instrumental in shaping the outcome of this study. I am grateful for his steadfast support, encouragement, and unwavering commitment to my academic success

.

TABLE OF CONTENTS

Page

Contents

LIST OF TABLES

LIST OF FIGURES

LIST OF SYMBOLS

A_s	Shell side cross flow velocity (m/s)
$\dot{m}$	mass flow rate (kg/s)
$\dot{w}$	Power (kW)
Af	Fin area (m2)
Aw	Unfinned tubes surface area (m2)
EF	Fin effectiveness
h	Heat transfer coefficient (kW/m2 °C)
K	Fluid thermal conductivity W/m K
Pr	Prandtl number
S	Fin pith (m)
tf	Thikness of fin (m)
Vmax	Maximum air velocity (m/s)
$Amin$	Minimum cross flow area (m2)
Cp	specific heat (kj/kg°C)
Ds	Shell diameter (m)
Gs	mass velocity(kg/m2 s)
LF	Length of fin (m)
Lt	Length of tube (m)
Nt	Total number of tubes
T	Temperature (°C)
Vs	Shell side fluid velocity (m/s)
pt	Tube pith (m)
$\dot{Q}$	Rate of heat transfer kW
$\dot{m}s$	Shell side fluid velocity (m/s)
Ab	Total surface area for tubes without fins (m2)
Ao	Total heating surface area (m2)

Df	Outer diameter of fin (m)
G	mass velocity (kg/m2 s)
Ho	Total heat transfer coefficint for shell side (kW/m2 °C)
Kf	Thermal conductivity of fin W/m°C
ReD	Renault number
St	Transverse pitch (m)
v	Fluid velocity (m/s)
$\boldsymbol{A}$	Area (m2)
$\boldsymbol{B}$	Baffle space (m)
$\boldsymbol{De}$	Equivalent diameter (m)
$\boldsymbol{EX}$	Exergy
$\boldsymbol{H}$	Enthalpy (kj/kg)
$\boldsymbol{LMTD}$	Logarithmic mean temperature (°C)
$\boldsymbol{Nr}$	Number of tubes in the center row
$\boldsymbol{Ntp}$	Number of tube passes
$\boldsymbol{U0}$	Overall heat transfer coefficient (kW/m2 °C)
$\boldsymbol{d}$	Tube diameter (m)

LIST OF ABBREVIATIONS

ORC	Organic rankine cycle
İn	inlet
Out	Outlet
R	Refrigerant
w	Water
a	Air
s	Shell side
HExU	Heat Exchanger Unit
HExPD	Heat exchanger pressure drop

CHAPTER 1
INTRODUCTION

1.1 Background and Motivation of Study

Energy is the driving force behind the functioning of our modern world. It powers our homes, businesses, and transportation systems, and enables us to perform a vast array of tasks with ease and efficiency. However, energy waste is a serious issue that has a detrimental impact on the environment and our limited natural resources. From the energy consumed by idle appliances to the emissions from power plants, energy waste not only harms the planet but also increases costs for consumers and businesses. It is essential that we take steps to reduce energy waste and transition to more sustainable forms of energy to ensure a healthy planet and a prosperous future for generations to come. Nowadays most scientific researches talk about how to increase energy efficiency by reducing or reusing wasted energy. The Organic Rankine cycle (ORC) is an applicable example of saving energy that promises an application for waste heat recovery due to its heat recovery efficiency and environmental_ friendly features. ORCs can be used in both large-scale power plants and small-scale, distributed systems, making them versatile for a wide range of applications. ORCs have a working principle similar to that in the conventional Rankine cycles which utilizes water and steam as working fluids to generate electricity. However, they utilize organic fluids as working fluids due to low boiling and condensing temperature. When any energy system or power planet is constructed to have good energy efficiency the first thing that comes to mind is the that this system must work perfectly and give us exquisite outputs. However, installing and working cost is not less important than the thing mentioned above, and usually, there is a trade-off between them so to have a good system design you should make a balance between required outputs and cost, in another word any energy system must have a characteristic combined of the maximum working efficiency and minimum cost containing (installing, working, equipment and maintenance). In order to achieve this characteristic, we have developed a unique and step by step design and optimization methodology for designing the condenser, evaporator, preheater and superheater.

1.2 Aim and objective

The aim of this study is to tackle the issue of the expensive investment in the Organic Rankine Cycle (ORC) mainly due to the high cost of its components, particularly the heat exchangers. Previous research has mostly focused on performance analysis only, neglecting the impact of heat transfer component designs on the system. On the other hand, some studies have only concentrated on designing heat transfer components without taking into account their effect on ORC performance. Therefore, our study encompasses both the performance analysis of a real ORC and the influence of optimal designs on it. SO, this study contributes to the body of knowledge in the field of sustainable energy generation through ORC technology, and may have significant implications for industrial operations seeking to harness waste heat for electricity production.

CHAPTER 2
INTRODUCTION TO ORGANIC RANKINE CYCLE

2.1 Organic Rankine cycle definition and the working principle

The Organic Rankine Cycle (ORC) is a thermodynamic cycle that converts heat into mechanical work, which is finally converted into useful electrical power. It is similar to the conventional Rankine Cycle, but instead of utilizing water as the working fluid, it uses an organic fluid having a lower boiling point, such as a hydrocarbon or refrigerant.

The work principle of ORC is that the working fluid in the ORC is evaporated by absorbing heat from a high-temperature source, such as industrial exhaust gases. The vaporized fluid then expands and produces rotational energy in a turbine. A generator then converts this energy into electrical power. The low-pressure vapor is condensed back into a liquid after expanding in the turbine by rejecting heat to a low-temperature sink. The condensed liquid is then returned to the high-temperature source by a pump, where the cycle is repeated.

2.2 The Organic Rankine Cycle system description

In this study the ORC includes 6 main components that are a condenser, a pump, a preheater, an evaporator, a superheater, and a turbine as it is shown in Figure 2.1. The exhaust gas comes from industrial operations enters the cycle at a high temperature through the superheater and then goes through the evaporator and finally exits from the preheater at a low temperature comparatively. The heat transfer process takes place between the exhaust gas and refrigerant in four stages three of them are energy-absorbing processes by the refrigerant and one is an exothermic process (condensation process).

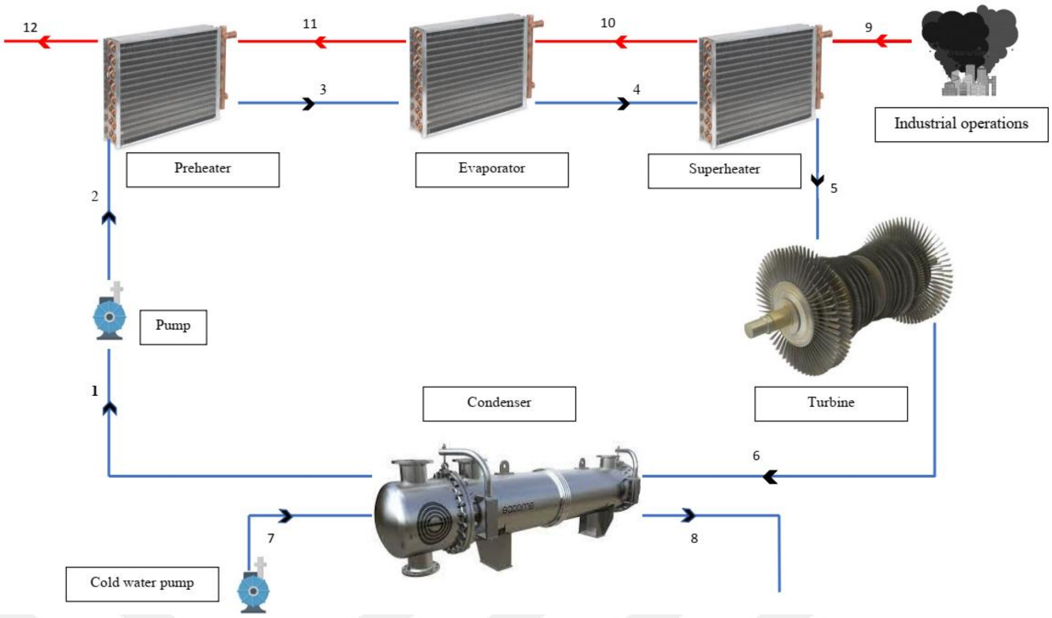

Figure 2.1. Organic Rankine cycle ORC

2.3 Refrigerant selection criteria

The selection of the working fluid in an Organic Rankine Cycle (ORC) system is a critical aspect that significantly impacts its thermal performance [1-2]. The choice of an organic fluid for the ORC should meet the following properties to ensure both optimal cycle performance and environmental considerations. These properties include economic viability, non-toxicity, non-flammability, environmental friendliness, and safety [3-4]. İn addition, the operating temperature range of the ORC system affects the choice of refrigerants. The appropriate choice of organic working fluid depending on the operating temperature range of the ORC system can minimize thermodynamic inefficiencies, increase energy conversion efficiency, and lower capital costs [5]. In our study, R245fa, R123, R236fa, R600a, and R142a are chosen due to their known and desirable properties that align with the efficient use of ORC for low tempeature heating source 375 °C in this study. Xu et al. focused on identifying pure working fluids for subcritical ORC systems, investigating the effects of nearly 30 working fluids on both simple and regenerative ORC systems. They presented maps to guide the selection of working fluids at different temperatures and constant pressures [6]. Bao, reviews the working fluid and expander options for the organic Rankine cycle, including an examination of the impact of working fluid category and thermodynamic and physical parameters on the performance of the organic Rankine cycle, as well as an overview of pure and mix fluids. [7].

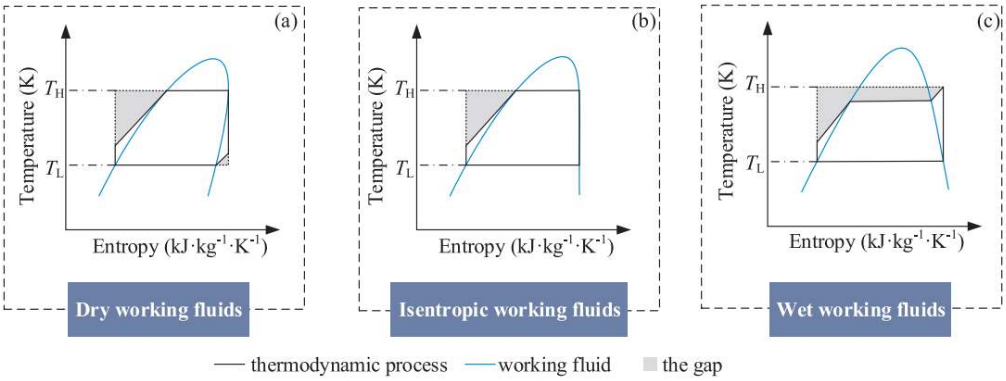

Figure 2.2. (T-s) diagram for dry, isentropic and wet working [6]

Table 2.1. Refrigerants' thermal and physical properties [8-15].

SHRAE number	Molecular structure	MM (g/mol)	Tb (K)	Tc (K)	Type
R245fa	CF3CH2CHF2	134.05	288	427	Dry
R123	CHCl2CF3	152.93	301	457	isentropic
R600	CH3CH2CH2CH3	58.123	273	425	Dry
R236fa	CF3CH2CF3	152.0393	272	398	isentropic
R142b	CClF2CH3	100.50	264	410	Isentropic
R600a	CH(CH3)3	58.1	261	425	Dry

ODP	GWP	ASHRAE 34 group
0	1030	A1
0.060	77	B1
0	20	A3
0	9810	A1
0.043	2300	A2
0	3	A3

MM: Molecular Mass, ODP: Ozone Depletion Potential (relative to R11), GWP: Global Warming Potential (relative to CO_2)

*A low toxicity, B high toxicity; 1 no flame; 2 lower flammability, 3 higher flammability

2.4 Problem description of ORC

The aim of this thesis is to investigate the feasibility of utilizing exhaust gas from industrial operations, having a temperature of 375 °C and a mass flow rate of approximately 21.8 kg/s at a pressure of 1 Bar, to generate electricity via an Organic Rankine cycle power plant. The cycle comprises a superheater, evaporator, and preheater, with all heat exchanger components being of the finned tube type, selected for their optimal heat transfer coefficient with air. To ensure maximum cost-effectiveness, a horizontal shell and tube condenser is employed, known for its low cost, simple structure, and high heat transfer efficiency, which is cooled using water at a temperature of 20 °C and exits at 35 °C. The study aims to perform a comprehensive performance analysis of the cycle with six different refrigerant types, namely R245fa, R600, R123, R236fa, R142b and R600a under variable pump outlet pressures. The pump inlet pressure is carefully selected to be as low as possible while still ensuring optimal performance for each refrigerant type. Specifically, we set the pump inlet pressure to be 3 bar for R245fa, 3.5 bar for R600, 2 bar for R123, 4 bar for R236fa and 5 bar for R142b and R600a. In this study, the pump outlet pressure is gradually increased from 10 bar until it reaches the maximum pressure at which the refrigerant can no longer vaporize. By conducting a detailed performance analysis, we aim to provide a deep understanding of Organic Rankine Cycl ORC and its behavior under many different conditions and with different distinct working fluids. The performance analysis of ORC is carried out in this thesis firstly for the ideal case (the pressure drop through the heat exchanger components is neglected) and then for the real case based on optimal designs of heat transfer units involved in the system after introducing a comprehensive and unique design and optimization methodology for each heat transfer units.

Table 2.2. Exhaust's (dry air) accepted nominal parameters:

Fluid	$\dot{m}a$ Kg/s	T9 °C	T12 °C	h9 kJ/kg	h12 kJ/kg
Exhaust (dry air)	21.8	375	150	784.3018	550.7663

$\dot{m}a$: Mass flow rate; T9: Exhaust temperature coming from industrial operations; T12: Exhaust temperature exits from the system; h: Enthalpy

Table 2.3. Refrigerant's accepted nominal parameters:

Organic fluid	P1** bar	P2* bar	$x1$	$x3$	$x4$
R245fa	3	22	0	0	1
R123	2	22	0	0	1
R600	2.5	22	0	0	1
R236fa	4	22	0	0	1
R142b	5	22	0	0	1
R600a	5	22	0	0	1

P1: pump inlet pressure; P2: pump outlet pressure; x: gas quality

*Moderate value in which the system has a good performance for all working fluids. ** minimum applicaple pressure inlet in where T1<T7.

2.5 Evaluation method

The mass, energy, and exergy balance equations of the ORC are given below (Eq. 1-14):

Table 2.4. The energy equations for the components of ORC cycles [16-17]

Components	Energy equations
	$\dot{Q}_{CON} = \dot{m}_R(h_1 - h_6) = \dot{m}_W\, Cp\, \Delta T$
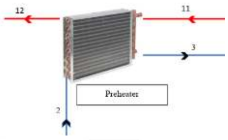	$\dot{Q}_{PRE} = \dot{m}_R(h_3 - h_2) = \dot{m}_a(h_{11} - h_{12})$
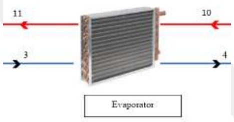	$\dot{Q}_{EVAP.} = \dot{m}_R(h_4 - h_3) = \dot{m}_a(h_{10} - h_{11})$
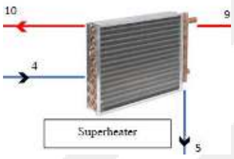	$\dot{Q}_{SUP.} = \dot{m}_R(h_5 - h_4) = \dot{m}_a(h_9 - h_{10})$
	$\dot{w}tot = \dot{m}_R(h_5 - h_6)$ $\dot{w}net = \dot{w}tot - \dot{w}pump$ $\eta_{Th} \cdot turbine = \frac{\dot{w}tot}{w_s} = \frac{h_5 - h_{s6}}{h_5 - h_6}$
	$\dot{w}pump = \dot{m}_R(h_2 - h_1)$ $\eta_{Th} \cdot pump = \frac{ws}{\dot{w}pump} = \frac{hs2 - h1}{h2 - h1}$

Total energy gained by the cycle heat exchanger components can be calculated by using the following equation:

$$\dot{Q}_{TOTAL} = \dot{Q}_{PRE} + \dot{Q}_{EVAP.} + \dot{Q}_{SUP.} = \dot{m}_a(h_9 - h_{12}) = \dot{m}_R(h_5 - h_2)$$

Thermal and exergy efficiencies are calculation as following:

$$\eta_{Th,ORC} = \frac{\dot{w}net}{\dot{Q}_{TOTAL}}$$

$$\eta_{EX,ORC} = \frac{\dot{w}net}{EXin}$$

$Exin = \dot{m}_a(\psi in - \psi out)$

$\psi = (H - H0) - T0(S - S0)$

Where:

$\dot{Q}_{CON}$ is condenser heat transfer rate (KW)

$\dot{Q}_{PRE}$ is preheater heat transfer rate (KW)

$\dot{Q}_{EVAP.}$is evaporator heat transfer rate (KW)

$\dot{Q}_{SUP.}$ is superheater heat transfer rate (KW)

$\dot{m}_R$ is refrigerant mass flow rate (kg/s)

h is enthalpy (kj/kg)

$\dot{m}_W$ is water mass flow rate (kg/s)

$\dot{m}_a$ is air mass flow rate (kg/s)

Cp is specific heat (kj/kg k)

$\dot{w}tot$ is total power output (KW)

$\dot{w}pump$ is total power consumed by the pump (KW)

$\dot{w}net$ is net useful power (KW)

η_{Th} is thermal efficiency %

$\eta_{Th,ORC}$ total organic Rankine cycle thermal efficiency %

$\eta_{EX,ORC}$ is exergy efficiency %

$Exin$ exergy inlet.

CHAPTER 3
ORC PERFORMANCE ANALYSIS FOR IDEAL CASE

3.1 ORC's performance calculations for ideal case

In this topic the performance analysis for ORC is carried out by assuming all the pressure drop through the heat exchanger components is negligible. The performance calculations are performed by using six different types of refrigerants.

Table 3.1. The flow parameters for ORC (ideal case)

State	Fluid	Pressure	Temperature	Enthalpy	Mass flow
		bar	°C	kJ/kg	kg/s
1	R245fa	3	45.58	260.65	21.11
2	R245fa	22	46.63	262.50	21.11
3	R245fa	22	126.60	384.96	21.11
4	R245fa	22	126.60	487.66	21.11
5	R245fa	22	136.60	503.64	21.11
6	R245fa	3	73.37	466.77	21.11
7	Water	1	20.00	84.01	69.40
8	Water	1	35.00	146.70	69.40
9	Exhaust gas	1	375.00	784.30	21.80
10	Exhaust gas	1	360.41	768.82	21.80
11	Exhaust gas	1	265.51	669.36	21.80
12	Exhaust gas	1	150.00	550.77	21.80
1	R600	3.5	37.225	289.8	10.68
2	R600	22	38.445	293.93	10.68
3	R600	22	119.67	526.21	10.68
4	R600	22	119.67	740.43	10.68
5	R600	22	129.67	770.61	10.68
6	R600	3.5	66.165	693.97	10.68
7	Water	1	20.00	84.01	68.85
8	Water	1	35.00	146.70	68.85
9	Exhaust gas	1	375	784.3018	21.80
10	Exhaust gas	1	361.0626	84.01	21.80

11	Exhaust gas	1	260.8866	146.70	21.80
12	Exhaust gas	1	150	550.7663	21.80
1	R123	2	48.047	249	22.83
2	R123	22	49.229	250.78	22.83
3	R123	22	152.72	370.82	22.83
4	R123	22	152.72	461.73	22.83
5	R123	22	162.72	473.75	22.83
6	R123	2	78.187	432.93	22.83
7	Water	1	20.00	84.01	66.98
8	Water	1	35.00	146.70	66.98
9	Exhaust gas	1	375	784.3018	21.80
10	Exhaust gas	1	363.1308	771.7073	21.80
11	Exhaust gas	1	272.3793	676.4905	21.80
12	Exhaust gas	1	150	550.7663	21.80
1	R236fa	4	37.09	245.56	27.33
2	R236fa	22	38.282	247.26	27.33
3	R236fa	22	106.19	343.21	27.33
4	R236fa	22	106.19	417.69	27.33
5	R236fa	22	116.19	433.53	27.33
6	R236fa	4	63.084	407.83	27.33
7	Water	1	20.00	84.01	70.74
8	Water	1	35.00	146.70	70.74
9	Exhaust gas	1	375	784.3018	21.80
10	Exhaust gas	1	356.2737	764.4465	21.80
11	Exhaust gas	1	267.1581	671.0682	21.80
12	Exhaust gas	1	150	550.7663	21.80
1	R142b	5	38.395	250	21.51
2	R142b	22	39.6	251.97	21.51
3	R142b	22	103.06	346.67	21.51
4	R142b	22	103.06	474	21.51
5	R142b	22	113.06	488.68	21.51
6	R142b	5	51.277	455.34	21.51
7	Water	1	20.00	84.01	70.44
8	Water	1	35.00	146.70	70.44
9	Exhaust gas	1	375	784.3018	21.80
10	Exhaust gas	1	361.3533	769.8242	21.80
11	Exhaust gas	1	241.2011	644.1953	21.80
12	Exhaust gas	1	150	550.7663	21.80
1	R600a	5	37.713	290.49	12.22

2	R600a	22	39.011	294.46	12.22
3	R600a	22	105.56	484.2	12.22
4	R600a	22	105.56	681.08	12.22
5	R600a	22	115.56	711	12.22
6	R600a	5	62.349	652.24	12.22
7	Water	1	20.00	84.01	70.52
8	Water	1	35.00	146.70	70.52
9	Exhaust gas	1	375	784.3018	21.8
10	Exhaust gas	1	359.1813	767.5239	21.8
11	Exhaust gas	1	253.728	657.1469	21.8
12	Exhaust gas	1	150	550.7663	21.8

Table 3.2. Heat exchanger components's heat transfer rate for ideal case

Ref.	$\dot{Q}_{pre}$ kW	$\dot{Q}_{evap}$ kW	$\dot{Q}_{sup}$ kW	$\dot{Q}_{con}$ kW
R245fa	2585.3	2168.26	337.46	4351.79
R600	2480.76	2287.98	322.33	4316.64
R123	2740.79	2075.73	274.56	4199.68
R236fa	2623	2036	433	4435.21
R142b	2036.8	2738.71	315.6	4416.4
R600a	2319.10	2406.22	365.76	4421.30

Table 3.3. ORC performance analysis for ideal case

Ref.	$\dot{W}_{pump}$ kW	$\dot{W}_{tur}$ kW	$\dot{W}_{net}$ kW	$\eta_{th,ORC}$ %	$\eta_{ex,ORC}$ %
R245fa	39.07	778.36	739.28	14.52	32.61
R600	44.13	818.57	774.43	15.21%	34.16%
R123	40.61	932.00	891.39	17.51%	39.32%
R236fa	47	702	655.87	12.88%	28.93%
R142b	42.4	717.1	674.771	13.25%	29.76%
R600a	48.48	718.25	669.77	13.16%	29.54%

Table 3.3. shows the performance parameters of ORC for six different refrigerants. The calculations were carried out under uniform working conditions for all fluids while assuming that the pressure through the heat exchanger components (Preheater, Evaporator, Superheater, and Condenser) is negligible.

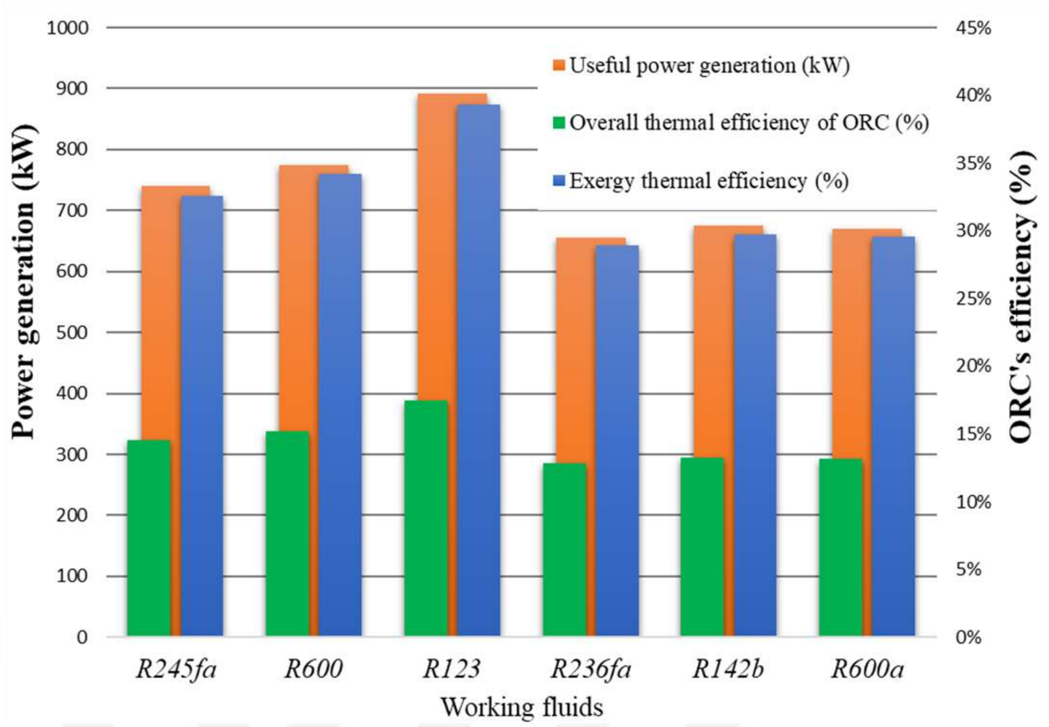

Figure 3.1. Performance analysis of ORC (Ideal case)

The values indicated in Figure 3.1. are calculated based on the ideal case, where the pressure drop across the heat transfer unit is neglected. The figure illustrates that R123 exhibits the best performance in the Organic Rankine Cycle (ORC) among the other fluids, namely R600, R245fa, R142b, R600a, and R236fa, respectively.

In the following chapters, a step-by-step design process is presented for each component of the heat exchangers used in the cycle, including the preheater, evaporator, superheater, and condenser. The design calculations are carried out for each heat exchanger unit by using the parameters that were obtained from the performance calculations conducted in this chapter.

CHAPTER 4
CONDENSER

4.1 Condenser definition

Condenser is one of Organic Rankine cycle components where the high pressure and temperature vapor coming from the expander condenses to a liquid state. Usually, the working fluid is cooled at the condenser by water and this type of condenser called water cooled condenser. the other type of condenser is cooled by air is called air cooled condenser. Both of condenser could be used of Rankine cycle. In case of shape there are many types of condensers but in our study, we used water cooled Shell and Tube condenser due to its high heat transfer coefficient and low manufacturing and operating cost. Horizontal shell and tube condenser is one of the most popular types of heat exchangers which could be used for wide range of pressures and temperatures consists from many circular tubes contained in a cylindrical shell. Heat transfer inside the condensers occurs between two fluids, one of them is a working fluid and the other is a cooling fluid. One of these two fluid enter the tubes side and the other enters from the shell side. Here in our case the refrigerant enters the shell side where the condensation occurs and the water which is cooling fluid enters from tube side as it is shown in **Figure 4.1**

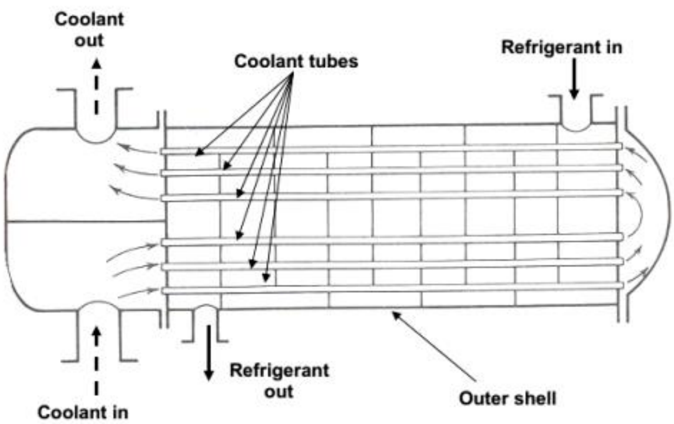

Figure 4.1.Schematic Diagram of a two-pass, Shell and Tube type condenser.

4.1.1 Condenser design methodology

In our study, the Kern's method has been employed for the design of the condenser, which plays a pivotal role in the efficient functioning of the ORC system. The condenser operates by receiving the superheated vapor from the turbine through the shell side, and the condensation process takes place inside the condenser until all the vapor is transformed into fluid. The fluid then exits the condenser through the other side. To achieve this, water has been used as a coolant that enters the condenser and passes through the tube passes. It is noteworthy that the temperature of the water entering the condenser has been maintained at 20 °C, and the mass flow rate of the coolant has been fixed at 80 kg/s. The water exits the condenser at a temperature of 35 °C. The selection of appropriate coolant and maintaining its flow rate and temperature are crucial factors in the efficient operation of the condenser and thereby achieving optimal performance of the ORC system.

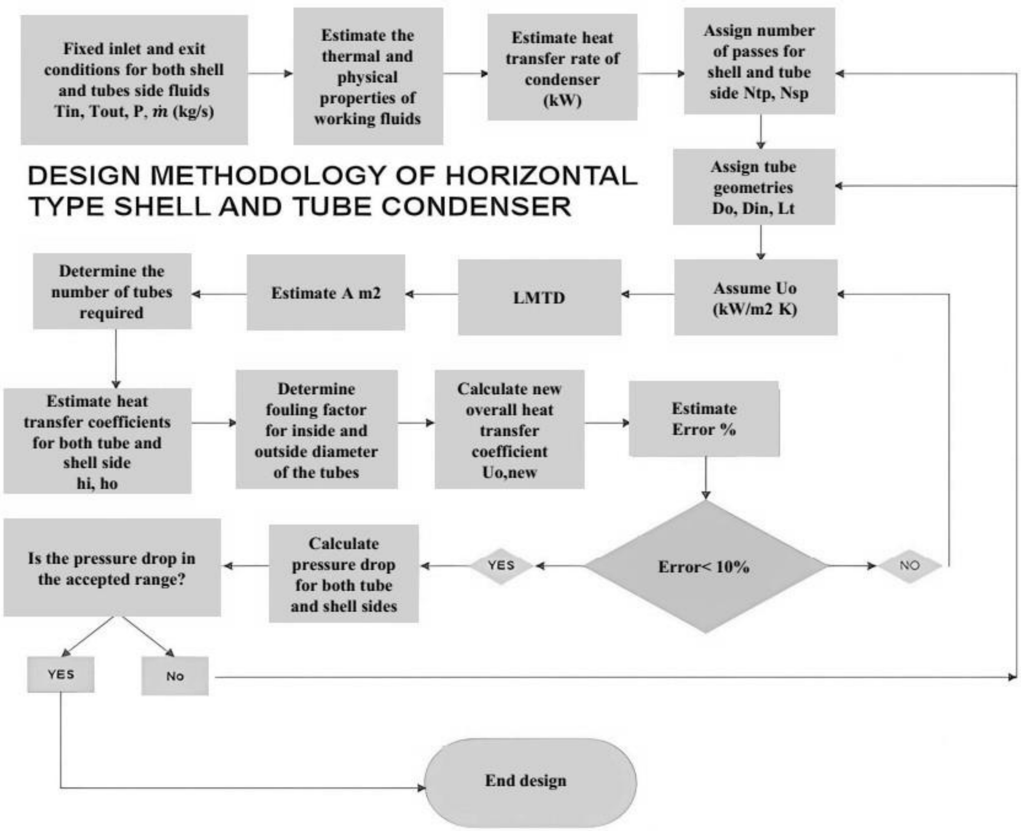

Figure 4.2. Flowchart for designing horizontal shell and tube condenser

4.1.2 Condenser design steps [18-21]

The design process for the horizontal shell and tube condenser involves several crucial steps to ensure optimal performance. Firstly, it is essential to define the inlet and outlet conditions of the refrigerant, including the inlet temperature, outlet temperatures, mass flow rate, and condenser pressure. Once these parameters are established, the physical and thermal properties of the coolant, in this case, water, must be obtained at the mean temperature Tavg, and the refrigerant in its liquid and vapor states at the saturated temperature, Tsat. The heat transfer rate for the condensation process is then calculated using an equation. This critical design process follows Kern's method, which is widely recognized as an effective approach for designing shell and tube heat exchangers, and it is essential for achieving the desired performance of the ORC system.

$$\dot{Q}cond = \dot{m}_R(h_6 - h_1) = \dot{m}_w\, c_{pw}\, \Delta T \quad (15)$$

Where:

$\dot{m}_R$= mass flow rate of refrigerant kg/s

$\dot{m}_w$= mass flow rate of water kg/s

c_{pw}= specific heat of water Kj/kg°C

2) Logarithmic mean temperature difference LMTD which could be determined by using the following equation:

$$LMTD = \frac{(T_1 - t_2) - (T2 - t_1)}{ln\left[\frac{T_1 - t_2}{T_2 - t_1}\right]} \quad (16)$$

Where: T_1 and T_2 are hot fluid inlet and outlet temperature respectively

t_1 and t_2 are cold fluid inlet and outlet temperature respectively

Note: If two of the working fluids proceed no isothermal process LMTD must be multiplied by correction factor F which could be determined by using following diagram:

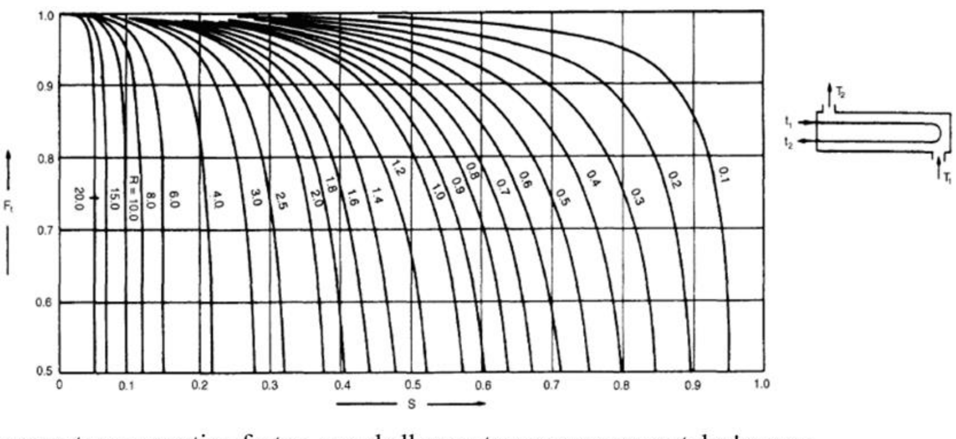

Temperature correction factor: one shell pass; two or more even tube 'passes

Figure 4.3. Temperature correction factor

Assuming a value of overall heat transfer coefficient Uo

3) Typical U-value for a horizontal shell and tube condenser using R245fa refrigerant can be in the range of 200-300 W/m^2·K.

4) Total heating surface area of the condenser from the equation:

$$A = \frac{\dot{Q}_{COND}}{U_0\ LMTD} \qquad (17)$$

5) Once the tube properties have been defined, the total number of tubes required for the condenser can be calculated. This is based on the total heating surface area. By using equation:

$$A = \pi\ dout\ Lt\ Nt \ldots\ldots\ldots\ldots\ldots\ldots \qquad (18)$$

6) Determine the shell geometries firstly we assign the layout of tubes which could be either square of triangular and then we calculate bundle diameter of tubes.

$$Db = dout\ \left(\frac{Nt}{K1}\right)^{1/n1} \ldots\ldots\ldots\ldots\ldots\ldots \qquad (19)$$

Where: Db= tube bundle diameter m

Nt= total number of tubes

K1 and $n1$ constants could be estimated from the Table3.

Table 4.1. K1 and n1 values

Triangular pitch *pt = 1.25do*					
No. passes	**1**	**2**	**4**	**6**	**8**
K1	*0.319*	*0.249*	*0.175*	*0.0743*	*0.0365*
n1	*2.142*	*2.207*	*2.285*	*2.499*	*2.675*
Squire pitch, pt = 1.25do					
No. passes	***1***	***2***	***4***	***6***	***8***
K1	*0.215*	*0.156*	*0.158*	*0.0402*	*0.0331*
n1	*2.207*	*2.291*	*2.263*	*2.617*	*2.643*

Inner shell diameter by using this formula:

$$Ds = Db + CD \ldots\ldots\ldots\ldots\ldots\ldots$$

(20)

Where:

CD = clearance defined from the chart diagram below

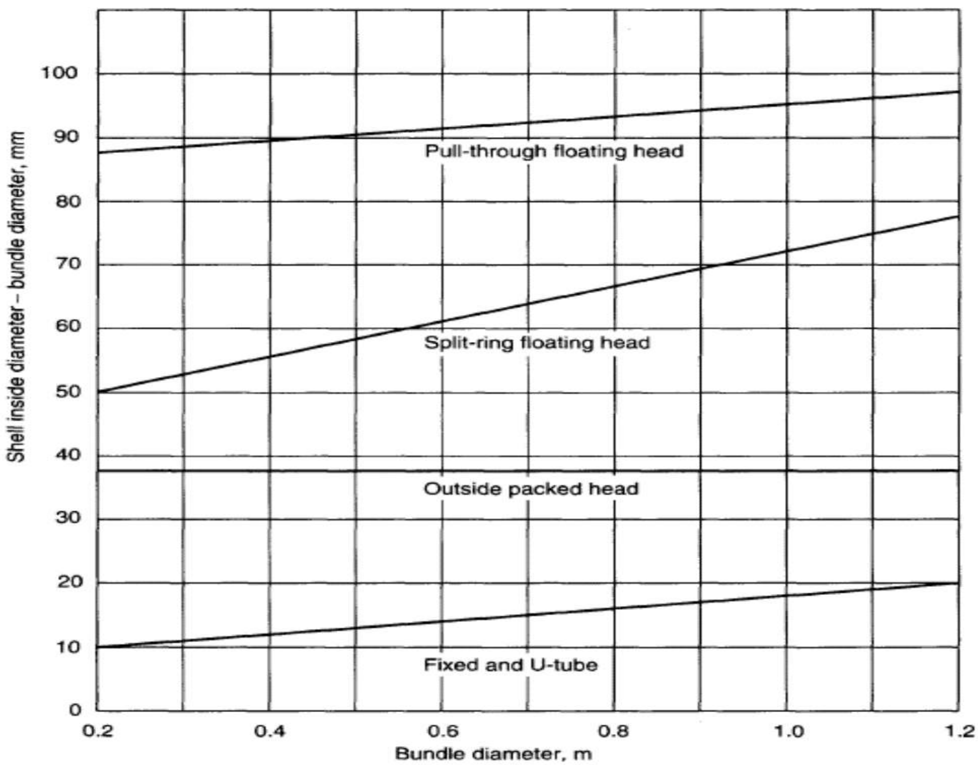

Figure 4.4 .Bundle diameter and shell and CD diagram

7) Heat transfer coefficient inside the tube hi for single phase flow, we use **Seider-Tate** and Hausen equations:

$$h_{i=}0.023\ Re^{0.8} p_r^{\frac{1}{3}}\ (\frac{K}{din}) \qquad (4000< \mathrm{Re}) \qquad (21)$$

$$h_{i=}0.116\left(R_e^{\frac{2}{3}}-125\right)p_r^{\frac{1}{3}}\left(1+\left(\frac{din}{L}\right)^{\frac{2}{3}}\right)(\frac{K}{din} \qquad (2300<\mathrm{Re}<4000) \qquad (22)$$

$$h_i\ = 1.86\left(Re\,Pr\frac{D}{L}\right)^{\frac{1}{3}}(\frac{k}{din}) \qquad (\mathrm{Re} < 2300) \qquad (23)$$

$$Re\ = \left(\frac{Gxdin}{\mu}\right)$$

Where:

G= mass velocity kg/m^2 s

din= tube inside diameter m

μ= fluid dynamic viscosity kg/m s

Pr: Prandtl number

K: fluid thermal conductivity W/m K

8) Heat transfer coefficient for shell side which is more complicated due to presence of both liquid and vapor use equation:

$$(h_c)b = 0{,}95k_L\left[\frac{\rho l(\rho l-\rho v)g}{\mu_{L}\Gamma n}\right]^{\frac{1}{3}}\left(N_{\gamma}'\right)^{\left(-\frac{1}{6}\right)} \tag{24}$$

$$\Gamma n = \frac{\dot{m}}{L \times N_t}$$

$$N\gamma' = \left(\frac{2}{3}Nr\right) \tag{26}$$

$$Nr = \frac{Db}{pt} \tag{27}$$

Where: Γn= is row density

Nr= number of tubes in the center raw

pt= tube pith which recommended to have a value of 1.25d

9) Uo over all heat transfer coefficient which can be written as:

$$\frac{1}{U} = \left[\frac{1}{h_o} + R_{do} + \frac{Ao}{Ai}\left(\frac{din - dout}{2k_W}\right) + \frac{Ao}{Ai}\left(\frac{1}{h_i}\right) + \frac{Ao}{Ai}R_{di}\right]$$

Where: R_{do} and R_{di}= fouling factors are estimated from Table.**4**

k_W= Tube wall thermal conductivity

Table 4.2. Fouling factors and coefficient

Fluid	Coefficient (W/m^2 °C)	R_{do} (m2 °C/W)
River water	3000-12000	0.0003-0.0001
Sea water	1000-3000	0.001-0.0003
Cooling water	3000-6000	0.0003-0.00017
Refrigerant	3000-5000	0.0003-0.0002
Air and industrial gases	5000-10000	0.0002-0.0001
Organic vapours	5000	0.0002
Organic liquids	5000	0.0002

10) Subsequently, we compare the value of Uo we estimated from equation and the value we assumed and check the Error percentage if it is in accepted limit or not, the limitation is given by Kern's method.

$$E\% = \frac{Uo.esti-Uo.assum}{Uo.\ assum} \times 100<30\% \tag{28}$$

11) If the design in accepted range the next step is to determine pressure drop for both shell and tubes sides. For calculation the pressure in tube side we use the following equation:

$$\Delta Pt = \Delta P\ tube + \Delta P\ Turing\ pass \tag{29}$$

$$\Delta P\ tube\ =\ fdarcy\left(\frac{L}{din}\right)\frac{\rho v^2}{2}\ Ntp \tag{30}$$

$$\Delta P\ Turing\ pass\ =\ K\ \frac{\rho v^2}{2}\ Ntp \tag{31}$$

Where: Ntp= number of tube passes

din= tube inner diameter m

K=Minor friction coefficient

Shell side pressure drop is estimated by using the following formula:

$$\Delta Ps\ =\ 8\,jh\,\left(\frac{Ds}{De}\right)\left(\frac{L}{BS}\right)\ \frac{\rho vs^2}{2} \tag{32}$$

Where:

jh: friction coefficient which is determined from the chart In figure 5 below

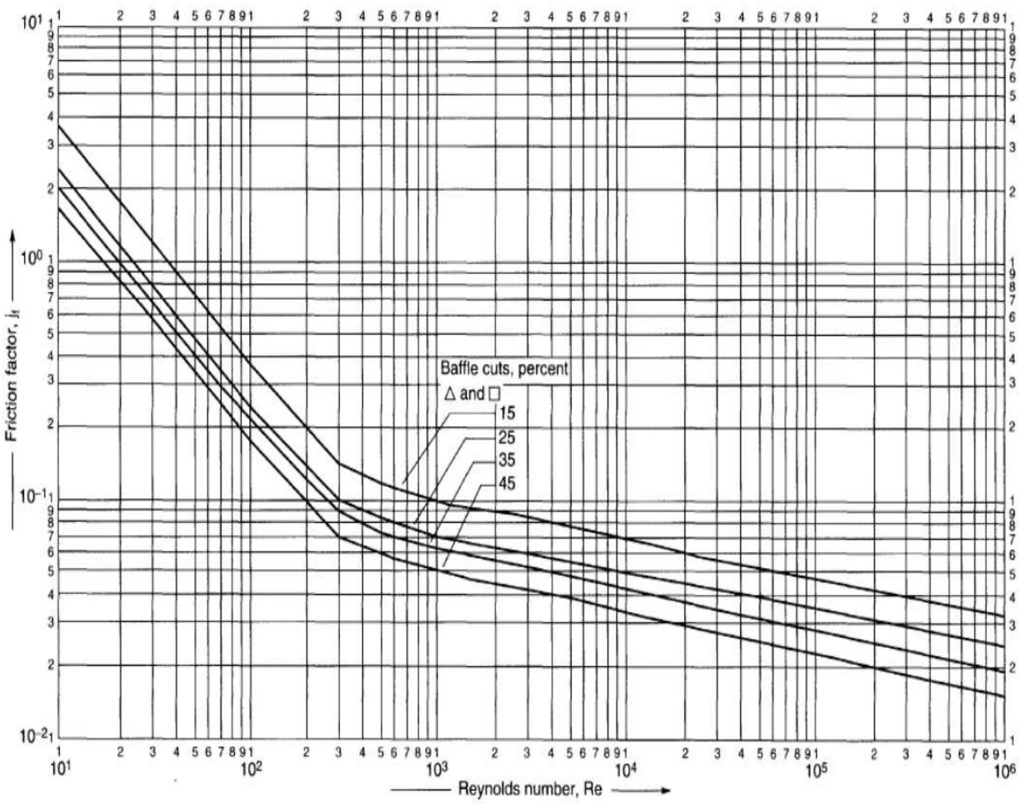

Figure 4.5. Shell side friction factor jh chart

$$Res = \frac{GDe}{\mu_s}$$

$$De = \frac{1{,}27}{dout}\left(p_t^2 - 0{,}785d_{0ut}^2\right) \text{ for square pitch type} \tag{34}$$

$$De = \frac{1{,}1}{do}\left(p_t^2 - 0{,}917d_{0ut}^2\right) \text{ for triangular pitch type.} \tag{35}$$

$$Bs\ =\ Ds. \tag{36}$$

$$Vs = (\frac{G}{\rho}) \quad (37)$$

$$Gs = \frac{\dot{m}s}{A_s} \quad (38)$$

$$A_s = \frac{pt - D_O}{Pt} x\ Ds\ x\ Bs \quad (39)$$

Where: Ds = Shell diameter m

De= equivalent diameter m

d_{0ut}= outside tube diameter m

pt = tube pitch m

Bs = baffle space m

Vs = shell side fluid velocity m/s

Gs = shell side mass velocity kg/m^2 s

$\dot{m}s$= shell side fluid velocity m/s

A_s= shell side cross flow velocity m/s

4.1.3 Condenser design limitations

To achieve an optimal design of the condenser with minimal cost, it is essential to strike a balance between heating surface area and pressure drop. Increasing the heating surface area results in a higher cost of materials and construction, while a smaller surface area leads to lower costs but increased pressure drop. Thus, to obtain the best compromise between cost and performance, certain limitations are imposed. In this study, we have proposed limitations that enable us to attain an optimum design with minimum surface area (i.e., minimum cost) and an allowable pressure drop. By setting appropriate constraints, we were able to ensure that the design satisfies the requirements of the ORC system while minimizing the cost of the condenser. This approach allowed us to achieve a balance between cost and performance, resulting in an efficient and cost-effective ORC system.

Table 4.3. Condenser design limitations

Error (E%)*	**v_t (m/s)** [21]**	**L_t/D_s*****	**ΔP_t (bar)**	**ΔP_s (bar)**
<10%	1.5< v_t < 2.5	5 < L_t/D_s<10	<2	<0.2

*To avoid overdesign for condenser. In Kern's it is indicated as 30%

**low-velocity cause low heat transfer; high velocity leads to tube erosion and more pressure drop

*** Preferred to have exemplary geometries of the design

4.1.4 Condenser design optimization procedure

Table 4.4. Condenser fixed properties and tube geometries

d_{out} (mm)	d_{in} (mm)	Material	Pitch (mm)	Tube layout	Shell No	Passes
25.4	21.3	Carbon steel	1.25 d_{out}	Triangular-square	1	

Length of tube and number of tube passes are variable values where

Length of tube = 1, 1.5, 2, 3 ....6m

Number of tube passes = 2, 4, 6, 8

Total number of design (44) design

The design which has a minimum surface area is called to be the optimum design among other designs.

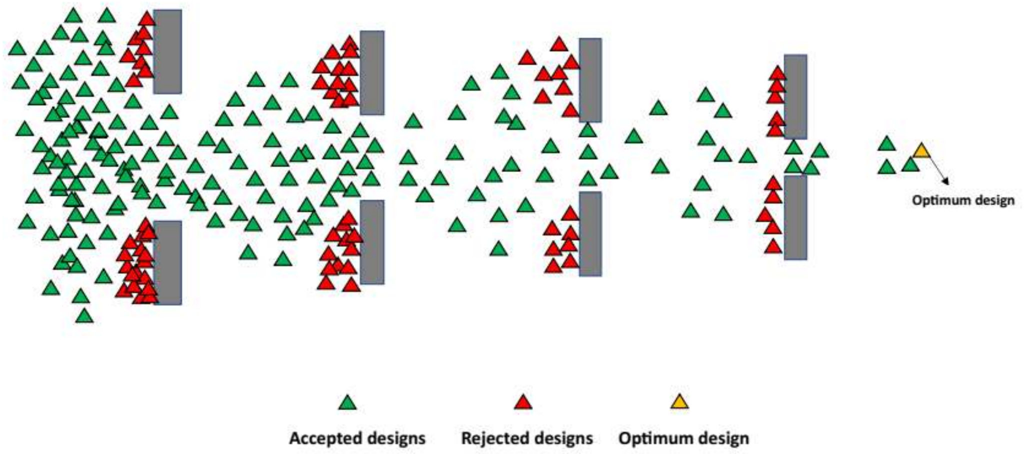

Figure 4.6. Optimization procedure mentioned in this study

4.1.4.1 Condenser optimization procedure for R245fa

The Figure 4.7 below depicted illustrates the results of an extensive analysis of various condenser designs, considering three key variables: the number of tube passes, total number of tubes, and tube length. These variables are plotted on the horizontal axis, while the condenser heat transfer (kW) is plotted on the vertical axis.

Each design is characterized by its respective number of tube passes, total number of tubes, and tube length, alongside the corresponding heating duty (kW). The tube length is systematically increased in increments of 50cm until it reaches 600cm for each number of tube passes. The number of tube passes is then gradually increased by 2, and the process is repeated until the number of tube passes reaches 8, resulting in a total of 44 distinct condenser designs being evaluated.

By examining the plotted graph, it becomes apparent that the optimal design is dependent on a careful balance between heating surface area and pressure drop. With this in mind, the suggested design limitations ensure that an optimum condenser design can be achieved that balances the desire for minimum surface area (minimum cost) with an acceptable level of pressure drop that would not negatively affect the overall performance of the ORC.

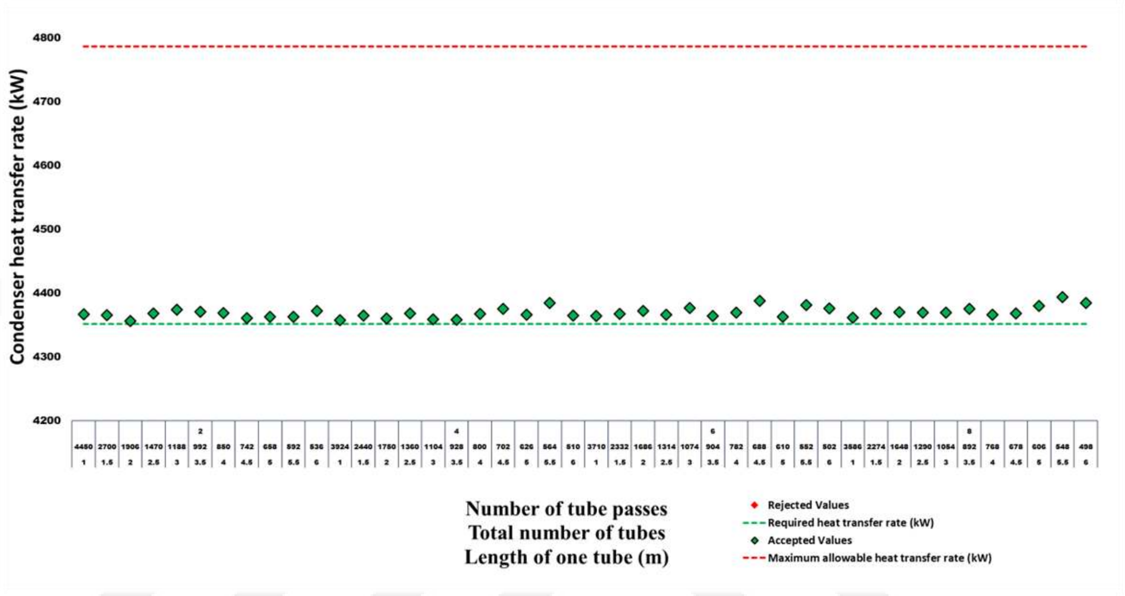

Figure 4.7. Rate of heat transfer through condenser (kW) with R245fa

Figure 4.7 depicts the evaluated condenser designs in terms of the total number of tubes, the number of tube passes, and tube length, with the Condenser heat transfer (kW) on the vertical axis. It is noteworthy that all the data points lie within the acceptable range, as indicated by the green shaded region between the minimum and maximum acceptable cooling duty values. The minimum required condenser cooling duty (KW), which was previously calculated in the Table 3.2, is represented by the green dashed line at 4351.79 KW. Similarly, the red dashed line represents the maximum acceptable cooling duty, which is approximately 10% higher than the required value, at 4787 KW. The location of all the data points in the green region suggests that each design meets the cooling duty requirements and falls within the acceptable range. Therefore, the presented condenser designs are deemed suitable for the ORC system, with the added advantage of being cost-effective and efficient.

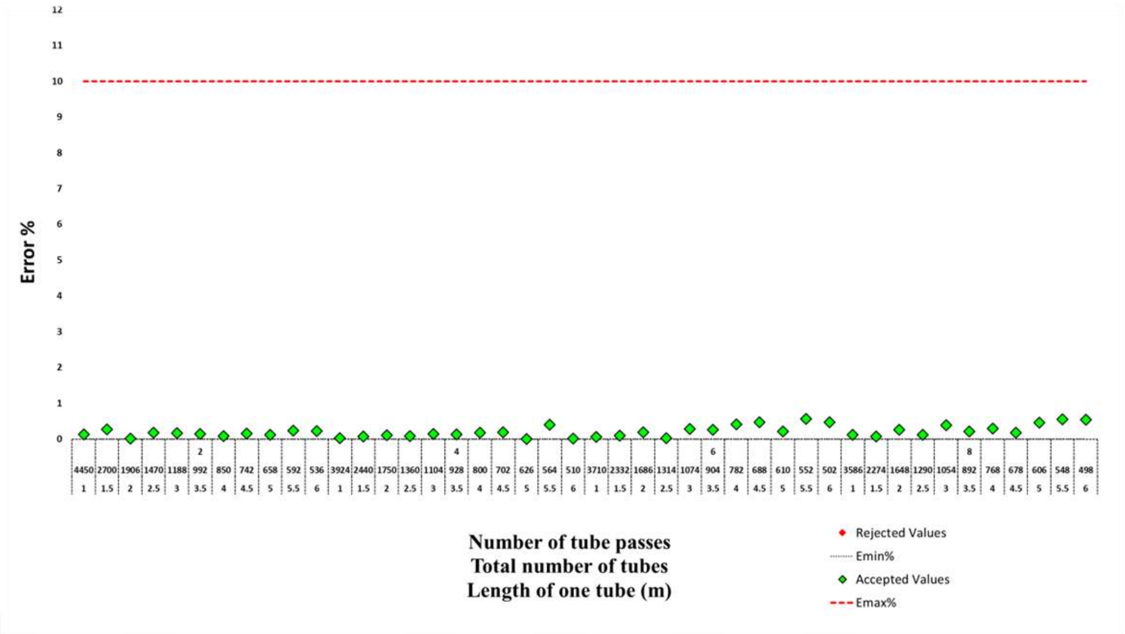

Figure 4.8. Condenser design error % diagram with R245fa

Figure 4.8 is a highly informative plot that offers a comprehensive evaluation of the design error for each of the condenser designs as a function of the number of tube passes, total number of tubes, and tube length. A critical constraint is highlighted by a bold red dashed line, indicating the maximum allowable design error of 10%. It is indeed encouraging to note that all 44 condenser designs presented in the plot fall within the accepted range, with each design represented by a vivid green color and a design error of less than 10%. This empirical evidence highlights the significant advancements made in optimizing condenser design, as each design not only meets the necessary performance criteria but also satisfies the essential design limitations. The results of this analysis are expected to be of immense value to the ORC industry as they provide crucial insights into achieving the optimal condenser design that ensures efficient and cost-effective operation.

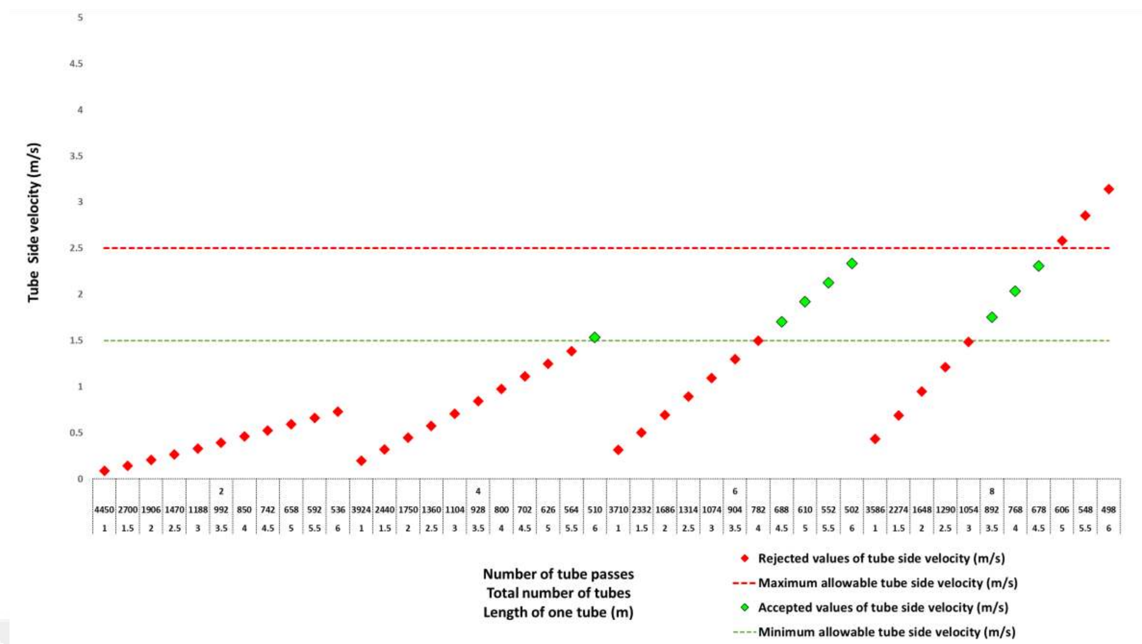

Figure 4.9. Condenser Tube side fluid velocity diagram with R245fa

Figure 4.9 provides an in-depth analysis of the fluid velocity within the tubes for each condenser design, in relation to the total number of tube passes, total number of tubes, and the length. This figure establishes an important threshold for the acceptable velocity range, with a lower limit of 1.5 m/s marked by a vibrant green dashed line, and an upper limit of 2.5 m/s denoted by a striking red dashed line.The empirical data in Figure 14 reveals that only 8 designs out of 44 met the desired range of fluid velocity within the tubes and passed all the pervious limitations. These designs are represented by a bold green color, while all other designs that failed to meet this crucial limitation are shown in a stark red color. The results of this analysis highlight the complexity and difficulty of optimizing condenser designs, as only a select few designs were capable of achieving the necessary fluid velocity within the tubes while also satisfying other essential performance criteria. In summary, Figure 14 serves as a valuable tool for condenser design optimization, as it enables engineers to visualize and analyze the fluid velocity within the tubes for each design and ensure that the acceptable range is maintained. The empirical data presented in this figure will contribute significantly to the development of more efficient and effective condenser designs that meet the necessary performance criteria.

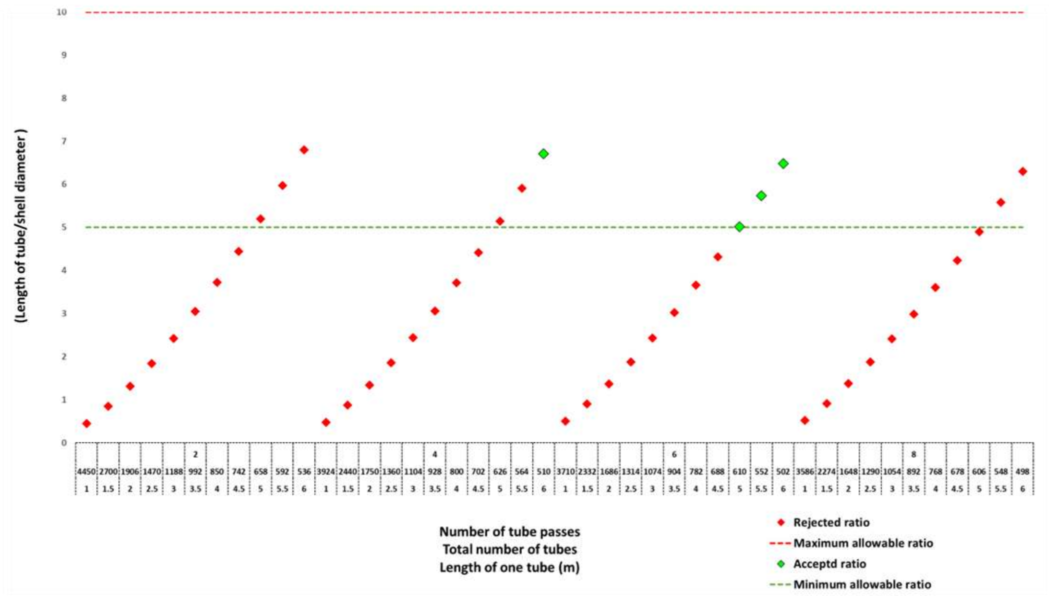

Figure 4.10. Condenser (Length of tube / shell diameter) diagram with R245fa

Figure 4.10 provides a comprehensive evaluation of the design goodness ratio, a critical metric for assessing the effectiveness and efficiency of each condenser design. The figure is expertly paired with the previous variables, including the number of tube passes, total number of tubes, and length of tubes, to provide a holistic assessment of each design. Notably, the figure establishes a vital threshold for the acceptable goodness ratio range, with a bold red dashed line representing the upper limit of 10 and a vibrant green dashed line denoting the lower limit of 5. Designs that fall within this accepted range are depicted in a bold green color, while those outside of the range are shown in a stark red color.

Intriguingly, the empirical data presented in the figure reveals that only 11 condenser designs achieved a value within the desired range. However, only four of these designs were able to surpass not only this critical design limitation but all prior limitations as well, earning them the coveted green color. These findings underscore the complexity and challenges of designing optimal condensers, as only a select few designs emerge as truly superior, with the ability to meet all necessary performance criteria. Overall, this figure provides critical insights into the design optimization process and highlights the need for meticulous evaluation and testing to achieve the desired performance outcomes.

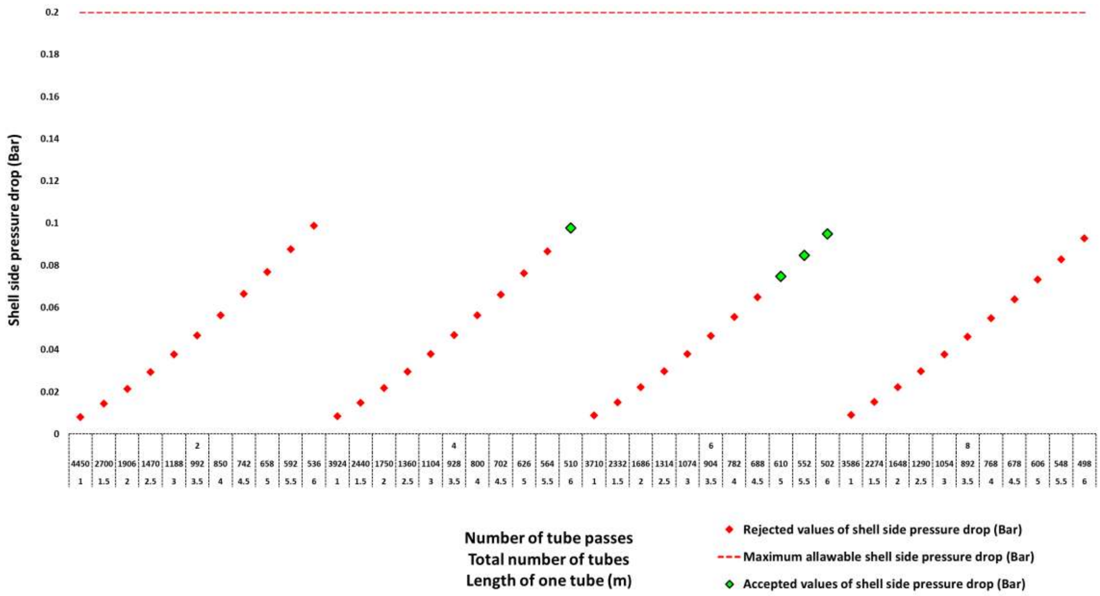

Figure 4.11. Shell side pressure drop through the condenser with R245fa

Figure 4.11 presents an informative graphical representation of the shell side pressure drop of each condenser design, meticulously correlated to the number of tube passes, total number of tubes, and tube length that were previously analyzed. Notably, this figure establishes a crucial threshold for the maximum allowable shell side pressure drop, clearly depicted by a striking dashed red line, emphasizing the importance of adhering to safe and optimal performance criteria. The green symbols within the figure represent the select few designs that have successfully passed all previous design limitations while also maintaining a shell side pressure drop of less than 0.2 bar. In contrast, the red symbols represent the designs that did not meet this critical threshold or failed to pass one or more of the previous design tests. Among the numerous designs evaluated, only four have emerged as optimal condenser designs, distinguished by a radiant green color to signify their exceptional performance and efficiency. These designs have ingeniously balanced the critical factors of pressure drop, tube passes, total tubes, and tube length to achieve an optimal result that meets all performance criteria, delivering an outstanding performance that is both safe and cost-effective. The empirical data presented in this figure highlights the significance of meticulous design optimization, underscoring the importance of meeting all critical design thresholds to achieve optimal performance.

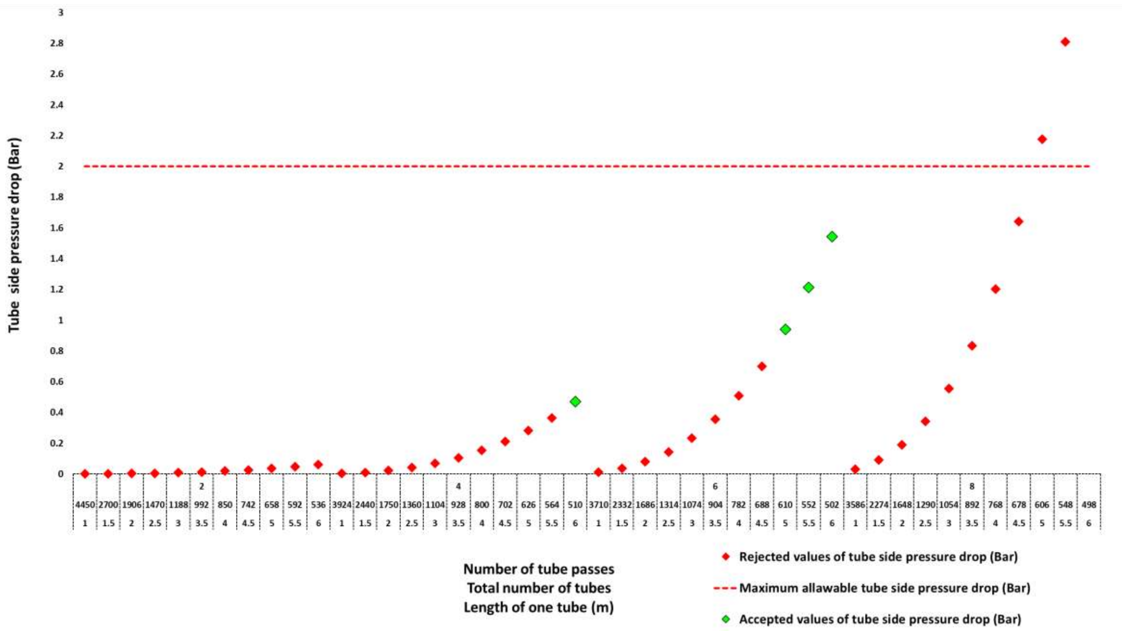

Figure 4.12. Tube side pressure drop through the condenser with R245fa

With an eloquent display of data, Figure 4.12. offers a comprehensive analysis of the tube side pressure drop (water side) for each condenser design, meticulously crafted to align with the number of tube passes, total number of tubes, and tube length evaluated previously. The maximum allowable tube side pressure drop is perceptively marked by a bold red dashed line, serving as a crucial threshold for evaluating the performance of each design.

The green symbols within the figure represent the successful designs that have not only remained under the 2 bar threshold but have also passed all prior design limitations. These designs have ingeniously optimized the number of tube passes, total number of tubes, and tube length to achieve a desirable tube side pressure drop, thereby demonstrating their exceptional performance and efficiency. On the other hand, the red symbols highlight the unfortunate candidates that failed to meet one or more critical performance criteria or exceeded the 2 bar threshold.

Of the plethora of designs evaluated, only four have emerged victorious, marked with a brilliant green color to signify their outstanding performance and efficiency. These designs have surpassed all prior design limitations and achieved a tube side pressure drop within the desirable range, making them the optimal condenser designs that embody safety, performance, and efficiency in perfect harmony.

Undoubtedly, the heating surface area of a condenser plays a crucial role in determining the cost and investment necessary for its installation and operation. A larger surface area usually entails a higher initial cost to manufacture and install the condenser, as it requires a larger quantity of materials and more labor for its assembly. However, in this study, the optimization procedure has been meticulously designed to create a condenser that not only embodies efficiency and elegance but also ingeniously minimizes the required heating surface area. The goal is to achieve a design that efficiently meets the critical performance parameters essential for the successful operation of the condenser, while minimizing the associated costs of manufacturing, installation, and operation.

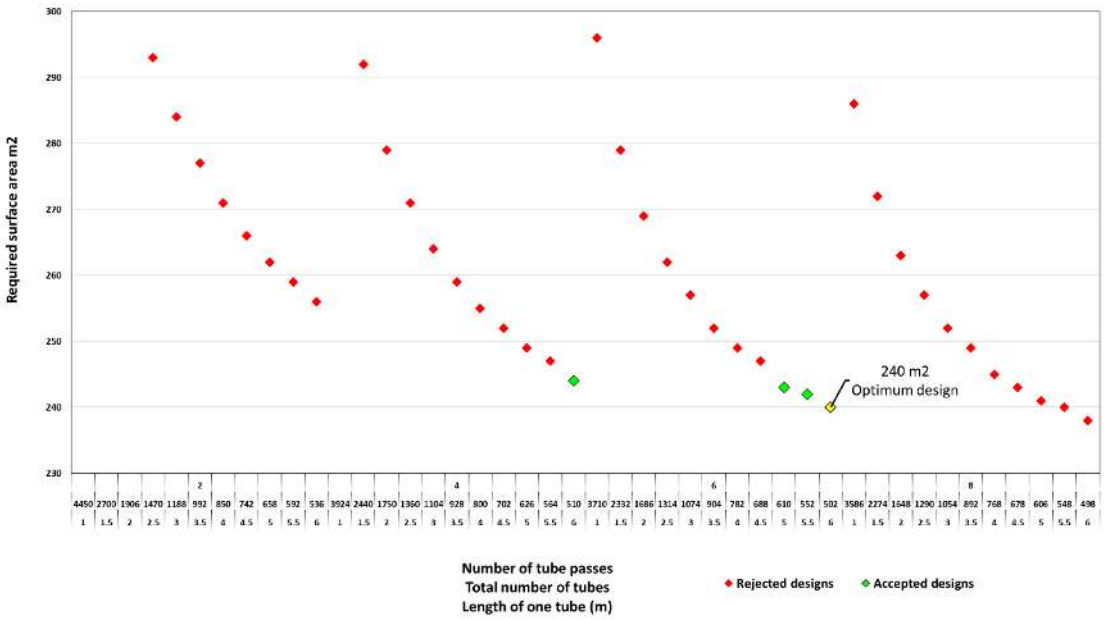

Figure 4.13. Condenser heating surface area m2 diagram with R245fa

Figure 4.13 provides a detailed comparison of various condenser designs that underwent the same performance tests. The designs that passed the tests are marked in green, while those that failed are marked in red. The optimal design has the smallest heating surface area of 240 m2 and includes six tube passes, a total of 502 tubes, and a tube length of six meters. This design strikes a balance between effectiveness, efficiency, and cost, providing exceptional and cost-effective performance.

Table 4.5. Condenser design results for R245fa

NO	Lt m	N_{tube} #	$N_{tube,pass}$ #	Error %	ΔP_t bar	ΔP_s bar	$\dot{Q}_{est}$ kW	Design Test Result accepted/not accepted
1	1	4450	2	0.14	0.000	0.01	4367	not accepted
2	1.5	2700	2	0.27	0.001	0.02	4366	not accepted
⋮	⋮	⋮	⋮	⋮	⋮	⋮	⋮	⋮
20	5	626	4	0.01	0.28	0.08	4367	not accepted
21	5.5	564	4	0.40	0.366	0.09	4385	not accepted
22	6	510	4	0.01	0.470	0.1	4365	accepted
⋮	⋮	⋮	⋮	⋮	⋮	⋮	⋮	⋮
30	4.5	688	6	0.47	0.699	0.07	4388	not accepted
31	5	610	6	0.22	0.941	0.08	4363	accepted
32	5.5	552	6	0.57	1.213	0.09	4382	accepted
33	**6**	**502**	**6**	**0.48**	**1.542**	**0.1**	**4377**	**accepted***
34	1	3586	8	0.13	0.032	0.01	4362	not accepted
⋮	⋮	⋮	⋮	⋮	⋮	⋮	⋮	⋮
43	5.5	548	8	0.56	2.810	0.08	4394	not accepted
44	6	498	8	0.55	3.579	0.09	4385	not accepted

*Minimal condenser area, ideal choice-lowest cost

** All the condenser design calculations are carried out assuming P2=22bar

4.1.4.2 Condenser optimization procedure for R600

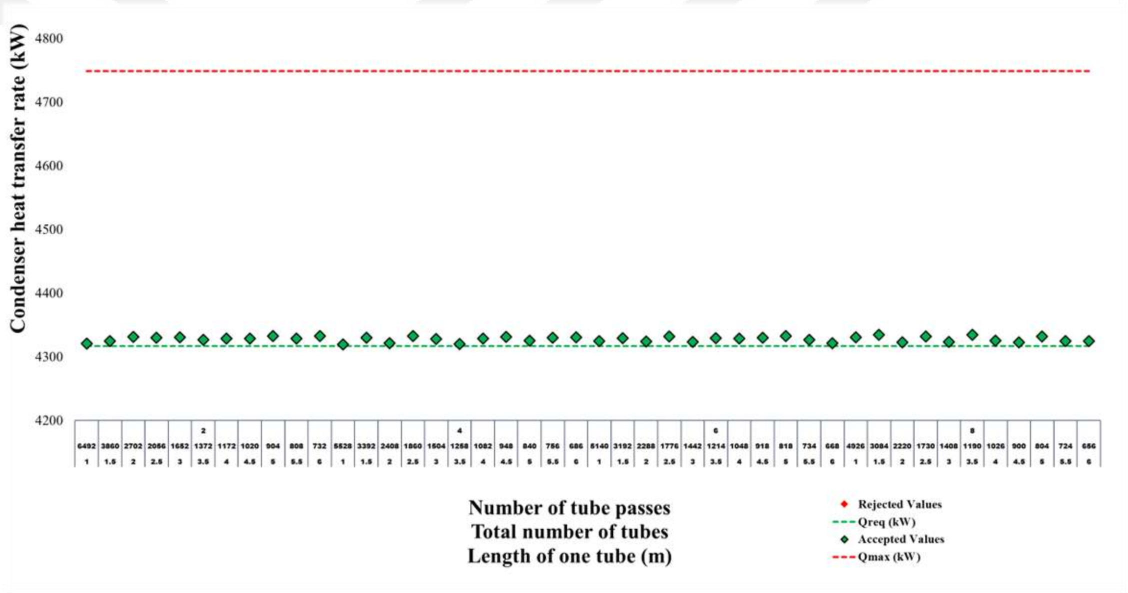

Figure 4.14. Rate of heat transfer through condenser (kW)diagram for R600

Figure 4.14 depicts the evaluated condenser designs in terms of the total number of tubes, the number of tube passes, and tube length, with the Condenser heat transfer (kW) on the vertical axis. It is noteworthy that all the data points lie within the acceptable range, as indicated by the green shaded region between the minimum and maximum acceptable cooling duty values. The minimum required condenser cooling duty (kW), which was previously calculated in the Table 3.2, is represented by the green dashed line at 4316.64 kW. Similarly, the red dashed line represents the maximum acceptable cooling duty, which is approximately 10% higher than the required value, at 4748.3 kW. The location of all the data points in the green region suggests that each design meets the cooling duty requirements and falls within the acceptable range. Therefore, the presented condenser designs are deemed suitable for the ORC system, with the added advantage of being cost-effective and efficient.

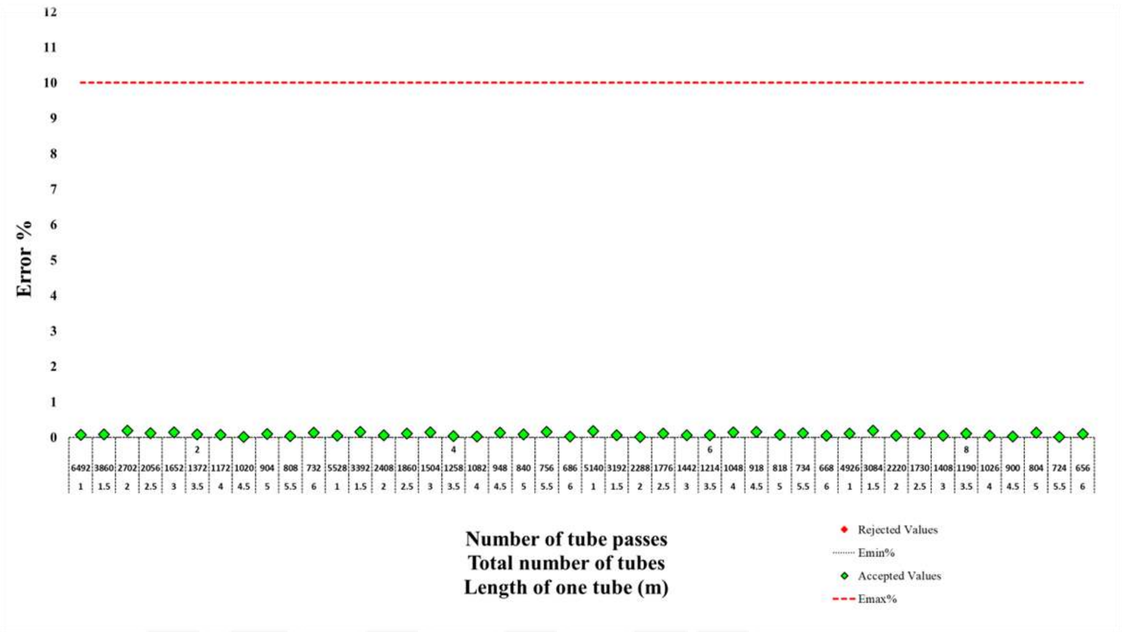

Figure 4.15. Condenser design error % diagram for R600

In Figure 4.15 the design error for all attempted condenser designs is shown. This limitation ensures that the final designs are neither overdesigned nor under designed. The suggested maximum design error is 10%, indicated by a red dashed line in the figure. It is noteworthy that all the points are located below this upper limit and are highlighted with a green symbol, indicating that all 44 suggested designs fall within the accepted range.

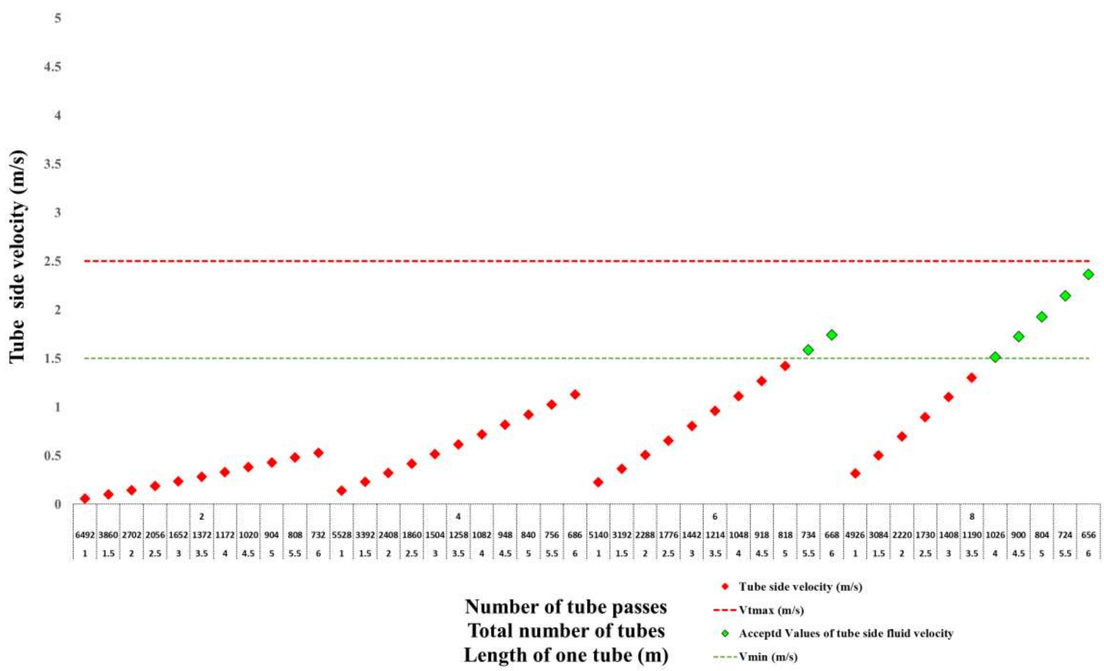

Figure 4.16. Condenser Tube side fluid velocity diagram with R600

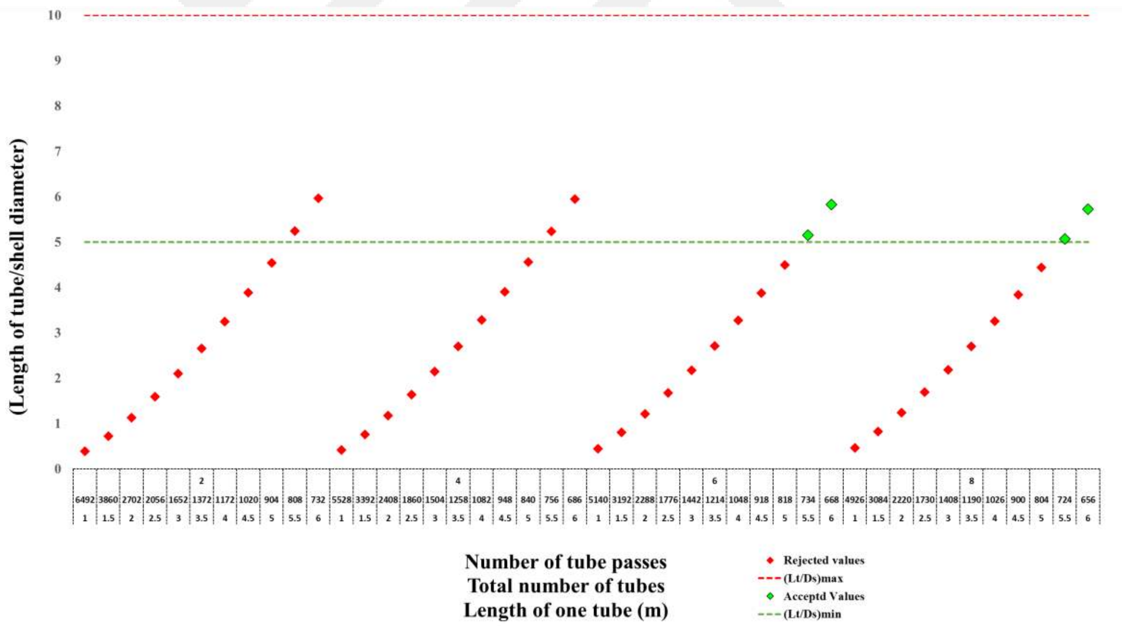

Figure 4.17. Condenser (length of tube / shell diameter) diagram with R600

In Figure 4.16 a detailed analysis of fluid velocity within the tubes for each condenser design is presented. This analysis considers the total number of tube passes, the total number of tubes, and their length. The figure sets an important threshold for acceptable velocity range, with a lower limit of 1.5 m/s marked by a green dashed line and an upper limit of 2.5 m/s denoted by a red dashed line. This limitation aims to prevent potential damage to the condenser and maintain high performance. Fluid velocity higher than 2.5 m/s can cause erosion in the tubes, while a low fluid velocity of less than 1.5 m/s can lead to a low heat transfer coefficient and reduced performance, resulting in larger heating surface areas and consequently, higher investment costs. The empirical data presented in Figure 18 shows that only 7 designs out of 44 met the desired range of fluid velocity within the tubes and passed all the pervious limitations, represented by a green color. All other designs that failed to meet this crucial limitation are shown in red. This analysis highlights the complexity and difficulty of optimizing condenser designs, as only a select few designs were capable of achieving the necessary fluid velocity within the tubes while also satisfying other essential performance criteria.

In summary, Figure 4.16 is a valuable tool for condenser design optimization, allowing engineers to visualize and analyze fluid velocity within the tubes for each design to ensure that the acceptable range is maintained. The empirical data presented in this figure will significantly contribute to the development of more efficient and effective condenser designs that meet the necessary performance criteria.

Figure 4.17 provides a crucial metric, known as the design goodness ratio, for evaluating condenser designs. The figure is analyzed alongside three parameters: the number of tube passes, the total number of tubes, and tube length. It establishes an acceptable goodness ratio range with red and green dashed lines marking the upper and lower limits. Designs within this range are depicted in green, while those outside the range are shown in red. According to the empirical data presented in the figure, only 8 condenser designs were able to achieve the desired value within the acceptable range. However, only 4 of these designs were able to surpass all critical design limitations, earning them the coveted green color, while the others were shown in red.

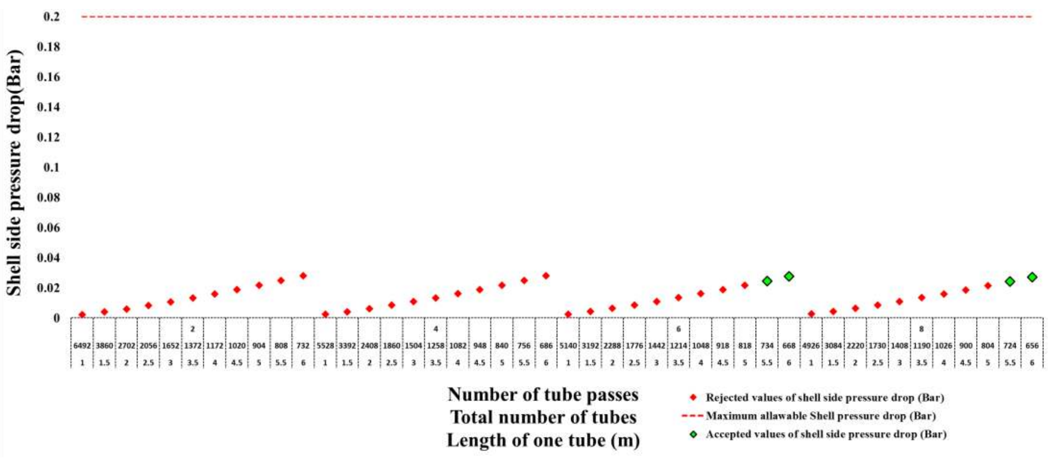

Figure 4.18. Shell side pressure drop through the condenser with R600

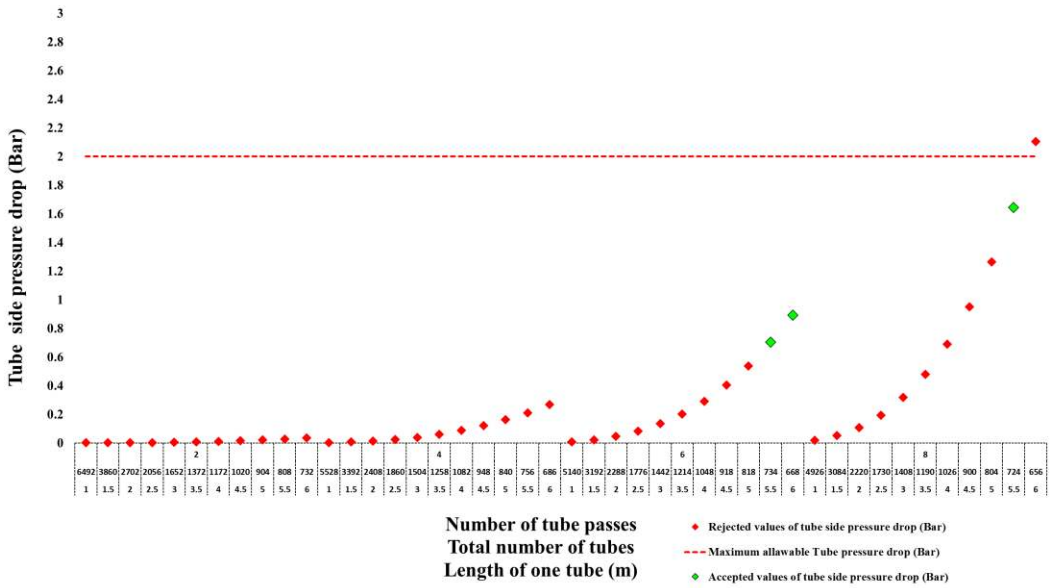

Figure 4.19. Tube side pressure drop through the condenser with R600

Figure 4.18 showcases a graph that depicts the pressure drop on the shell side of each condenser design with utmost clarity and precision. The graph takes into consideration the number of tube passes, the total number of tubes, and the tube length of each condenser design. A red dashed line is drawn in the graph that represents a crucial maximum limit which is 0.2 bar for the allowable shell side pressure drop. This line emphasizes the importance of complying with safe and optimal performance criteria to ensure efficient and secure operation.

The graph portrays green symbols that indicate a small number of designs that have successfully surpassed all previous design limitations while keeping a shell side pressure drop of less than 0.2 bar. In contrast, the red symbols denote designs that failed to meet this critical limitation or couldn't pass one or more of the previous design tests. Among all the designs analyzed, only four have emerged as optimal condenser designs, distinguished by their green color to signify their exceptional performance and efficiency. These optimal designs have ingeniously maintained a balance among the critical factors of pressure drop, tube passes, total tubes, and tube length to achieve an optimal result that meets all performance criteria. This outstanding performance is both safe and cost-effective, making it a valuable asset to any system.

Figure 4.19 presents detailed information on the tube side pressure drop for each condenser design. This information is essential for evaluating the performance of each design, as it includes the number of tubes, tube length, and tube passes. The red dashed line on the chart shows the maximum tube side pressure drop that cannot be exceeded. The green symbols on the chart represent successful condenser designs that have met all performance criteria. These designs have optimized the tube passes, total number of tubes, and tube length to achieve an ideal tube side pressure drop below 2 bars. In contrast, the red symbols indicate designs that failed to meet the performance criteria or exceeded the 2 bar threshold. Out of the 44 designs evaluated, only three managed to pass all the tests and achieve the desired pressure drop levels, making them exceptional in terms of their performance and efficiency. Overall, the data presented in Figure 4.18 and Figure 4.19 provide critical insights that can help in making informed decisions about condenser design and performance evaluation.

The cost of installing and operating a condenser is largely dependent on the size of its heating surface area. A larger surface area typically leads to a higher initial cost. In light of this, this study has been conducted to optimize the design of the condenser, with the aim of making it efficient while keeping the heating surface area as small as possible. The overarching objective of this optimization is to develop a condenser that satisfies performance requirements while simultaneously reducing manufacturing, installation, and operational costs. The chart below shows the final results of the optimization procedure for the condenser. Out of all the designs that met the suggested limitations, the one with the lowest heating surface area was chosen as the best.

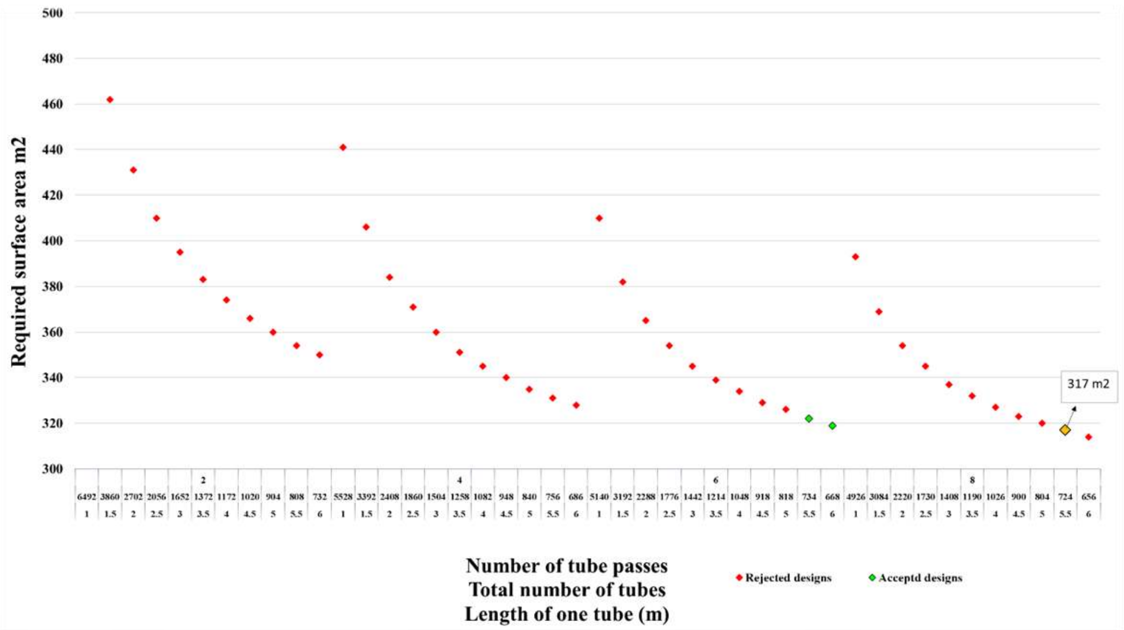

Figure 4.20. Condenser heating surface area m2 diagram with R600

A detailed comparison of different condenser designs that underwent the same performance tests is presented in Figure 4.20. The designs that passed the tests are marked in green, while those that failed are marked in red. The optimal design has a heating surface area of 317 m2, which is the smallest among all the designs. It includes 8 tube passes, a total of 724 tubes, and a tube length of 5.5 meters. This design offers a balanced solution between effectiveness, efficiency, and cost, providing outstanding and cost-effective performance.

Table 4.6. Condenser design results for R600

NO	Length	N_{tube}	$N_{tube,passes}$	Error	ΔP_t	ΔP_s	$\dot{Q}_{est}$	Design Test Result
	m	#	#	%	bar	bar	kW	accepted/not accepted
1	1	6492	2	0.067	0.0022	0.0002	4320.44045	not accepted
:	:	:	:	:	:	:	:	:
32	5.5	734	6	0.117	0.0245	0.7030	4326.26739	accepted
33	6	668	6	0.049	0.0275	0.8925	4321.23161	accepted
34	1	4926	8	0.102	0.0026	0.0173	4330.17523	not accepted
:	:	:	:	:	:	:	:	:
43	**5.5**	**724**	**8**	**0.018**	**0.0242**	**1.6428**	**4324.40219**	**accepted***
44	6	656	8	0.100	0.0271	2.1033	4324.59786	not accepted

*Minimal condenser area, ideal choice-lowest cost

** All the condenser design calculations are carried out assuming P2=22bar

4.1.4.3 Condenser optimization procedure for R123

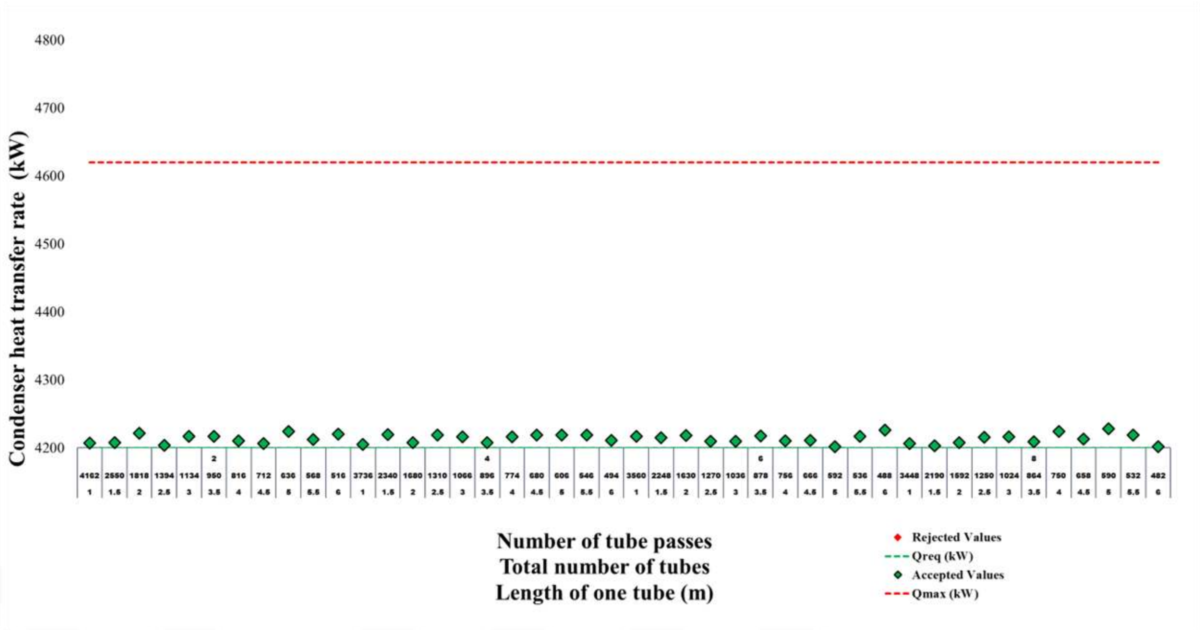

Figure 4.21. Rate of heat transfer through condenser (kW)diagram with R123

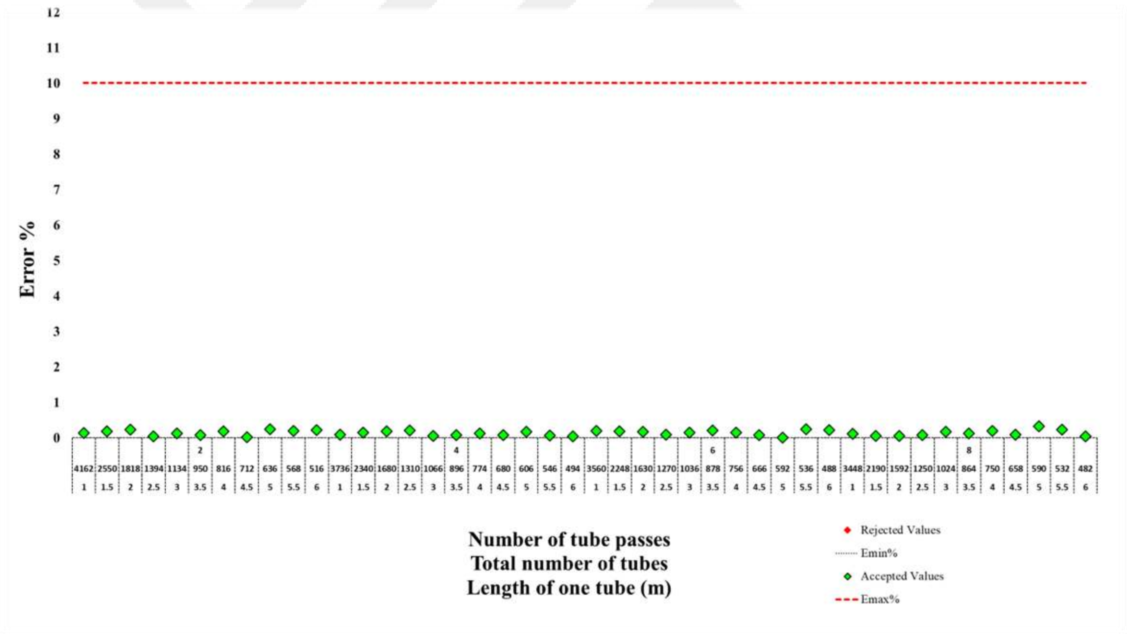

Figure 4.22. Condenser design error % diagram with R123

Figure 4.21 depicts the evaluated condenser designs in terms of the total number of tubes, the number of tube passes, and tube length, with the Condenser heat transfer (kW) on the vertical axis. It is noteworthy that all the data points lie within the acceptable range, as indicated by the green shaded region between the minimum and maximum acceptable cooling duty values. The minimum required condenser cooling duty (kW), which was previously calculated in the Table 3.2, is represented by the green dashed line at 4199.68 kW. Similarly, the red dashed line represents the maximum acceptable cooling duty, which is approximately 10% higher than the required value, at 4619.6 kW. The location of all the data points in the green region suggests that each design meets the cooling duty requirements and falls within the acceptable range. Therefore, the presented condenser designs are deemed suitable for the ORC system, with the added advantage of being cost-effective and efficient.

In Figure 4.22, the design error for all attempted condenser designs is shown. This limitation ensures that the final designs are neither overdesigned nor underdesigned. The suggested maximum design error is 10%, indicated by a red dashed line in the figure. It is noteworthy that all the points are located below this upper limit and are highlighted with a green symbol, indicating that all 44 suggested designs fall within the accepted range.

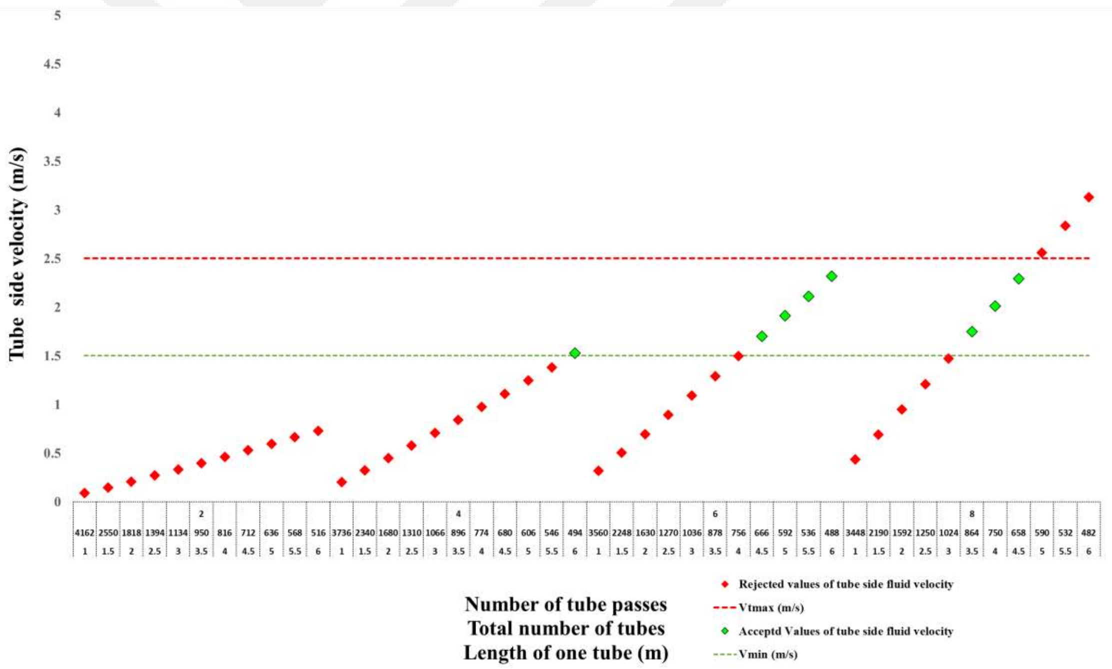

Figure 4.23. Condenser Tube side fluid velocity diagram with R123

In **Figure 4.23** a detailed analysis of fluid velocity within the tubes for each condenser design is presented. This analysis considers the total number of tube passes, the total number of tubes, and their length. The figure sets an important limit for acceptable velocity range, with a lower limit of 1.5 m/s marked by a green dashed line and an upper limit of 2.5 m/s denoted by a red dashed line. This limitation aims to prevent potential damage to the condenser and maintain high performance. Fluid velocity higher than 2.5 m/s can cause erosion in the tubes, while a low fluid velocity of less than 1.5 m/s can lead to a low heat transfer coefficient and reduced performance, resulting in larger heating surface areas and consequently, higher investment costs. The empirical data presented in Figure 4.23 shows that only 7 designs out of 44 met the desired range of fluid velocity within the tubes and passed all the pervious limitations, represented by a green color. All other designs that failed to meet this crucial limitation are shown in red. This analysis highlights the complexity and difficulty of optimizing condenser designs, as only a select few designs were capable of achieving the necessary fluid velocity within the tubes while also satisfying other essential performance criteria. In summary, Figure 4.23 is a valuable tool for condenser design optimization, allowing engineers to visualize and analyze fluid velocity within the tubes for each design to ensure that the acceptable range is maintained. The empirical data presented in this figure will significantly contribute to the development of more efficient and effective condenser designs that meet the necessary performance criteria.

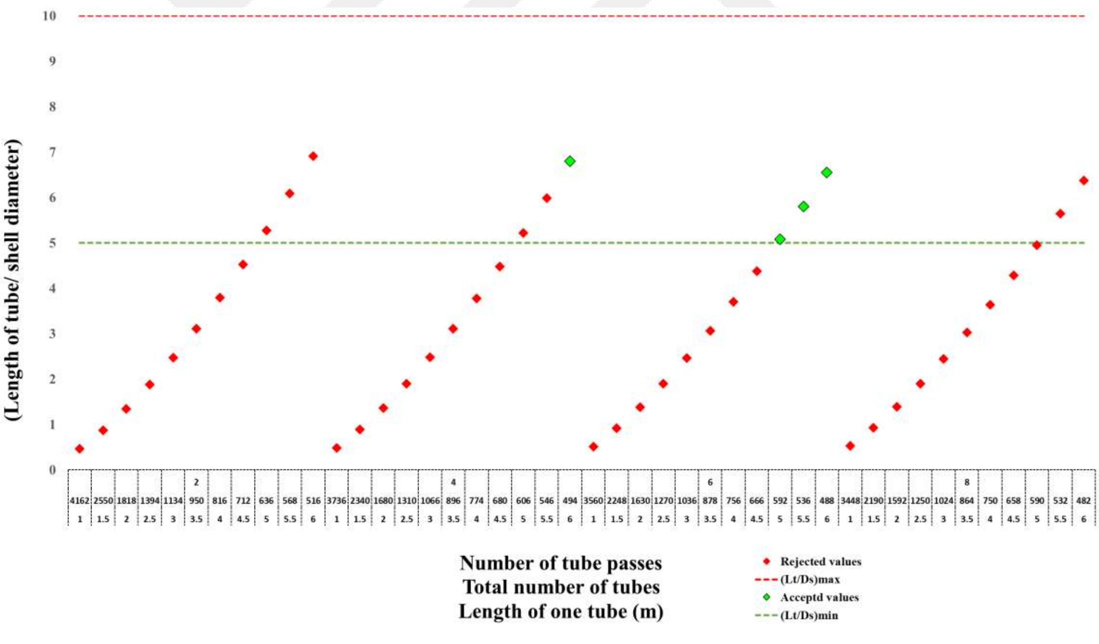

Figure 4.24. Condenser (Length of tube/shell diameter) diagram with R123

Figure 4.24 provides a crucial metric, known as the design goodness ratio, for evaluating condenser designs. The figure is analyzed alongside three parameters: the number of tube passes, the total number of tubes, and tube length. It establishes an acceptable goodness ratio range with red and green dashed lines marking the upper and lower limits. Designs within this range are depicted in green, while those outside the range are shown in red. According to the empirical data presented in the figure, only 11 condenser designs were able to achieve the desired value within the acceptable range. However, only 4 of these designs were able to surpass all critical design limitations, earning them the coveted green color, while the others were shown in red.

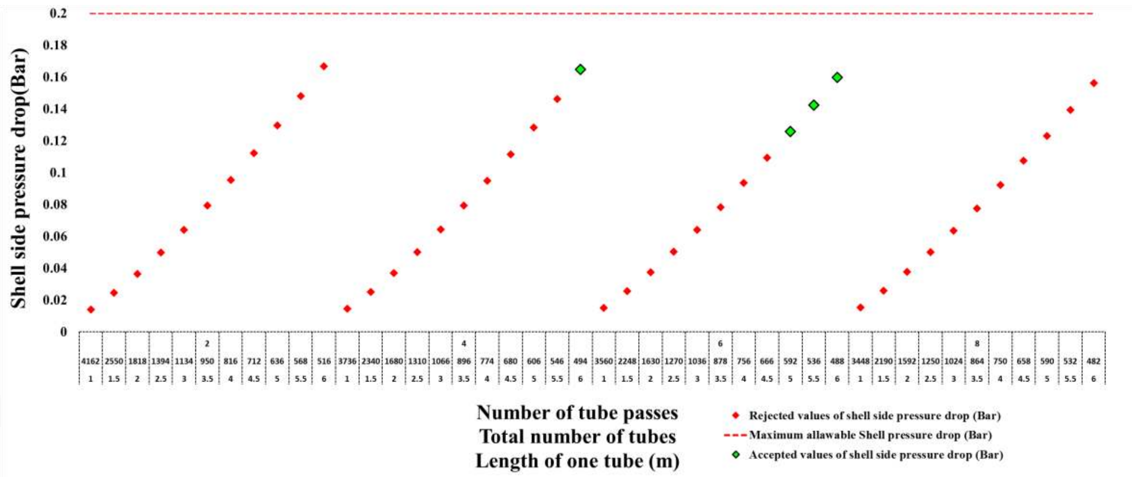

Figure 4.25. Shell side pressure drop through the condenser with R123

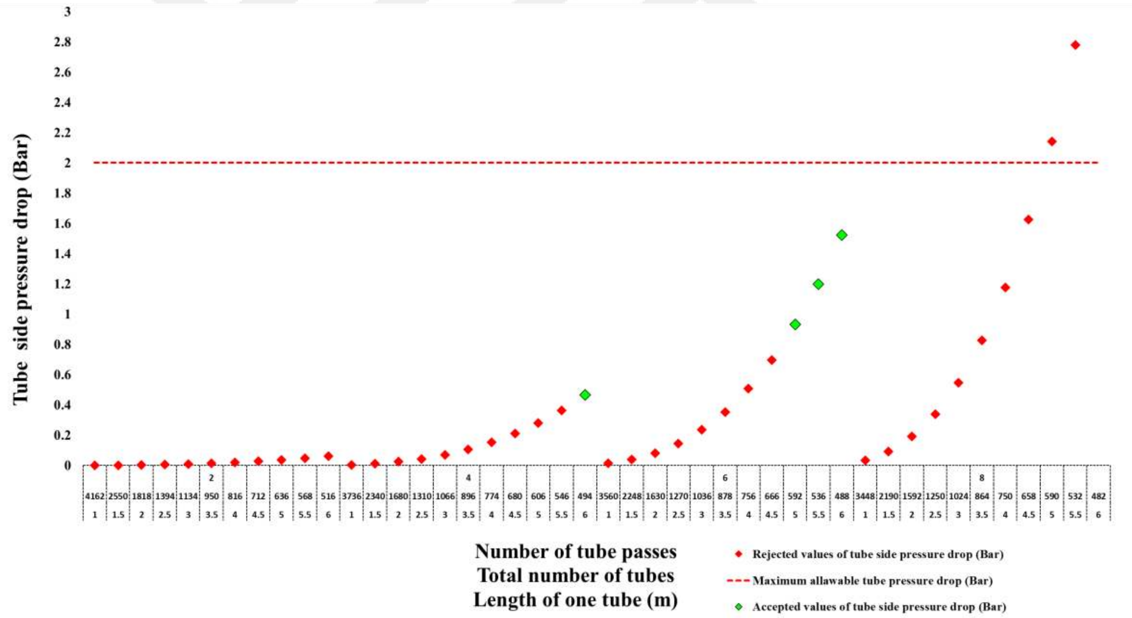

Figure 4.26. Tube side pressure drop through the condenser with R123

Figure 4.25 showcases a graph that depicts the pressure drop on the shell side of each condenser design with utmost clarity and precision. The graph takes into consideration the number of tube passes, the total number of tubes, and the tube length of each condenser design. A red dashed line is drawn in the graph that represents a crucial maximum limit which is 0.2 bar for the allowable shell side pressure drop. This line emphasizes the importance of complying with safe and optimal performance criteria to ensure efficient and secure operation. The graph portrays green symbols that indicate a small number of designs that have successfully surpassed all previous design limitations while keeping a shell side pressure drop of less than 0.2 bar. In contrast, the red symbols denote designs that failed to meet this critical limitation or couldn't pass one or more of the previous design tests. Among all the designs analyzed, only 4 have emerged as optimal condenser designs, distinguished by their green color to signify their exceptional performance and efficiency. These optimal designs have ingeniously maintained a balance among the critical factors of pressure drop, tube passes, total tubes, and tube length to achieve an optimal result that meets all performance criteria. This outstanding performance is both safe and cost-effective, making it a valuable asset to any system.

Figure 4.26 presents detailed information on the tube side pressure drop for each condenser design. This information is essential for evaluating the performance of each design, as it includes the number of tubes, tube length, and tube passes. The red dashed line on the chart shows the maximum tube side pressure drop that cannot be exceeded. The green symbols on the chart represent successful condenser designs that have met all performance criteria. These designs have optimized the tube passes, total number of tubes, and tube length to achieve an ideal tube side pressure drop below 2 bars. In contrast, the red symbols indicate designs that failed to meet the performance criteria or exceeded the 2 bar threshold. Out of the 44 designs evaluated, only 4 managed to pass all the tests and achieve the desired pressure drop levels, making them exceptional in terms of their performance and efficiency. Overall, the data presented in Figure 28 provides critical insights that can help in making informed decisions about condenser design and performance evaluation.

The cost of installing and operating a condenser is largely dependent on the size of its heating surface area. A larger surface area typically leads to a higher initial cost. In light of this, this study has been conducted to optimize the design of the condenser, with the aim of making it efficient while keeping the heating surface area as small as possible. The overarching objective of this optimization is to develop a condenser that satisfies performance requirements while simultaneously reducing manufacturing, installation, and operational costs. The chart 29 below shows the final results of the optimization procedure for the condenser. Out of all the designs that met the suggested limitations, the one with the lowest heating surface area was chosen as the best.

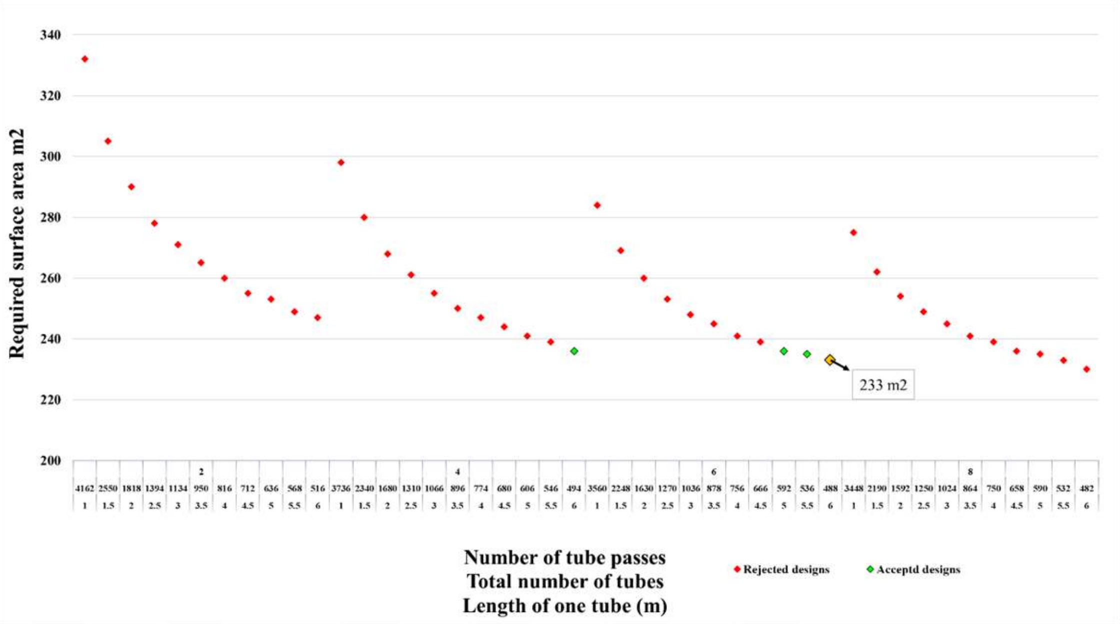

Figure 4.27. Condenser heating surface area m2 diagram with R123

A detailed comparison of different condenser designs that underwent the same performance tests is presented in Figure 29. The designs that passed the tests are marked in green, while those that failed are marked in red. The optimal design which marked by yellow color and has a heating surface area of 233 m2, which is the smallest among all the designs. It includes 6 tube passes, a total of 488 tubes, and a tube length of 6 meters. This design offers a balanced solution between effectiveness, efficiency, and cost, providing outstanding and cost-effective performance.

Table 4.7. Condenser design results for R123

NO	Length	N_{tube}	$N_{tube,passes}$	Error	ΔP_t	ΔP_s	$\dot{Q}_{est}$	Design Test Result
	m	#	#	%	bar	bar	kW	accepted/not accepted
1	1	4162	2	0.137	0.014	0.0004	4207.28633	not accepted
⋮	⋮	⋮	⋮	⋮	⋮	⋮	⋮	⋮
22	6	494	4	0.036	0.165	0.4666	4210.66035	accepted
23	1	3560	6	0.199	0.015	0.0132	4216.9765	not accepted
⋮	⋮	⋮	⋮	⋮	⋮	⋮	⋮	⋮
31	5	592	6	0.006	0.126	0.9312	4201.64064	accepted
32	5.5	536	6	0.242	0.142	1.1992	4216.90664	accepted
33	**6**	**488**	**6**	**0.216**	**0.160**	**1.5216**	**4225.83961**	**accepted***
44	6	482	8	0.042	0.156	3.55897179	4201.91777	not accepted

*Minimal condenser area, ideal choice-lowest cost

** All the condenser design calculations are carried out assuming P2=22bar.

4.1.4.4 Condenser optimization procedure for R236fa

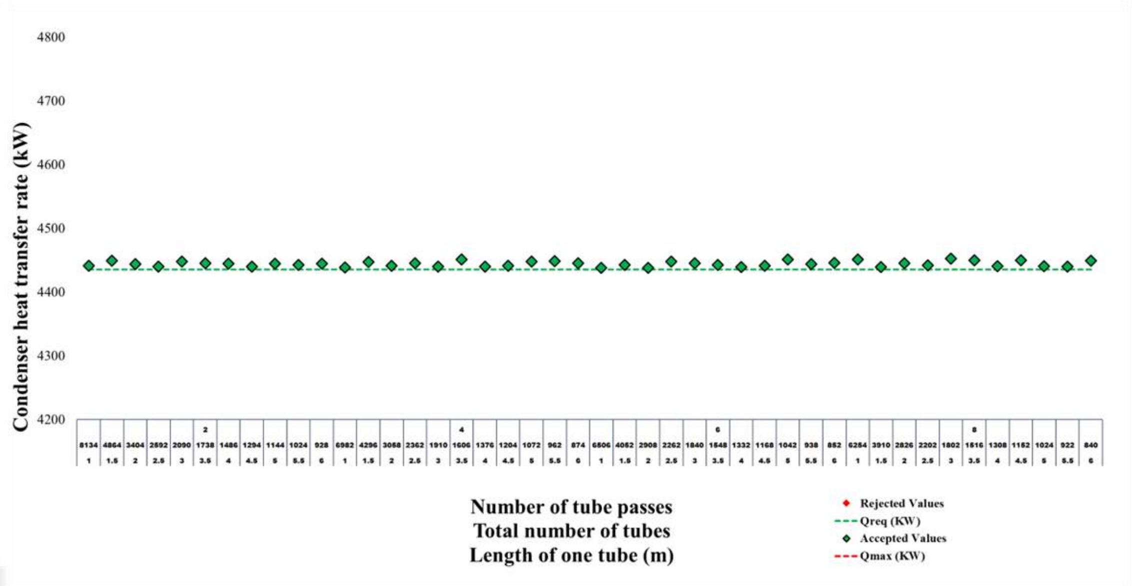

Figure 4.28.Rate of heat transfer through condenser (kW)diagram with R236fa

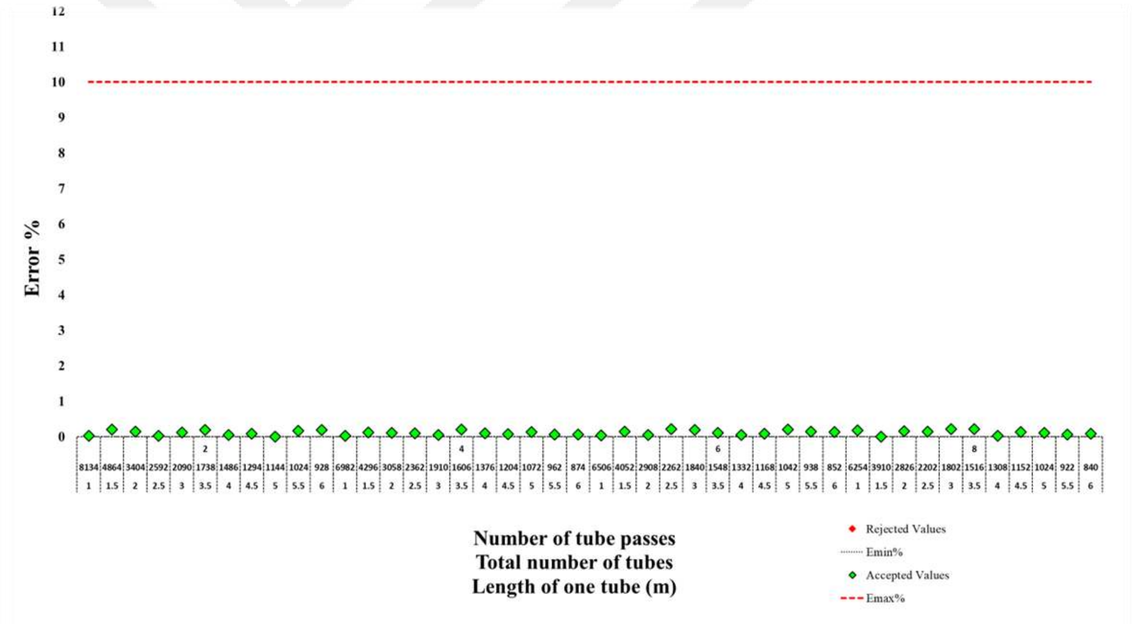

Figure 4.29. Condenser design error % diagram with R236fa

Figure 4.28 depicts the evaluated condenser designs in terms of the total number of tubes, the number of tube passes, and tube length, with the Condenser heat transfer (kW) on the vertical axis. It is noteworthy that all the data points lie within the acceptable range, as indicated by the green shaded region between the minimum and maximum acceptable cooling duty values. The minimum required condenser cooling duty (kW), which was previously calculated in the Table 3.2, is represented by the green dashed line at 4435.21 kW. The maximum acceptable cooling duty, which is approximately 10% higher than the required value, at 4878.7 kW. The location of all the data points in the green region suggests that each design meets the cooling duty requirements and falls within the acceptable range. Therefore, the presented condenser designs are deemed suitable for the ORC system, with the added advantage of being cost-effective and efficient.

In Figure 4.29, the design error for all attempted condenser designs is shown. This limitation ensures that the final designs are neither overdesigned nor underdesigned. The suggested maximum design error is 10%, indicated by a red dashed line in the figure. It is noteworthy that all the points are located below this upper limit and are highlighted with a green symbol, indicating that all 44 suggested designs fall within the accepted range.

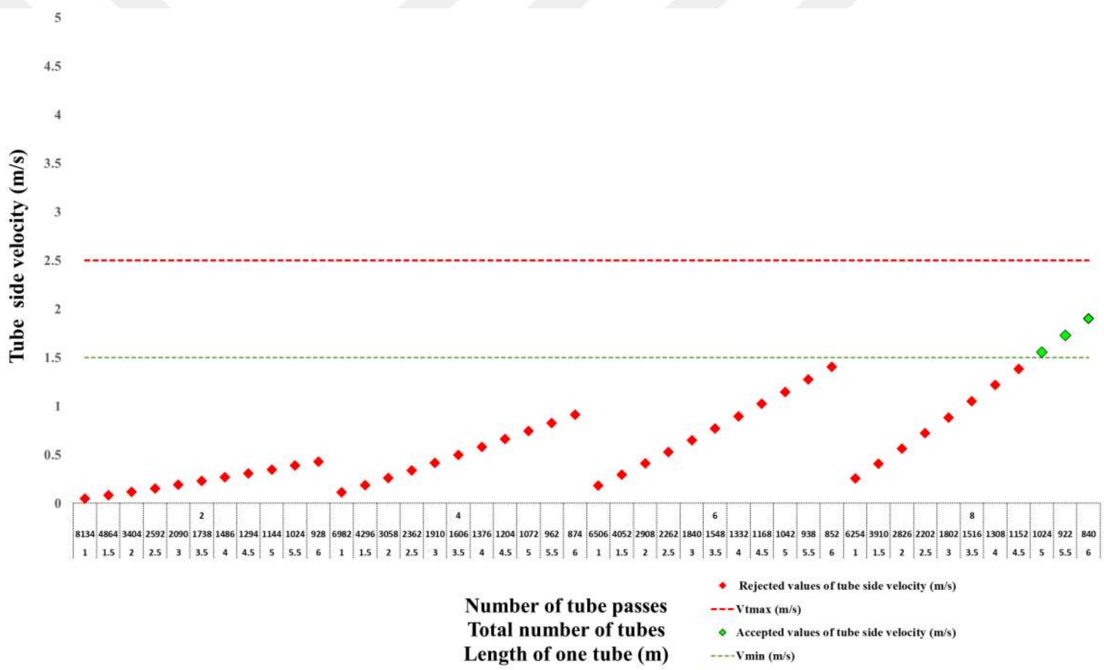

Figure 4.30. Condenser Tube side fluid velocity diagram with R236fa

In **Figure 4.30**, a detailed analysis of fluid velocity within the tubes for each condenser design is presented. This analysis considers the total number of tube passes, the total number of tubes, and their length. The figure sets an important limit for acceptable velocity range, with a lower limit of 1.5 m/s marked by a green dashed line and an upper limit of 2.5 m/s denoted by a red dashed line. This limitation aims to prevent potential damage to the condenser and maintain high performance. Fluid velocity higher than 2.5 m/s can cause erosion in the tubes, while a low fluid velocity of less than 1.5 m/s can lead to a low heat transfer coefficient and reduced performance, resulting in larger heating surface areas and consequently, higher investment costs. The empirical data presented in Figure 32 shows that only 3 designs out of 44 met the desired range of fluid velocity within the tubes and passed all the pervious limitations, represented by a green color. All other designs that failed to meet this crucial limitation are shown in red. This analysis highlights the complexity and difficulty of optimizing condenser designs, as only a select few designs were capable of achieving the necessary fluid velocity within the tubes while also satisfying other essential performance criteria. In summary, Figure 4.30 is a valuable tool for condenser design optimization, allowing engineers to visualize and analyze fluid velocity within the tubes for each design to ensure that the acceptable range is maintained. The empirical data presented in this figure will significantly contribute to the development of more efficient and effective condenser designs that meet the necessary performance criteria.

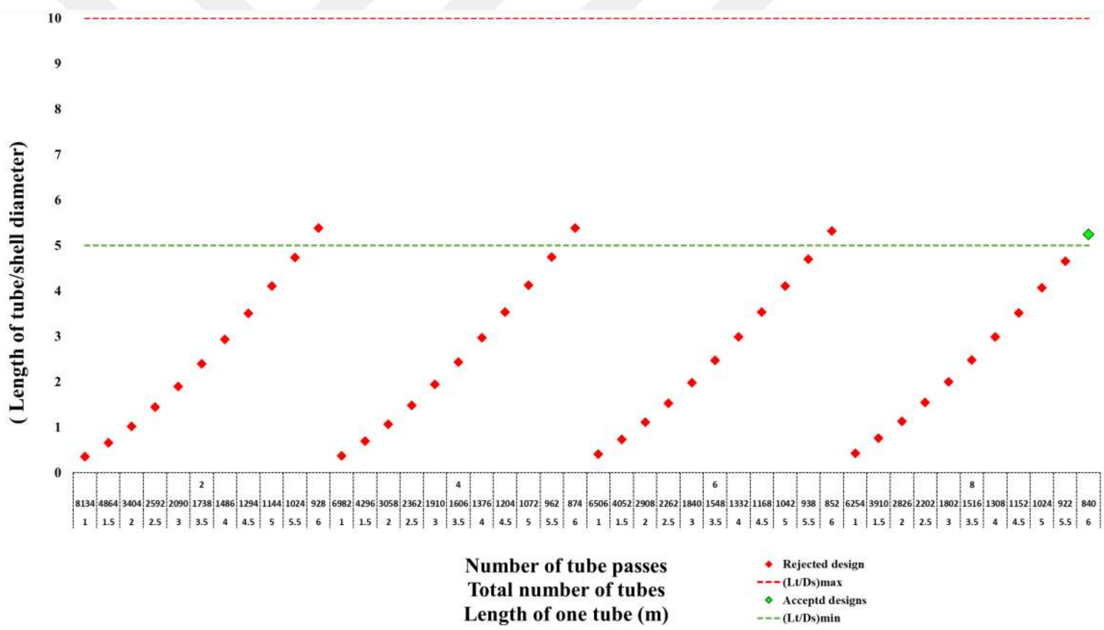

Figure 4.31. Condenser (Length of tube/ shell diameter) diagram with R236fa

Figure 4.31 provides a crucial metric, known as the design goodness ratio, for evaluating condenser designs. The figure is analyzed alongside three parameters: the number of tube passes, the total number of tubes, and tube length. It establishes an acceptable goodness ratio range with red and green dashed lines marking the upper and lower limits. Designs within this range are depicted in green, while those outside the range are shown in red. According to the empirical data presented in the figure, only 4 condenser designs were able to achieve the desired value within the acceptable range. However, only one of these designs were able to surpass all critical design limitations, earning it the coveted green color, while the others were shown in red.

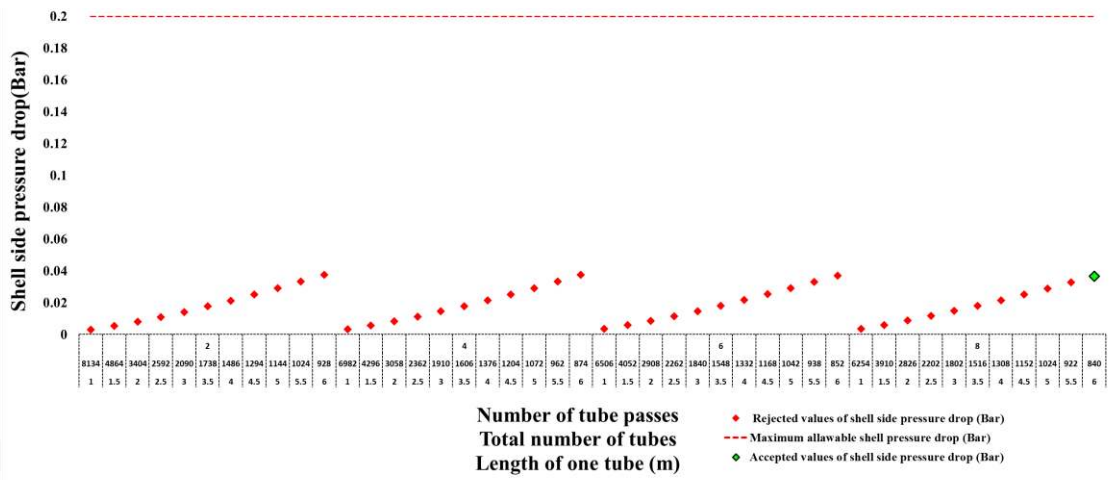

Figure 4.32. Shell side pressure drop through the condenser for R236fa

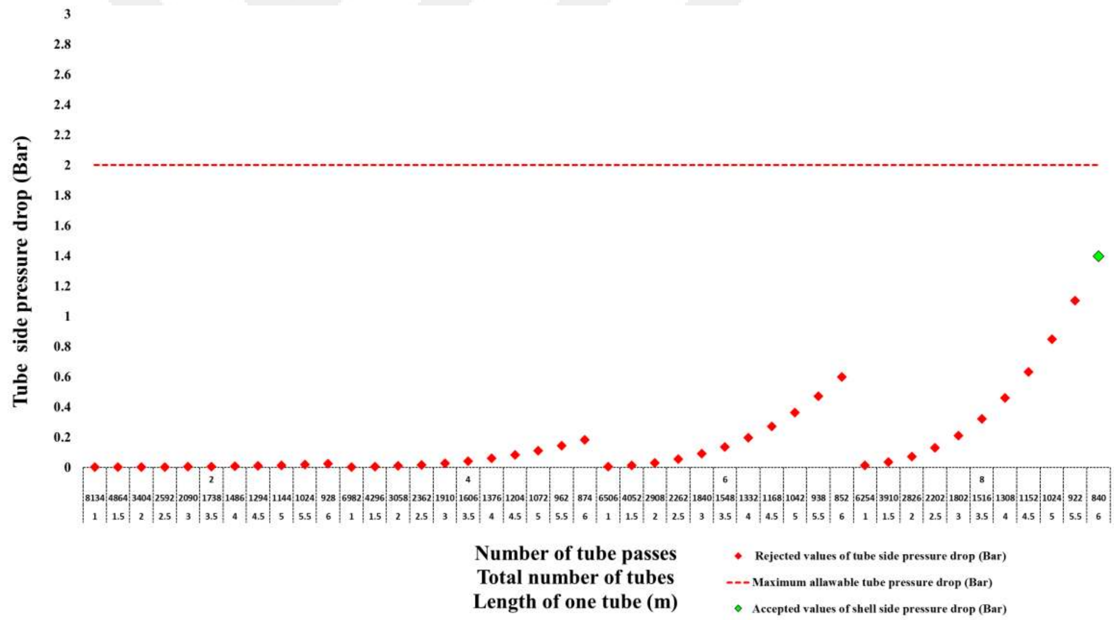

Figure 4.33. Tube side pressure drop through the condenser for R236fa

Figure 4.32 showcases a graph that depicts the pressure drop on the shell side of each condenser design with utmost clarity and precision. The graph takes into consideration the number of tube passes, the total number of tubes, and the tube length of each condenser design. A red dashed line is drawn in the graph that represents a crucial maximum limit which is 0.2 bar for the allowable shell side pressure drop. This line emphasizes the importance of complying with safe and optimal performance criteria to ensure efficient and secure operation. The graph portrays green symbols that indicate a small number of designs that have successfully surpassed all previous design limitations while keeping a shell side pressure drop of less than 0.2 bar. In contrast, the red symbols denote designs that failed to meet this critical limitation or couldn't pass one or more of the previous design tests. Among all the designs analyzed, only one have emerged as optimal condenser designs, distinguished by their green color to signify their exceptional performance and efficiency. These optimal designs have ingeniously maintained a balance among the critical factors of pressure drop, tube passes, total tubes, and tube length to achieve an optimal result that meets all performance criteria. This outstanding performance is both safe and cost-effective, making it a valuable asset to any system.

Figure 4.33, presents detailed information on the tube side pressure drop for each condenser design. This information is essential for evaluating the performance of each design, as it includes the number of tubes, tube length, and tube passes. The red dashed line on the chart shows the maximum tube side pressure drop that cannot be exceeded. The green symbols on the chart represent successful condenser designs that have met all performance criteria. These designs have optimized the tube passes, total number of tubes, and tube length to achieve an ideal tube side pressure drop below 2 bars. In contrast, the red symbols indicate designs that failed to meet the performance criteria or exceeded the 2 bar threshold. Out of the 44 designs evaluated, only one managed to pass all the tests and achieve the desired pressure drop levels, making them exceptional in terms of their performance and efficiency. Overall, the data presented in Figure 4.33 provides critical insights that can help in making informed decisions about condenser design and performance evaluation.

The cost of installing and operating a condenser is largely dependent on the size of its heating surface area. A larger surface area typically leads to a higher initial cost. In light of this, this study has been conducted to optimize the design of the condenser, with the aim of making it efficient while keeping the heating surface area as small as possible. The overarching objective of this optimization is to develop a condenser that satisfies performance requirements while simultaneously reducing manufacturing, installation, and operational costs. The chart 4.34 below shows the final results of the optimization procedure for the condenser. Out of all the designs that met the suggested limitations, the one with the lowest heating surface area was chosen as the best.

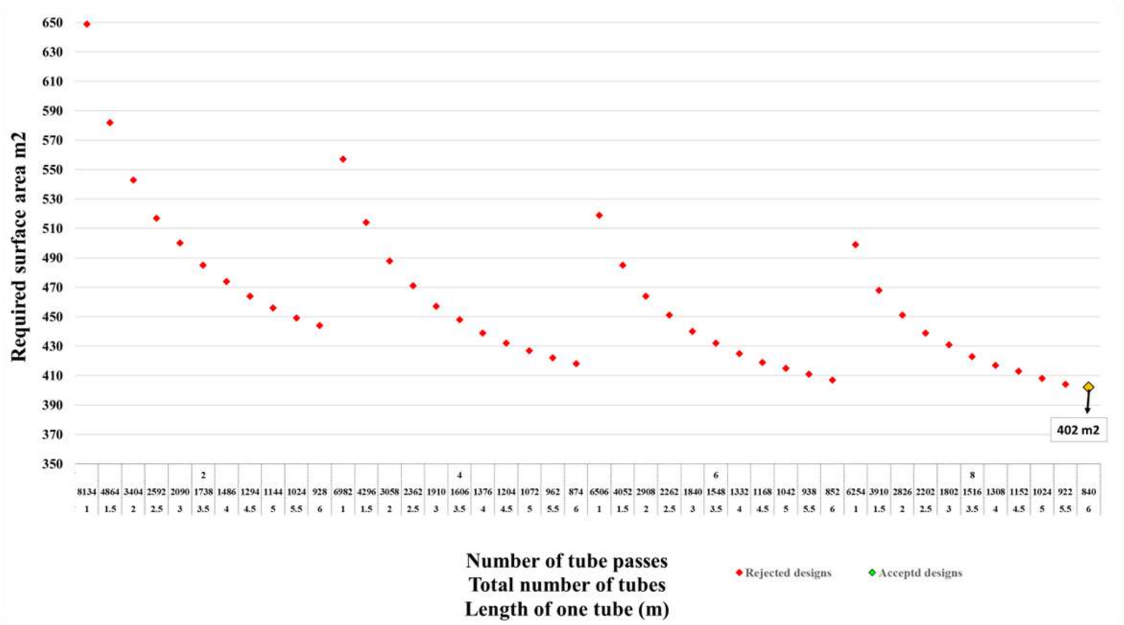

Figure 4.34. Condenser heating surface area m2 diagram for R236fa

A detailed comparison of different condenser designs that underwent the same performance tests is presented in Figure 4.34. The designs that passed the tests are marked in green, while those that failed are marked in red. The optimal design has a heating surface area of 402 m2, which is the smallest among all the designs. It includes 8 tube passes, a total of 840 tubes, and a tube length of 6 meters. This design offers a balanced solution between effectiveness, efficiency, and cost, providing outstanding and cost-effective performance.

Table 4.8. Condenser design results for R236fa

NO	Length	N_{tube}	$N_{tube,passes}$	Error	ΔP_t	ΔP_s	$\dot{Q}_{est}$	Design Test Result
	m	#	#	%	bar	bar	kW	accepted/not accepted
1	1	8134	2	0.023549	0.00300529	0.00013888	4441.27065	not accepted
2	1.5	4864	2	0.19856661	0.00533663	0.00044352	4448.83523	not accepted
⋮	⋮	⋮	⋮	⋮	⋮	⋮	⋮	⋮
42	5	1024	8	0.10200874	0.02886609	0.84634976	4440.15742	not accepted
43	5.5	922	8	0.05503533	0.03269895	1.10122754	4440.02432	not accepted
44	**6**	**840**	**8**	**0.07946653**	**0.03661361**	**1.39533852**	**4449.28745**	**accepted***

*Minimal condenser area, ideal choice-lowest cost

** All the condenser design calculations are carried out assuming P2=22bar

4.1.4.5 Condenser optimization procedure for R142b

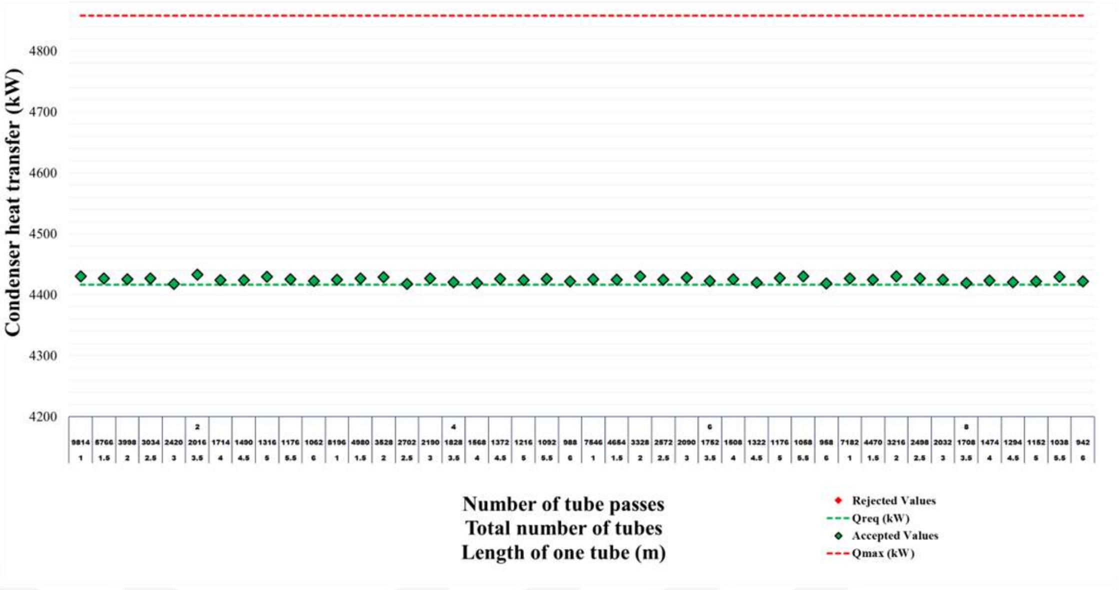

Figure 4.35. Rate of heat transfer through condenser (kW)diagram for R142b

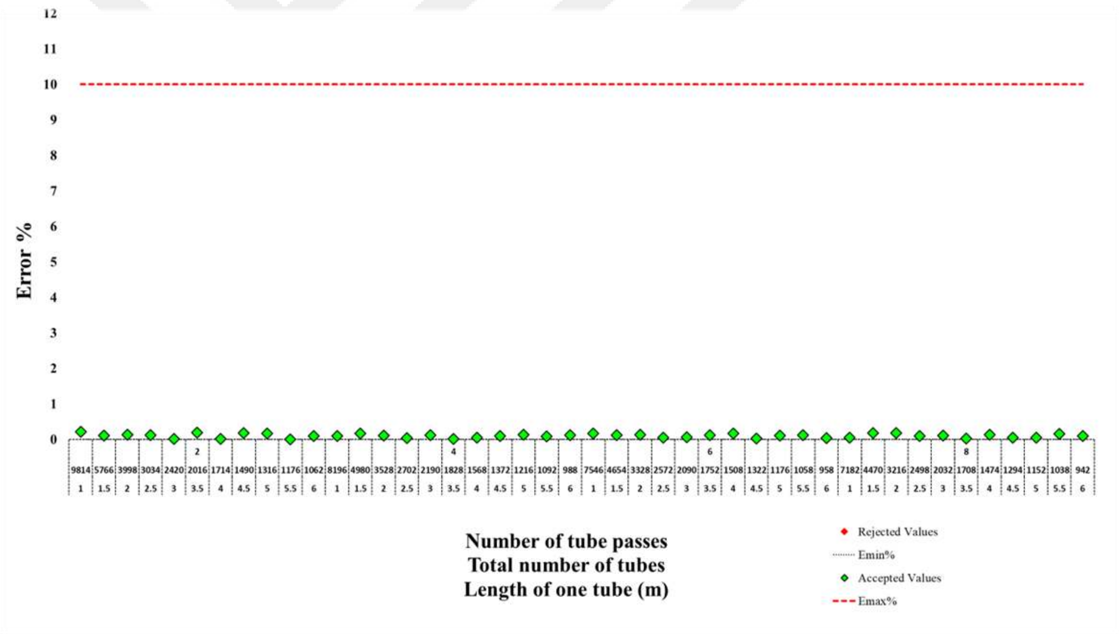

Figure 4.36. Condenser design error % diagram for R142b

Figure 4.35 depicts the evaluated condenser designs in terms of the total number of tubes, the number of tube passes, and tube length, with the Condenser heat transfer (kW) on the vertical axis. It is noteworthy that all the data points lie within the acceptable range, as indicated by the green shaded region between the minimum and maximum acceptable cooling duty values. The minimum required condenser cooling duty (kW), which was previously calculated in the Table 3.2, is represented by the green dashed line at 4416.4 kW. Similarly, the red dashed line represents the maximum acceptable cooling duty, which is approximately 10% higher than the required value, at 4858.04 kW. The location of all the data points in the green region suggests that each design meets the cooling duty requirements and falls within the acceptable range. Therefore, the presented condenser designs are deemed suitable for the ORC system, with the added advantage of being cost-effective and efficient.

In Figure 4.36, the design error for all attempted condenser designs is shown. This limitation ensures that the final designs are neither overdesigned nor underdesigned. The suggested maximum design error is 10%, indicated by a red dashed line in the figure. It is noteworthy that all the points are located below this upper limit and are highlighted with a green symbol, indicating that all 44 suggested designs fall within the accepted range.

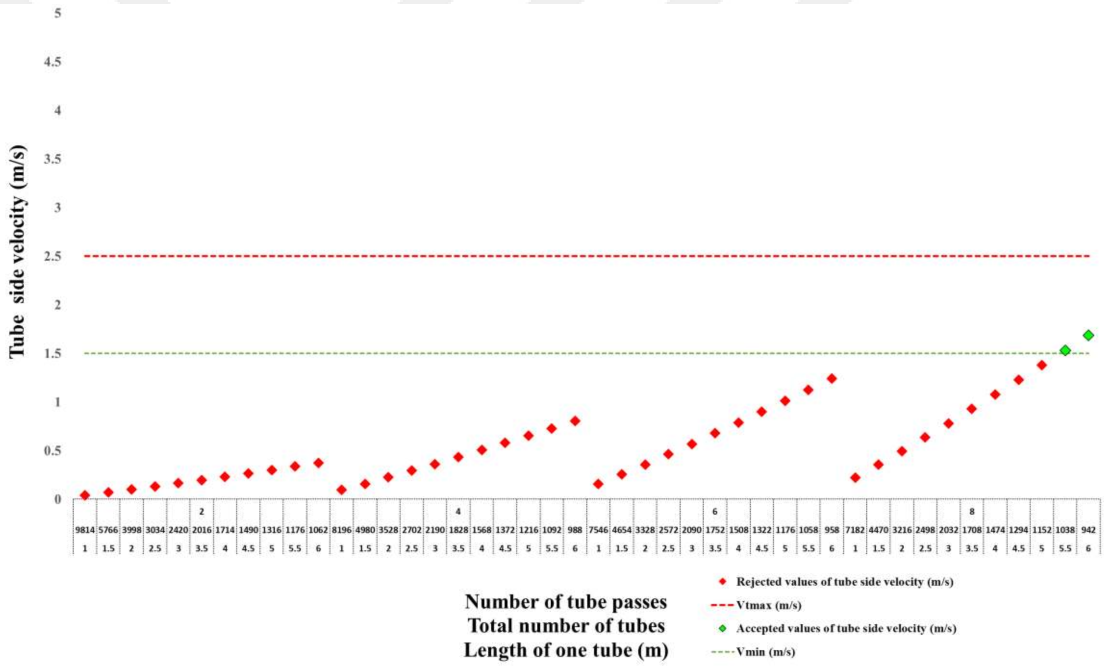

Figure 4.37. Condenser Tube side fluid velocity diagram for R142b

In **Figure 4.37**, a detailed analysis of fluid velocity within the tubes for each condenser design is presented. This analysis considers the total number of tube passes, the total number of tubes, and their length. The figure sets an important limit for acceptable velocity range, with a lower limit of 1.5 m/s marked by a green dashed line and an upper limit of 2.5 m/s denoted by a red dashed line. This limitation aims to prevent potential damage to the condenser and maintain high performance. Fluid velocity higher than 2.5 m/s can cause erosion in the tubes, while a low fluid velocity of less than 1.5 m/s can lead to a low heat transfer coefficient and reduced performance, resulting in larger heating surface areas and consequently, higher investment costs. The empirical data presented in Figure 25 shows that only 2 designs out of 44 met the desired range of fluid velocity within the tubes, represented by a green color. All other designs that failed to meet this crucial limitation are shown in red. This analysis highlights the complexity and difficulty of optimizing condenser designs, as only a select few designs were capable of achieving the necessary fluid velocity within the tubes while also satisfying other essential performance criteria. In summary, Figure 4.37 is a valuable tool for condenser design optimization, allowing engineers to visualize and analyze fluid velocity within the tubes for each design to ensure that the acceptable range is maintained. The empirical data presented in this figure will significantly contribute to the development of more efficient and effective condenser designs that meet the necessary performance criteria.

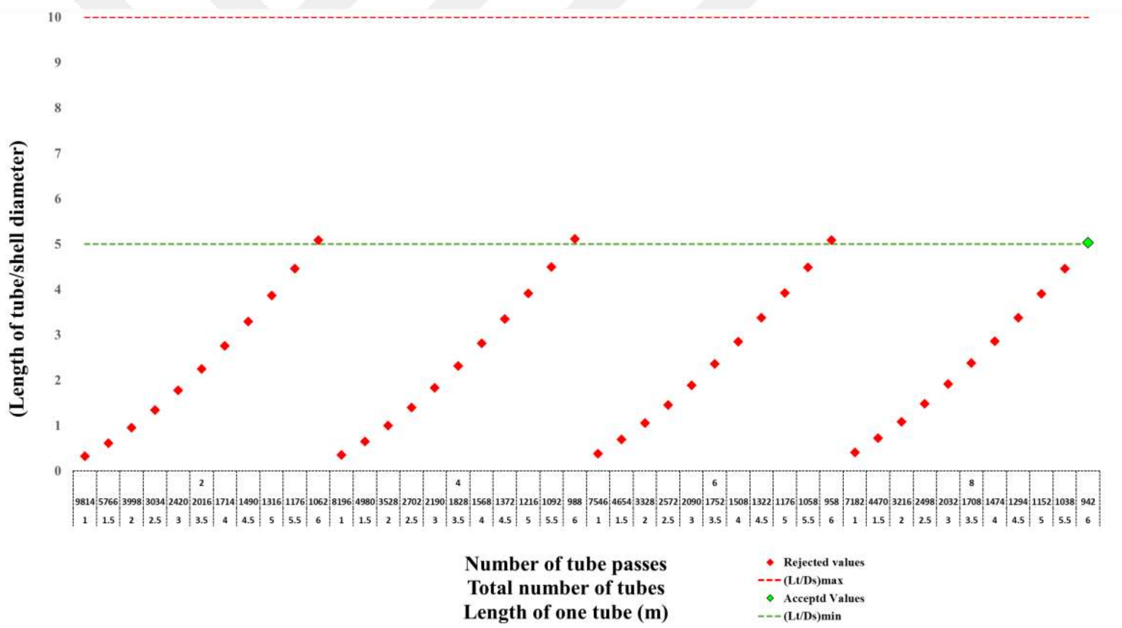

Figure 4.38. Condenser (Length of tube/ shell diameter) diagram for R142b

Figure 4.38. provides a crucial metric, known as the design goodness ratio, for evaluating condenser designs. The figure is analyzed alongside three parameters: the number of tube passes, the total number of tubes, and tube length. It establishes an acceptable goodness ratio range with red and green dashed lines marking the upper and lower limits. Designs within this range are depicted in green, while those outside the range are shown in red. According to the empirical data presented in the figure, only 4 condenser designs were able to achieve the desired value within the acceptable

range. However, only one of these designs were able to surpass all critical design limitations, earning it the coveted green color, while the others were shown in red.

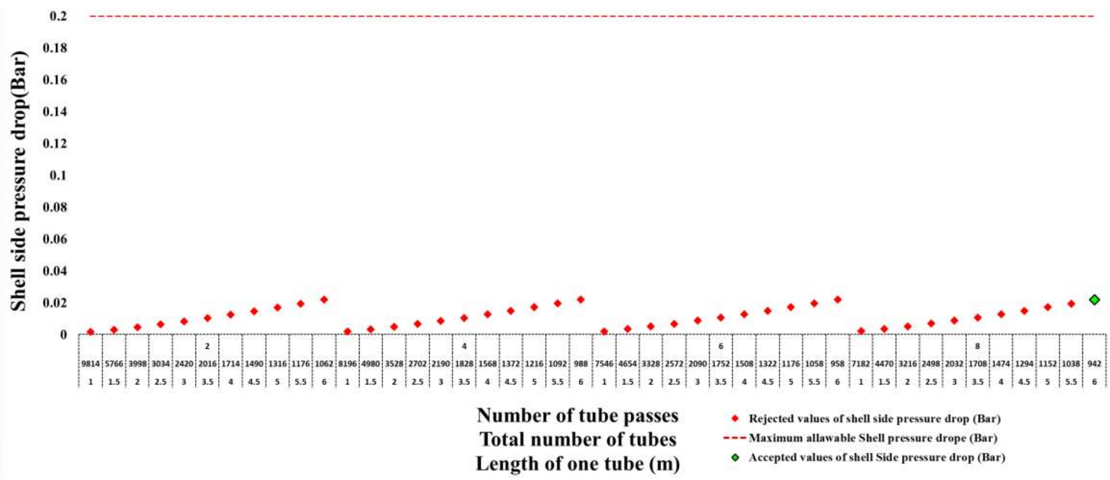

Figure 4.39. Shell side pressure drop through the condenser for R142b

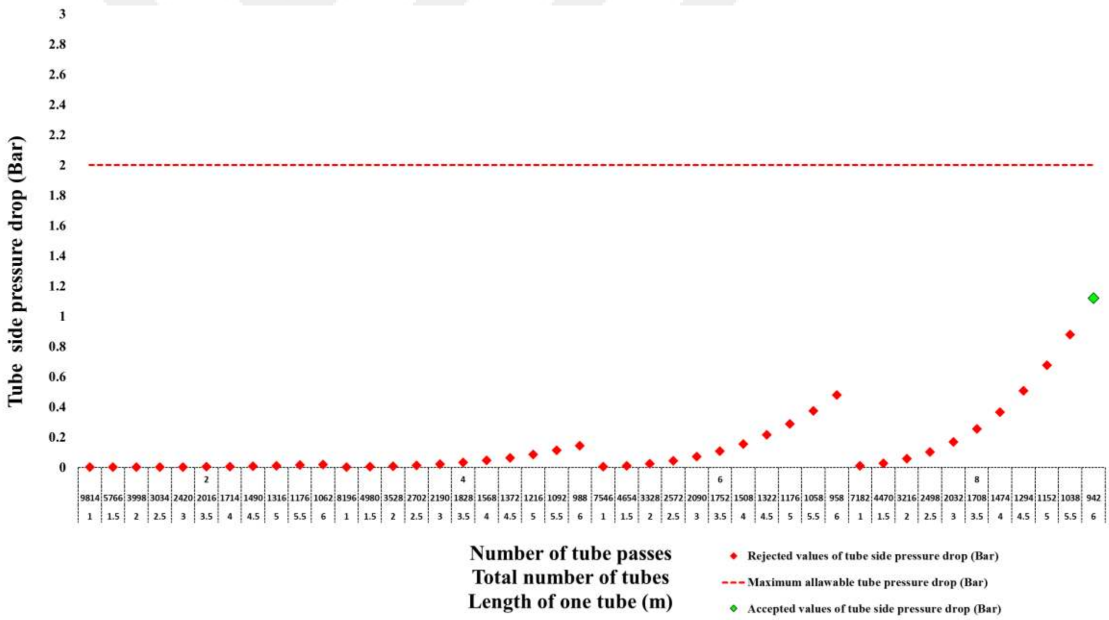

Figure 4.40. Tube side pressure drop through the condenser for R142b

Figure 4.39. showcases a graph that depicts the pressure drop on the shell side of each condenser design with utmost clarity and precision. The graph takes into consideration the number of tube passes, the total number of tubes, and the tube length of each condenser design. A red dashed line is drawn in the graph that represents a crucial maximum limit which is 0.2 bar for the allowable shell side pressure drop. This line emphasizes the importance of complying with safe and optimal performance criteria to ensure efficient and secure operation. The graph portrays green symbols that

indicate a small number of designs that have successfully surpassed all previous design limitations while keeping a shell side pressure drop of less than 0.2 bar. In contrast, the red symbols denote designs that failed to meet this critical limitation or couldn't pass one or more of the previous design tests. Among all the designs analyzed, only one has emerged as an optimal condenser design, distinguished by its green color to signify their exceptional performance and efficiency. This optimal design has maintained a balance among the critical factors of pressure drop, tube passes, total tubes, and tube length to achieve an optimal result that meets all performance criteria. This outstanding performance is both safe and cost-effective, making it a valuable asset to any system.

Figure 4.40., presents detailed information on the tube side pressure drop for each condenser design. This information is essential for evaluating the performance of each design, as it includes the number of tubes, tube length, and tube passes. The red dashed line on the chart shows the maximum tube side pressure drop that cannot be exceeded. The green symbols on the chart represent successful condenser designs that have met all performance criteria. These designs have optimized the tube passes, total number of tubes, and tube length to achieve an ideal tube side pressure drop below 2 bars. In contrast, the red symbols indicate designs that failed to meet the performance criteria or exceeded the 2 bar threshold. Out of the 44 designs evaluated, only one managed to pass all the tests and achieve the desired pressure drop levels, making it exceptional in terms of its performance and efficiency.

The cost of installing and operating a condenser is largely dependent on the size of its heating surface area. A larger surface area typically leads to a higher initial cost. In light of this, this study has been conducted to optimize the design of the condenser, with the aim of making it efficient while keeping the heating surface area as small as possible. The overarching objective of this optimization is to develop a condenser that satisfies performance requirements while simultaneously reducing manufacturing, installation, and operational costs. The chart 43 below shows the final results of the optimization procedure for the condenser. Out of all the designs only one design met the suggested limitations, and was chosen as the best.

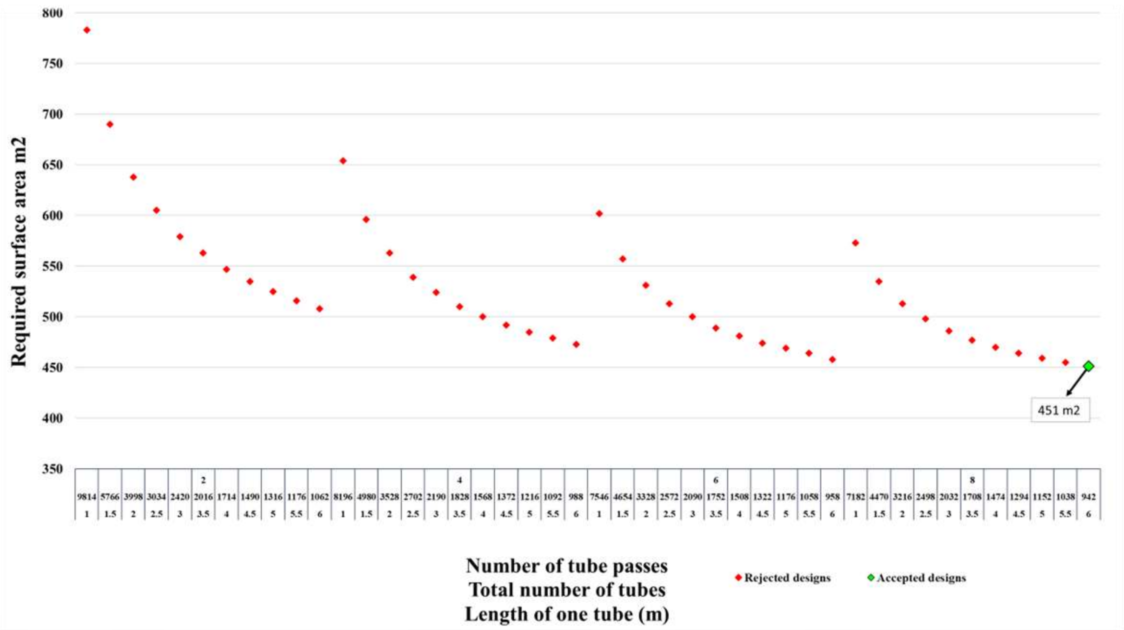

Figure 4.41. Condenser heating surface area m2 diagram for R142b

A detailed comparison of different condenser designs that underwent the same performance tests is presented in Figure 4.41. The design that passed the tests is marked in green, while those that failed are marked in red. The optimal design has a heating surface area of 451 m2, which is the smallest among all the designs. It includes 8 tube passes, a total of 942 tubes, and a tube length of 6 meters. This design offers a balanced solution between effectiveness, efficiency, and cost, providing outstanding and cost-effective performance.

Table 4.9. Condenser design results for R142b

NO	Length	N_{tube}	$N_{tube,passes}$	Error	ΔP_t	ΔP_s	$\dot{Q}_{est}$	Design Test Result
	m	#	#	%	bar	bar	kW	accepted/not accepted
1	1	9814	2	0.218142	0.001725	0.00010	4430.206	not accepted
2	1.5	5766	2	0.109894	0.003084	0.000324	4426.796	not accepted
⋮	⋮	⋮	⋮	⋮	⋮	⋮	⋮	⋮
43	5.5	1038	8	0.158637	0.01941	0.876751	4429.486	not accepted
44	6	942	8	0.094179	0.02176	1.118917	4422.16	accepted*

*Minimal condenser area, ideal choice-lowest cost

** All the condenser design calculations are carried out assuming P2=22bar

4.1.4.6 Condenser optimization procedure for R600a

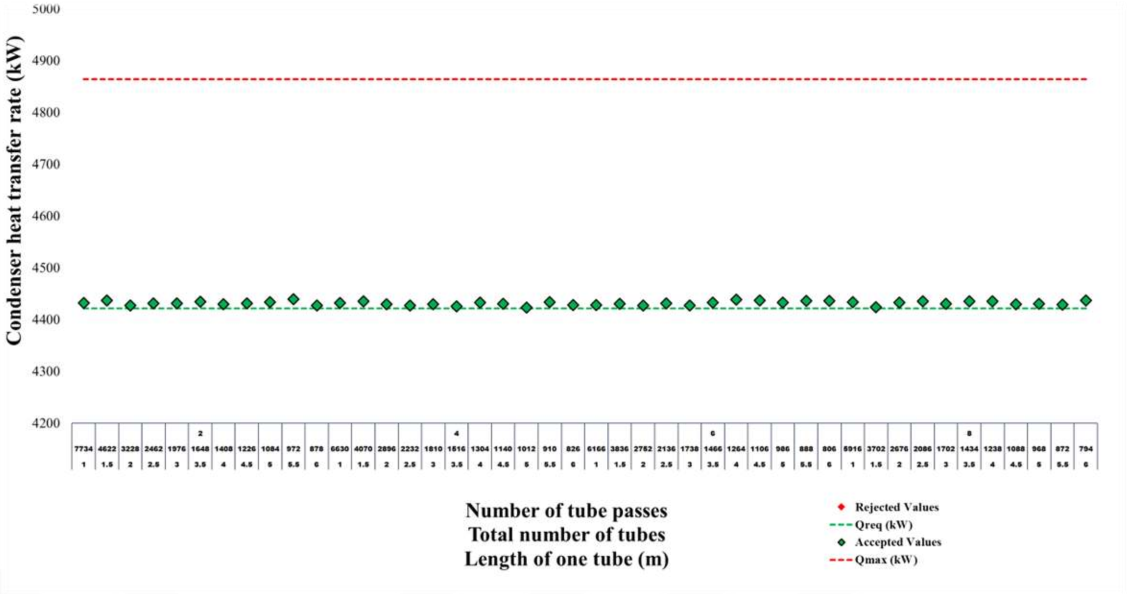

Figure 4.42. Rate of heat transfer through condenser (kW)diagram for R600a

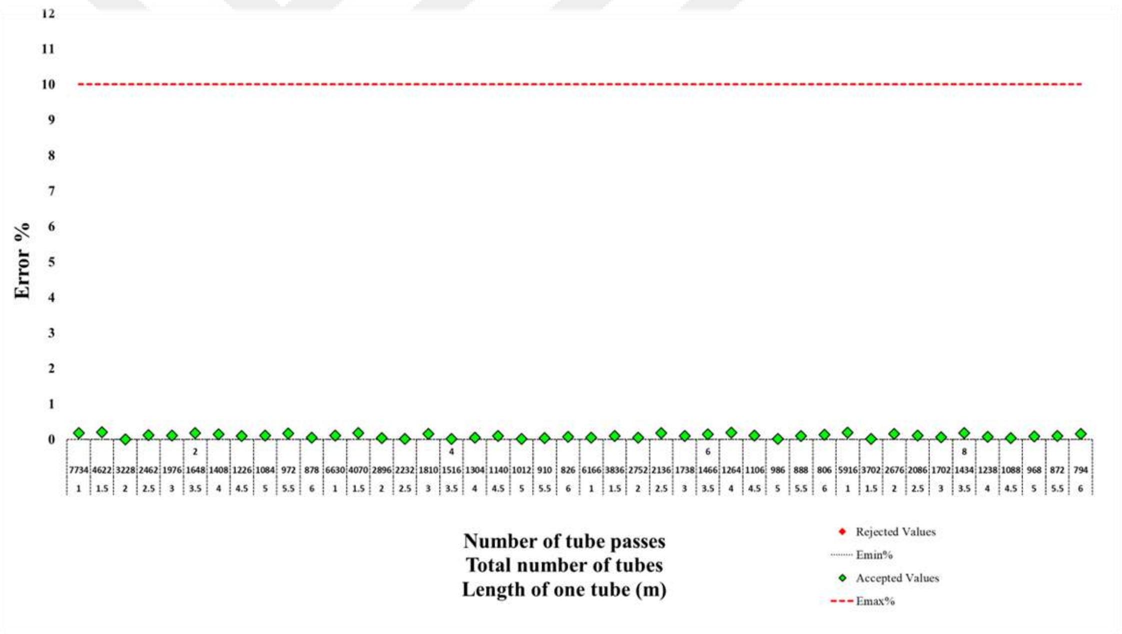

Figure 4.43. Condenser design error % diagram for R600a

Based on the number of tubes, tube passes, tube length on horizontal axis, and condenser heat transfer (kW) on the vertical axis, Figure 4.42. shows the evaluated condenser designs. All data points fall within the acceptable range, which is indicated by the green shaded area between the minimum and maximum acceptable cooling duty values. The minimum required condenser cooling duty, previously calculated in Table 3.2, is represented by the green dashed line at 4421.3 kW. The maximum acceptable cooling duty, which is around 10% higher than the required value, is represented by the red dashed line at 4863.43 kW. All data points within the green region show that each design meets the cooling duty requirements and falls within the acceptable range. Therefore, the presented condenser designs are suitable for the ORC system, and they are both cost-effective and efficient.

Figure 4.43. displays the design error for all attempted condenser designs. The suggested maximum design error of 10% is indicated by the red dashed line. All 44 suggested designs fall within the accepted range, which is highlighted with a green symbol, indicating that each design is suitable for the ORC system and avoids overdesigning or underdesigning.

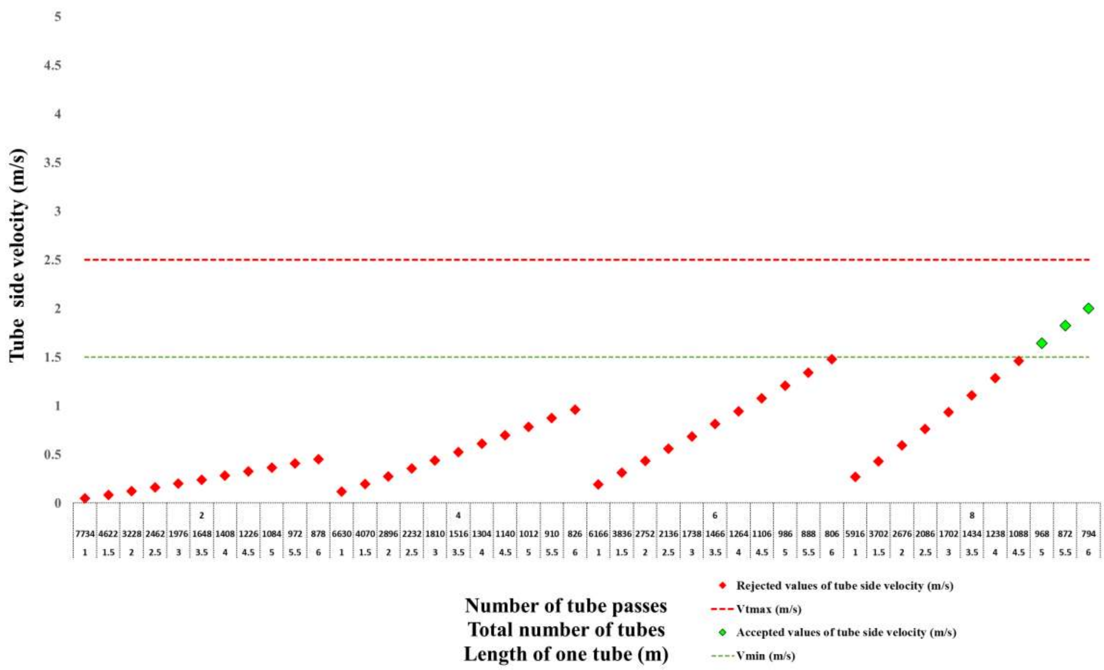

Figure 4.44. Condenser Tube side fluid velocity diagram for R600a

Figure 4.44. provides a detailed analysis of fluid velocity within the tubes for each condenser design. The green dashed line marks the lower limit of 1.5 m/s, and the upper limit of 2.5 m/s is denoted by the red dashed line. Fluid velocity outside of this range can cause damage to the condenser and reduce performance. Only three out of 44 designs met the desired fluid velocity range, while the rest failed to meet the criteria. Figure 4.44. is a valuable tool for condenser design optimization, allowing engineers to ensure that the acceptable range of fluid velocity is maintained.

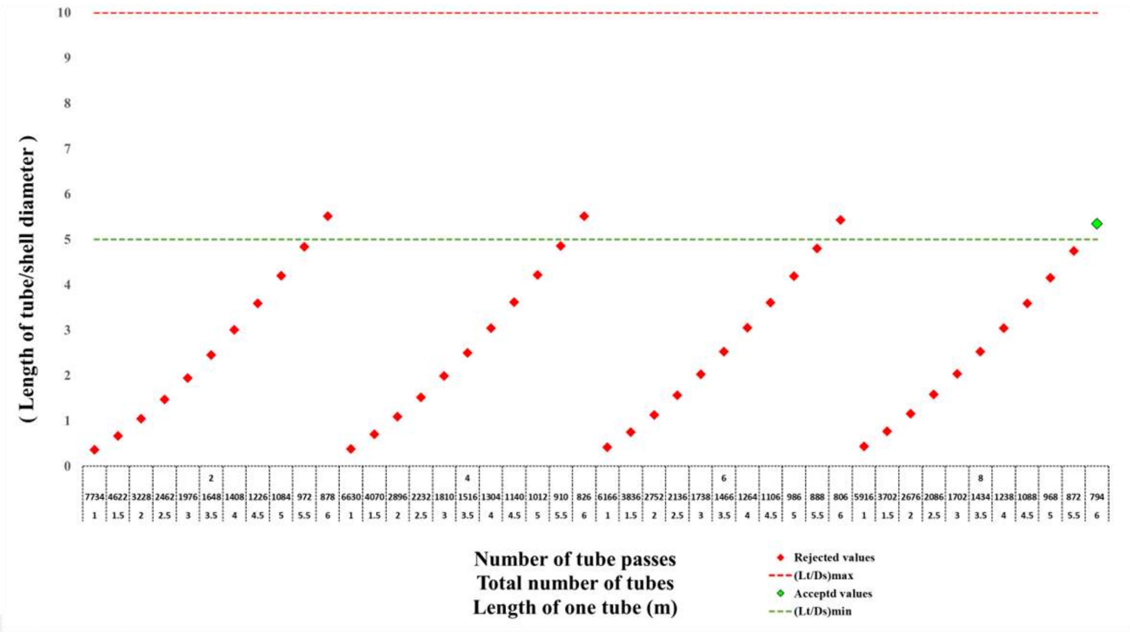

Figure 4.45. Condenser (Length of tube/ shell diameter) diagram for R600a

Figure 4.45. provides a crucial metric, known as the design goodness ratio, for evaluating condenser designs. The figure is analyzed alongside three parameters: the number of tube passes, the total number of tubes, and tube length. It establishes an acceptable goodness ratio range with red and green dashed lines marking the upper and lower limits. Designs within this range are depicted in green, while those outside the range are shown in red. According to the empirical data presented in the figure, only 4 condenser designs were able to achieve the desired value within the acceptable range. However, only one of these designs were able to surpass all critical design limitations, earning it the coveted green color, while the others were shown in red.

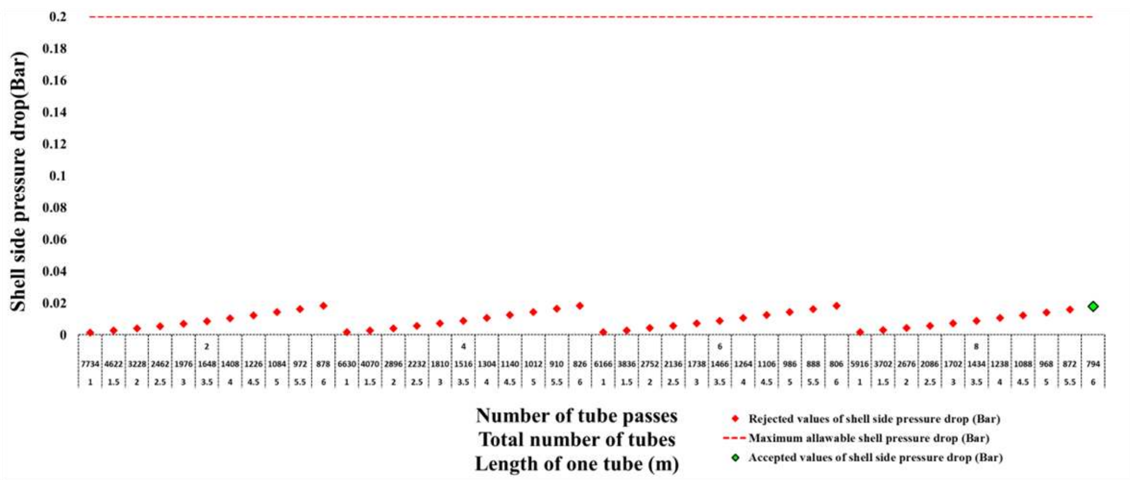

Figure 4.46. Shell side pressure drop through the condenser for R600a

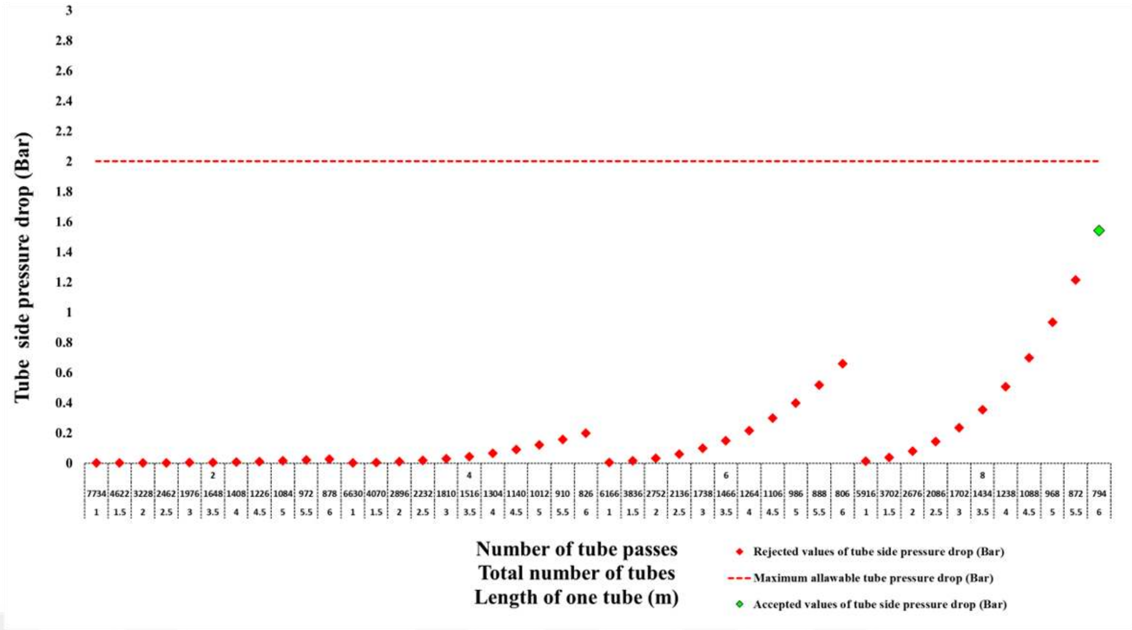

Figure 4.47. Tube side pressure drop through the condenser for R600a

Figure 4.46. showcases a graph that depicts the pressure drop on the shell side of each condenser design with utmost clarity and precision. The graph takes into consideration the number of tube passes, the total number of tubes, and the tube length of each condenser design. A red dashed line is drawn in the graph that represents a crucial maximum limit which is 0.2 bar for the allowable shell side pressure drop. This line emphasizes the importance of complying with safe and optimal performance criteria to ensure efficient and secure operation. The graph portrays green symbols that indicate a small number of designs that have successfully surpassed all previous design limitations while keeping a shell side pressure drop of less than 0.2 bar. In contrast, the red symbols denote designs that failed to meet this critical limitation or couldn't pass one or more of the previous design tests. Among all the designs analyzed, only one has emerged as an optimal condenser design, distinguished by its green color to signify their exceptional performance and efficiency. This optimal design has maintained a balance among the critical factors of pressure drop, tube passes, total tubes, and tube length to achieve an optimal result that meets all performance criteria. This outstanding performance is both safe and cost-effective, making it a valuable asset to any system.

Figure 4.47., presents detailed information on the tube side pressure drop for each condenser design. This information is essential for evaluating the performance of each

design, as it includes the number of tubes, tube length, and tube passes. The red dashed line on the chart shows the maximum tube side pressure drop that cannot be exceeded. The green symbols on the chart represent successful condenser designs that have met all performance criteria. These designs have optimized the tube passes, total number of tubes, and tube length to achieve an ideal tube side pressure drop below 2 bars. In contrast, the red symbols indicate designs that failed to meet the performance criteria or exceeded the 2 bar threshold. Out of the 44 designs evaluated, only one managed to pass all the tests and achieve the desired pressure drop levels, making it exceptional in terms of its performance and efficiency.

The cost of installing and operating a condenser is largely dependent on the size of its heating surface area. A larger surface area typically leads to a higher initial cost. In light of this, this study has been conducted to optimize the design of the condenser, with the aim of making it efficient while keeping the heating surface area as small as possible. The overarching objective of this optimization is to develop a condenser that satisfies performance requirements while simultaneously reducing manufacturing, installation, and operational costs. The chart 50 below shows the final results of the optimization procedure for the condenser. Out of all the designs only one design met the suggested limitations, and was chosen as the best.

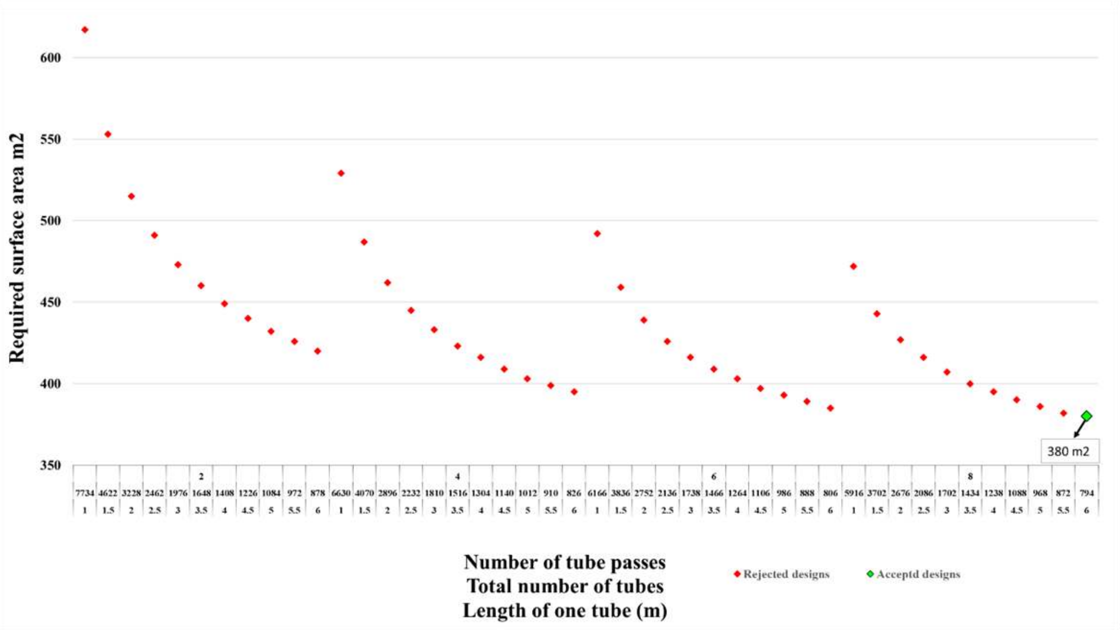

Figure 4.48. Condenser heating surface area m2 diagram for R600a

A detailed comparison of different condenser designs that underwent the same performance tests is presented in Figure 4.48. The design that passed the tests is marked in green, while those that failed are marked in red. The optimal design has a heating surface area of 380 m2, which is the smallest among all the designs. It includes 8 tube passes, a total of 794 tubes, and a tube length of 6 meters. This design offers a balanced solution between effectiveness, efficiency, and cost, providing outstanding and cost-effective performance.

Table 4.10. Condenser design results for R600a

NO	Length	N_{tube}	$N_{tube,passes}$	Error	ΔP_t	ΔP_s	$\dot{Q}_{est}$	Design Test Result
	m	#	#	%	bar	bar	kW	accepted/not accepted
1	1	7734	2	0.179771968	0.001475338	0.000151301	4431.783812	not accepted
2	1.5	4622	2	0.196410819	0.002620131	0.000483544	4436.407243	not accepted
19	4.5	1140	4	0.099979178	0.012398583	0.089132383	4430.386095	not accepted
⋮	⋮	⋮	⋮	⋮	⋮	⋮	⋮	⋮
41	4.5	1088	8	0.038982785	0.01232025	0.698412556	4429.760222	not accepted
42	5	968	8	0.079838215	0.014143403	0.934200875	4430.198903	not accepted
43	5.5	872	8	0.095681161	0.016018631	1.214468224	4428.615836	not accepted
44	**6**	**794**	**8**	**0.14895389**	**0.01793873**	**1.54047308**	**4436.72491**	**accepted***

*Minimal condenser area, ideal choice-lowest cost

** All the condenser design calculations are carried out assuming P2=22bar

4.1.4.7 Condenser optimization procedure results discussion

R600:

The graphical representations showcases the analysis of various condenser designs based on three key parameters, namely the number of tube passes, the total number of tubes, and the length of tubes that are poltted on horizontal axis. The corresponding condenser heat transfer (kW), design error%, tube side velocity, (length of tubes/shell diameter) ratio, shell side pressure drop, tube side pressure drop, and heating surface area that are plotted on the vertical axis. The study evaluated a total of 44 different condenser designs. On x axis the length of tubes was gradually incremented by 50cm for each number of tube passes until it reached 600cm, after which the number of tube passes was increased by 2, and the process was repeated until it reached 8. The green dashed line indicates the minimum accepted value, while the red dashed line represents the maximum accepted value. The green and red symbols represent the attempted designs that passed or failed the design limitations, respectively. The study revealed that only three condenser designs successfully passed all the design limitations, indicating them as good condenser design recommendations. These optimal designs correspond to the number of tube passes 6, 6, and 8, the number of tubes 734, 668, and 724, and the length of tubes 5.5, 6, and 5.5 m, respectively, with corresponding heating surface areas of 322, 319, and 317 m2, respectively. The design with the minimum surface area 317 m2 was deemed as the optimal design among the 44 evaluated designs. These findings can provide valuable insights for further research in the field of condenser design.

<u>R123:</u>

The graphical representations showcases the analysis of various condenser designs based on three key parameters, namely the number of tube passes, the total number of tubes, and the length of tubes that are poltted on horizontal axis. The corresponding condenser heat transfer (kW), design error%, tube side velocity, (length of tubes/shell diameter) ratio, shell side pressure drop, tube side pressure drop, and heating surface area are plotted on the vertical axis. The study evaluated a total of 44 distinct condenser designs. On x -axis the length of tubes was gradually incremented by 50cm for each number of tube passes until it reached 600cm, after which the number of tube passes was increased by 2, and the process was repeated until it reached 8. The green dashed line indicates the minimum accepted value, while the red dashed line represents the maximum accepted value. The green and red symbols represent the attempted designs that passed or failed the design limitations, respectively. The study revealed that only four condenser designs successfully passed all the design limitations, indicating them as good condenser design recommendations. These optimal designs correspond to the number of tube passes 4, 6, 6 and 6 the number of tubes 494, 592, 536, and 488 and the length of tubes 6, 5, 5.5 and 6 m, respectively, with corresponding heating surface areas of 236, 236, 235 and 233 m2, respectively. The design with the minimum surface area was 233 m2 deemed as the optimal design among the 44 evaluated designs. These findings can provide valuable insights for further research in the field of condenser design.

<u>R236:</u>

The graphical representations showcases the analysis of various condenser designs based on three key parameters, namely the number of tube passes, the total number of tubes, and the length of tubes that are poltted. The corresponding condenser heat transfer (kW), design error%, tube side velocity, (length of tubes/shell diameter) ratio, shell side pressure drop, tube side pressure drop, and heating surface area are plotted on the vertical axis. The study evaluated a total of 44 distinct condenser designs. The length of tubes was gradually incremented by 50cm for each number of tube passes until it reached 600cm, after which the number of tube passes was increased by 2, and the process was repeated until it reached 8. The green dashed line indicates the minimum accepted value, while the red dashed line represents the maximum accepted value. The green and red symbols represent the attempted designs that passed or failed the design limitations, respectively. The study revealed that only a single condenser designs successfully passed all the design limitations, indicating it as an optimal design among other 44 designs. These optimal design correspond to the number of tube passes 8,total number of tubes 840 and the length of tubes 6 m, respectively, with corresponding heating surface areas of 402 m2, respectively.

<u>R142b:</u>

The graphical representations showcases the analysis of various condenser designs based on three key parameters, namely the number of tube passes, the total number of tubes, and the length of tubes that are poltted on horizontal axis. The corresponding condenser heat transfer (kW), design error%, tube side velocity, (length of tubes/shell diameter) ratio, shell side pressure drop, tube side pressure drop, and heating surface area are plotted on the vertical axis. The study evaluated a total of 44 distinct condenser designs, each characterized by three variables, namely the number of tube passes, the total number of tubes, and the length of tubes, along with the associated heating duty (kW), design error%, tube side velocity, (length of tubes/shell diameter) ratio, shell side pressure drop, tube side pressure drop, and heating surface area. The length of tubes was gradually incremented by 50cm for each number of tube passes until it reached 600cm, after which the number of tube passes was increased by 2, and the process was repeated until it reached 8. The green dashed line indicates the minimum accepted value, while the red dashed line represents the maximum accepted value. The green and red symbols represent the attempted designs that passed or failed the design limitations, respectively. The study revealed that only a single condenser designs successfully passed all the design limitations, indicating it as an optimal design among other 44 designs. These optimal design correspond to the number of tube passes 8, total number of tubes 942 and the length of tubes 6 m, respectively, with corresponding heating surface areas of 451 m2, respectively.

R600a:

The graphical representations showcases the analysis of various condenser designs based on three key parameters, namely the number of tube passes, the total number of tubes, and the length of tubes that are poltted on the horizontal axis. The corresponding condenser heat transfer (kW), design error%, tube side velocity, (length of tubes/shell diameter) ratio, shell side pressure drop, tube side pressure drop, and heating surface area are plotted on the vertical axis. The study evaluated a total of 44 distinct condenser designs, each characterized by three variables, namely the number of tube passes, the total number of tubes, and the length of tubes, along with the associated heating duty (kW), design error%, tube side velocity, (length of tubes/shell diameter) ratio, shell side pressure drop, tube side pressure drop, and heating surface area. The length of tubes was gradually incremented by 50cm for each number of tube passes until it reached 600cm, after which the number of tube passes was increased by 2, and the process was repeated until it reached 8. The green dashed line indicates the minimum accepted value, while the red dashed line represents the maximum accepted value. The green and red symbols represent the attempted designs that passed or failed the design limitations, respectively. The study revealed that only a single condenser designs successfully passed all the design limitations, indicating it as an optimal design among other 44 designs. These optimal design correspond to the number of tube passes 8, total number of tubes 794 and the length of tubes 6 m, respectively, with corresponding heating surface areas of 380 m2, respectively.

CHAPTER 5
PREHEATER, EVAPORATOR, AND SUPERHEATER

Finned tube heat exchangers are a type of heat transfer equipment that have gained immense popularity in the industrial and commercial sectors owing to their unparalleled heat transfer efficiency. These heat exchangers are comprised of a series of tubes that are enveloped by fins, which are essentially thin metallic strips that are meticulously attached to the tubes to increase their surface area. By augmenting the surface area, these fins facilitate superior heat dissipation, thus enabling the heat exchanger to transfer heat more effectively and expeditiously.

In our study, we have extensively utilized finned tube heat exchangers for each of the preheater, superheater, and evaporator components. This strategic selection can be attributed to the low heat transfer coefficient of industrial air that is introduced on the shell side. Consequently, finned tube heat exchangers have proved to be a robust and reliable solution, which can effectively and efficiently transfer heat from one fluid to another, thus meeting the complex requirements of our project. One of the most significant advantages of finned tube heat exchangers is their remarkably high heat transfer coefficient, which greatly surpasses that of other types of heat exchangers. This unique feature enables them to transfer heat much more efficiently, making them a preferred choice in various applications where swift and proficient heat transfer is of paramount importance. Furthermore, these heat exchangers are relatively easy to maintain and repair, thanks to their simplistic design with few moving parts, coupled with the use of durable and robust materials. Additionally, finned tube heat exchangers can be customized to be compact and lightweight, making them suitable for a diverse range of industrial and commercial applications. In summary, finned tube heat exchangers are an immensely reliable and efficient solution for transferring heat from one fluid to another. Their widespread usage in diverse industries and applications is a testament to their superior performance and reliability. In our study, their selection for preheater, superheater, and evaporator components highlights their indispensability and efficiency in tackling the low heat transfer coefficient of industrial air.

5.1 Design methodology (preheater, Evaporator and superheater)

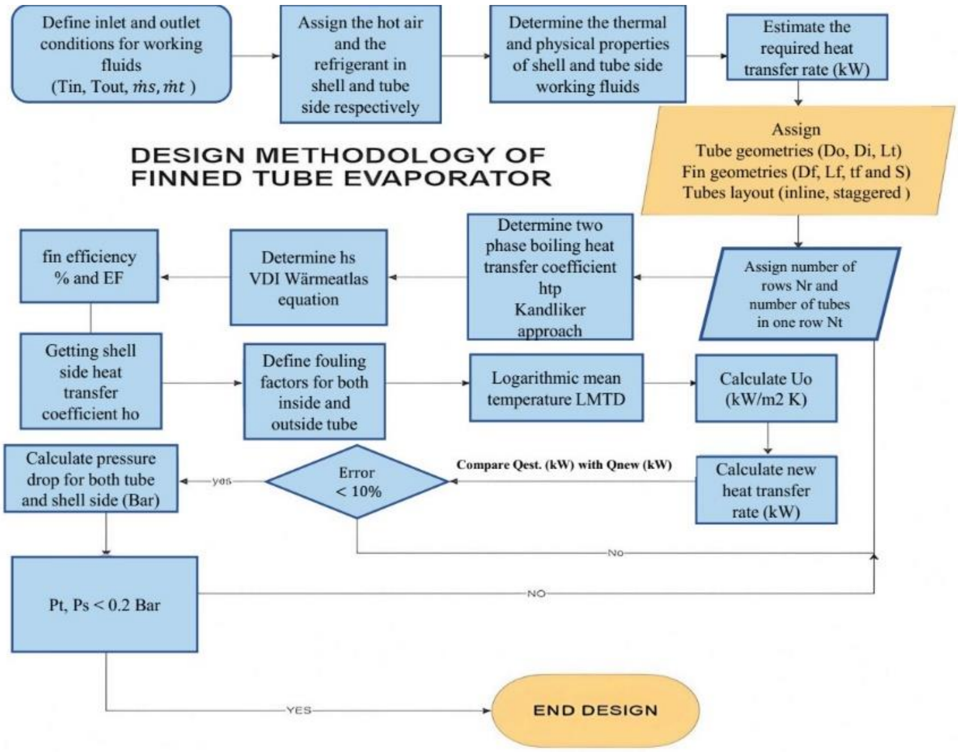

Figure 5.1. Finned tube evaporator design methodology

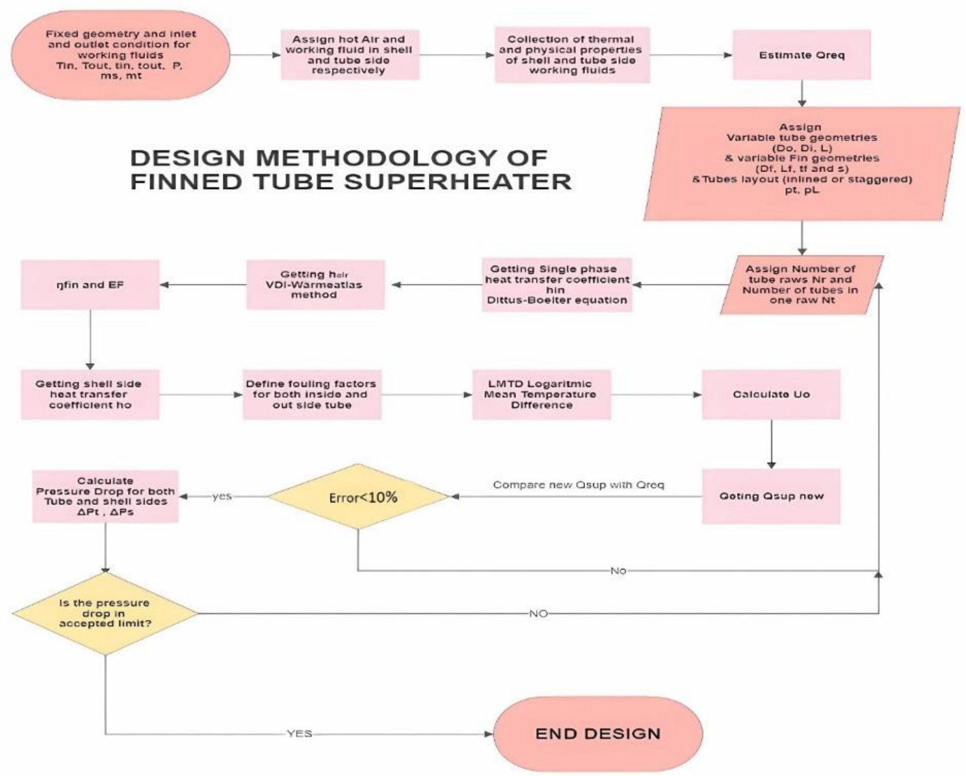

Figure 5.2. Finned tube superheater and preheater design methodology

In our study, we have developed a practical and effective design methodology for finned tube evaporators, which is presented in **Figure 5.1**. This methodology incorporates several important design considerations and limitations to ensure the optimal performance of the evaporator. To achieve a well-designed evaporator, our methodology includes detailed steps, which will be thoroughly discussed in the following topic. Furthermore, **Figure 5.2** demonstrates a design methodology for single-phase finned tube heat exchangers, specifically for preheater and superheater components. While the methodology for the heat exchangers is similar to that for the evaporator, the main difference lies in calculation the heat trasnfer coefficient inside the tubes in which the refrigerants flow inside. Our methodology for the heat exchangers takes into account various factors such as the desired heat transfer rate and pressure drop, as well as the materials used in the structure and other practical considerations. These steps ensure that the heat exchangers are designed to operate at optimal efficiency and reliability.

5.2 Design steps (preheater, Evaporator and superheater) [19-26]

1) The first step is to define the thermal and physical properties of working fluids based on given temperature and pressure data, and then we can easily estimate the required heat transfer Qreq and mass flow rate of refrigerant which is located in tube side.

2) The second step is to assign the tube and fin properties and geometries including the tube and fin material, outer diameter and inner diameter of tube (*dout, din*), Length of tube *Lt*, outer diameter of fin *Df*, length of fin *Lf*, thickness of fin tf and spacing between to following fins which called as fin pitch S, then we decide the layout of tubes either it is inline (St,SL) or staggered layout manner (*St,SL* and *Sr*) .

3) The third step is assigning the number of raws *Nr* and number of tubes per one raw nt then getting the total number of tube *N=Nr x nt*.

4) In forth step we calculate in tube heat transfer coefficient hi there are many methods we can use for calculation such as **Dittus-Boelter equation:**

$$h_i = 0{,}023\ R_e^{0{,}8}\ Pr^{0{,}4}\left(\frac{k}{din}\right) \tag{40}$$

This formula is used only for single flow (liquid or vapor only) and for two phase heat transfer coefficient htp there are also many approaches which could be applied like **(Kandlikar 1990)** approach to see in details go to A General Correlation for

Saturated Two-Phase Flow Boiling Heat Transfer Inside Horizontal and Vertical Tubes.

To calculate air side heat transfer coefficient there is a **VDI-Wärmeatlas method** given for forced convection on finned tubes in cross flow (VDI-Wärmeatlas, 2010) which is given as :

$h_D = 0{,}22\, R_{eD}^{0{,}6}\, Pr^{\frac{1}{3}} \left(\frac{Ao}{Ab}\right)^{-0{,}15} \left(\frac{k}{dout}\right)$..................*(eq27) inline layout*

$h_D = 0{,}38\, R_{eD}^{0{,}6}\, Pr^{\frac{1}{3}} \left(\frac{Ao}{Ab}\right)^{-0{,}15} \left(\frac{k}{dout}\right)$.................*(eq28)staggered layout*

$Ao = Af + Aw$

$$Ao = \frac{N\, L_T\, \pi}{S+t_f}\, (0.5\,(Df2 - dout2) + Df\ \ tf\ +\ Do\ S) \quad (41)$$

$$Ab = N\, Lt\, \pi\, dout\, kair \quad (42)$$

$$ReD = \left(\frac{\rho a\ V_{MAX}\ DO}{\mu a}\right) \quad (43)$$

$$Vmax = \frac{\dot{m}_a}{\rho\, Am_i n} \quad (44)$$

$$Amin = nt\, Lt(\, St - dout\ - \frac{2t_f L_f}{t_f + s}\,) \quad (45)$$

$$ho = EF\ hD \quad (46)$$

$$EF = \frac{n_f A_F + Aw}{A_o} \quad (47)$$

$$Af = \frac{NL_T\pi}{S+t_f}\, (0.5\,(Df2 - dout2) + Df\ \ tf\,) \quad (48)$$

$$Aw = \frac{NL_T\pi}{S+t_f}\, (dout\ \ tf) \quad (49)$$

$$nf = \frac{tanh\, m\psi}{m\, \psi} \quad (50)$$

$$\psi = 0.5\, dout\, \left(\frac{Df}{dout} - 1\right)\left(1 + 0.35\, Ln\left(\frac{Df}{dout}\right)\right) \quad (51)$$

$$m = \sqrt{\frac{2\, hD}{k_f}} \quad (52)$$

Where:

Pr = *Prandtl number*

$kair$ = *themal conductivity of air KW/m °C*

$dout$= *tube outer diameter m*

N= total number of tube

Lt=length of stright tube m

S= fin pith m

tf= thikness of fin

Df= outer diameter of fin m

LF=length of fin m

St= transverse pitch m

ρa*= density of dry air kg/m*^{3}

μa= air dynamic viscosity kg/ms

Ao= Total heating surface area m^2

Af =fin area m^2

Aw= unfinned tubes surface area m^2

Ab= Total surface area for tubes without fins m^2

ReD= Renault number

Vmax= maximum air velocity m/s

Amin= minimum cross flow aream2

ho= total heat transfer coefficint for shell side KW/m^2 *°C*

EF= fin effectiveness

n_f *= fin efficiency*

Kf = thermal conductivity of fin W/m°C

5) After we calculate heat transfer correlations for both tube and shell side we determine fouling factors Rdi,Rdo from **Table 8**

6) now we can esrimate overall heat transfer coefficient Uo by using the formula:

$$\frac{1}{U} = \left[\frac{1}{h_o} + R_{do} + \frac{Ao}{Ai}\left(\frac{din - dout}{2k_W}\right) + \frac{Ao}{Ai}\left(\frac{1}{h_i}\right) + \frac{Ao}{Ai}R_{di}\right]$$

(53)

7) The next step is to determine DTLM which can be written as:

$$DTLM = \frac{(Ta,in - TR,out) - (Ta,out - TR,in)}{Ln\left(\frac{Ta,in - TR,out}{Ta,out - TR,in}\right)} \quad (54)$$

Where: Ta, in and Ta, out are inlet and outlet air temperature respectively

TR, in and TR, out are inlet and outlet refrigerant temperature respectively

8) $\dot{Q}evap = A_0 U0\ DTLM$ (55)

9) $E = \frac{Q - Qreq}{Qreq} \times 100\%$ (56)

The error should be 0 < Error <10%

10) Pressure drops for both shell and tube sides

i) Tube side:

$\Delta P\ tube\ = \Delta Pf + \Delta P\ u$

$$\Delta P\ tube\ =\ \left[f\ \left(\frac{Lt}{din}\right)Nr\ +K\ (Nr-1)\right]\frac{\rho Ref.\ v^2}{2} \tag{57}$$

Where:

ΔPf = pressure drop due to friction Kpa

ΔPu= pressure drop due to U bending

f = darcy friction factor

Lt= length straight tube m

din= inner tube diameter m

Nr= number of tube rows

K= 1.5 for 180° elbow

ρRef.= density of refrigerant kg/m^3

v= velocity of fluid inside the tube m/s

This equation used for single phase flow (liquid or vapor only)

For calculation two phase pressure drop inside horizontal and U_bend tube we can use Müller-Stenhagen & Heck and Paliwoda (1992) respectively.

$$\left(\frac{dP}{dL}\right)_{f,L} = \zeta_l \frac{G^2}{2\rho_L d} = B1$$

$$\left(\frac{dP}{dL}\right)_{f,V} = \zeta_g \frac{G^2}{2\rho_V d} = B2$$

$$\zeta_l = \frac{64}{Re_V}, \zeta_g = \frac{64}{Re_V} \qquad \text{for } Re_L, Re_V \leq 1187$$

$$\zeta_l = \frac{0.3164}{Rel^{0.25}}, \zeta_g = \frac{0.3164}{Re_V^{0.25}} \qquad \text{for } Re_L, Re_V > 1187$$

$$Re_L = \frac{Gdin}{\mu_L} \text{ and } Re_V = \frac{Gdin}{\mu_V}$$

$$\int_0^L \left(\frac{dP}{dL}\right)_f dL = \left\{-\frac{3}{4}(1-x)^{\frac{4}{3}}[B1 + 2(B2 - B1)x] + \frac{1}{4}B2x^4 - \frac{9}{14}(B2 - B1)(1 -\right.$$

Where: G = *mass velocity kg/sm^2*

Re_L, Re_V= Renault number for saturated liquid and vapor state

x= vapour qualiy

B1= single phase pressure drop for liquid state kPa

B1= single phase pressure drop for vapor state kPa

For two phase pressure drop for U_bend:

$$\Delta p = f\frac{G^2}{2\rho_V}\beta$$

$$\beta = [\vartheta + C(1-\vartheta)x](1-x)^{0.333} + x^{2.276}$$

$$\vartheta = \frac{\Delta p_L}{\Delta p_V} = \frac{\rho_V}{\rho_L}\left(\frac{\mu_L}{\mu_V}\right)^{0.25}$$

Table 1. Palowoda friction factor coefficient based on the curvature ratio, D/d

Paliwoda (1992)friction factor coefficients based on the curvature ratio, D/d.

D/d	2.0	2.5	3.0	3.5	4.0	5.0	6.0	8.0
f	0.280	0.210	0.190	0.175	0.160	0.140	0.130	0.120

ii) Shell side:

$$\Delta Ps = \Delta Pacc + \Delta Pf$$

$$\Delta Ps = (ka + kf)\ 0.5\ \rho\ Vmax2$$

$$Ka = 1 + \sigma 2$$

$$\sigma = \frac{S_t - Do - \left(\frac{2L_f t_F}{tF+s}\right)}{Pt}$$

$$Kf = 4.71Re - 0.286 \left(\frac{Lf}{S}\right) 0.51 \left(\frac{St-Do}{Sl-Do}\right)^{0.536} \left(\frac{Do}{St-Do}\right)^{0.36} \qquad 10^3 < Re < 10^5$$

For high fin tube in staggered arrays Re ($5x10^2$ –$5x10^4$)

$$Kf = 4.567\ Re^{-0.242} \left(\frac{0.5\,(Df^2 - Do^2) + Df\ tf + Do\ S}{Do\,(t_f + s)}\right)^{0.504} \left(\frac{St}{Do}\right)^{0.376} \left(\frac{Sl}{Do}\right)^{0.546}$$

Where:

ΔPs= total shell side pressure drops Kpa

$\Delta Pacc$= pressure drop due to acceleration Kpa

ΔPf= pressure drop due to friction Kpa

Ka= acceleration factor

Kf= friction factor

5.3 Design limitation for (preheater, evaporator and superheater)

Just like in the case of the condenser, when designing the heat exchangers for the ORC, there exists a trade-off between the heating surface area and the pressure drop. This means that a design with minimum heating surface area (and hence minimum cost) will lead to a maximum pressure drop, which could negatively impact the overall performance of the ORC. To address this challenge, our study has proposed some limitations that will help us achieve an optimum design with the minimum required heating surface area and an allowable amount of pressure drop. These limitations have been carefully selected to ensure that the performance of the ORC is not compromised, while also keeping the cost of the heat exchanger design to a minimum. The proposed methodology and design limitations will be discussed in detail in the upcoming sections of this thesis.

Table 5.1. Preheater, evaporator, and superheater design limitation

Error (E%) *	**ΔP_s (bar)**	**ΔP_t (bar)**
<10%	<0.2	<0.2

*To avoid overdesign or under design

5.4 Design optimization for (preheater, evaporator and superheater)

In our design method for the heat exchanger unit, we have a set of parameters that are fixed while others are variable. By adjusting the variable parameters, we can generate multiple designs for each heat exchanger unit. Among these designs, the one with the minimum heating surface area is considered to be the optimal design. This approach allows us to explore different design possibilities and choose the most efficient one for our application. By using this method, we can achieve an optimal balance between heat transfer efficiency and cost-effectiveness, which is essential for the successful implementation of the heat exchanger unit in the overall system.
The logic of the optimization procedure in the preheater, evaporator, and superheater is similar to that in the condenser as it is shown in **Figure 4.6.**

5.4.1 Design optimization procedure for evaporator

Table 5.2. Evaporator's fixed properties and parameters

Tube fixed geometries	
Do (mm)	57.15
Din (mm)	53.8
Ltube (mm)	2000
Material	Carbon steel
Fin fixed geometries	
Df (mm)	89.6
Lf (mm)	15.8
tf (mm)	0.4
S (mm)	4
Material	Alaminum
Dbend	3 x Do
Tube layout	Staggered (°60)

Nr= (2 – 11) raws & nt=(2-60) tubes per rows

$$Nt = Nr\ X\ nt;\ (\mathbf{2x2, 2x4, 2x6} \ldots\ldots\ldots\ldots\ldots\ldots\ldots\ldots\ldots\ldots\ldots.\mathbf{11x60})$$

(300 design) attempted in all calculations for evaporator and each design is tested by previous mentioned limitations.

5.4.1.1 Evaporator optimization procedure for R245fa

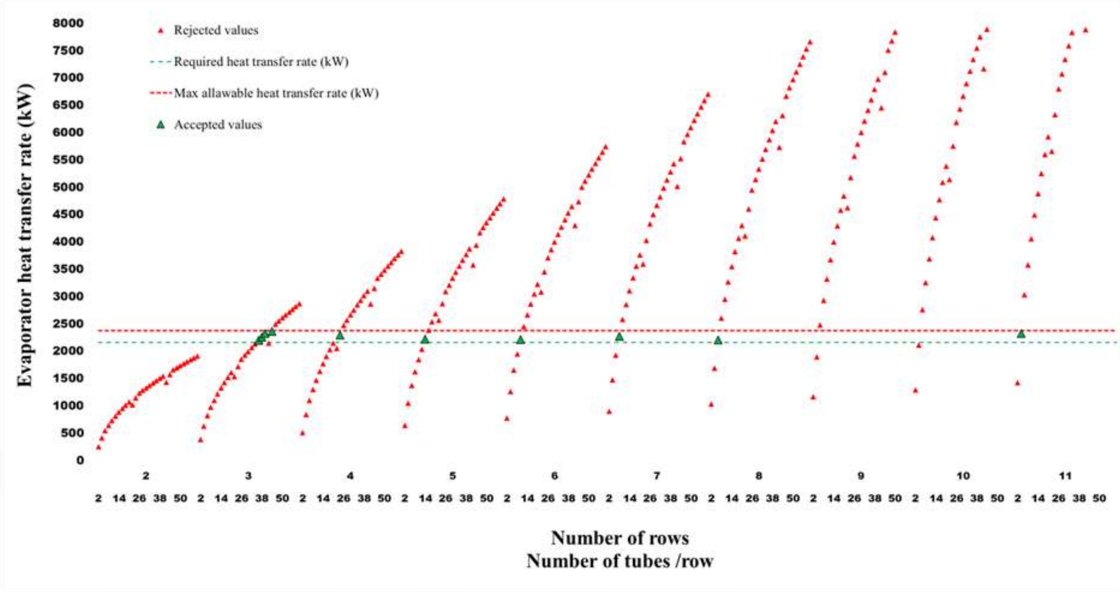

Figure 5.3. Evaporator heat transfer rate (kW) diagram for R245fa

In order to obtain an optimum design for the evaporator unit, a methodology was developed and implemented as illustrated in Figure 5.3. The design process involved fixing certain parameters while varying others to achieve multiple designs for each heat exchanger unit. The variable parameters were the number of tube rows, the number of tubes in one row that are poltted in horizontal axis, and the heating duty of the evaporator that are poltted on vertical axis. In horizontal axis, starting with two tubes in one row, the number of tubes in one row was gradually increased until 60, at which point the number of rows was increased by one, and the process was repeated until a total of 11 rows were achieved.

In this way, a total of 300 evaporator designs were evaluated based on their heating duty, with the aim of achieving a minimum heating surface area and an acceptable level of pressure drop for the overall performance of the ORC system. The required heating duty was calculated in Table 3.2 to be 2168.26 KW, and a maximum accepted value of 10% more than the required value, or 2385 KW, was established.

The resulting designs were plotted in Figure 5.3, with the red and green points indicating the attempted evaporator designs, and the green dashed line representing the minimum required heating duty. Additionally, the red dashed line represented the maximum accepted value for the heating duty. Out of the 300 designs attempted, only 10 of them fell within the accepted range and were highlighted in green, while the others were outside the accepted range and were shown in red.

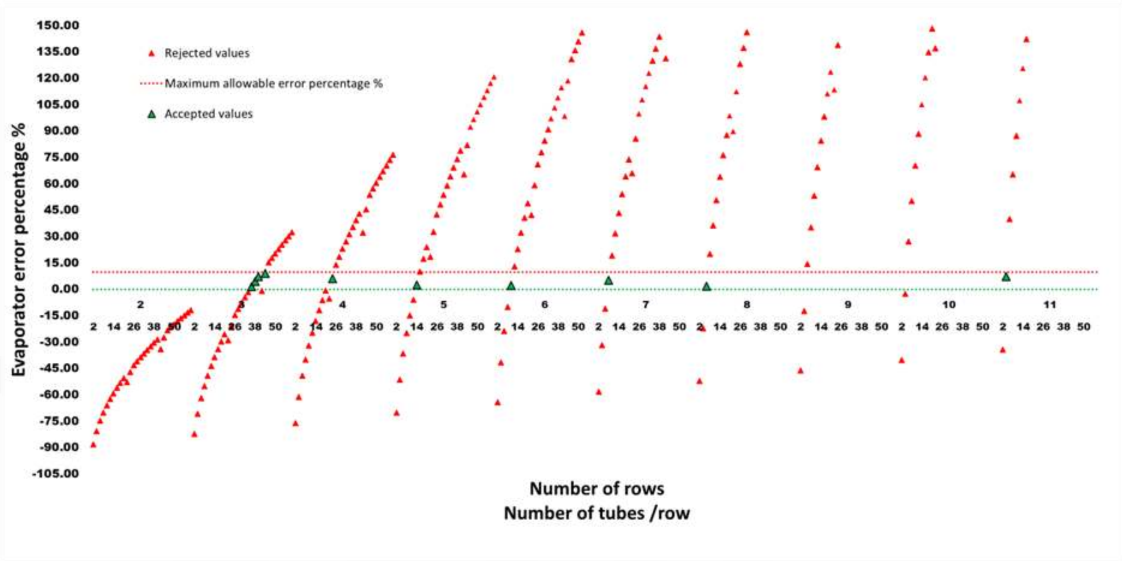

Figure 5.4. Evaporator design error% diagram with R245fa

Figure 5.4 showcases the percentage design error of each evaporator design in relation to the total number of tube rows and the total number of tubes in one row. The maximum allowable design error is indicated by a red dashed line at 10%. The green triangles indicate evaporator designs that have a design error value of less than 10%, while the red triangles indicate designs that exceed the maximum allowable limit or have negative values. The results show that only 10 designs in green color passed this limitation successfully, indicating their ability to satisfy the desired design criteria. On the other hand, the remaining designs in red color had values greater than 10% or less than zero, indicating their unsuitability for use in the proposed system. This limitation insured that the accepted green designs were out of overdesigning or underdesigning.

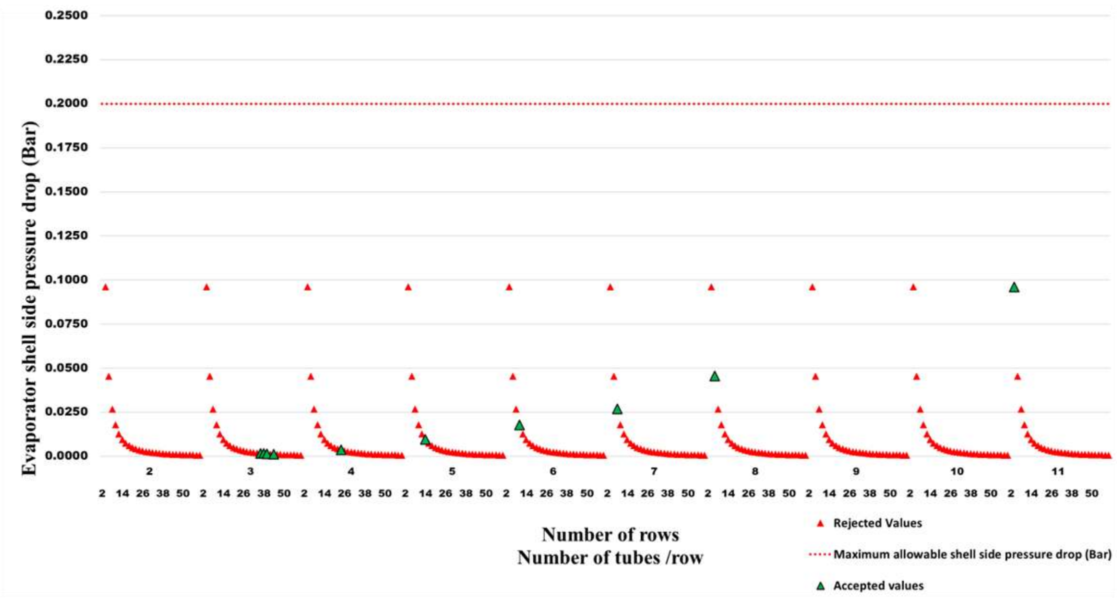

Figure 5.5. Shell side pressure drop through the evaporator with R245fa

In Figure 5.5, the shell side pressure drop is presented for each evaporator design, with the total number of tube rows and the total number of tubes in one row as design variables. The maximum allowable shell side pressure drop of 0.2 bar is indicated by a red dashed line. Designs that passed all previous tests and have a shell side pressure drop value less than 0.2 bar are represented by green triangles. Conversely, designs that did not pass one of the previous tests or have a value of more than 0.2 bar are represented by red triangles. It is clear from this figure that only the ten designs out of 300 that passed all the previous tests that are depicted in green color, while the rejected designs are shown in red triangles, even if they have a value of shell side pressure drop less than 0.2 bar, as they did not pass the previous tests. This result shows that the proposed methodology, which takes into account multiple constraints and limitations, was able to identify only a small set of feasible evaporator designs.

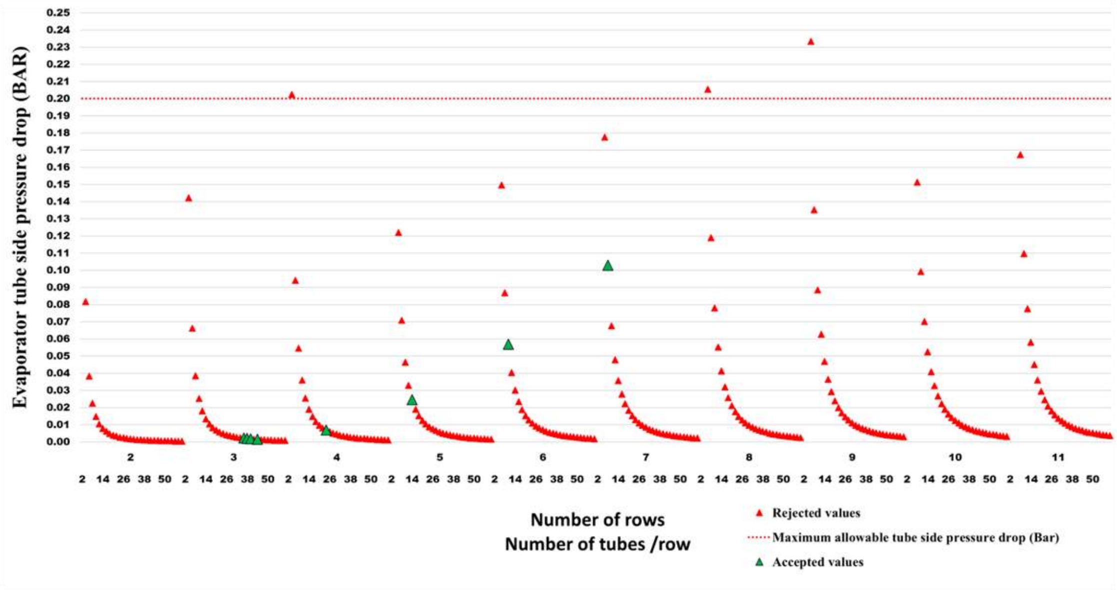

Figure 5.6. Tube side pressure drop through the evaporator with R245fa

Figure 5.6 depicts the tube side pressure drop for each evaporator design obtained through our methodology, considering the total number of tube rows and the total number of tubes in one row. The maximum allowable tube side pressure drop is denoted by a red dashed line at 0.2 bar. The successful designs that passed all the previous limitations and also have a tube side pressure drop value less than 0.2 bar are depicted as green triangles. On the other hand, the rejected designs that failed to pass one of the previous limitations or have a tube side pressure drop value more than 0.2 bar are indicated as red triangles. It is apparent from this figure that out of the 300 designs obtained through our methodology, only 8 designs were able to pass all the limitations successfully and are represented as green triangles, indicating their acceptability for further consideration.

Efficient design of an evaporator is crucial from both an economic and practical standpoint, as it involves optimizing the heating surface area to achieve maximum efficiency while minimizing investment and operational costs. Increasing the heating surface area can enhance the evaporator's efficiency, leading to lower energy consumption. However, a larger heating surface area also leads into increased material, manufacturing, and installation costs. Hence, determining the optimal heating surface area that balances the investment and operational costs is vital. By achieving an optimized heating surface area, a well-designed evaporator can lead to substantial cost savings over the long term. During the optimization process, the focus was on achieving the minimum heating surface area while ensuring that the pressure drop remains within an acceptable limit of less than 0.2 bar.

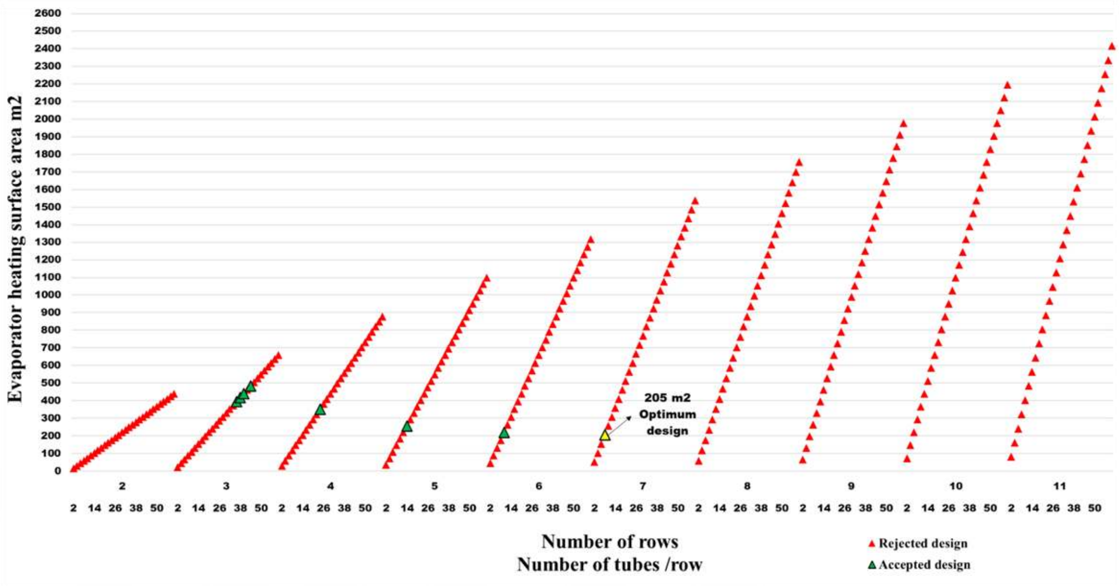

Figure 5.7. Evaporator heating surface area m2 diagram with R245fa

Figure 5.7 provides a representation of the heating surface area for each of the 300 evaporator designs based on the total number of tube rows and the total number of tubes in one row. It is worth noting that only 8 designs satisfy all the previous limitations and can be considered as good evaporator designs, and these designs are represented as green and yellow triangles in the figure. Conversely, the rejected designs, which failed to pass one or more of the previous tests, are shown as red triangles. The optimum design that is associated with the yellow triangle with the minimum surface area of 205 m2, corresponding to 8 tubes in one row and 7 number of tube rows. This design ensures the lowest possible cost and investment while also maintaining the required performance, making it the ideal choice for the evaporator. As such, the optimization process for the heating surface area of the evaporator has yielded a favorable result that can lead to significant cost savings and improved efficiency. Therefore, it can be concluded that the optimization of the heating surface area is a critical aspect of the evaporator design process that must be carefully considered.

Table 5.3. Finned tube evaporator design results with R245fa

NO	$N_{tube/raw}$	N_{raw}	N_{total}	Error	ΔP_t	ΔP_s	A	$\dot{Q}_{est}$	Design Test Result
	#	#	#	%	bar	bar	m^2	kW	accepted/not accepted
1	2	2	4	-88	0.297	0.346	15	261	not accepted
2	4	2	8	-80	0.081	0.096	29	424	not accepted
⋮	⋮	⋮	⋮	⋮	⋮	⋮	⋮	⋮	⋮
48	36	3	108	2	0.002	0.002	396	2205	accepted
49	38	3	114	5	0.002	0.002	418	2268	accepted
50	40	3	120	7	0.002	0.001	440	2330	accepted
51	42	3	126	-1	0.002	0.001	462	2154	not accepted
52	44	3	132	9	0.002	0.001	484	2371	accepted
⋮	⋮	⋮	⋮	⋮	⋮	⋮	⋮	⋮	⋮
71	22	4	88	-5	0.008	0.004	323	2060	not accepted
72	24	4	96	6	0.007	0.004	352	2306	accepted
⋮	⋮	⋮	⋮	⋮	⋮	⋮	⋮	⋮	⋮
96	12	5	60	-6	0.033	0.013	220	2046	not accepted
97	14	5	70	3	0.024	0.01	257	2226	accepted
98	16	5	80	10	0.019	0.008	294	2392	not accepted
⋮	⋮	⋮	⋮	⋮	⋮	⋮	⋮	⋮	⋮
124	8	6	48	-10	0.086	0.027	176	1958	not accepted
125	10	6	60	2	0.056	0.018	220	2220	accepted
⋮	⋮	⋮	⋮	⋮	⋮	⋮	⋮	⋮	⋮
153	6	7	42	-11	0.176	0.045	154	1936	not accepted
154	**8**	**7**	**56**	**5**	**0.102**	**0.027**	**205**	**2285**	**accepted***
⋮	⋮	⋮	⋮	⋮	⋮	⋮	⋮	⋮	⋮
181	2	8	16	-52	1.646	0.346	59	1042	not accepted
⋮	⋮	⋮	⋮	⋮	⋮	⋮	⋮	⋮	⋮
211	2	9	18	-46	1.871	0.346	66	1172	not accepted
⋮	⋮	⋮	⋮	⋮	⋮	⋮	⋮	⋮	⋮
241	2	10	20	-40	2.096	0.346	73	1303	not accepted
⋮	⋮	⋮	⋮	⋮	⋮	⋮	⋮	⋮	⋮
299	58	11	638	378	0.004	0.001	2341	10367	not accepted
300	60	11	660	387	0.004	0.001	2422	10551	not accepted

*Minimal evaporator area, ideal choice-lowest cost

** All the evaporator design calculations are carried out assuming P2=22bar with R245fa.

5.4.1.2 Evaporator optimization procedure for R600

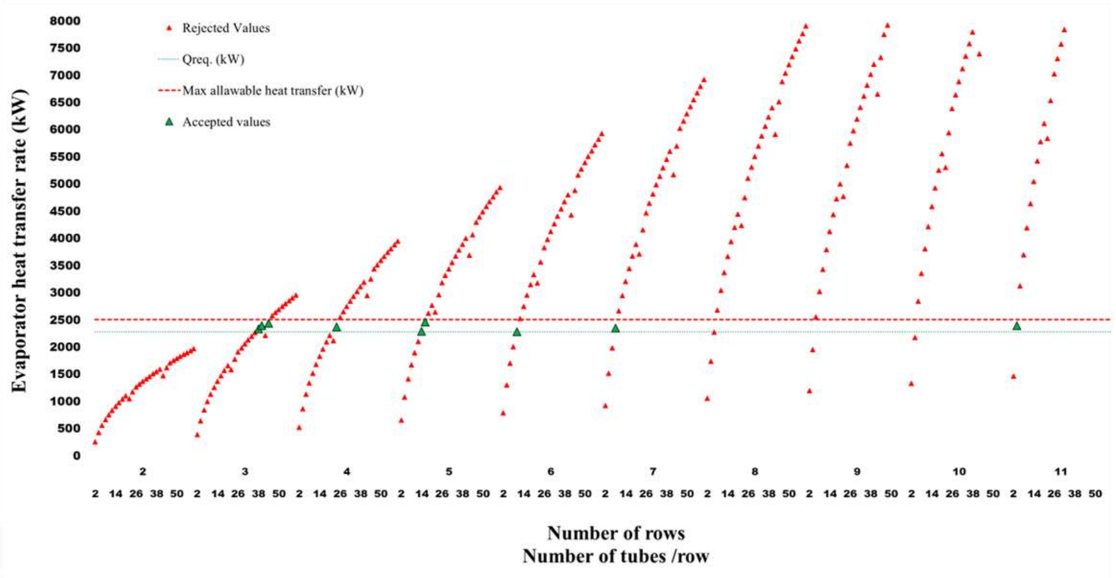

Figure 5.8. Evaporator heat transfer rate (kW) diagram for R600

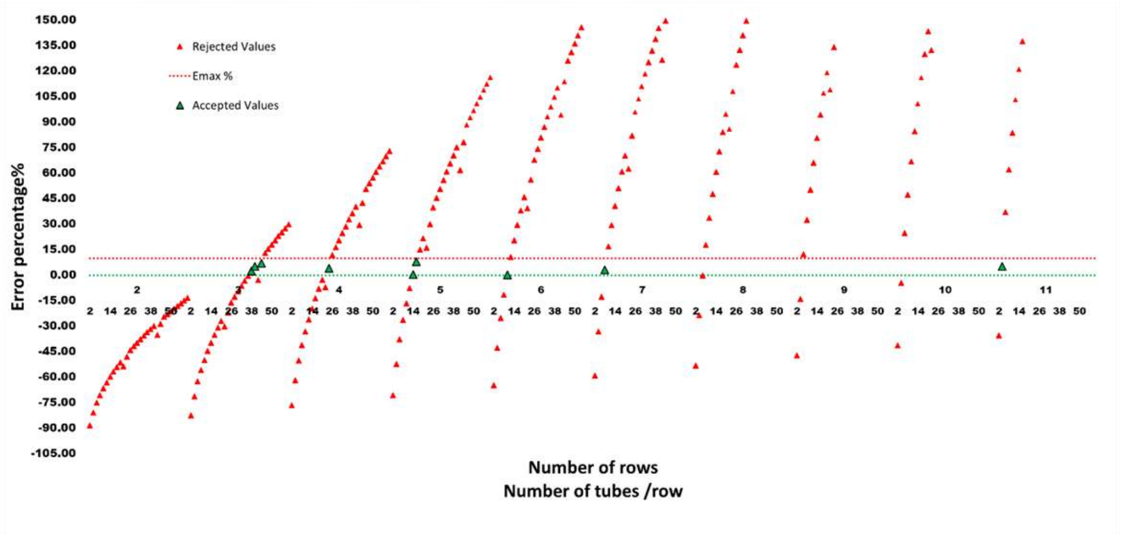

Figure 5.9. Evaporator design error% diagram R600

Figure 5.8 indicates 300 designs for evaporator and each design corrosponds to certain prameters including the number of tube rows, the number of tubes in one row that are poltted on horizontal axis, while the heating duty of the evaporator is poltted on vertical axis. In horizontal axis, Starting with two tubes in one row, this number was gradually increased until 60, at which point the number of rows was increased by one, and the process was repeated until a total of 11 rows were achieved. In this way, a total of 300 evaporator designs were evaluated based on their heating duty. The minimum accepted heating duty was calculated in Table 3.2 to be 2287.98 kW, and the maximum accepted value of 10% more than the required value which is equal to 2516.78 kW. The resulting designs were plotted in Figure 5.8, with the red and green points indicating the attempted evaporator designs, and the green dashed line representing the minimum required heating duty. Additionally, the red dashed line represented the maximum accepted value for the heating duty. Out of the 300 designs attempted, only 9 of them fell within the accepted range and were highlighted in green, while the others were outside the accepted range and were shown in red.

Figure 5.9 showcases the percentage design error of each evaporator design in relation to the total number of tube rows and the total number of tubes in one row. The maximum allowable design error is indicated by a red dashed line at 10%. The green triangles indicate evaporator designs that have a design error value of less than 10%, while the red triangles indicate designs that exceed the maximum allowable limit or have negative values. The results show that only 9 designs in green color passed this limitation successfully, indicating their ability to satisfy the desired design criteria. On the other hand, the remaining designs in red color had values greater than 10% or less than zero, indicating their unsuitability for use in the proposed system. This limitation insured that the accepted green designs were out of overdesigning or underdesigning.

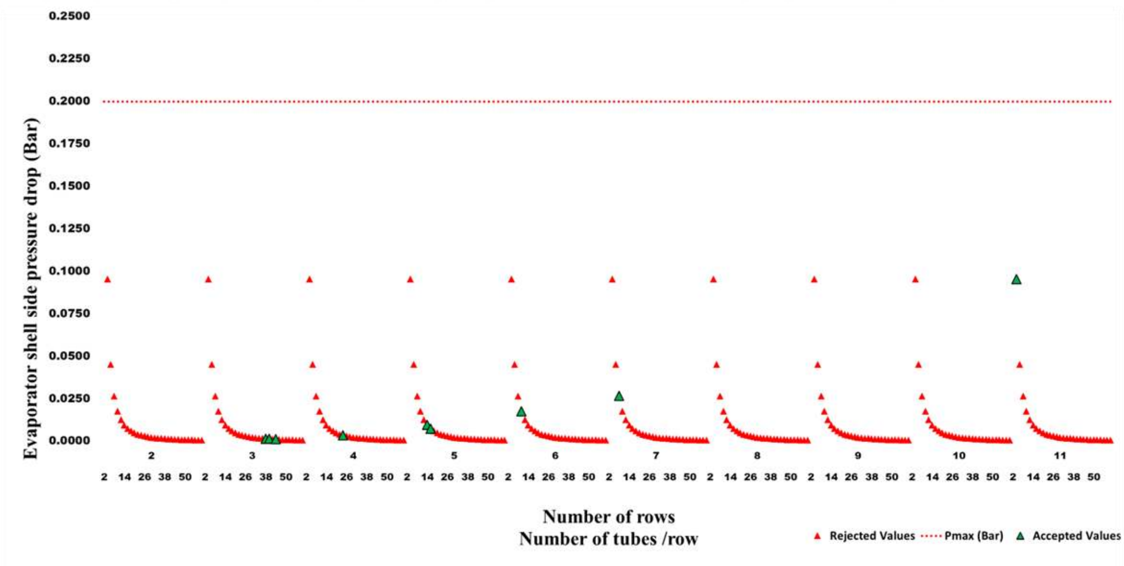

Figure 5.10. Shell side pressure drop through the evaporator with R600

In Figure 5.10, the shell side pressure drop is presented for each evaporator design, corresponding to the total number of tube rows and the total number of tubes in one row for each evaporator design. The maximum allowable shell side pressure drop of

0.2 bar is indicated by a red dashed line. Designs that passed all previous tests and have a shell side pressure drop value less than 0.2 bar are represented by green triangles. Conversely, designs that did not pass one of the previous tests or have a value of more than 0.2 bar are represented by red triangles. It is clear from this figure that only the 9 designs out of 300 that passed all the previous tests that are depicted in green color, while the rejected designs are shown in red triangles, even if they have a value of shell side pressure drop less than 0.2 bar, as they did not pass the previous limitations.

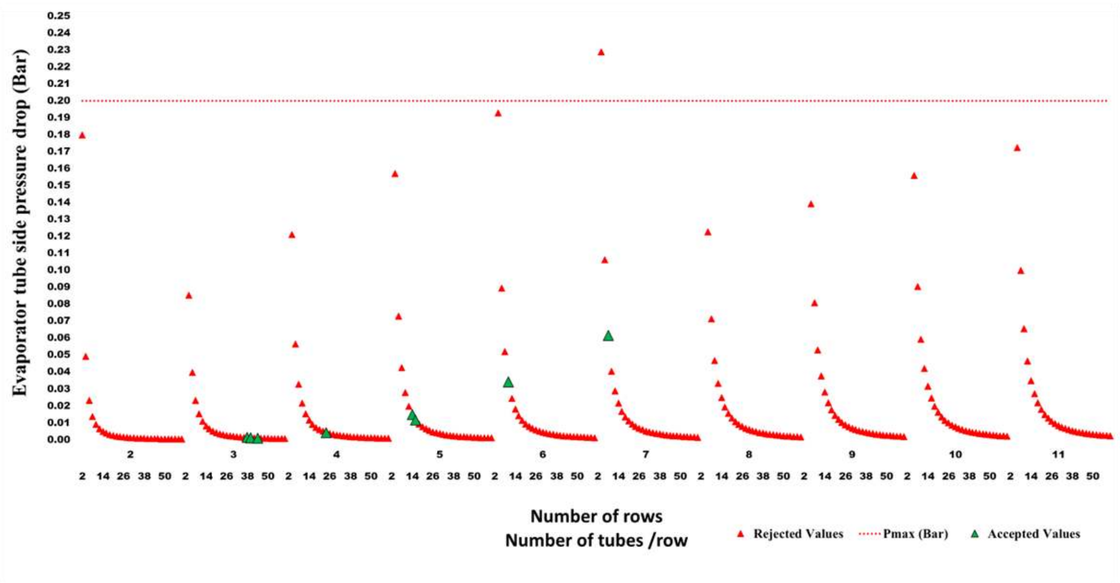

Figure 5.11. Tube side pressure drop through the evaporator with R600

Figure 5.11 depicts the tube side pressure drop for each evaporator design obtained through our methodology, considering the total number of tube rows and the total number of tubes in one row. The maximum allowable tube side pressure drop is denoted by a red dashed line at 0.2 bar. The successful designs that passed all the previous limitations and also have a tube side pressure drop value less than 0.2 bar are depicted as green triangles. On the other hand, the rejected designs that failed to pass one of the previous limitations or have a tube side pressure drop value more than 0.2 bar are indicated as red triangles. It is apparent from this figure that out of the 300 designs obtained through our methodology, only 8 designs were able to pass all the limitations successfully and are represented as green triangles, indicating their acceptability for further consideration.

The results of the evaporator optimization procedure are indicated in the following chart in case of heating surface area as it is the last step in the optimization process, in which all the perfect designs that successfully passed all the limitations suggested in this study are shown as green triangles while the optimal desing which has successfully passed all the tests and has the smallest area among other accepted designs is in yellow color.

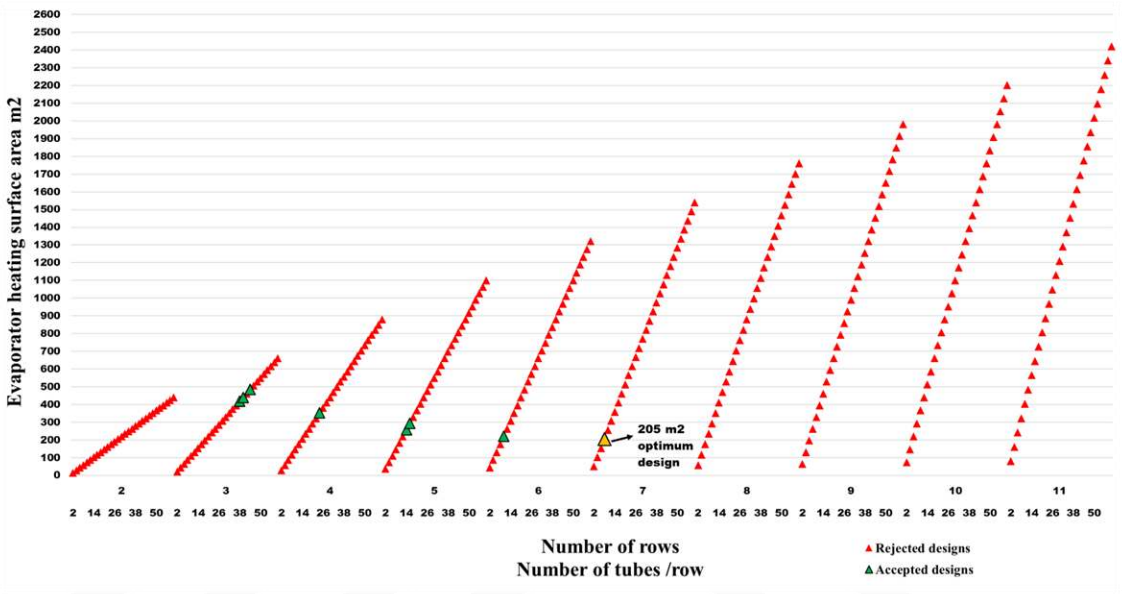

Figure 5.12. Evaporator heating surface area m2 diagram R600

Figure 5.12 provides a representation of the heating surface area for each of the 300 evaporator designs based on the total number of tube rows and the total number of tubes in one row. It is worth noting that only 8 designs satisfy all the previous limitations and can be considered as good evaporator designs, and these designs are represented as green and yellow triangles in the figure. Conversely, the rejected designs, which failed to pass one or more of the previous tests, are shown as red triangles. The optimum design that is associated with the yellow triangle with the minimum surface area of 205 m2, corresponding to 8 tubes in one row and 7 number of tube rows. This design ensures the lowest possible cost and investment while also maintaining the required performance, making it the ideal choice for the evaporator. As such, the optimization process for the heating surface area of the evaporator has yielded a favorable result that can lead to significant cost savings and improved efficiency. Therefore, it can be concluded that the optimization of the heating surface area is a critical aspect of the evaporator design process that must be carefully considered.

Table 5.4. Finned tube evaporator design results with R600

NO	$N_{tube/raw}$	N_{raw}	N_{total}	Error	ΔP_t	ΔP_s	A	$\dot{Q}_{est}$	Design Test Result
	#	#	#	%	bar	bar	m^2	kW	accepted/not accepted
1	2	2	4	-88.27224263	0.179894879	0.344290301	14.67592152	268.329394	not accepted
⋮	⋮	⋮	⋮	⋮	⋮	⋮	⋮	⋮	⋮
47	34	3	102	-3.392373452	0.001583231	0.001896892	374.2359988	2210.368535	not accepted
48	36	3	108	-0.463522728	0.001425238	0.001709646	396.2498811	2277.380216	not accepted
49	38	3	114	2.38531902	0.00129042	0.001549619	418.2637634	2342.561304	accepted design
50	40	3	120	5.160563963	0.001174405	0.001411713	440.2776456	2406.058507	accepted design
51	42	3	126	-2.852574773	0.00107381	0.001291976	462.2915279	2222.719051	not accepted
52	44	3	132	6.993367927	0.000985986	0.001187309	484.3054102	2447.992797	accepted design
53	46	3	138	13.0973459	0.000908833	0.001095252	506.3192925	2587.650931	not accepted
⋮	⋮	⋮	⋮	⋮	⋮	⋮	⋮	⋮	⋮
71	22	4	88	-7.045695176	0.004953057	0.004191031	322.8702735	2126.781062	not accepted
72	24	4	96	4.087320556	0.004213592	0.003576283	352.2221165	2381.502853	accepted design
⋮	⋮	⋮	⋮	⋮	⋮	⋮	⋮	⋮	⋮
96	12	5	60	-7.619503738	0.019792173	0.012684914	220.1388228	2113.652405	not accepted
97	14	5	70	0.496671857	0.014826164	0.009567266	256.8286266	2299.34933	accepted design
98	16	5	80	8.024934803	0.011547738	0.007495059	293.5184304	2471.594898	accepted design
99	18	5	90	15.07702406	0.009265799	0.006044245	330.2082342	2632.945681	not accepted
123	6	6	36	-25.14704676	0.089508148	0.045259608	132.0832937	1712.624753	not accepted
124	8	6	48	-11.61780461	0.052000453	0.02667546	176.1110583	2022.171859	not accepted
125	10	6	60	0.217838077	0.034156783	0.017714873	220.1388228	2292.969653	accepted design
126	12	6	72	10.85659551	0.024244464	0.012684914	264.1665874	2536.382886	not accepted
⋮	⋮	⋮	⋮	⋮	⋮	⋮	⋮	⋮	⋮
153	6	7	42	-12.67155456	0.106091129	0.045259608	154.097176	1998.062212	not accepted
154	**8**	**7**	**56**	**3.11256128**	**0.06160021**	**0.02667546**	**205.462901**	**2359.2005**	**accepted design***
⋮	⋮	⋮	⋮	⋮	⋮	⋮	⋮	⋮	⋮
300	60	11	660	376.0396867	0.002289177	0.000676388	2421.527051	10891.71924	not accepted

*Minimal evaporator area, ideal choice-lowest cost

** All the evaporator design calculations are carried out assuming P2=22bar R600.

5.4.1.3 Evaporator optimization procedure for R123

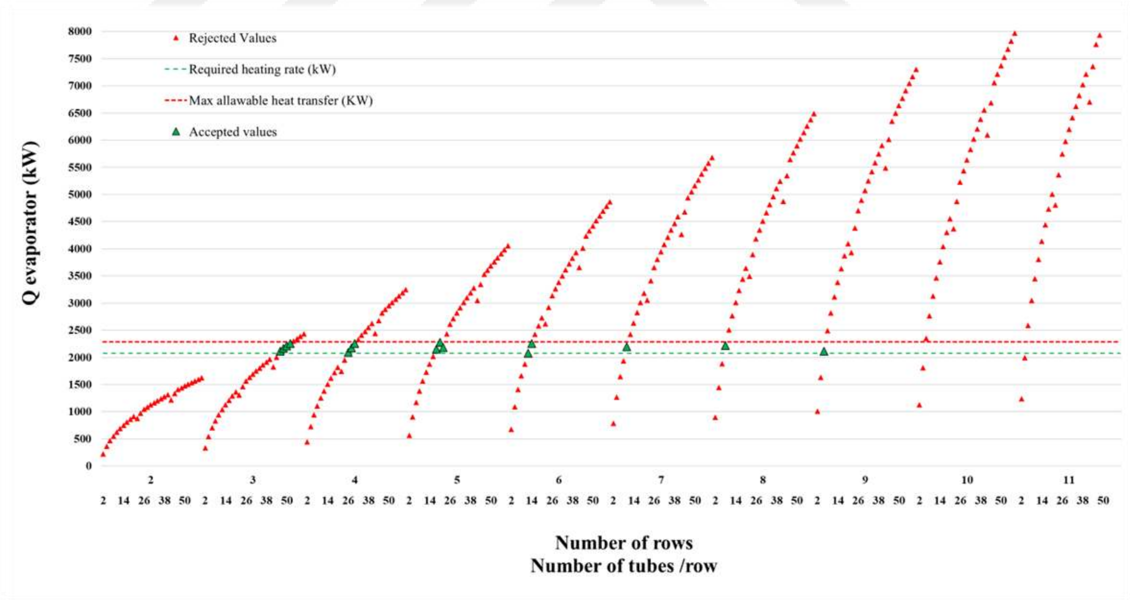

Figure 5.13. Evaporator heat transfer rate (kW) with R123

Figure 5.13 indicates 300 designs for evaporator and each design corrosponds to certain prameters including the number of tube rows, the number of tubes in one row that are poltted on horizontal axis, while the heating duty of the evaporator is poltted on vertical axis. In horizontal axis, Starting with two tubes in one row, this number was gradually increased until 60, at which point the number of rows was increased by one, and the process was repeated until a total of 11 rows were achieved. In this way, a total of 300 evaporator designs were evaluated based on their heating duty. The minimum accepted heating duty was calculated in Table 3.2 to be 2075.73 kW, and the maximum accepted value of 10% more than the required value which is equal to 2283.3 kW. The resulting designs were plotted in Figure 5.13, with the red and green points indicating the attempted evaporator designs, and the green dashed line representing the minimum required heating duty. Additionally, the red dashed line represented the maximum accepted value for the heating duty. Out of the 300 designs attempted, only 15 of them fell within the accepted range and were highlighted in green, while the others were outside the accepted range and were shown in red.

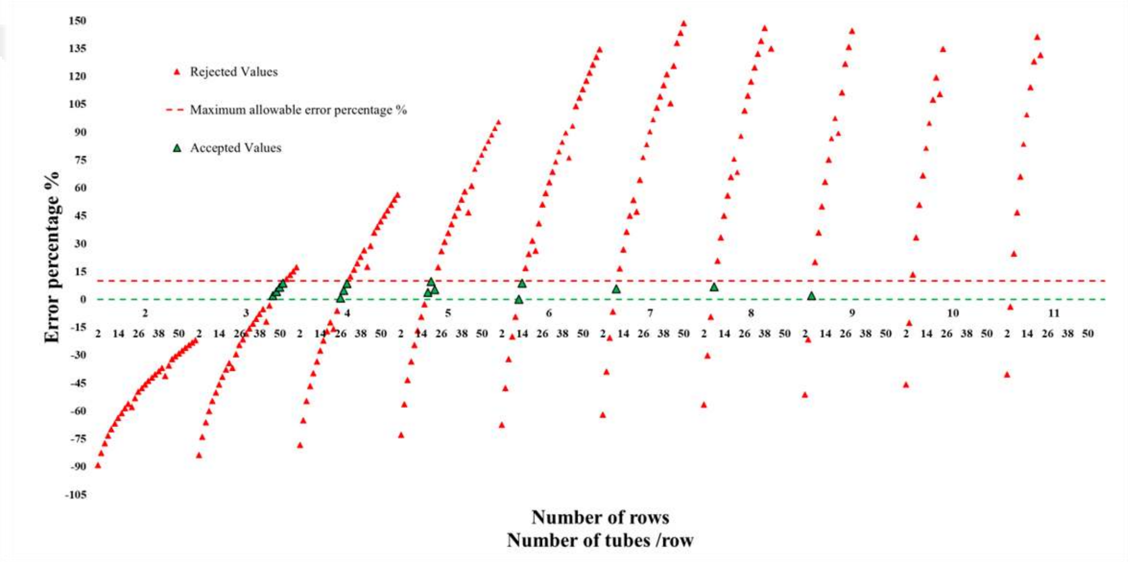

Figure 5.14. Evaporator design error% diagram with R123

Figure 5.14 showcases the percentage design error of each evaporator design in relation to the total number of tube rows and the total number of tubes in one row. The maximum allowable design error is indicated by a red dashed line at 10%. The green triangles indicate evaporator designs that have a design error value of less than 10%, while the red triangles indicate designs that exceed the maximum allowable limit or have negative values. The results show that only 15 designs in green color passed this limitation successfully, indicating their ability to satisfy the desired design criteria. On the other hand, the remaining designs in red color had values greater than 10% or less than zero, indicating their unsuitability for use in the proposed system. This limitation insured that the accepted green designs were out of overdesigning or underdesigning.

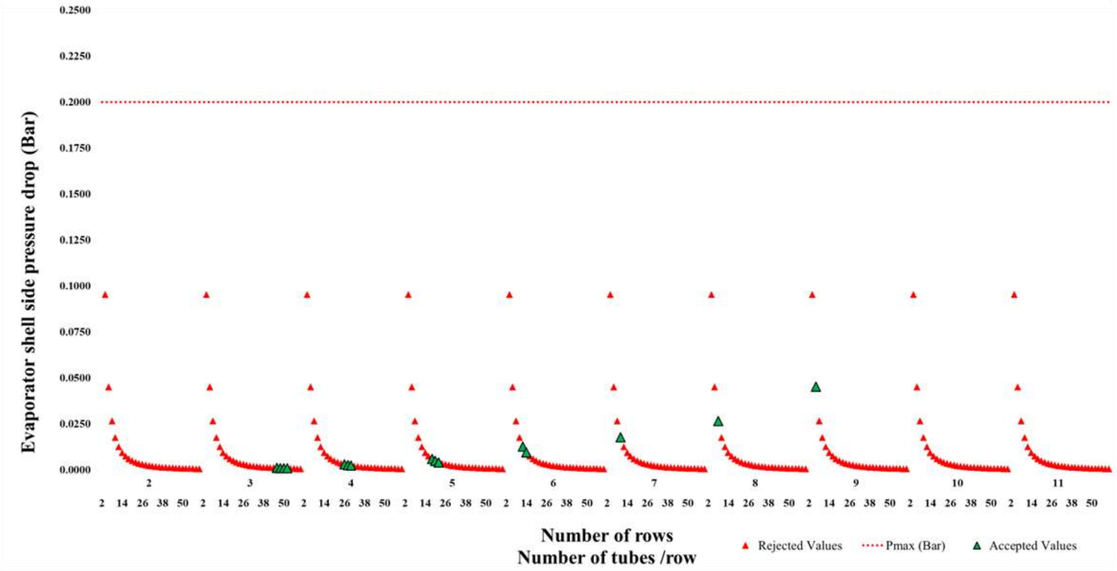

Figure 5.15. Shell side pressure drop through the evaporator with R123

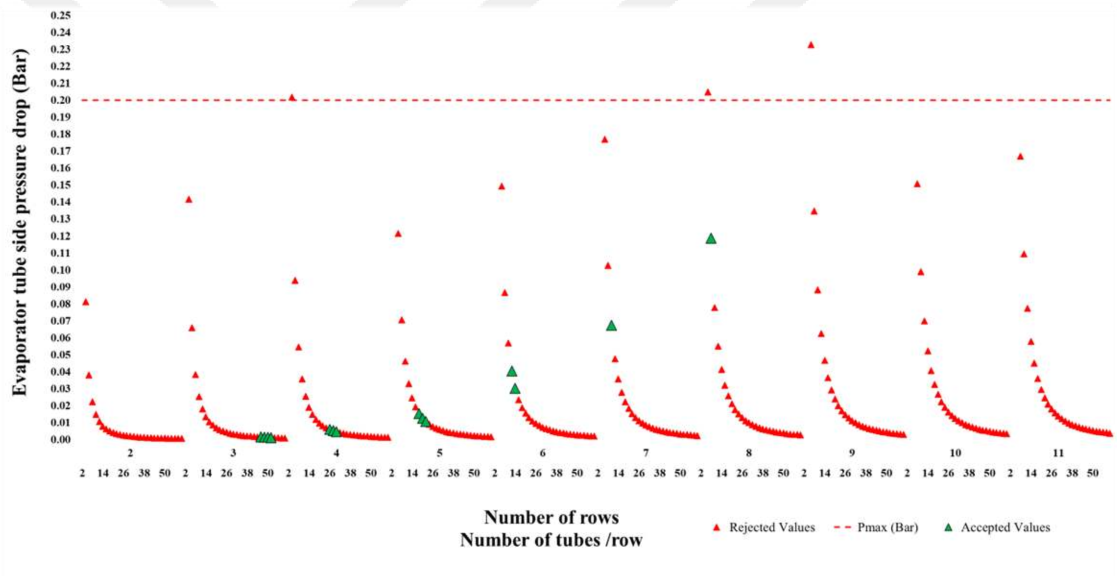

Figure 5.16. Tube side pressure drop through the evaporator with R123

In Figure 5.15, the shell side pressure drop is presented for each evaporator design, corresponding to the total number of tube rows and the total number of tubes in one row for each evaporator design. The maximum allowable shell side pressure drop of 0.2 bar is indicated by a red dashed line. Designs that passed all previous tests and have a shell side pressure drop value less than 0.2 bar are represented by green triangles. Conversely, designs that did not pass one of the previous tests or have a value of more than 0.2 bar are represented by red triangles. It is clear from this figure that only the 15 designs out of 300 that passed all the previous tests that are depicted in green color, while the rejected designs are shown in red triangles, even if they have a value of shell side pressure drop less than 0.2 bar, as they did not pass the previous limitations.

Figure 5.16 depicts the tube side pressure drop for each evaporator design obtained through our methodology, considering the total number of tube rows and the total number of tubes in one row. The maximum allowable tube side pressure drop is denoted by a red dashed line at 0.2 bar. The successful designs that passed all the previous limitations and also have a tube side pressure drop value less than 0.2 bar are depicted as green triangles. On the other hand, the rejected designs that failed to pass one of the previous limitations or have a tube side pressure drop value more than 0.2 bar are indicated as red triangles. It is apparent from this figure that out of the 300 designs obtained through our methodology, only 14 designs were able to pass all the limitations successfully and are represented as green triangles, indicating their acceptability for further consideration.

The results of the evaporator optimization procedure are indicated in the following chart in case of heating surface area as it is the last step in the optimization process, in which all the perfect designs that successfully passed all the limitations suggested in this study are shown as green triangles while the optimal desing which has successfully passed all the tests and has the smallest area among other accepted designs is in yellow color.

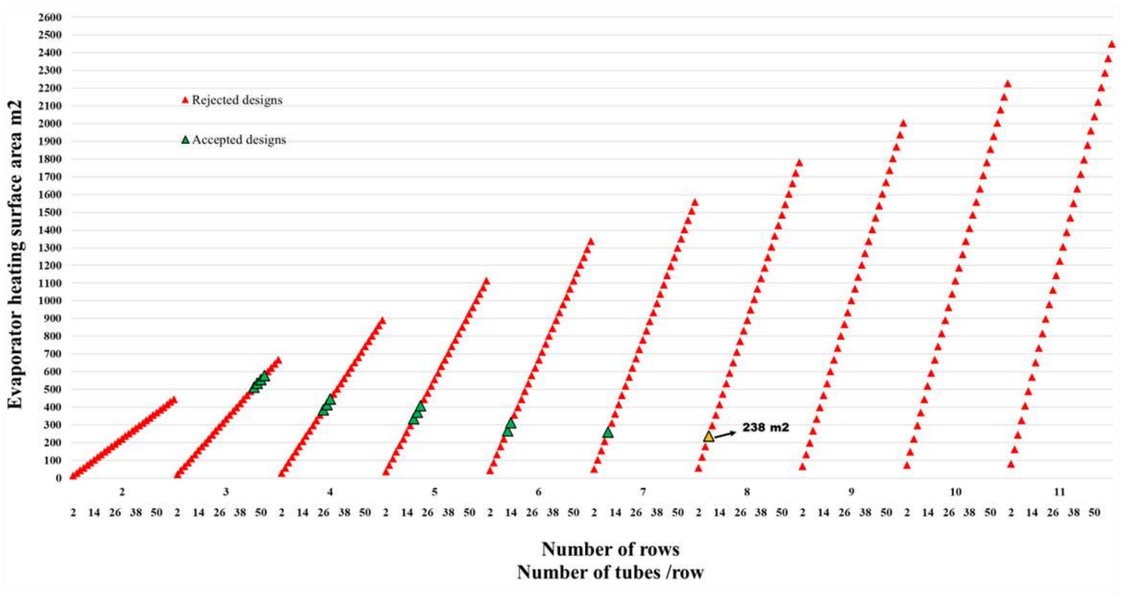

Figure 5.17. Evaporator heating surface area m2 diagram R123

Figure 5.17 provides a representation of the heating surface area for each of the 300 evaporator designs based on the total number of tube rows and the total number of tubes in one row. It is worth noting that only 14 designs satisfy all the previous limitations and can be considered as good evaporator designs, and these designs are represented as green and yellow triangles in the figure. Conversely, the rejected designs, which failed to pass one or more of the previous tests, are shown as red triangles. The optimum design that is associated with the yellow triangle with the minimum surface area of 238 m2, corresponding to 8 tubes in one row and 8 number of tube rows. This design ensures the lowest possible cost and investment while also maintaining the required performance, making it the ideal choice for the evaporator. As such, the optimization process for the heating surface area of the evaporator has yielded a favorable result that can lead to significant cost savings and improved efficiency. Therefore, it can be concluded that the optimization of the heating surface area is a critical aspect of the evaporator design process that must be carefully considered.

Table 5.5. Finned tube evaporator design results with R123

NO	$N_{tube/raw}$	N_{raw}	N_{total}	Error	ΔP_t	ΔP_s	A	$\dot{Q}_{est}$	Design Test Result
	#	#	#	%	bar	bar	m^2	kW	accepted/not accepted
1	2	2	4	-89.15	0.298	0.344	14.85	225.21	not accepted
2	4	2	8	-82.52	0.081	0.095	29.70	362.75	not accepted
⋮	⋮	⋮	⋮	⋮	⋮	⋮	⋮	⋮	⋮
53	46	3	138	2.00	0.001	0.001	512.35	2117.23	accepted design
54	48	3	144	4.31	0.001	0.001	534.63	2165.09	accepted design
55	50	3	150	6.57	0.001	0.001	556.90	2212.03	accepted design
56	52	3	156	8.78	0.001	0.001	579.18	2258.08	accepted design
57	54	3	162	10.96	0.001	0.001	601.45	2303.30	not accepted
⋮	⋮	⋮	⋮	⋮	⋮	⋮	⋮	⋮	⋮
72	24	4	96	-6.12	0.007	0.004	356.42	1948.76	not accepted
73	26	4	104	0.75	0.006	0.003	386.12	2091.35	accepted design
74	28	4	112	4.76	0.005	0.003	415.82	2174.62	accepted design
75	30	4	120	8.64	0.005	0.002	445.52	2255.05	accepted design
76	32	4	128	12.39	0.004	0.002	475.22	2332.91	not accepted
⋮	⋮	⋮	⋮	⋮	⋮	⋮	⋮	⋮	⋮
99	18	5	90	3.66	0.015	0.006	334.14	2151.80	accepted design
100	20	5	100	9.63	0.013	0.005	371.27	2275.66	accepted design
101	22	5	110	5.20	0.011	0.004	408.39	2183.63	accepted design
102	24	5	120	17.35	0.009	0.004	445.52	2435.96	not accepted
⋮	⋮	⋮	⋮	⋮	⋮	⋮	⋮	⋮	⋮
125	10	6	60	-9.42	0.057	0.018	222.76	1880.25	not accepted
126	12	6	72	0.06	0.040	0.013	267.31	2077.00	accepted design
127	14	6	84	8.75	0.030	0.010	311.86	2257.37	accepted design
128	16	6	96	16.82	0.023	0.007	356.42	2424.94	not accepted
⋮	⋮	⋮	⋮	⋮	⋮	⋮	⋮	⋮	⋮
154	8	7	56	-6.61	0.103	0.027	207.91	1938.54	not accepted
155	10	7	70	5.68	0.067	0.018	259.89	2193.63	accepted design
156	12	7	84	16.74	0.048	0.013	311.86	2423.17	not accepted
⋮	⋮	⋮	⋮	⋮	⋮	⋮	⋮	⋮	⋮
183	6	8	48	-9.32	0.205	0.045	178.21	1882.34	not accepted
184	**8**	**8**	**64**	**6.73**	**0.119**	**0.027**	**237.61**	**2215.48**	**accepted design***
⋮	⋮	⋮	⋮	⋮	⋮	⋮	⋮	⋮	⋮
298	56	11	616	314.72	0.004	0.001	2287.01	8608.37	not accepted
299	58	11	638	322.43	0.004	0.001	2368.69	8768.59	not accepted
300	60	11	660	330.03	0.004	0.001	2450.37	8926.23	not accepted

*Minimal evaporator area, ideal choice-lowest cost

** All the evaporator design calculations are carried out assuming P2=22bar R123.

5.4.1.4 Evaporator optimization procedure for R236fa

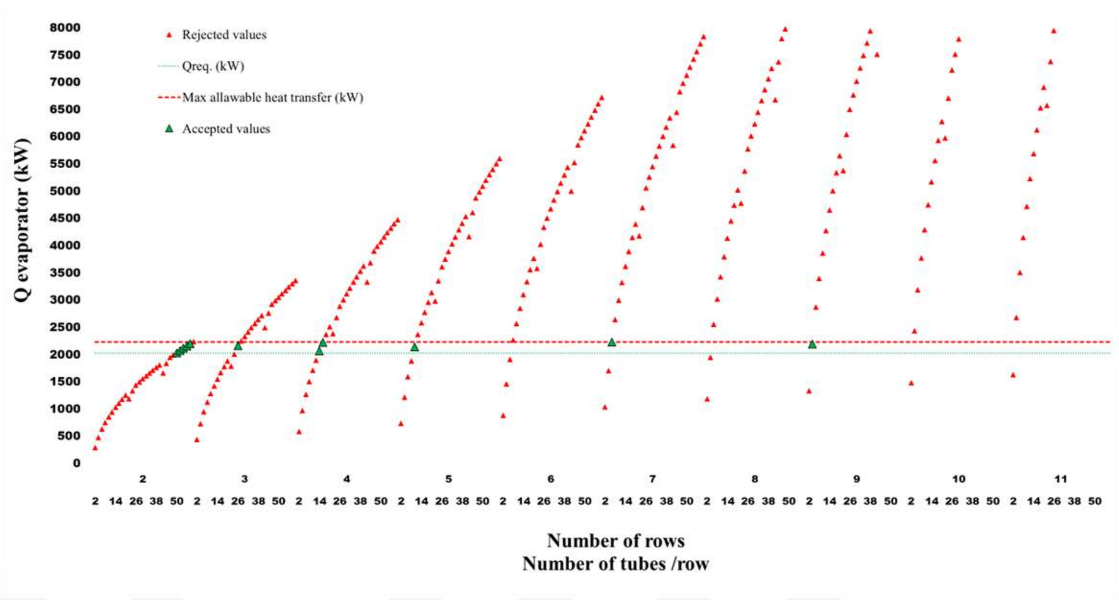

Figure 5.18. Evaporator heat transfer rate (kW) with R236fa

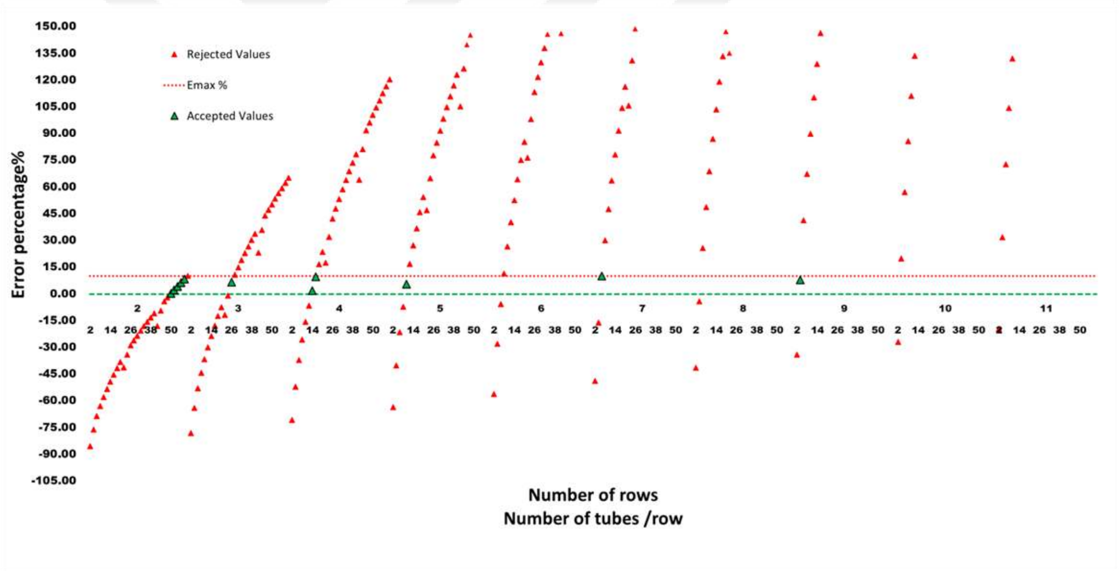

Figure 5.19. Evaporator design error% diagram R236fa

Figure 5.18 indicates 300 designs for evaporator and each design corrosponds to certain prameters including the number of tube rows, the number of tubes in one row that are poltted on horizontal axis, while the heating duty of the evaporator is poltted on vertical axis. In horizontal axis, Starting with two tubes in one row, this number was gradually increased until 60, at which point the number of rows was increased by one, and the process was repeated until a total of 11 rows were achieved. In this way, a total of 300 evaporator designs were evaluated based on their heating duty. The minimum accepted heating duty was calculated in Table 3.2 to be 2036 kW, and the maximum accepted value of 10% more than the required value which is equal to 2239.6 kW. The resulting designs were plotted in Figure 5.18, with the red and green points indicating the attempted evaporator designs, and the green dashed line representing the minimum required heating duty. Additionally, the red dashed line represented the maximum accepted value for the heating duty. Out of the 300 designs attempted, only 11 of them fell within the accepted range and were highlighted in green, while the others were outside the accepted range and were shown in red.

Figure 5.19 showcases the percentage design error of each evaporator design in relation to the total number of tube rows and the total number of tubes in one row. The maximum allowable design error is indicated by a red dashed line at 10%. The green triangles indicate evaporator designs that have a design error value of less than 10%, while the red triangles indicate designs that exceed the maximum allowable limit or have negative values. The results show that only 11 designs in green color passed this limitation successfully, indicating their ability to satisfy the desired design criteria. On the other hand, the remaining designs in red color had values greater than 10% or less than zero, indicating their unsuitability for use in the proposed system. This limitation insured that the accepted green designs were out of overdesigning or underdesigning.

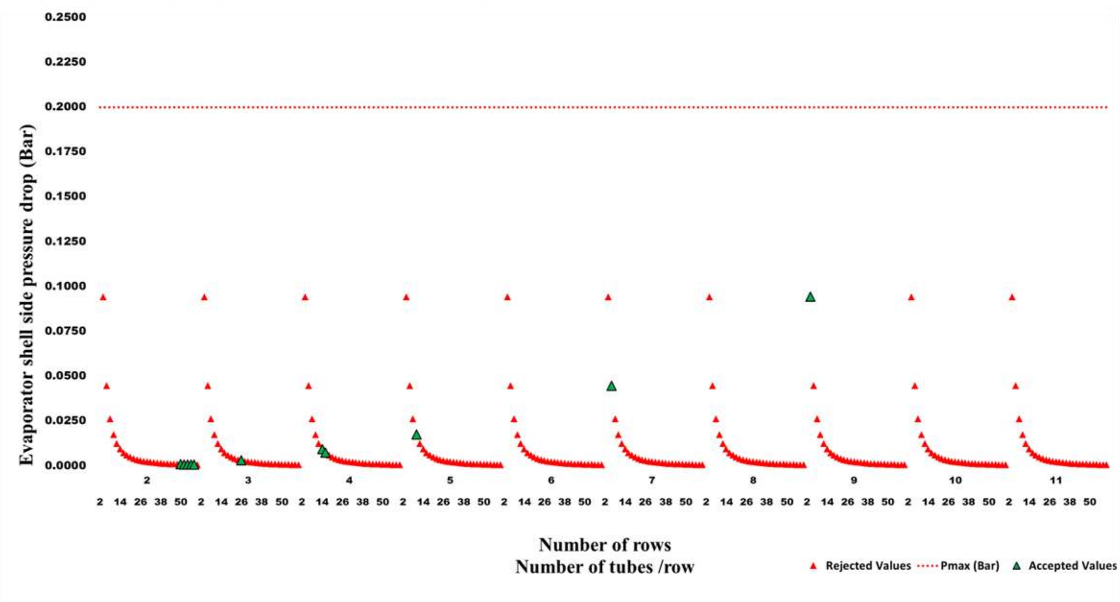

Figure 5.20. Shell side pressure drop through the evaporator with R236fa

In Figure 5.20, the shell side pressure drop is presented for each evaporator design, corresponding to the total number of tube rows and the total number of tubes in one row for each evaporator design. The maximum allowable shell side pressure drop of

0.2 bar is indicated by a red dashed line. Designs that passed all previous tests and have a shell side pressure drop value less than 0.2 bar are represented by green triangles. Conversely, designs that did not pass one of the previous tests or have a value of more than 0.2 bar are represented by red triangles. It is clear from this figure that only the 11 designs out of 300 that passed all the previous tests that are depicted in green color, while the rejected designs are shown in red triangles, even if they have a value of shell side pressure drop less than 0.2 bar, as they did not pass the previous limitations.

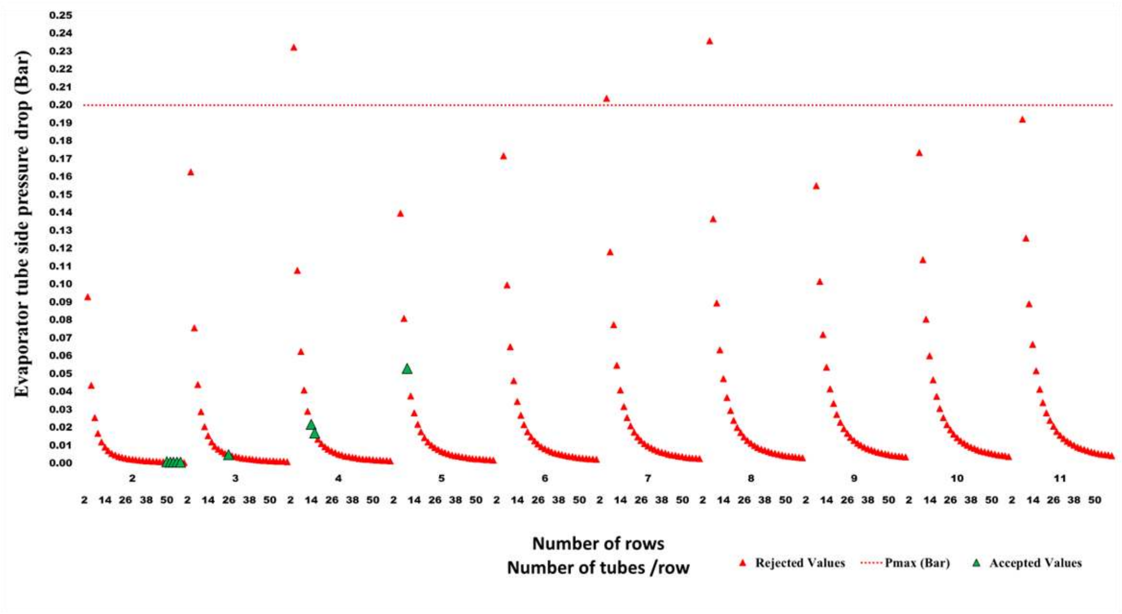

Figure 5.21. Tube side pressure drop through the evaporator with R236fa

Figure 5.21 above depicts the tube side pressure drop for each evaporator design obtained through our methodology, considering the total number of tube rows and the total number of tubes in one row. The maximum allowable tube side pressure drop is denoted by a red dashed line at 0.2 bar. The successful designs that passed all the previous limitations and also have a tube side pressure drop value less than 0.2 bar are depicted as green triangles. On the other hand, the rejected designs that failed to pass one of the previous limitations or have a tube side pressure drop value more than 0.2 bar are indicated as red triangles. It is apparent from this figure that out of the 300 designs obtained through our methodology, only 9 designs were able to pass all the limitations successfully and are represented as green triangles, indicating their acceptability for further consideration.

The results of the evaporator optimization procedure are indicated in the following chart in case of heating surface area as it is the last step in the optimization process, in which all the perfect designs that successfully passed all the limitations suggested in this study are shown as green triangles while the optimal desing which has successfully passed all the tests and has the smallest area among other accepted designs is in yellow color.

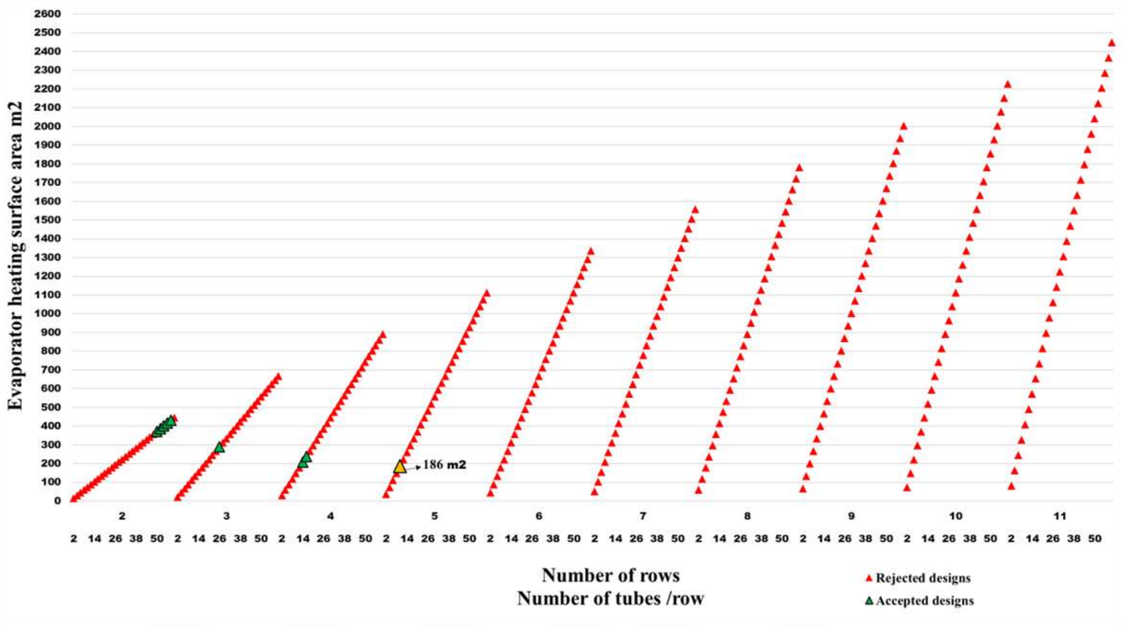

Figure 5.22. Evaporator heating surface area m2 diagram R236fa

Figure 5.22 provides a representation of the heating surface area for each of the 300 evaporator designs based on the total number of tube rows and the total number of tubes in one row. It is worth noting that only 9 designs satisfy all the previous limitations and can be considered as good evaporator designs, and these designs are represented as green and yellow triangles in the figure. Conversely, the rejected designs, which failed to pass one or more of the previous tests, are shown as red triangles. The optimum design that is associated with the yellow triangle with the minimum surface area of 186 m2, corresponding to 10 tubes in one row and 5 number of tube rows. This design ensures the lowest possible cost and investment while also maintaining the required performance, making it the ideal choice for the evaporator. As such, the optimization process for the heating surface area of the evaporator has yielded a favorable result that can lead to significant cost savings and improved efficiency. Therefore, it can be concluded that the optimization of the heating surface area is a critical aspect of the evaporator design process that must be carefully considered.

Table 5.6. Finned tube evaporator design results with R236fa

NO	$N_{tube/raw}$	N_{raw}	N_{total}	Error	ΔP_t	ΔP_s	A	$\dot{Q}_{est}$	Design Test Result
	#	#	#	%	bar	bar	m^2	kW	accepted/not accepted
1	2	2	4	-85.359662	0.34225091	0.3401664	14.8507083	298.025572	not accepted
2	4	2	8	-76.0143743	0.0930251	0.09435423	29.7014166	488.262624	not accepted
⋮	⋮	⋮	⋮	⋮	⋮	⋮	⋮	⋮	⋮
25	50	2	100	0.23550098	0.00086695	0.0009291	371.267708	2040.44077	accepted design
26	52	2	104	2.30317002	0.00080703	0.00086528	386.118416	2082.53121	accepted design
27	54	2	108	4.33140699	0.00075331	0.00080802	400.969124	2123.81895	accepted design
28	56	2	112	6.32239121	0.00070495	0.00075644	415.819833	2164.34836	accepted design
29	58	2	116	8.2781052	0.00066126	0.0007098	430.670541	2204.15979	accepted design
30	60	2	120	10.2003587	0.00062163	0.00066749	445.521249	2243.29008	not accepted
⋮	⋮	⋮	⋮	⋮	⋮	⋮	⋮	⋮	⋮
43	26	3	78	6.63997131	0.00485228	0.00305107	289.588812	2170.81317	accepted design
⋮	⋮	⋮	⋮	⋮	⋮	⋮	⋮	⋮	⋮
66	12	4	48	-6.4842891	0.02910823	0.01252448	178.2085	1903.64958	not accepted
67	14	4	56	1.82925321	0.02178348	0.00944576	207.909916	2072.88394	accepted design
68	16	4	64	9.54379543	0.0169519	0.00739953	237.611333	2229.92477	accepted design
69	18	4	72	16.7719991	0.01359139	0.00596697	267.31275	2377.06547	not accepted
⋮	⋮	⋮	⋮	⋮	⋮	⋮	⋮	⋮	⋮
95	**10**	**5**	**50**	**5.55092338**	**0.05313422**	**0.01749195**	**185.633854**	**2148.644**	**accepted design***
⋮	⋮	⋮	⋮	⋮	⋮	⋮	⋮	⋮	⋮
299	58	11	638	495.529579	0.0045893	0.0007098	2368.68798	12122.8788	not accepted
300	60	11	660	506.101973	0.00430761	0.00066749	2450.36687	12338.0954	not accepted

*Minimal evaporator area, ideal choice-lowest cost

** All the evaporator design calculations are carried out assuming P2=22bar.

5.4.1.5 Evaporator optimization procedure for R142b

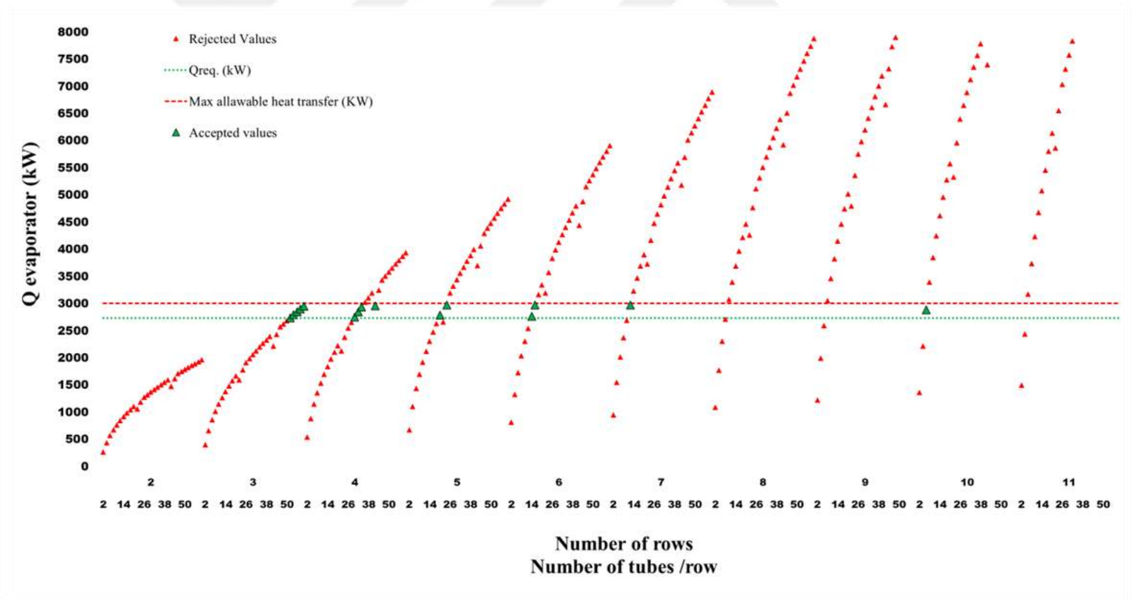

Figure 5.23. Evaporator heat transfer rate (kW) R142b

Figure 5.23 indicates 300 designs for evaporator and each design corrosponds to certain prameters including the number of tube rows, the number of tubes in one row that are poltted on horizontal axis, while the heating duty of the evaporator is poltted on vertical axis. In horizontal axis, Starting with two tubes in one row, this number was gradually increased until 60, at which point the number of rows was increased by one, and the process was repeated until a total of 11 rows were achieved. In this way, a total of 300 evaporator designs were evaluated based on their heating duty. The minimum accepted heating duty was calculated in Table 3.2 to be 2738.71 kW, and the maximum accepted value of 10% more than the required value which is equal to 3012.57 kW. The resulting designs were plotted in Figure 5.23, with the red and green points indicating the attempted evaporator designs, and the green dashed line representing the minimum required heating duty. Additionally, the red dashed line represented the maximum accepted value for the heating duty. Out of the 300 designs attempted, only 15 of them fell within the accepted range and were highlighted in green, while the others were outside the accepted range and were shown in red.

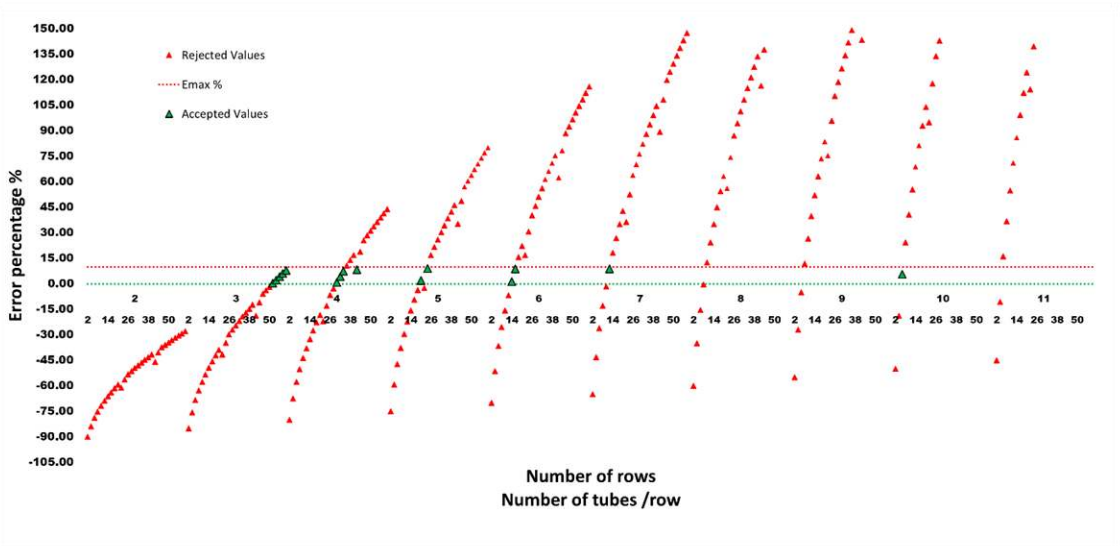

Figure 5.24. Evaporator design error% diagram R142b

Figure 5.24 represents the percentage design error of each evaporator design in relation to the total number of tube rows and the total number of tubes in one row. The maximum allowable design error is indicated by a red dashed line at 10%. The green triangles indicate evaporator designs that have a design error value of less than 10%, while the red triangles indicate designs that exceed the maximum allowable limit or have negative values. The results show that only 15 designs in green color passed this limitation successfully, indicating their ability to satisfy the desired design criteria. On the other hand, the remaining designs in red color had values greater than 10% or less than zero, indicating their unsuitability for use in the proposed system. This limitation insured that the accepted green designs were out of overdesigning or underdesigning.

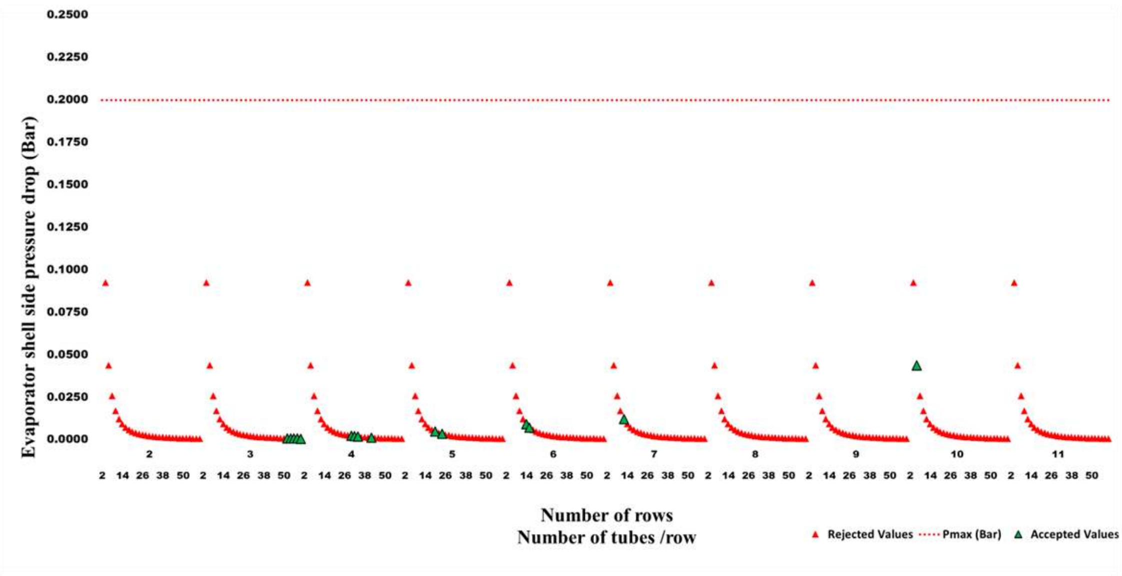

Figure 5.25. Shell side pressure drop through the evaporator R142b

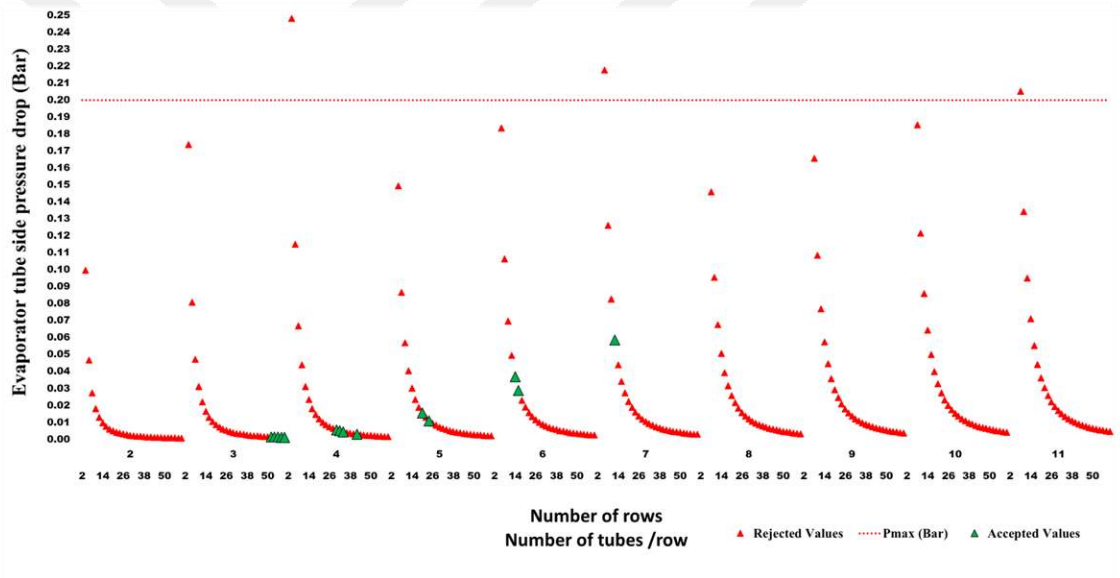

Figure 5.26. Tube side pressure drop through the evaporator with R142b

In Figure 5.25, the shell side pressure drop is presented for each evaporator design, corresponding to the total number of tube rows and the total number of tubes in one row for each evaporator design. The maximum allowable shell side pressure drop of 0.2 bar is indicated by a red dashed line. Designs that passed all previous tests and have a shell side pressure drop value less than 0.2 bar are represented by green triangles. Conversely, designs that did not pass one of the previous tests or have a value of more than 0.2 bar are represented by red triangles. It is clear from this figure that only the 15 designs out of 300 that passed all the previous tests that are depicted in green color, while the rejected designs are shown in red triangles, even if they have a value of shell side pressure drop less than 0.2 bar, as they did not pass the previous limitations.

Figure 5.26 depicts the tube side pressure drop for each evaporator design obtained through our methodology, considering the total number of tube rows and the total number of tubes in one row. The maximum allowable tube side pressure drop is denoted by a red dashed line at 0.2 bar. The successful designs that passed all the previous limitations and also have a tube side pressure drop value less than 0.2 bar are depicted as green triangles. On the other hand, the rejected designs that failed to pass one of the previous limitations or have a tube side pressure drop value more than 0.2 bar are indicated as red triangles. It is apparent from this figure that out of the 300 designs obtained through our methodology, only 14 designs were able to pass all the limitations successfully and are represented as green triangles, indicating their acceptability for further consideration.

The results of the evaporator optimization procedure are indicated in the following chart in case of heating surface area as it is the last step in the optimization process, in which all the perfect designs that successfully passed all the limitations suggested in this study are shown as green triangles while the optimal desing which has successfully passed all the tests and has the smallest area among other accepted designs is in yellow color.

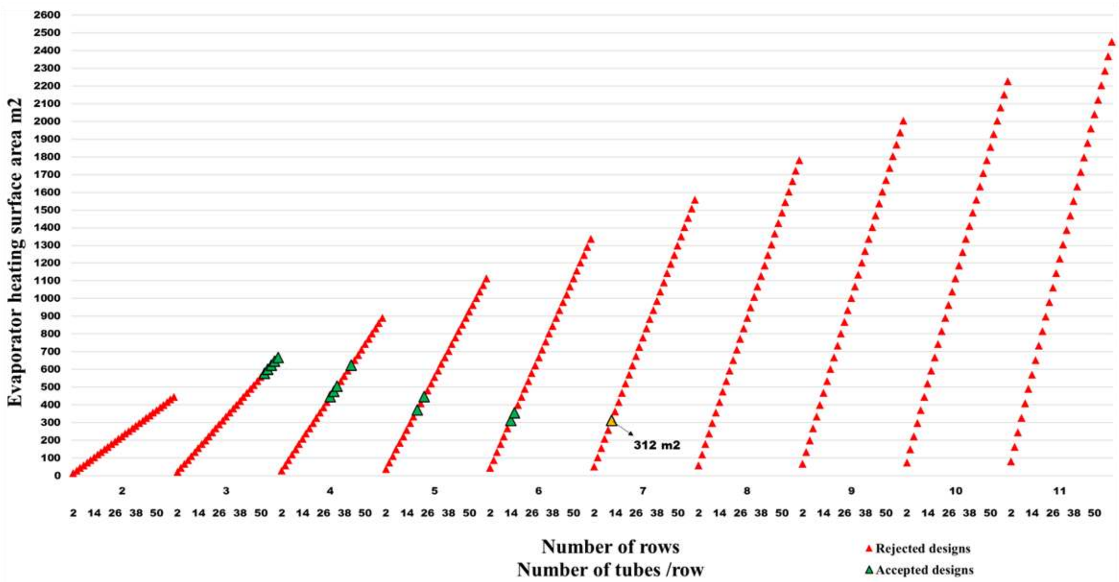

Figure 5.27. Evaporator heating surface area m2 diagram R142b

Figure 5.27 provides a representation of the heating surface area for each of the 300 evaporator designs based on the total number of tube rows and the total number of tubes in one row. It is worth noting that only 14 designs satisfy all the previous limitations and can be considered as good evaporator designs, and these designs are represented as green and yellow triangles in the figure. Conversely, the rejected designs, which failed to pass one or more of the previous tests, are shown as red triangles. The optimum design that is associated with the yellow triangle with the minimum surface area of 312 m2, corresponding to 12 tubes in one row and 7 number of tube rows. This design ensures the lowest possible cost and investment while also maintaining the required performance, making it the ideal choice for the evaporator. As such, the optimization process for the heating surface area of the evaporator has yielded a favorable result that can lead to significant cost savings and improved efficiency. Therefore, it can be concluded that the optimization of the heating surface area is a critical aspect of the evaporator design process that must be carefully considered.

Table 5.7. Finned tube evaporator design results with R142b

NO	$N_{tube/raw}$	N_{raw}	N_{total}	Error	ΔP_t	ΔP_s	A	$\dot{Q}_{est}$	Design Test Result
	#	#	#	%	bar	bar	m^2	kW	accepted/not accepted
1	2	2	4	-89.97	0.366	0.333	14.85	274.57	not accepted
2	4	2	8	-83.75	0.100	0.092	29.70	444.91	not accepted
⋮	⋮	⋮	⋮	⋮	⋮	⋮	⋮	⋮	⋮
56	52	3	156	0.36	0.001	0.001	579.18	2748.55	accepted design
57	54	3	162	2.33	0.001	0.001	601.45	2802.42	accepted design
58	56	3	168	4.26	0.001	0.001	623.73	2855.32	accepted design
59	58	3	174	6.16	0.001	0.001	646.01	2907.31	accepted design
60	60	3	180	8.02	0.001	0.001	668.28	2958.43	accepted design
⋮	⋮	⋮	⋮	⋮	⋮	⋮	⋮	⋮	⋮
73	26	4	104	-6.42	0.007	0.003	386.12	2562.90	not accepted
74	28	4	112	-2.75	0.006	0.003	415.82	2663.33	not accepted
75	30	4	120	0.78	0.006	0.002	445.52	2760.18	accepted design
76	32	4	128	4.20	0.005	0.002	475.22	2853.83	accepted design
77	34	4	136	7.52	0.004	0.002	504.92	2944.59	accepted design
78	36	4	144	10.73	0.004	0.002	534.63	3032.71	not accepted
79	38	4	152	13.86	0.004	0.001	564.33	3118.42	not accepted
80	40	4	160	16.91	0.003	0.001	594.03	3201.93	not accepted
81	42	4	168	8.26	0.003	0.001	623.73	2965.04	accepted design
82	44	4	176	18.99	0.003	0.001	653.43	3258.72	not accepted
83	46	4	184	25.63	0.003	0.001	683.13	3440.77	not accepted
84	48	4	192	28.42	0.002	0.001	712.83	3516.93	not accepted
⋮	⋮	⋮	⋮	⋮	⋮	⋮	⋮	⋮	⋮
97	14	5	70	-15.53	0.030	0.009	259.89	2313.47	not accepted
98	16	5	80	-9.30	0.023	0.007	297.01	2483.92	not accepted
99	18	5	90	-3.48	0.019	0.006	334.14	2643.45	not accepted
100	20	5	100	2.02	0.015	0.005	371.27	2793.93	accepted design
101	22	5	110	-2.50	0.013	0.004	408.39	2670.32	not accepted
102	24	5	120	8.95	0.011	0.003	445.52	2983.89	accepted design
103	26	5	130	16.98	0.009	0.003	482.65	3203.62	not accepted
104	28	5	140	21.56	0.008	0.003	519.77	3329.16	not accepted
⋮	⋮	⋮	⋮	⋮	⋮	⋮	⋮	⋮	⋮
126	12	6	72	-6.69	0.049	0.012	267.31	2555.41	not accepted
127	14	6	84	1.37	0.037	0.009	311.86	2776.17	accepted design
128	16	6	96	8.84	0.029	0.007	356.42	2980.70	accepted design
129	18	6	108	15.83	0.023	0.006	400.97	3172.14	not accepted
130	20	6	120	22.42	0.019	0.005	445.52	3352.72	not accepted
131	22	6	132	17.00	0.016	0.004	490.07	3204.39	not accepted
⋮	⋮	⋮	⋮	⋮	⋮	⋮	⋮	⋮	⋮
154	8	7	56	-12.90	0.126	0.026	207.91	2385.49	not accepted
155	10	7	70	-1.43	0.083	0.017	259.89	2699.56	not accepted
156	**12**	**7**	**84**	**8.86**	**0.059**	**0.012**	**311.86**	**2981.31**	**accepted design***
157	14	7	98	18.26	0.044	0.009	363.84	3238.86	not accepted
158	16	7	112	26.98	0.034	0.007	415.82	3477.49	not accepted
⋮	⋮	⋮	⋮	⋮	⋮	⋮	⋮	⋮	⋮
299	58	11	638	289.24	0.005	0.001	2368.69	10660.12	not accepted
300	60	11	660	296.08	0.005	0.001	2450.37	10847.57	not accepted

*Minimal evaporator area, ideal choice-lowest cost

5.4.1.6 Evaporator optimization procedure for R600a

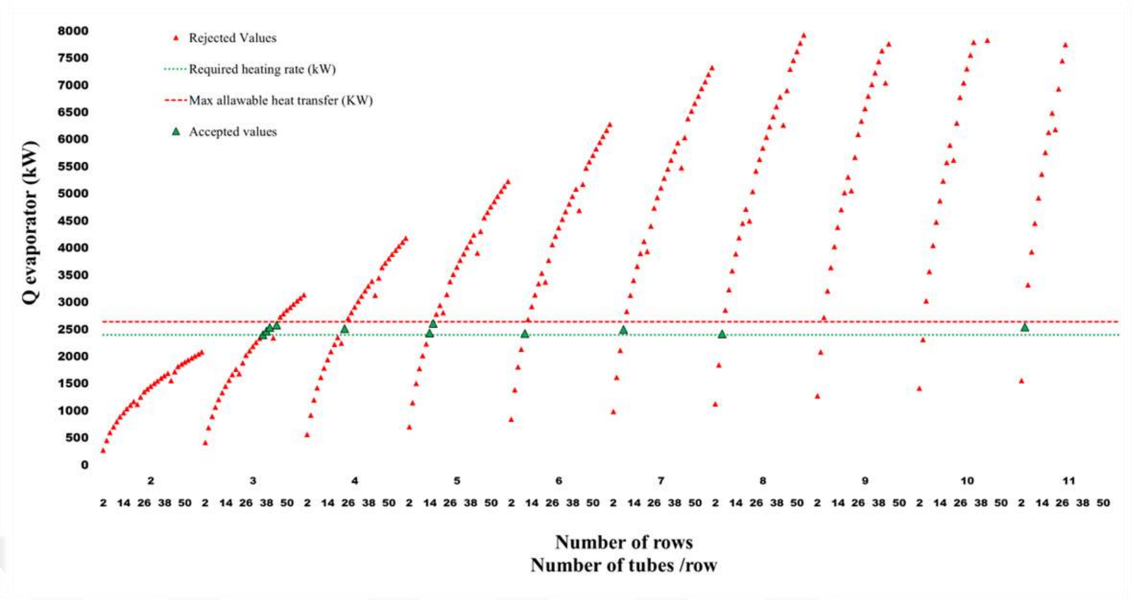

Figure 5.28. Evaporator heat transfer rate (kW) R600a

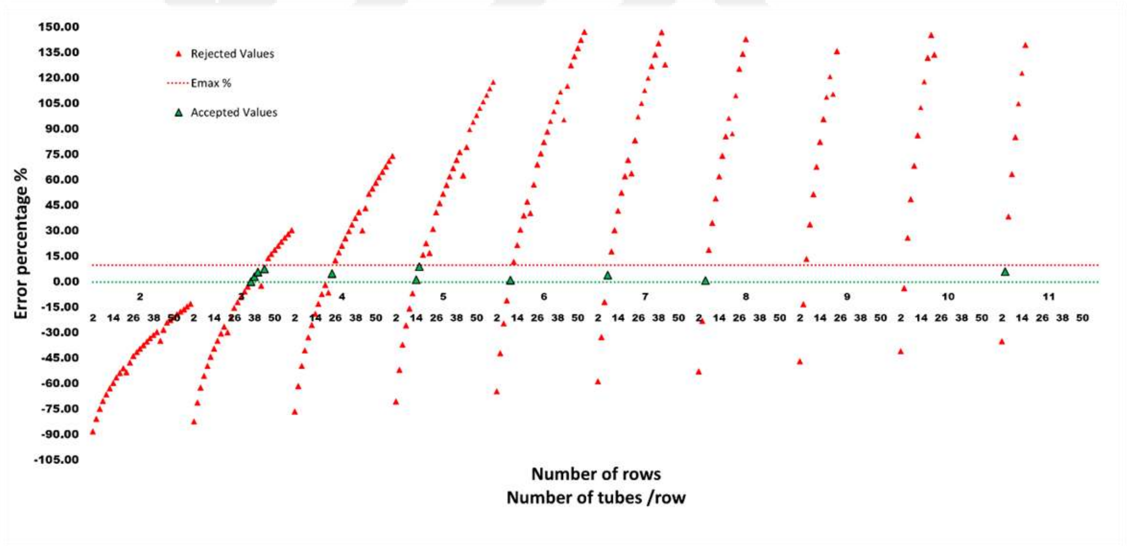

Figure 5.29. Evaporator design error% diagram R600a

Figure 5.28 indicates 300 designs for evaporator and each design corrosponds to certain prameters including the number of tube rows, the number of tubes in one row that are poltted on horizontal axis, while the heating duty of the evaporator is poltted on vertical axis. In horizontal axis, Starting with two tubes in one row, this number was gradually increased until 60, at which point the number of rows was increased by one, and the process was repeated until a total of 11 rows were achieved. In this way, a total of 300 evaporator designs were evaluated based on their heating duty. The minimum accepted heating duty was calculated in Table 3.2 to be 2406.22 kW, and the maximum accepted value of 10% more than the required value which is equal to 2646.8 kW. The resulting designs were plotted in Figure 5.28, with the red and green points indicating the attempted evaporator designs, and the green dashed line representing the minimum required heating duty. Additionally, the red dashed line represented the maximum accepted value for the heating duty. Out of the 300 designs attempted, only 11 of them fell within the accepted range and were highlighted in green, while the others were outside the accepted range and were shown in red.

Figure 5.29 showcases the percentage design error of each evaporator design in relation to the total number of tube rows and the total number of tubes in one row. The maximum allowable design error is indicated by a red dashed line at 10%. The green triangles indicate evaporator designs that have a design error value of less than 10%, while the red triangles indicate designs that exceed the maximum allowable limit or have negative values. The results show that only 11 designs in green color passed this limitation successfully, indicating their ability to satisfy the desired design criteria. On the other hand, the remaining designs in red color had values greater than 10% or less than zero, indicating their unsuitability for use in the proposed system. This limitation insured that the accepted green designs were out of overdesigning or underdesigning.

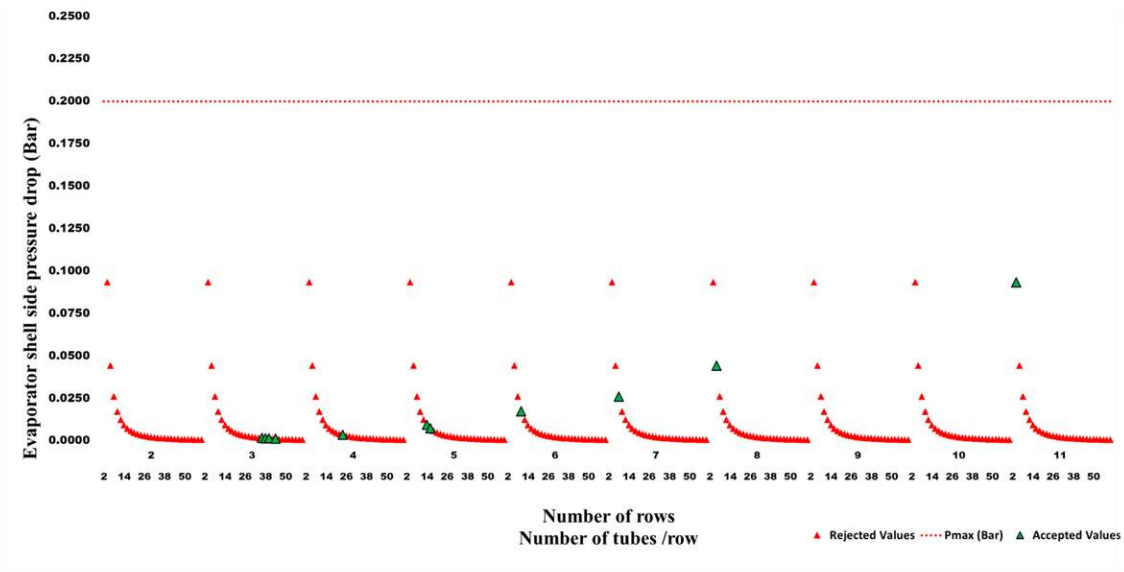

Figure 5.30. Shell side pressure drop through the evaporator R600a

In Figure 5.30, the shell side pressure drop is presented for each evaporator design, corresponding to the total number of tube rows and the total number of tubes in one row for each evaporator design. The maximum allowable shell side pressure drop of 0.2 bar is indicated by a red dashed line. Designs that passed all previous tests and have a shell side pressure drop value less than 0.2 bar are represented by green triangles. Conversely, designs that did not pass one of the previous tests or have a value of more than 0.2 bar are represented by red triangles. It is clear from this figure that only the 11 designs out of 300 that passed all the previous tests that are depicted in green color, while the rejected designs are shown in red triangles, even if they have a value of shell side pressure drop less than 0.2 bar, as they did not pass the previous limitations.

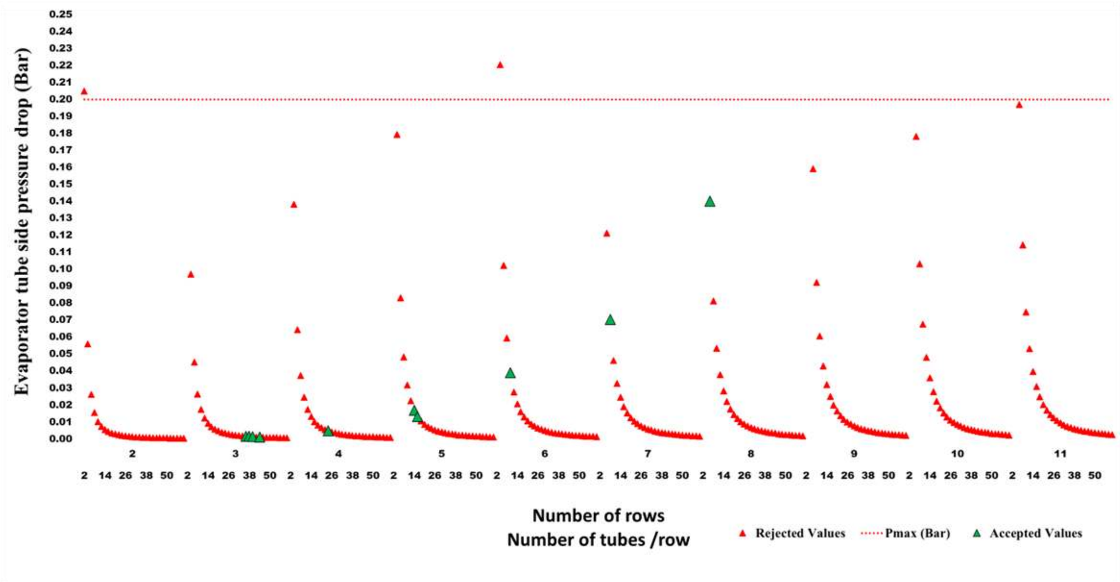

Figure 5.31. Tube side pressure drop through the evaporator with R600a

Figure 5.31 indicates the tube side pressure drop for each evaporator design obtained through our methodology, considering the total number of tube rows and the total number of tubes in one row. The maximum allowable tube side pressure drop is denoted by a red dashed line at 0.2 bar. The successful designs that passed all the previous limitations and also have a tube side pressure drop value less than 0.2 bar are depicted as green triangles. On the other hand, the rejected designs that failed to pass one of the previous limitations or have a tube side pressure drop value more than 0.2 bar are indicated as red triangles. It is apparent from this figure that out of the 300 designs obtained through our methodology, only 10 designs were able to pass all the limitations successfully and are represented as green triangles, indicating their acceptability for further consideration.

The results of the evaporator optimization procedure are indicated in the following chart in case of heating surface area as it is the last step in the optimization process, in which all the perfect designs that successfully passed all the limitations suggested in this study are shown as green triangles while the optimal desing which has successfully passed all the tests and has the smallest area among other accepted designs is in yellow color.

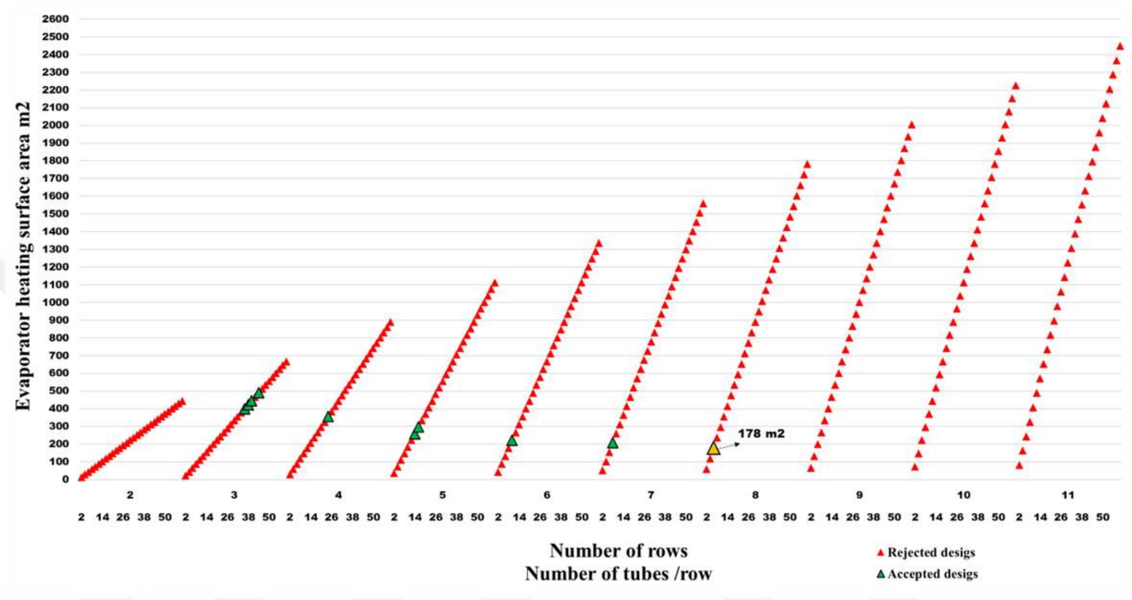

Figure 5.32. Evaporator heating surface area m2 diagram R600a

Figure 5.32 provides a representation of the heating surface area for each of the 300 evaporator designs based on the total number of tube rows and the total number of tubes in one row. It is worth noting that only 10 designs satisfy all the previous limitations and can be considered as good evaporator designs, and these designs are represented as green and yellow triangles in the figure. Conversely, the rejected designs, which failed to pass one or more of the previous tests, are shown as red triangles. The optimum design that is associated with the yellow triangle with the minimum surface area of 178 m2, corresponding to 6 tubes in one row and 8 number of tube rows. This design ensures the lowest possible cost and investment while also maintaining the required performance, making it the ideal choice for the evaporator. As such, the optimization process for the heating surface area of the evaporator has yielded a favorable result that can lead to significant cost savings and improved efficiency. Therefore, it can be concluded that the optimization of the heating surface area is a critical aspect of the evaporator design process that must be carefully considered.

Table 5.8. Finned tube evaporator design results with R600a

NO	$N_{tube/raw}$	N_{raw}	N_{total}	Error	ΔP_t	ΔP_s	A	$\dot{Q}_{est}$	Design Test Result
	#	#	#	%	bar	bar	m^2	kW	accepted/not accepted
1	2	2	4	-88.16	0.205	0.337	14.85	285.00	not accepted
2	4	2	8	-80.70	0.056	0.093	29.70	464.42	not accepted
⋮	⋮	⋮	⋮	⋮	⋮	⋮	⋮	⋮	⋮
47	34	3	102	-2.68	0.002	0.002	378.69	2341.63	not accepted
48	36	3	108	0.25	0.002	0.002	400.97	2412.35	accepted design
49	38	3	114	3.11	0.001	0.002	423.25	2481.12	accepted design
50	40	3	120	5.90	0.001	0.001	445.52	2548.11	accepted design
51	42	3	126	-2.25	0.001	0.001	467.80	2352.05	not accepted
52	44	3	132	7.70	0.001	0.001	490.07	2591.44	accepted design
53	46	3	138	13.86	0.001	0.001	512.35	2739.64	not accepted
⋮	⋮	⋮	⋮	⋮	⋮	⋮	⋮	⋮	⋮
71	22	4	88	-6.36	0.006	0.004	326.72	2253.16	not accepted
72	24	4	96	4.89	0.005	0.003	356.42	2523.97	accepted design
73	26	4	104	12.78	0.004	0.003	386.12	2713.63	not accepted
⋮	⋮	⋮	⋮	⋮	⋮	⋮	⋮	⋮	⋮
96	12	5	60	-6.78	0.023	0.012	222.76	2243.06	not accepted
97	14	5	70	1.39	0.017	0.009	259.89	2439.61	accepted design
98	16	5	80	8.96	0.013	0.007	297.01	2621.85	accepted design
99	18	5	90	16.05	0.011	0.006	334.14	2792.49	not accepted
⋮	⋮	⋮	⋮	⋮	⋮	⋮	⋮	⋮	⋮
124	8	6	48	-10.77	0.059	0.026	178.21	2147.02	not accepted
125	10	6	60	1.15	0.039	0.017	222.76	2433.92	accepted design
126	12	6	72	11.86	0.028	0.012	267.31	2691.68	not accepted
⋮	⋮	⋮	⋮	⋮	⋮	⋮	⋮	⋮	⋮
153	6	7	42	-11.81	0.121	0.044	155.93	2122.01	not accepted
154	8	7	56	4.10	0.070	0.026	207.91	2504.85	accepted design
155	10	7	70	18.01	0.046	0.017	259.89	2839.57	not accepted
⋮	⋮	⋮	⋮	⋮	⋮	⋮	⋮	⋮	⋮
182	4	8	32	-22.80	0.303	0.093	118.81	1857.69	not accepted
183	**6**	**8**	**48**	**0.79**	**0.140**	**0.044**	**178.21**	**2425.15**	**accepted design***
184	8	8	64	18.97	0.081	0.026	237.61	2862.69	not accepted
⋮	⋮	⋮	⋮	⋮	⋮	⋮	⋮	⋮	⋮
299	58	11	638	370.66	0.003	0.001	2368.69	11325.00	not accepted
300	60	11	660	378.97	0.003	0.001	2450.37	11525.05	not accepted

*Minimal evaporator area, ideal choice-lowest cost

** All the evaporator design calculations are carried out assuming P2=22bar R600a.

5.4.2 Design optimization procedure for preheater

Table 5.9. Preheater's fixed properties and parameters

Tube fixed geometries	
Do (mm)	57.15
Din (mm)	53.8
Ltube (mm)	2000
Material	Carbon steel
Fin fixed geometries	
Df (mm)	89.6
Lf (mm)	15.8
tf (mm)	0.4
S (mm)	4
Material	Alaminum
Dbend	3 x Do
Tube layout	Staggered (°60)

Nr= (2 – 21) raws & nt=(2-60) tubes per rows

$Nt = Nr \; X \; nt$; $(\mathbf{2x2, 2x4, 2x6} \ldots\ldots\ldots\ldots\ldots\ldots\ldots\ldots\ldots\ldots. \mathbf{21x60})$

(600 design) attempted in all calculations for preheater and each design is tested by previous mentioned limitations.

In contrast to the evaporator design process, the optimization procedure for preheater design involved analyzing 600 designs. In the figures, the number of tube rows starts at 7, as the acceptable designs start to appear after this value. The results are presented in the figure, where the heating duty is plotted against the number of tubes in one row and number of rows for each preheater design.

5.4.2.1 Preheater optimization procedure for R245fa

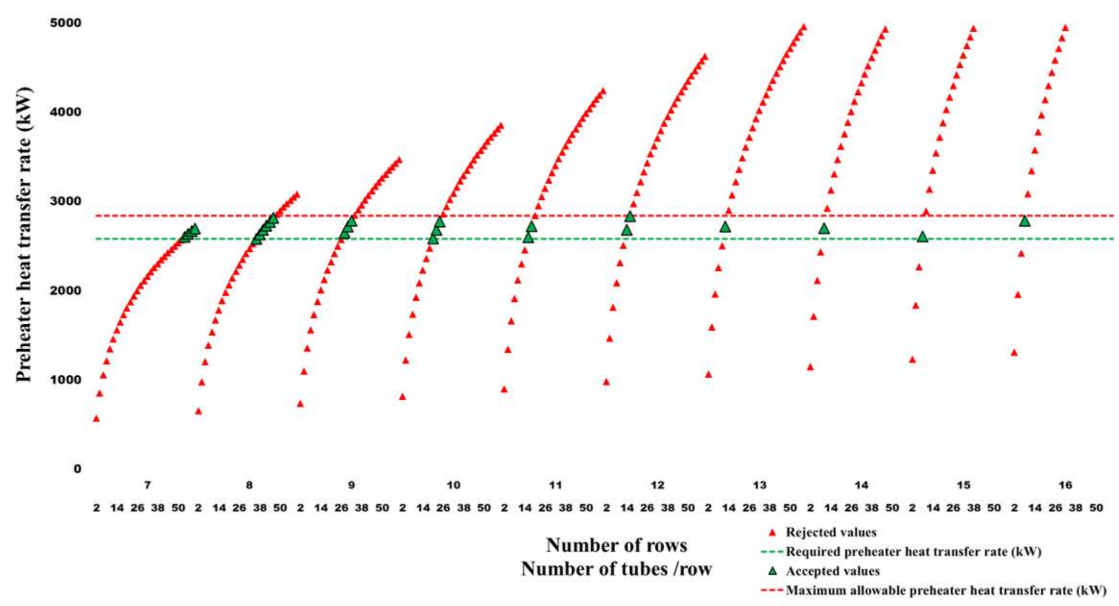

Figure 5.33. Heat transfer rate through the preheater for R245fa

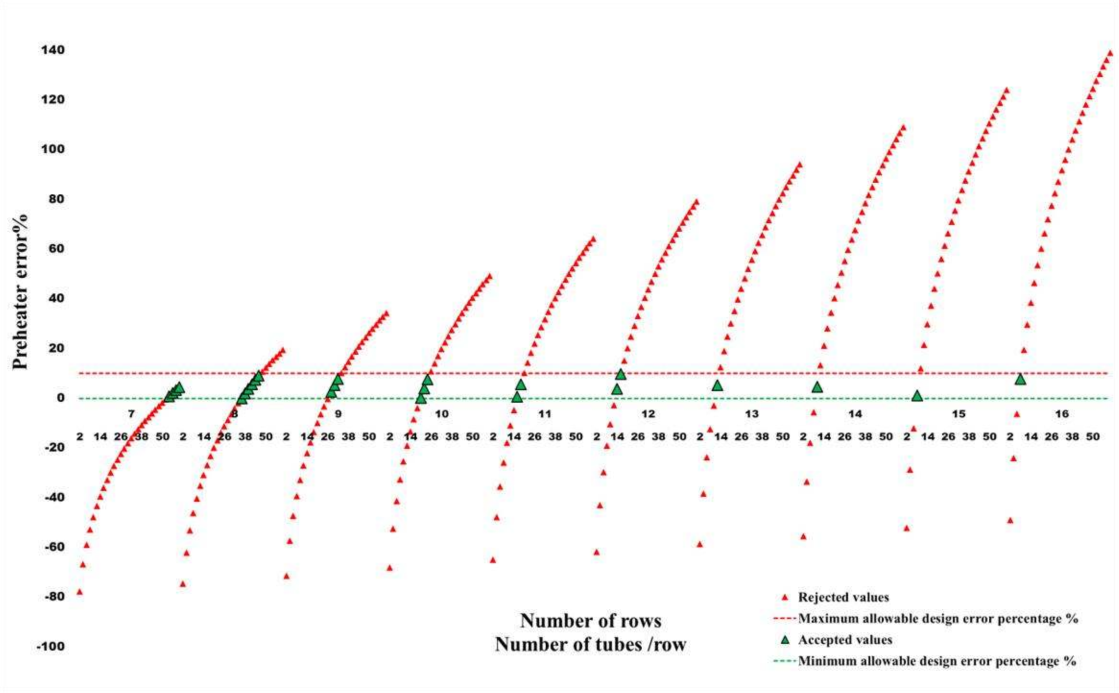

Figure 5.34. Preheater design error % diagram R245fa

Figure 5.33 shows a representation of the correlation between the preheater heating duty (kW) and the total number of tube rows and tubes in one row. The green triangles illustrated in the figure refer to the designs that meet the acceptable values of heating duty that are within the range of two design limitations. These limitations include the upper limit that is represented by a red dashed line, which indicates the maximum permissible preheater heat transfer which is equal to 2844 kW, and the lower limit, which is represented by a dashed green line, which corresponds to the minimum required heating rate at 2585.3 kW. On the other hand, the rejected designs that have a heating duty value (kW) outside of the defined range are represented by red triangles. Figure 5.34, illustates the percentage design error of 300 out of 600 reached preheater designs, corresponding to the total number of tube rows and tubes in one row for each preheater design. The maximum allowable design error, is set at 10%, which is indicated by a red dashed line. The green triangles correspond to preheater designs that have a design error value of less than 10%, which are placed inside the accepted range. Conversely, the red triangles represent designs with values that exceed the maximum allowable limit or less than zero, indicating unsatisfactory designs. Notably, out of the 600 preheater designs ,only 24 were able to meet this limitation successfully and are represented by green triangles, while the remaining designs were represented by red triangles due to a design error value greater than 10% or less than zero. Overall, this figure insured that all the accepted desings were out of overdesigning or underdesigning.

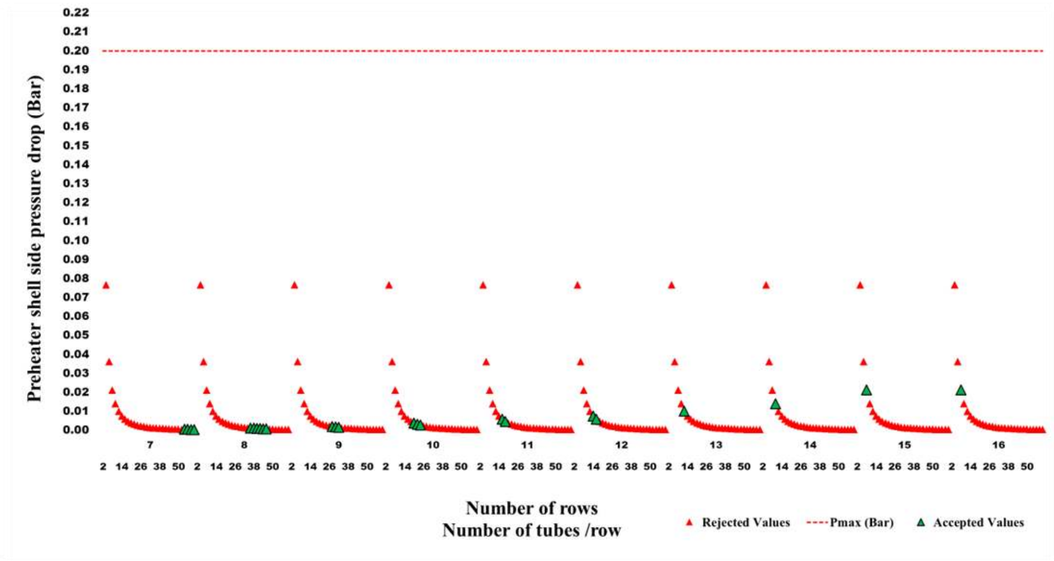

Figure 5.35. Shell side pressure drop through the preheater diagram R245fa

Figure 5.35 portrays the shell side pressure drop corresponding to the total number of tube rows and the total number of tubes in one row for each preheater design. The red dashed line illustrates the maximum allowable shell side pressure drop of 0.2 bar. The green triangles refer to the designs that have successfully passed all previous tests and have a shell side pressure drop value less than 0.2 bar. On the other hand, the red triangles represent the rejected designs that either have a value exceeding 0.2 bar or failed to pass one of the previous tests. It is noteworthy that only 24 preheater designs out of 600 designs have meeted all the design requirements and successfully have passed all the limitations. Conversely, the remaining designs, although having a shell side pressure drop value less than 0.2 bar they are still rejected as they failed to pass the pervious limitations (heat transfer and design error).

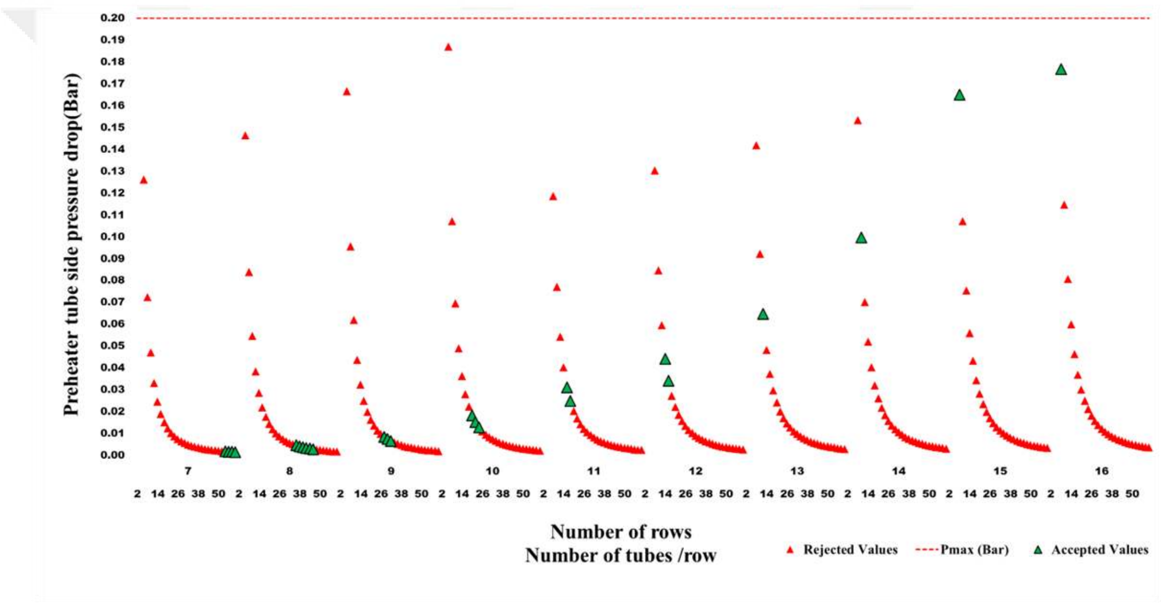

Figure 5.36. Tube side pressure drop through the preheater diagram R245fa

Figure 5.36 presents the tube side pressure drop for each preheater design, with respect to the total number of tube rows and the total number of tubes in one row. the red dashed line indicates the maximum allowable tube side pressure drop of 0.2 bar. The green triangles represent the designs that have successfully passed all the previous tests, as well as this limitation, exhibiting a tube side pressure drop value of less than 0.2 bar. Conversely, the red triangles signify the rejected designs that failed to pass one of the pervious tests or have a tube side pressure drop value exceeding the maximum limit. It is noteworthy that only 24 designs, out of the 600 total designs were able to satisfy all the design requirements and constraints, that are reprsented as green triangles. Although, the red triangle designs, have a tube side pressure drop value less than 0.2 bar, they were rejected due to their inability to fulfill the previous requirements (heating duty and design error).

The optimization of the heating surface area of the heat exchangers that are involved in the system has an impact on both the cost and performance of the cycle. The significance of this step lies in its ability to strike a balance between decreasing the surface area while keeping the pressure drop in low level as the pressure drop has a nigative impact on the overall performace of ORC. Therefore, achieving an optimum heating surface area is critical to any design process, as it can lead to substantial cost savings over time. The optimization process, therefore, aimed to determine the minimum heating surface area required to satisfy the pressure drop limitation of 0.2bar, thus maximizing efficiency of ORC while minimizing equipment costs. The result of the preheater optimization procedure is indicated in the following as a heating surface area of each preheater design as it is the last step in the optimization process, in which all the perfect designs that have successfully passed all the limitations that were suggested in this study are shown as green triangles while the optimal desing which has the smallest heating surface area is represented in a yellow color.

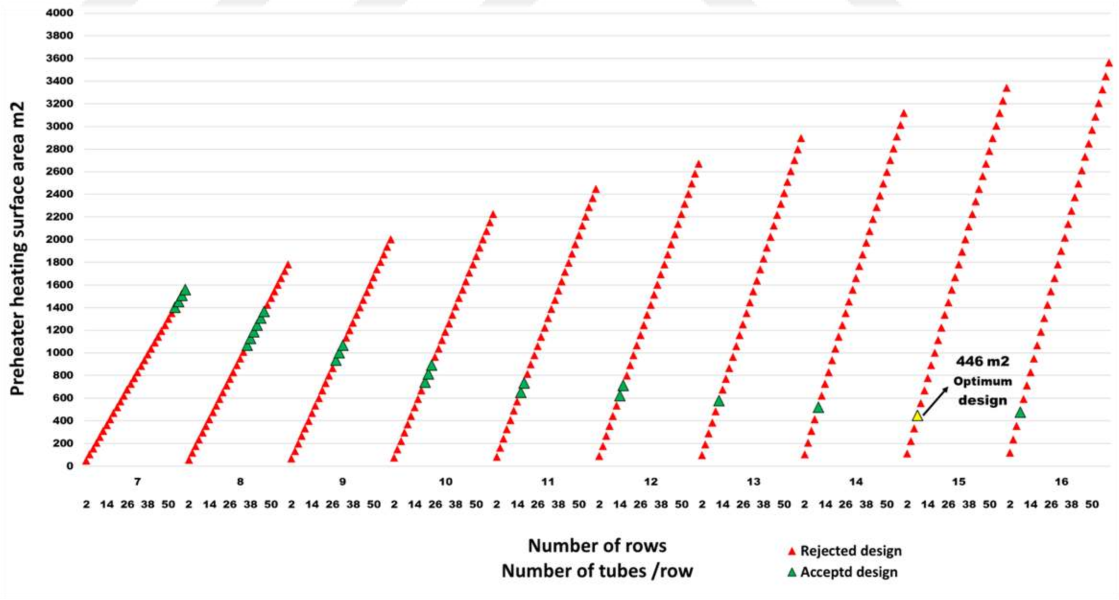

Figure 5.37. Preheater heating surface area diagram R245fa

In Figure 5.37, the heating surface area for each preheater design is plotted against the total number of tube rows and the total number of tubes in one row. The green triangles indicate the optimal designs that passed all previous limitations, while the red triangles represent the designs that failed to meet one or more of the previous requirements. It is noteworthy that out of the 600 designs, only 24 satisfied all constraints and are depicted in green, while the remaining designs are rejected.

The optimized preheater design, denoted by the yellow triangle, has the smallest heating surface area of 446 m2, corresponding to 8 tubes in one row and 15 tube rows. This design is the most cost-effective option with a minimum investment, while still meeting the required performance. Therefore, it is the preferred choice for the preheater, resulting in significant cost save.

Table 5.10. Finned tube preheater design result for R245fa

NO	$N_{tube/raw}$	N_{raw}	N_{total}	Error	ΔP_t	ΔP_s	A	$\dot{Q}_{est}$	Design Test Result
	#	#	#	%	bar	bar	m^2	kW	accepted/not accepted
1	2	7	14	-77.6761863	1.06421176	0.2773901	51.9774791	577.146875	Not accepted
2	4	7	28	-66.7301804	0.2767124	0.07683552	103.954958	860.138535	Not accepted
⋮	⋮	⋮	⋮	⋮	⋮	⋮	⋮	⋮	⋮
26	52	7	364	-0.39373578	0.00199368	0.00070147	1351.41446	2575.16233	Not accepted
27	54	7	378	0.89411173	0.00185535	0.00065501	1403.39194	2608.45759	Acceptable design
28	56	7	392	2.14450062	0.00173117	0.00061317	1455.36941	2640.78441	Acceptable design
29	58	7	406	3.35979525	0.00161927	0.00057533	1507.34689	2672.20393	Acceptable design
30	60	7	420	4.54213642	0.00151807	0.00054101	1559.32437	2702.77149	Acceptable design
31	2	8	16	-74.48707	1.23621491	0.2773901	59.4028333	659.596428	Not accepted
⋮	⋮	⋮	⋮	⋮	⋮	⋮	⋮	⋮	⋮
47	34	8	272	-1.97391673	0.00519593	0.00151882	1009.84817	2534.30925	Not accepted
48	36	8	288	0.07335387	0.00465787	0.00136874	1069.251	2587.23819	Acceptable design
49	38	8	304	2.03231219	0.00420047	0.0012405	1128.65383	2637.88396	Acceptable design
50	40	8	320	3.91105795	0.00380827	0.00112999	1188.05667	2686.45596	Acceptable design
51	42	8	336	5.71659601	0.00346937	0.00103406	1247.4595	2733.13529	Acceptable design
52	44	8	352	7.45502751	0.00317447	0.0009502	1306.86233	2778.07968	Acceptable design
53	46	8	368	9.13170067	0.00291621	0.00087646	1366.26516	2821.42741	Acceptable design
54	48	8	384	10.7513313	0.00268873	0.00081124	1425.668	2863.3004	Not accepted
⋮	⋮	⋮	⋮	⋮	⋮	⋮	⋮	⋮	⋮
73	26	9	234	-0.17025575	0.00987362	0.00247619	868.766436	2580.94005	Not accepted
74	28	9	252	2.65770281	0.00856596	0.00216325	935.594624	2654.05244	Acceptable design
75	30	9	270	5.3305875	0.00750524	0.00190767	1002.42281	2723.15565	Acceptable design
76	32	9	288	7.86619347	0.00663263	0.00169608	1069.251	2788.70973	Acceptable design
77	34	9	306	10.2793437	0.00590589	0.00151882	1136.07919	2851.09791	Not accepted
⋮	⋮	⋮	⋮	⋮	⋮	⋮	⋮	⋮	⋮
99	18	10	180	-3.94732452	0.02241839	0.00484566	668.281874	2483.28992	Not accepted
100	20	10	200	0.19119117	0.01830772	0.00399707	742.535416	2590.28469	Acceptable design
101	22	10	220	4.0189036	0.01524443	0.00335858	816.788957	2689.24414	Acceptable design
102	24	10	240	7.58341887	0.01289909	0.00286544	891.042499	2781.39904	Acceptable design
103	26	10	260	10.9219381	0.0110626	0.00247619	965.29604	2867.71117	Not accepted
⋮	⋮	⋮	⋮	⋮	⋮	⋮	⋮	⋮	⋮
126	12	11	132	-10.8692441	0.05423147	0.01017812	490.073374	2304.33464	Not accepted
127	14	11	154	-4.77086009	0.04028793	0.00767408	571.75227	2461.99871	Not accepted
128	16	11	176	0.69507074	0.03115097	0.00601024	653.431166	2603.3117	Acceptable design
129	18	11	198	5.65794303	0.02483283	0.00484566	735.110061	2731.61891	Acceptable design
130	20	11	220	10.2103103	0.0202783	0.00399707	816.788957	2849.31316	Not accepted
⋮	⋮	⋮	⋮	⋮	⋮	⋮	⋮	⋮	⋮
156	12	12	144	-2.76644808	0.05951466	0.01017812	534.625499	2513.81961	Not accepted
157	14	12	168	3.88633445	0.04420986	0.00767408	623.729749	2685.81677	Acceptable design
158	16	12	192	9.84916808	0.03418147	0.00601024	712.833999	2839.9764	Acceptable design
159	18	12	216	15.2632106	0.02724728	0.00484566	801.938249	2979.9479	Not accepted
⋮	⋮	⋮	⋮	⋮	⋮	⋮	⋮	⋮	⋮
185	10	13	130	-2.8421321	0.09214151	0.01421965	482.64802	2511.86292	Not accepted
186	12	13	156	5.33634791	0.06479785	0.01017812	579.177624	2723.30457	Acceptable design
187	14	13	182	12.543529	0.04813179	0.00767408	675.707228	2909.63483	Not accepted
⋮	⋮	⋮	⋮	⋮	⋮	⋮	⋮	⋮	⋮
214	8	14	112	-5.5972515	0.1534325	0.02142276	415.819833	2440.63366	Not accepted
215	10	14	140	4.63155005	0.0996595	0.01421965	519.774791	2705.08314	Acceptable design
216	12	14	168	13.4391439	0.07008104	0.01017812	623.729749	2932.78954	Not accepted
217	14	14	196	21.2007235	0.05205371	0.00767408	727.684707	3133.4529	Not accepted
⋮	⋮	⋮	⋮	⋮	⋮	⋮	⋮	⋮	⋮
243	6	15	90	-12.0183213	0.28809632	0.03637093	334.140937	2274.62707	Not accepted
244	**8**	**15**	**120**	**1.14580196**	**0.16501611**	**0.02142276**	**445.521249**	**2614.96464**	**Acceptable design**
245	10	15	150	12.1052322	0.1071775	0.01421965	556.901562	2898.30336	Not accepted
273	6	16	96	-6.15287606	0.30833838	0.03637093	356.417	2426.26887	Not accepted
274	8	16	128	7.88885542	0.17659973	0.02142276	475.222666	2789.29562	Acceptable design
275	10	16	160	19.5789143	0.11469549	0.01421965	594.028333	3091.52359	Not accepted
⋮	⋮	⋮	⋮	⋮	⋮	⋮	⋮	⋮	⋮
596	52	26	1352	269.966124	0.00796645	0.00070147	5019.53941	9564.88865	Not accepted
597	54	26	1404	274.749558	0.00741185	0.00065501	5212.59862	9688.55675	Not accepted
598	56	26	1456	279.393859	0.00691411	0.00061317	5405.65783	9808.62782	Not accepted
599	58	26	1508	283.907811	0.00646567	0.00057533	5598.71703	9925.32889	Not accepted
600	60	26	1560	288.299364	0.00606018	0.00054101	5791.77624	10038.8655	Not accepted

*Minimal Preheater area, ideal choice-lowest cost

** All the preheater design calculations are carried out assuming P2=22bar

5.4.2.2 Preheater optimization procedure for R600

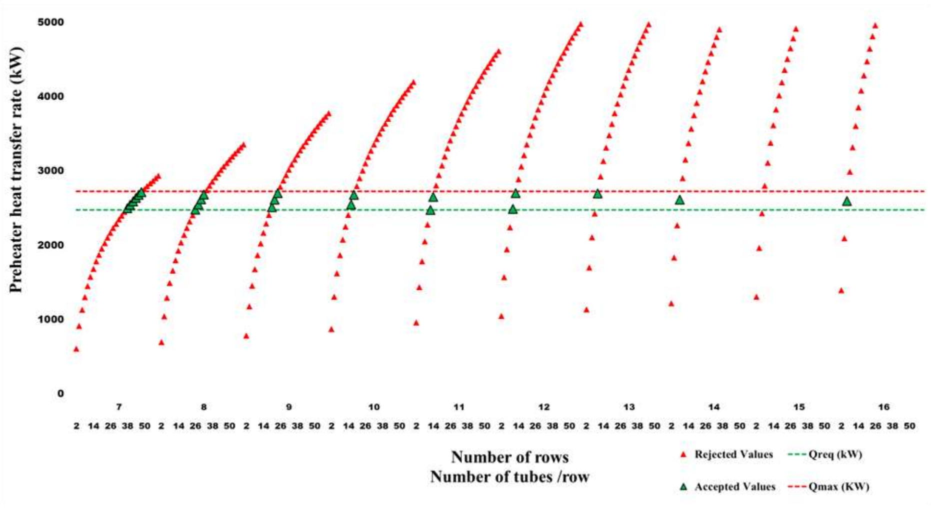

Figure 5.38. Heat transfer rate through the preheater for R600

Figure 5.38 represents the preheater heating duty (kW) accordeing to the total number of tube rows and tubes in one row of each preheater design. The green triangles illustrated in the figure refer to the designs that meet the acceptable values of heating duty that are within the range of two design limitations. These limitations include the upper limit that is represented by a red dashed line, which indicates the maximum permissible preheater heat transfer which is equal to 2728.88 kW, and the lower limit, which is represented by a dashed green line, which corresponds to the minimum required heating rate at 2480.76 kW. On the other hand, the rejected designs that have a heating duty value (kW) outside of the defined range are represented by red triangles.

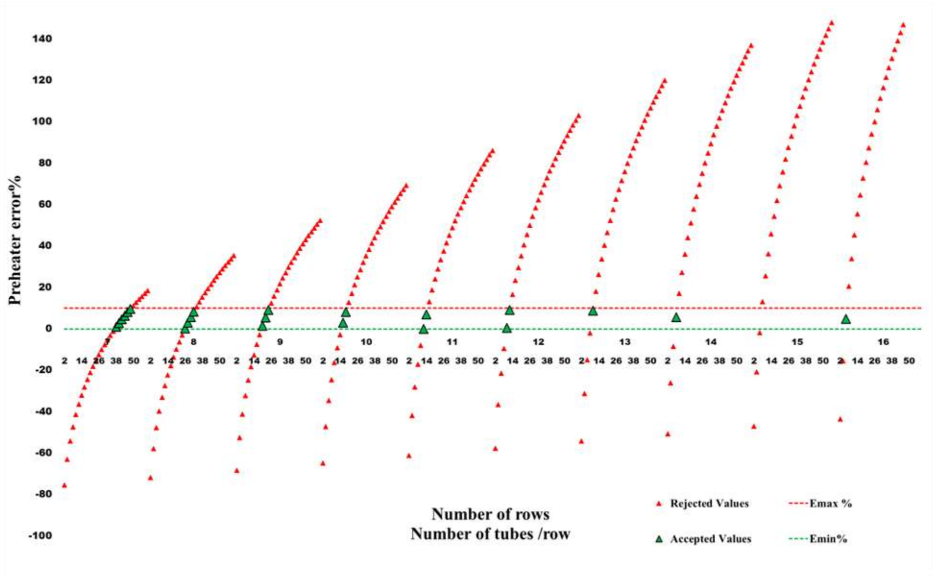

Figure 5.39. Preheater design error % diagram R600

Figure 5.39, illustates the percentage design error, corresponding to the total number of tube rows and tubes in one row for each preheater design. The maximum allowable design error, is set at 10%, which is indicated by a red dashed line. The green triangles correspond to preheater designs that have a design error value of less than 10%, which are placed inside the accepted range. Conversely, the red triangles represent designs with values that exceed the maximum allowable limit or less than zero, indicating unsatisfactory designs. Notably, out of the 600 preheater designs ,only 22 were able to meet this limitation successfully and are represented by green triangles, while the remaining designs were represented by red triangles due to a design error value greater than 10% or less than zero. Overall, this figure insured that all the accepted desings were out of overdesigning or underdesigning.

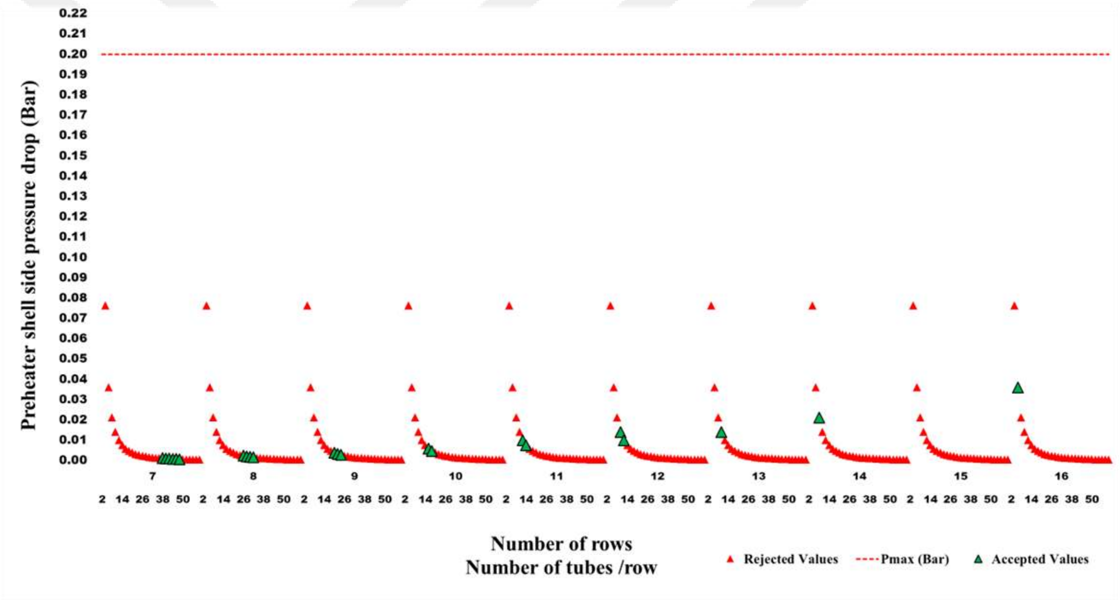

Figure 5.40. Shell side pressure drop through the preheater diagram R600

Figure 5.40 presents the shell side pressure drop corresponding to the total number of tube rows and the total number of tubes in one row for each preheater design. The red dashed line illustrates the maximum allowable shell side pressure drop of 0.2 bar. The green triangles refer to the designs that have successfully passed all previous tests and have a shell side pressure drop value less than 0.2 bar. On the other hand, the red triangles represent the rejected designs that either have a value exceeding 0.2 bar or failed to pass one of the previous tests. It is noteworthy that only 22 preheater designs out of 600 designs have meeted all the design requirements and successfully have passed all the limitations. Conversely, the remaining designs, although having a shell side pressure drop value less than 0.2 bar they are still rejected as they failed to pass the pervious limitations (heat transfer and design error).

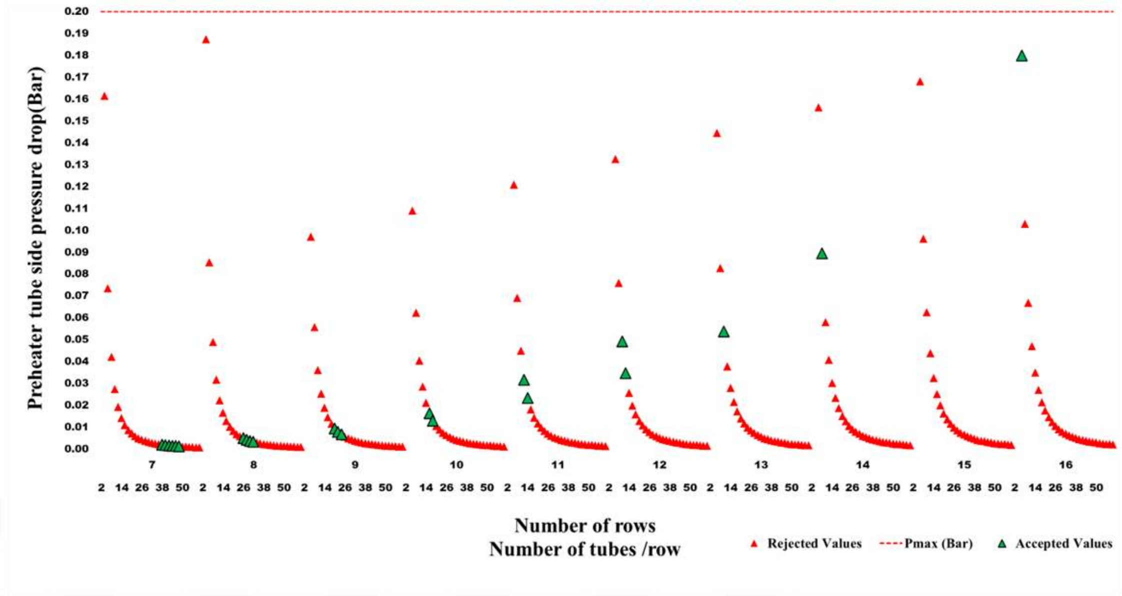

Figure 5.41. Tube side pressure drop through the preheater diagram R600

Figure 5.41 presents the tube side pressure drop for each preheater design, with respect to the total number of tube rows and the total number of tubes in one row. the red dashed line indicates the maximum allowable tube side pressure drop of 0.2 bar. The green triangles represent the designs that have successfully passed all the previous tests, as well as this limitation, exhibiting a tube side pressure drop value of less than 0.2 bar. Conversely, the red triangles signify the rejected designs that failed to pass one of the pervious tests or have a tube side pressure drop value exceeding the maximum limit. It is noteworthy that only 22 designs, out of the 600 total designs were able to satisfy all the design requirements and constraints, that are represented as green triangles. Although, the red triangle designs, have a tube side pressure drop value less than 0.2 bar, they were rejected due to their inability to fulfill the previous requirements (heating duty and design error).

The result of the preheater optimization procedure is indicated in the following as a heating surface area of each preheater design as it is the last step in the optimization process, in which all the perfect designs that have successfully passed all the limitations that were suggested in this study are shown as green triangles while the optimal desing which has the smallest heating surface area is represented in a yellow color.

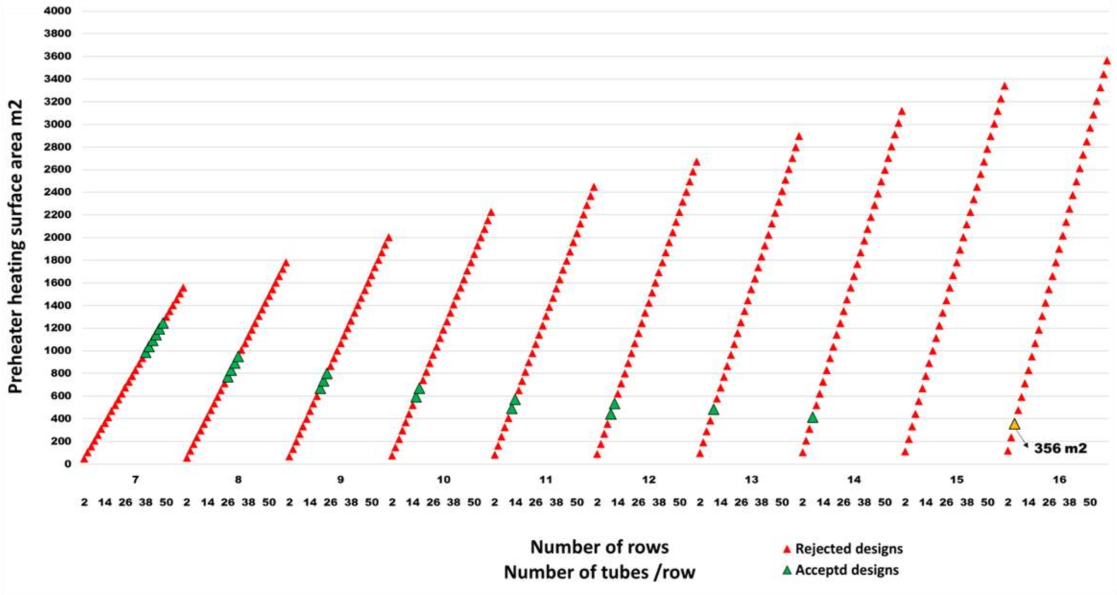

Figure 5.42. Preheater heating surface area diagram R600

In Figure 5.42, the heating surface area for each preheater design is plotted against the total number of tube rows and the total number of tubes in one row. The green triangles indicate the optimal designs that passed all previous limitations, while the red triangles represent the designs that failed to meet one or more of the previous requirements. It is noteworthy that out of the 600 designs, only 22 satisfied all constraints and are depicted in green, while the remaining designs are rejected.

The optimized preheater design, denoted by the yellow triangle, and has the smallest heating surface area of 356 m2, corresponding to 6 tubes in one row and 16 tube rows. This design is the most cost-effective option with a minimum investment, while still meeting the required performance. Therefore, it is the preferred choice for the preheater, resulting in significant cost savings.

The following table shows in detail all the preheater final designs parameters including the geometrical and performace ones as it could be used in future studies regarding this field of energy generation.

Table 5.11. Finned tube preheater design result for R600

	$N_{tube/raw}$	N_{raw}	N_{total}	Error	ΔP_t	ΔP_s	A	$\dot{Q}_{est}$	Design Test Result
NO	#	#	#	%	bar	bar	m^2	kW	accepted/not accepted
1	2	7	14	-75.2703	0.620948	0.27588	51.97748	613.4835	Not accepted
2	4	7	28	-62.9622	0.161415	0.076415	103.955	918.8177	Not accepted
⋮	⋮	⋮	⋮	⋮	⋮	⋮	⋮	⋮	⋮
18	36	7	252	-1.01884	0.002344	0.001361	935.5946	2455.483	Not accepted
19	38	7	266	0.951577	0.002114	0.001234	987.5721	2504.364	Acceptable design
20	40	7	280	2.841873	0.001916	0.001124	1039.55	2551.258	Acceptable design
21	42	7	294	4.659012	0.001746	0.001028	1091.527	2596.337	Acceptable design
22	44	7	308	6.409065	0.001598	0.000945	1143.505	2639.751	Acceptable design
23	46	7	322	8.097354	0.001468	0.000872	1195.482	2681.634	Acceptable design
24	48	7	336	9.728576	0.001353	0.000807	1247.459	2722.1	Acceptable design
25	50	7	350	11.3069	0.001252	0.000749	1299.437	2761.255	Not accepted
⋮	⋮	⋮	⋮	⋮	⋮	⋮	⋮	⋮	⋮
42	24	8	192	-2.95797	0.005902	0.00285	712.834	2407.378	Not accepted
43	26	8	208	0.104871	0.005062	0.002462	772.2368	2483.359	Acceptable design
44	28	8	224	2.989029	0.004392	0.002151	831.6397	2554.908	Acceptable design
45	30	8	240	5.716264	0.003848	0.001897	891.0425	2622.565	Acceptable design
46	32	8	256	8.304492	0.003401	0.001687	950.4453	2686.772	Acceptable design
47	34	8	272	10.76865	0.003028	0.00151	1009.848	2747.902	Not accepted
⋮	⋮	⋮	⋮	⋮	⋮	⋮	⋮	⋮	⋮
69	18	9	162	-2.71374	0.011662	0.004819	601.4537	2413.437	Not accepted
70	20	9	180	1.549492	0.009524	0.003975	668.2819	2519.197	Acceptable design
71	22	9	198	5.49539	0.007931	0.00334	735.1101	2617.085	Acceptable design
72	24	9	216	9.172282	0.006711	0.00285	801.9382	2708.3	Acceptable design
73	26	9	234	12.61798	0.005755	0.002462	868.7664	2793.779	Not accepted
⋮	⋮	⋮	⋮	⋮	⋮	⋮	⋮	⋮	⋮
97	14	10	140	-2.74122	0.021204	0.007632	519.7748	2412.755	Not accepted
98	16	10	160	2.936059	0.016395	0.005977	594.0283	2553.594	Acceptable design
99	18	10	180	8.095846	0.01307	0.004819	668.2819	2681.596	Acceptable design
100	20	10	200	12.83277	0.010673	0.003975	742.5354	2799.108	Not accepted
⋮	⋮	⋮	⋮	⋮	⋮	⋮	⋮	⋮	⋮
125	10	11	110	-7.86097	0.044966	0.014141	408.3945	2285.746	Not accepted
126	12	11	132	0.025167	0.031624	0.010122	490.0734	2481.382	Acceptable design
127	14	11	154	6.98466	0.023491	0.007632	571.7523	2654.03	Acceptable design
128	16	11	176	13.22966	0.018163	0.005977	653.4312	2808.954	Not accepted
⋮	⋮	⋮	⋮	⋮	⋮	⋮	⋮	⋮	⋮
154	8	12	96	-9.45784	0.075975	0.021305	356.417	2246.132	Not accepted
155	10	12	120	0.51531	0.049351	0.014141	445.5212	2493.541	Acceptable design
156	12	12	144	9.118364	0.034705	0.010122	534.6255	2706.962	Acceptable design
157	14	12	168	16.71054	0.025779	0.007632	623.7297	2895.306	Not accepted
⋮	⋮	⋮	⋮	⋮	⋮	⋮	⋮	⋮	⋮
184	8	13	104	-1.91266	0.082732	0.021305	386.1184	2433.309	Not accepted
185	10	13	130	8.891586	0.053736	0.014141	482.648	2701.337	Acceptable design
186	12	13	156	18.21156	0.037786	0.010122	579.1776	2932.543	Not accepted
⋮	⋮	⋮	⋮	⋮	⋮	⋮	⋮	⋮	⋮
213	6	14	84	-8.30977	0.156243	0.036171	311.8649	2274.613	Not accepted
214	8	14	112	5.632522	0.089489	0.021305	415.8198	2620.487	Acceptable design
215	10	14	140	17.26786	0.058121	0.014141	519.7748	2909.132	Not accepted
⋮	⋮	⋮	⋮	⋮	⋮	⋮	⋮	⋮	⋮
272	4	16	64	-15.3422	0.395217	0.076415	237.6113	2100.155	Not accepted
273	**6**	**16**	**96**	**4.788836**	**0.17986**	**0.036171**	**356.417**	**2599.557**	**Acceptable design***
274	8	16	128	20.72288	0.103003	0.021305	475.2227	2994.842	Not accepted
⋮	⋮	⋮	⋮	⋮	⋮	⋮	⋮	⋮	⋮
599	58	26	1508	335.1652	0.003768	0.000572	5598.717	10795.4	Not accepted
600	60	26	1560	340.2258	0.003532	0.000538	5791.776	10920.94	Not accepted

*Minimal Preheater area, ideal choice-lowest cost

** All the preheater design calculations are carried out assuming P2=22bar.

5.4.2.3 Preheater optimization procedure for R123

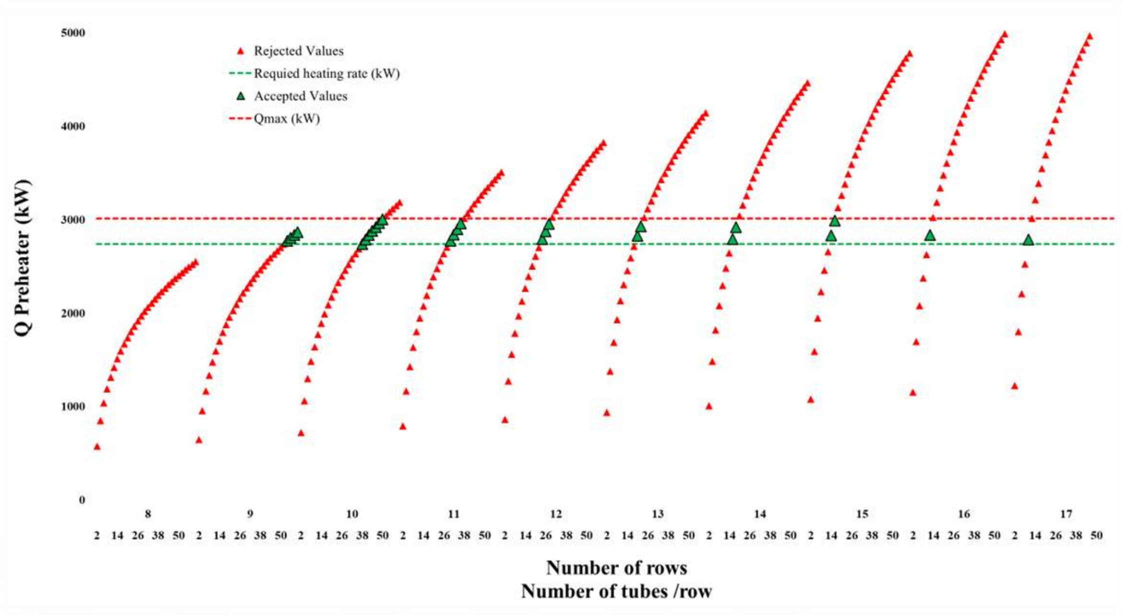

Figure 5.43. Heat transfer rate through the preheater R123

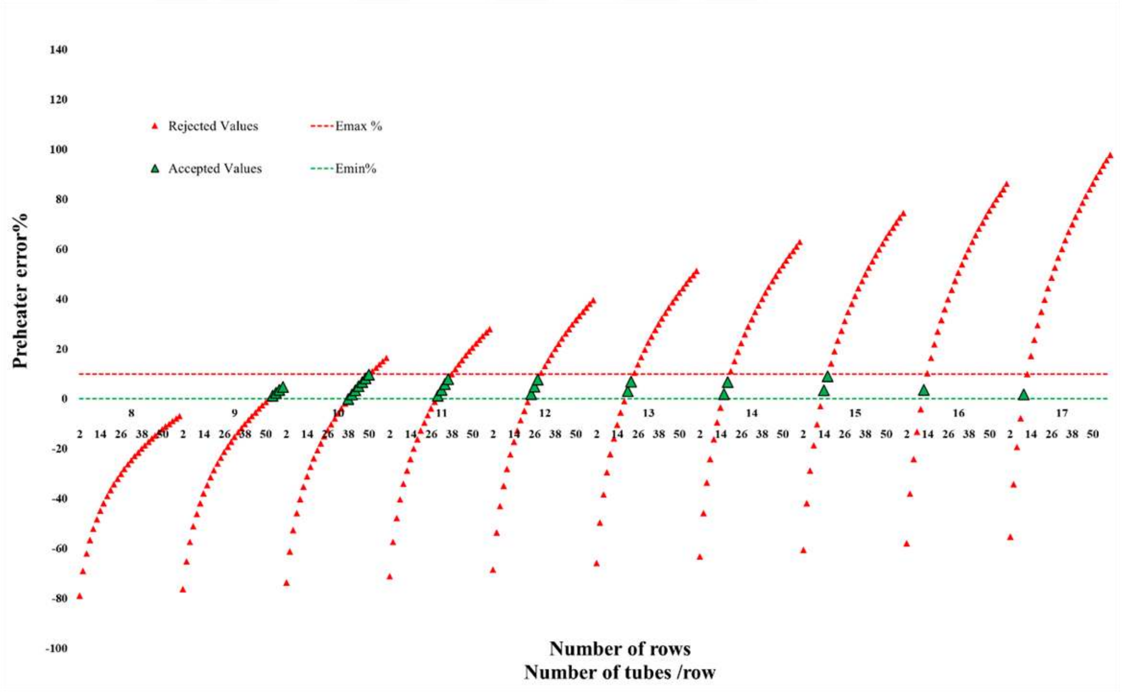

Figure 5.44. Preheater design error % diagram R123

Figure 5.43 represents the preheater heating duty (kW) accordeing to the total number of tube rows and tubes in one row of each preheater design. The green triangles illustrated in the figure refer to the designs that meet the acceptable values of heating duty that are within the range of two design limitations. These limitations include the upper limit that is represented by a red dashed line, which indicates the maximum permissible preheater heat transfer which is equal to 3014.869 kW, and the lower limit, which is represented by a dashed green line, which corresponds to the minimum required heating rate at 2740.79 kW. On the other hand, the rejected designs that have a heating duty value (kW) outside of the defined range are represented by red triangles. Figure 5.44, illustates the percentage design error, corresponding to the total number of tube rows and tubes in one row for each preheater design. The maximum allowable design error, is set at 10%, which is indicated by a red dashed line. The green triangles correspond to preheater designs that have a design error value of less than 10%, which are placed inside the accepted range. Conversely, the red triangles represent designs with values that exceed the maximum allowable limit or less than zero, indicating unsatisfactory designs. Notably, out of the 600 preheater designs ,only 27 were able to meet this limitation successfully and are represented by green triangles, while the remaining designs were represented by red triangles due to a design error value greater than 10% or less than zero. Overall, this figure insured that all the accepted desings were out of overdesigning or underdesigning.

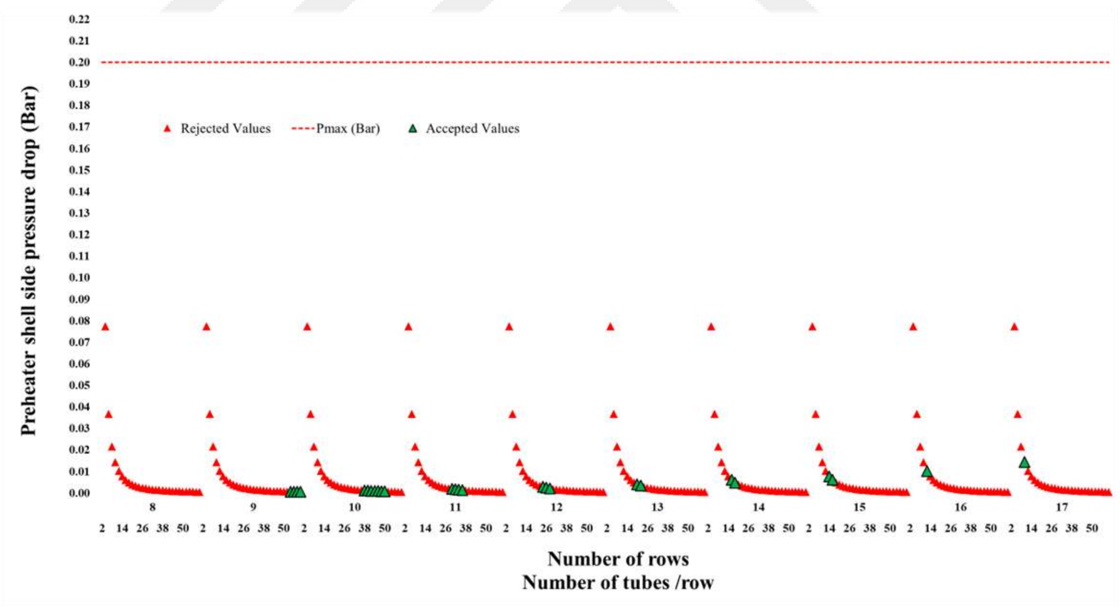

Figure 5.45. Shell side pressure drop through the preheater diagram R123

Figure 5.45 presents the shell side pressure drop corresponding to the total number of tube rows and the total number of tubes in one row for each preheater design. The red dashed line illustrates the maximum allowable shell side pressure drop of 0.2 bar. The green triangles refer to the designs that have successfully passed all previous tests and have a shell side pressure drop value less than 0.2 bar. On the other hand, the red triangles represent the rejected designs that either have a value exceeding 0.2 bar or failed to pass one of the previous tests. It is noteworthy that only 27 preheater designs out of 600 designs have meeted all the design requirements and successfully have passed all the limitations. Conversely, the remaining designs, although having a shell side pressure drop value less than 0.2 bar they are still rejected as they failed to pass the pervious limitations (heat transfer and design error).

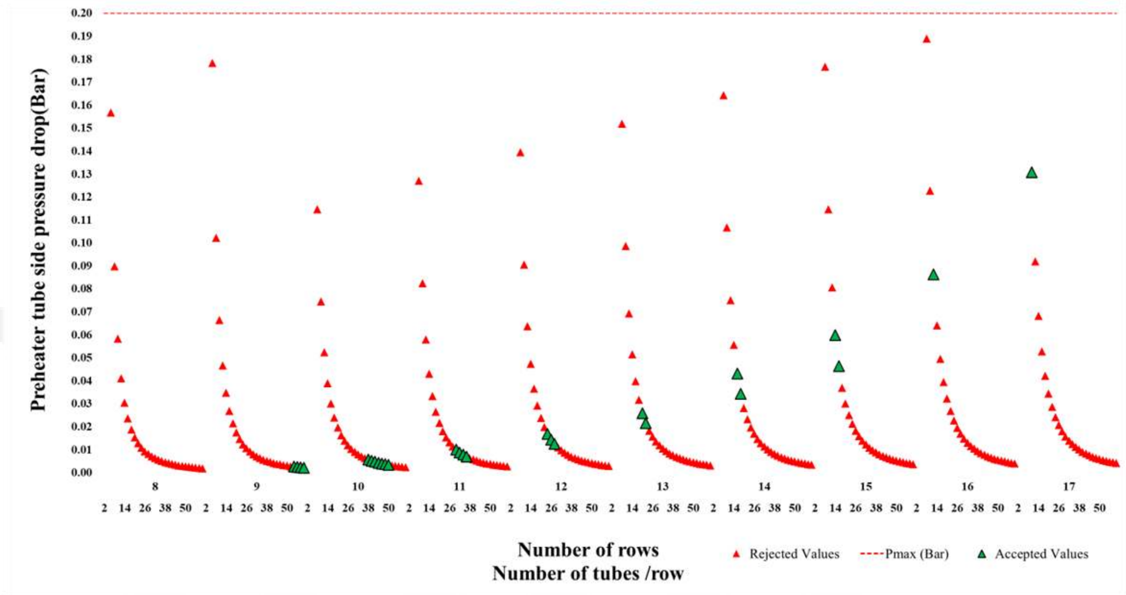

Figure 5.46. Tube side pressure drop through the preheater diagram R123

Figure 5.46 presents the tube side pressure drop for each preheater design, with respect to the total number of tube rows and the total number of tubes in one row. the red dashed line indicates the maximum allowable tube side pressure drop of 0.2 bar. The green triangles represent the designs that have successfully passed all the previous tests, as well as this limitation, exhibiting a tube side pressure drop value of less than 0.2 bar. Conversely, the red triangles signify the rejected designs that failed to pass one of the pervious tests or have a tube side pressure drop value exceeding the maximum limit. It is noteworthy that only 27 designs, out of the 600 total designs were able to satisfy all the design requirements and constraints, that are represented as green triangles. Although, the red triangle designs, have a tube side pressure drop value less than 0.2 bar, they were rejected due to their inability to fulfill the previous requirements (heating duty and design error.

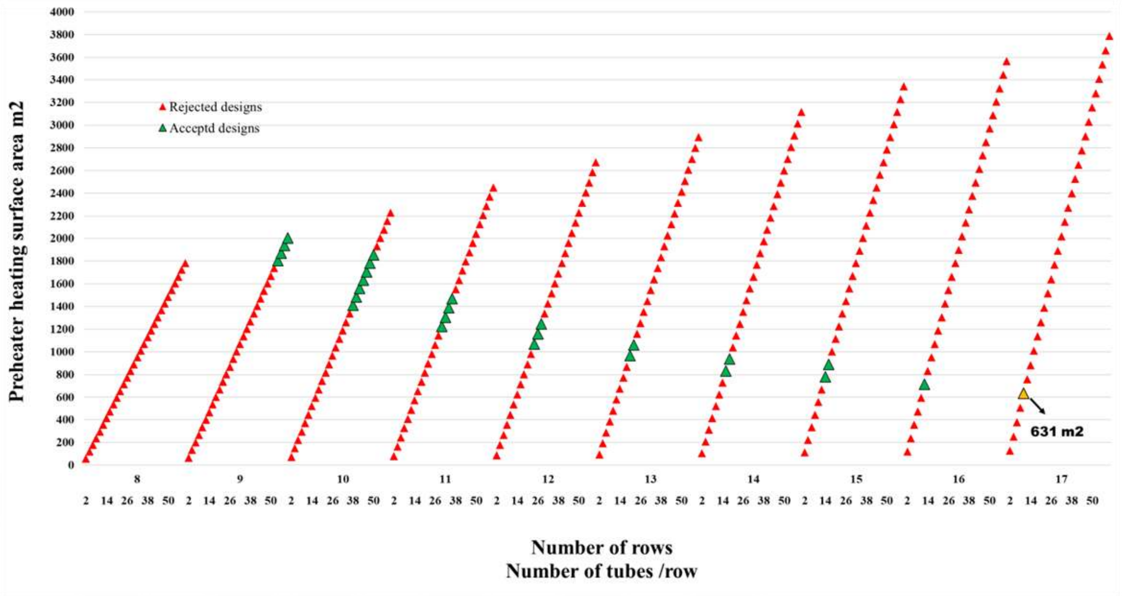

Figure 5.47. Preheater heating surface area diagram R123

In Figure 5.47, the heating surface area for each preheater design is plotted against the total number of tube rows and the total number of tubes in one row. The green triangles indicate the optimal designs that passed all previous limitations, while the red triangles represent the designs that failed to meet one or more of the previous requirements. It is noteworthy that out of the 600 designs, only 27 satisfied all constraints and are depicted in green, while the remaining designs are rejected.

The optimized preheater design, denoted by the yellow triangle, has the smallest heating surface area of 631 m2, corresponding to 10 tubes in one row and 17 tube rows. This design is the most cost-effective option with a minimum investment, while still meeting the required performance. Therefore, it is the preferred choice for the preheater, resulting in significant cost savings in the long run. The results of this optimization process demonstrate the importance of considering both operational costs and efficiency in preheater design, leading to a cost-effective and optimal design.

Table 5.12. records in detail all the preheater final designs parameters including the geometrical and performace ones as it could be used in future studies regarding this field of energy generation.

Table 5.12. Finned tube preheater design result for R123

NO	$N_{tube/raw}$	N_{raw}	N_{total}	Error	ΔP_t	ΔP_s	A	$\dot{Q}_{est}$	Design Test Result
	#	#	#	%	bar	bar	m^2	kW	accepted/not accepted
1	2	8	16	-78.9350054	1.3248474	0.2796332	59.4028333	577.34606	Not accepted
2	4	8	32	-69.0041274	0.34395676	0.07746055	118.805667	849.530004	Not accepted
⋮	⋮	⋮	⋮	⋮	⋮	⋮	⋮	⋮	⋮
57	54	9	486	1.23634728	0.00260239	0.00066045	1804.36106	2774.66989	Acceptable design
58	56	9	504	2.44108225	0.00242787	0.00061825	1871.18925	2807.68908	Acceptable design
59	58	9	522	3.61156241	0.00227063	0.00058011	1938.01743	2839.76941	Acceptable design
60	60	9	540	4.74989541	0.00212843	0.0005455	2004.84562	2870.96867	Acceptable design
61	2	10	20	-73.6687568	1.69375243	0.2796332	74.2535416	721.682575	Not accepted
62	4	10	40	-61.2551593	0.43936924	0.07746055	148.507083	1061.9125	Not accepted
⋮	⋮	⋮	⋮	⋮	⋮	⋮	⋮	⋮	⋮
79	38	10	380	0.02277474	0.0057067	0.00125076	1410.81729	2741.40849	Acceptable design
80	40	10	400	1.78959757	0.00517299	0.00113935	1485.07083	2789.83329	Acceptable design
81	42	10	420	3.48653673	0.00471187	0.00104262	1559.32437	2836.34273	Acceptable design
82	44	10	440	5.11947519	0.00431068	0.00095807	1633.57791	2881.09805	Acceptable design
83	46	10	460	6.69356405	0.0039594	0.00088372	1707.83146	2924.24043	Acceptable design
84	48	10	480	8.21334048	0.00365002	0.00081796	1782.085	2965.89422	Acceptable design
85	50	10	500	9.68282261	0.00337609	0.0007595	1856.33854	3006.16956	Acceptable design
86	52	10	520	11.1055867	0.00313236	0.00070729	1930.59208	3045.16445	Not accepted
87	54	10	540	12.4848303	0.00291452	0.00066045	2004.84562	3082.96655	Not accepted
⋮	⋮	⋮	⋮	⋮	⋮	⋮	⋮	⋮	⋮
105	30	11	330	1.31425054	0.00994144	0.00192343	1225.18344	2776.80505	Acceptable design
106	32	11	352	3.65277961	0.00878392	0.0017101	1306.86233	2840.89909	Acceptable design
107	34	11	374	5.87649598	0.00782006	0.00153138	1388.54123	2901.84636	Acceptable design
108	36	11	396	7.99723612	0.00700872	0.00138007	1470.22012	2959.97127	Acceptable design
109	38	11	418	10.0250522	0.00631914	0.00125076	1551.89902	3015.54933	Not accepted
110	40	11	440	11.9685573	0.00572798	0.00113935	1633.57791	3068.81662	Not accepted
⋮	⋮	⋮	⋮	⋮	⋮	⋮	⋮	⋮	⋮
130	20	12	240	-4.7782659	0.02377205	0.00403	891.042499	2609.82232	Not accepted
131	22	12	264	-1.2920777	0.01978955	0.00338626	980.146749	2705.37122	Not accepted
132	24	12	288	1.9497126	0.01674112	0.00288907	1069.251	2794.2217	Acceptable design
133	26	12	312	4.98210011	0.01435459	0.00249662	1158.35525	2877.3329	Acceptable design
134	28	12	336	7.83290734	0.01245039	0.00218111	1247.4595	2955.46737	Acceptable design
135	30	12	360	10.524637	0.01090612	0.00192343	1336.56375	3029.24187	Not accepted
⋮	⋮	⋮	⋮	⋮	⋮	⋮	⋮	⋮	⋮
159	18	13	234	-0.93324739	0.03169912	0.00488555	868.766436	2715.20598	Not accepted
160	20	13	260	3.15687861	0.0258787	0.00403	965.29604	2827.30751	Acceptable design
161	22	13	286	6.9335825	0.02154252	0.00338626	1061.82564	2930.81882	Acceptable design
162	24	13	312	10.445522	0.01822347	0.00288907	1158.35525	3027.0735	Not accepted
163	26	13	338	13.7306085	0.01562515	0.00249662	1254.88485	3117.11064	Not accepted
⋮	⋮	⋮	⋮	⋮	⋮	⋮	⋮	⋮	⋮
188	16	14	224	1.87609232	0.04301624	0.00605967	831.639666	2792.20392	Acceptable design
189	18	14	252	6.68727204	0.0342807	0.00488555	935.594624	2924.06798	Acceptable design
190	20	14	280	11.0920231	0.02798534	0.00403	1039.54958	3044.79271	Not accepted
191	22	14	308	15.1592427	0.02329548	0.00338626	1143.50454	3156.26642	Not accepted
192	24	14	336	18.9413314	0.01970582	0.00288907	1247.4595	3259.92531	Not accepted
⋮	⋮	⋮	⋮	⋮	⋮	⋮	⋮	⋮	⋮
215	10	15	150	-10.1517987	0.11465054	0.01433618	556.901562	2462.54538	Not accepted
216	12	15	180	-2.90332953	0.08059705	0.01026165	668.281874	2661.21028	Not accepted
217	14	15	210	3.46270957	0.05984815	0.00773713	779.662186	2835.68968	Acceptable design
218	16	15	240	9.15295606	0.0462571	0.00605967	891.042499	2991.64706	Acceptable design
219	18	15	270	14.3077915	0.03686228	0.00488555	1002.42281	3132.92998	Not accepted
220	20	15	300	19.0271676	0.03009199	0.00403	1113.80312	3262.2779	Not accepted
⋮	⋮	⋮	⋮	⋮	⋮	⋮	⋮	⋮	⋮
245	10	16	160	-4.16191861	0.12269597	0.01433618	594.028333	2626.71507	Not accepted
246	12	16	192	3.56978184	0.0862494	0.01026165	712.833999	2838.6243	Acceptable design
247	14	16	224	10.3602235	0.06404316	0.00773713	831.639666	3024.73566	Not accepted
248	16	16	256	16.4298198	0.04949796	0.00605967	950.445332	3191.0902	Not accepted
⋮	⋮	⋮	⋮	⋮	⋮	⋮	⋮	⋮	⋮
273	6	17	102	-19.3311222	0.35176558	0.03666779	378.693062	2210.95992	Not accepted
274	8	17	136	-7.75403264	0.20138004	0.02159802	504.924083	2528.26297	Not accepted
275	**10**	**17**	**170**	**1.82796148**	**0.1307414**	**0.01433618**	**631.155103**	**2790.88476**	**Acceptable design***
276	12	17	204	10.0428932	0.09190174	0.01026165	757.386124	3016.03832	Not accepted
⋮	⋮	⋮	⋮	⋮	⋮	⋮	⋮	⋮	⋮
303	6	18	108	-14.5858941	0.37344312	0.03666779	400.969124	2341.01639	Not accepted
304	8	18	144	-2.32779926	0.21378024	0.02159802	534.625499	2676.98432	Not accepted
305	10	18	180	7.81784157	0.13878683	0.01433618	668.281874	2955.05445	Acceptable design
306	12	18	216	16.5160046	0.09755409	0.01026165	801.938249	3193.45234	Not accepted
⋮	⋮	⋮	⋮	⋮	⋮	⋮	⋮	⋮	⋮
599	58	27	1566	210.834687	0.00717043	0.00058011	5814.0523	8519.30824	Not accepted
600	60	27	1620	214.249686	0.00672033	0.0005455	6014.53687	8612.906	Not accepted

*Minimal Preheater area, ideal choice-lowest cost

** All the preheater design calculations are carried out assuming P2=22bar.

5.4.2.4 Preheater optimization procedure for R236fa

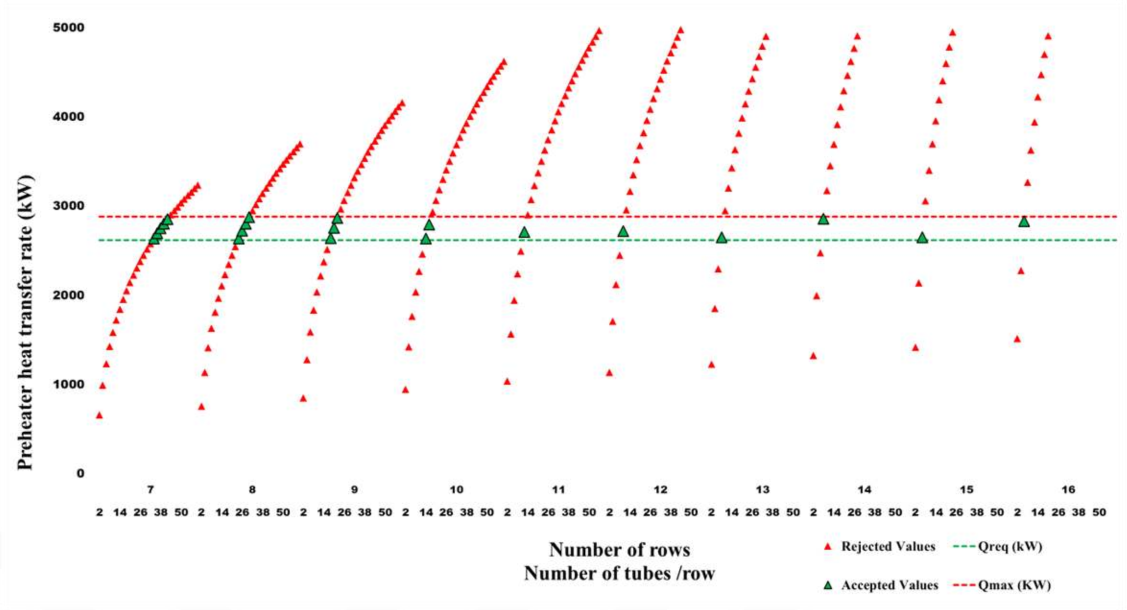

Figure 5.48. Heat transfer rate through the preheater R236fa

Figure 5.48 represents the preheater heating duty (kW) accordeing to the total number of tube rows and tubes in one row of each preheater design. The green triangles illustrated in the figure refer to the designs that meet the acceptable values of heating duty that are within the range of two design limitations. These limitations include the upper limit that is represented by a red dashed line, which indicates the maximum permissible preheater heat transfer which is equal to 2885.3 kW, and the lower limit, which is represented by a dashed green line, which corresponds to the minimum required heating rate at 2623 kW. On the other hand, the rejected designs that have a heating duty value (kW) outside of the defined range are represented by red triangles.

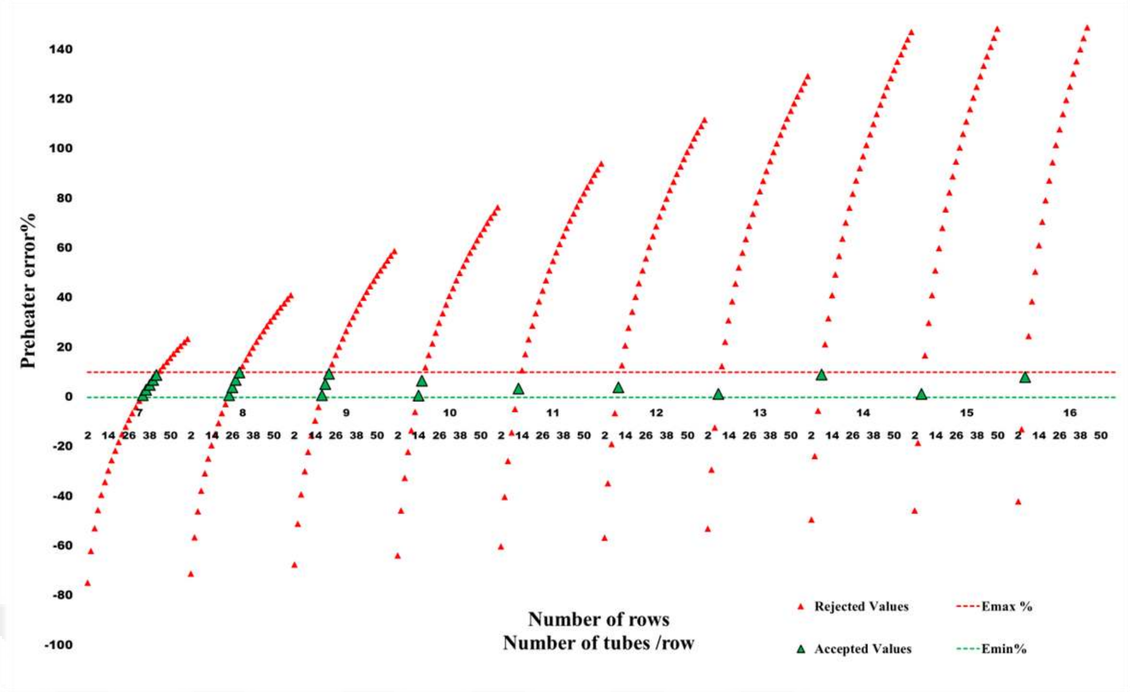

Figure 5.49. Preheater design error % diagram R236fa

Figure 5.49, illustates the percentage design error, corresponding to the total number of tube rows and tubes in one row for each preheater design. The maximum allowable design error, is set at 10%, which is indicated by a red dashed line. The green triangles correspond to preheater designs that have a design error value of less than 10%, which are placed inside the accepted range. Conversely, the red triangles represent designs with values that exceed the maximum allowable limit or less than zero, indicating unsatisfactory designs. Notably, out of the 600 preheater designs ,only 20 were able to meet this limitation successfully and are represented by green triangles, while the remaining designs were represented by red triangles due to a design error value greater than 10% or less than zero. Overall, this figure insured that all the accepted desings were out of overdesigning or underdesigning.

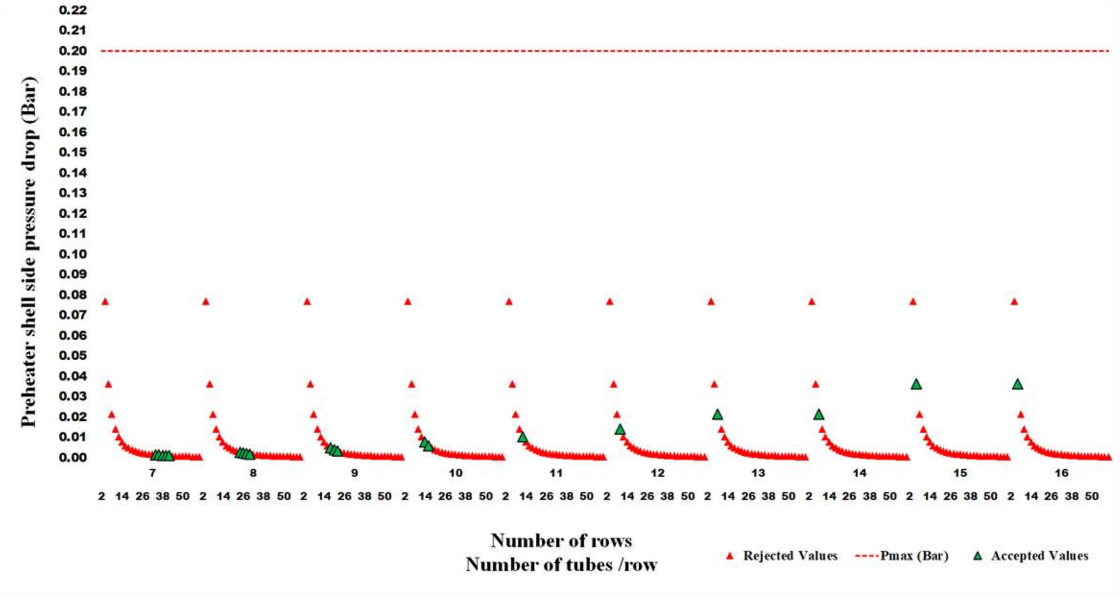

Figure 5.50. Shell side pressure drop through the preheater diagram R236fa

Figure 5.50 presents the shell side pressure drop corresponding to the total number of tube rows and the total number of tubes in one row for each preheater design. The red dashed line illustrates the maximum allowable shell side pressure drop of 0.2 bar. The green triangles refer to the designs that have successfully passed all previous tests and have a shell side pressure drop value less than 0.2 bar. On the other hand, the red triangles represent the rejected designs that either have a value exceeding 0.2 bar or failed to pass one of the previous tests. It is noteworthy that only 20 preheater designs out of 600 designs have meeted all the design requirements and successfully have passed all the limitations. Conversely, the remaining designs, although having a shell side pressure drop value less than 0.2 bar they are still rejected as they failed to pass the pervious limitations (heat transfer and design error).

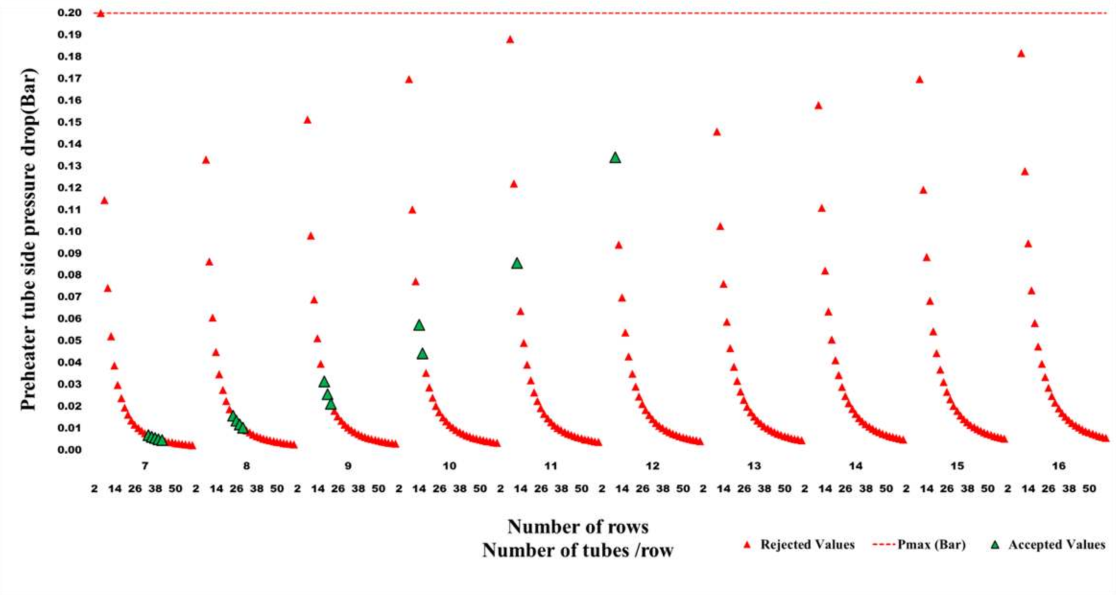

Figure 5.51. Tube side pressure drop through the preheater diagram R236fa

Figure 5.51 presents the tube side pressure drop for each preheater design, with respect to the total number of tube rows and the total number of tubes in one row. the red dashed line indicates the maximum allowable tube side pressure drop of 0.2 bar. The green triangles represent the designs that have successfully passed all the previous tests, as well as this limitation, exhibiting a tube side pressure drop value of less than 0.2 bar. Conversely, the red triangles signify the rejected designs that failed to pass one of the pervious tests or have a tube side pressure drop value exceeding the maximum limit. It is noteworthy that only 16 designs, out of the 600 total designs were able to satisfy all the design requirements and constraints, that are represented as green triangles. Although, the red triangle designs, have a tube side pressure drop value less than 0.2 bar, they were rejected due to their inability to fulfill the previous requirements (heating duty and design error.

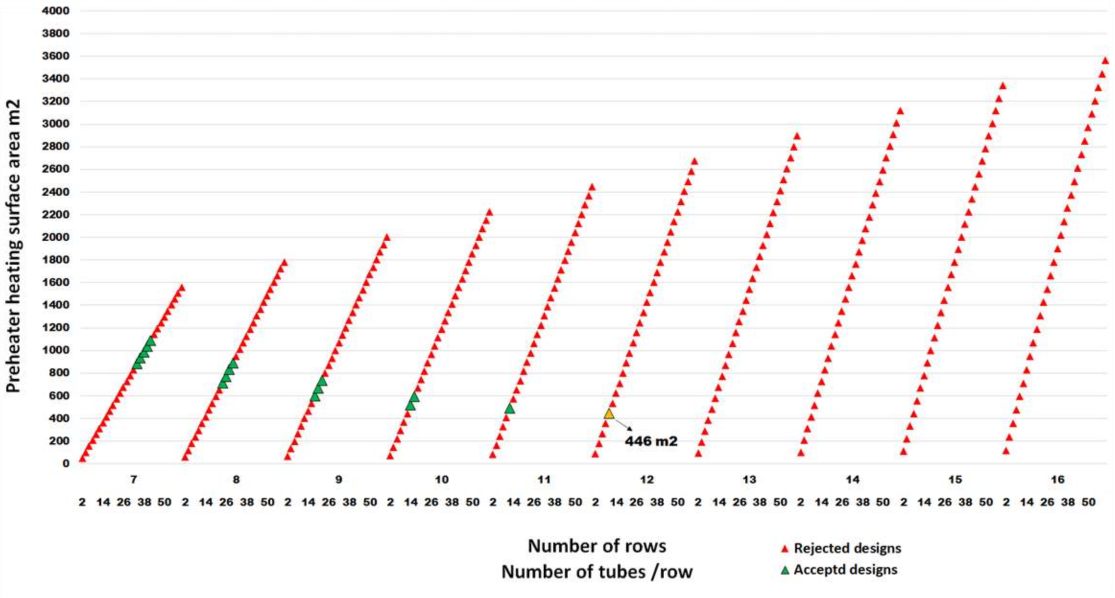

Figure 5.52. Preheater heating surface area diagram R236fa

In Figure 5.52, the heating surface area for each preheater design is plotted against the total number of tube rows and the total number of tubes in one row. The green triangles indicate the optimal designs that passed all previous limitations, while the red triangles represent the designs that failed to meet one or more of the previous requirements. It is noteworthy that out of the 600 designs, only 16 satisfied all constraints and are depicted in green, while the remaining designs are rejected. The optimized preheater design, denoted by the yellow triangle, has the smallest heating surface area of 446 m2, corresponding to 10 tubes in one row and 12 tube rows. This design is the most cost-effective option with a minimum investment, while still meeting the required performance. Therefore, it is the preferred choice for the preheater, resulting in significant cost savings in the long run. The results of this optimization process demonstrate the importance of considering both operational costs and efficiency in preheater design, leading to a cost-effective and optimal design.

Table 5.13 records in detail all the preheater final designs parameters including the geometrical and performace ones as it could be used in future studies regarding this field of energy generation.

Table 5.13. Finned tube preheater design result for R236fa

NO	$N_{tube/raw}$	N_{raw}	N_{total}	Error	ΔP_t	ΔP_s	A	$\dot{Q}_{est}$	Design Test Result
	#	#	#	%	bar	bar	m^2	kW	accepted/not accepted
1	2	7	14	-74.6286118	1.69625713	0.27792728	51.9774791	665.384054	Not accepted
2	4	7	28	-61.8703467	0.43957711	0.0769852	103.954958	999.979312	Not accepted
⋮	⋮	⋮	⋮	⋮	⋮	⋮	⋮	⋮	⋮
16	32	7	224	-1.45398527	0.00790708	0.00169944	831.639666	2584.44459	Not accepted
17	34	7	238	0.81382565	0.00703885	0.00152183	883.617145	2643.91966	Acceptable design
18	36	7	252	2.97953588	0.00630806	0.00137146	935.594624	2700.71707	Acceptable design
19	38	7	266	5.05292701	0.00568699	0.00124296	987.572103	2755.09334	Acceptable design
20	40	7	280	7.04240085	0.0051546	0.00113223	1039.54958	2807.26881	Acceptable design
21	42	7	294	8.95523046	0.00469468	0.00103611	1091.52706	2857.43423	Acceptable design
22	44	7	308	10.7977561	0.00429456	0.00095209	1143.50454	2905.75587	Not accepted
23	46	7	322	12.5755402	0.00394424	0.0008782	1195.48202	2952.37962	Not accepted
⋮	⋮	⋮	⋮	⋮	⋮	⋮	⋮	⋮	⋮
41	22	8	176	-2.64566359	0.01883416	0.00336521	653.431166	2553.19191	Not accepted
42	24	8	192	0.78667819	0.01593017	0.0028711	712.833999	2643.2077	Acceptable design
43	26	8	208	4.00441031	0.01365706	0.00248108	772.236832	2727.59519	Acceptable design
44	28	8	224	7.03543759	0.01184363	0.00216752	831.639666	2807.08619	Acceptable design
45	30	8	240	9.90241834	0.01037318	0.00191144	891.042499	2882.27496	Acceptable design
46	32	8	256	12.6240168	0.00916392	0.00169944	950.445332	2953.65096	Not accepted
47	34	8	272	15.2158007	0.00815713	0.00152183	1009.84817	3021.62247	Not accepted
⋮	⋮	⋮	⋮	⋮	⋮	⋮	⋮	⋮	⋮
67	14	9	126	-9.31580785	0.05122977	0.00768917	467.797312	2378.26228	Not accepted
68	16	9	144	-3.961262	0.03958658	0.00602208	534.625499	2518.68934	Not accepted
69	18	9	162	0.90841053	0.03153991	0.00485522	601.453687	2646.40022	Acceptable design
70	20	9	180	5.38149584	0.02574225	0.00400495	668.281874	2763.71031	Acceptable design
71	22	9	198	9.52362846	0.02142402	0.00336521	735.110061	2872.3409	Acceptable design
72	24	9	216	13.385013	0.0181194	0.0028711	801.938249	2973.60866	Not accepted
73	26	9	234	17.0049616	0.01553287	0.00248108	868.766436	3068.54458	Not accepted
⋮	⋮	⋮	⋮	⋮	⋮	⋮	⋮	⋮	⋮
95	10	10	100	-13.3645171	0.11012138	0.01424756	371.267708	2272.08178	Not accepted
96	12	10	120	-5.86473943	0.07738072	0.01019813	445.521249	2468.76919	Not accepted
97	14	10	140	0.7602135	0.05743909	0.00768917	519.774791	2642.51364	Acceptable design
98	16	10	160	6.70970889	0.04438101	0.00602208	594.028333	2798.54371	Acceptable design
99	18	10	180	12.1204561	0.03535717	0.00485522	668.281874	2940.44469	Not accepted
100	20	10	200	17.0905509	0.02885589	0.00400495	742.535416	3070.78923	Not accepted
101	22	10	220	21.6929205	0.02401388	0.00336521	816.788957	3191.48989	Not accepted
⋮	⋮	⋮	⋮	⋮	⋮	⋮	⋮	⋮	⋮
125	10	11	110	-4.70096876	0.12204572	0.01424756	408.394479	2499.28996	Not accepted
126	12	11	132	3.54878663	0.08575227	0.01019813	490.073374	2715.64611	Acceptable design
127	14	11	154	10.8362348	0.06364841	0.00768917	571.75227	2906.76501	Not accepted
128	16	11	176	17.3806798	0.04917544	0.00602208	653.431166	3078.39808	Not accepted
⋮	⋮	⋮	⋮	⋮	⋮	⋮	⋮	⋮	⋮
154	8	12	96	-6.45756027	0.20647728	0.02146473	356.417	2453.22201	Not accepted
155	**10**	**12**	**120**	**3.96257954**	**0.13397005**	**0.01424756**	**445.521249**	**2726.49814**	**Acceptable design***
156	12	12	144	12.9623127	0.09412382	0.01019813	534.625499	2962.52302	Not accepted
157	14	12	168	20.9122562	0.06985773	0.00768917	623.729749	3171.01637	Not accepted
⋮	⋮	⋮	⋮	⋮	⋮	⋮	⋮	⋮	⋮
599	58	26	1508	353.599485	0.01014033	0.00057648	5598.71703	11895.9933	Not accepted
600	60	26	1560	358.933081	0.00950231	0.00054208	5791.77624	12035.871	Not accepted

*Minimal Preheater area, ideal choice-lowest cost

** All the preheater design calculations are carried out assuming P2=22bar.

5.4.2.5 Preheater optimization procedure for R142b

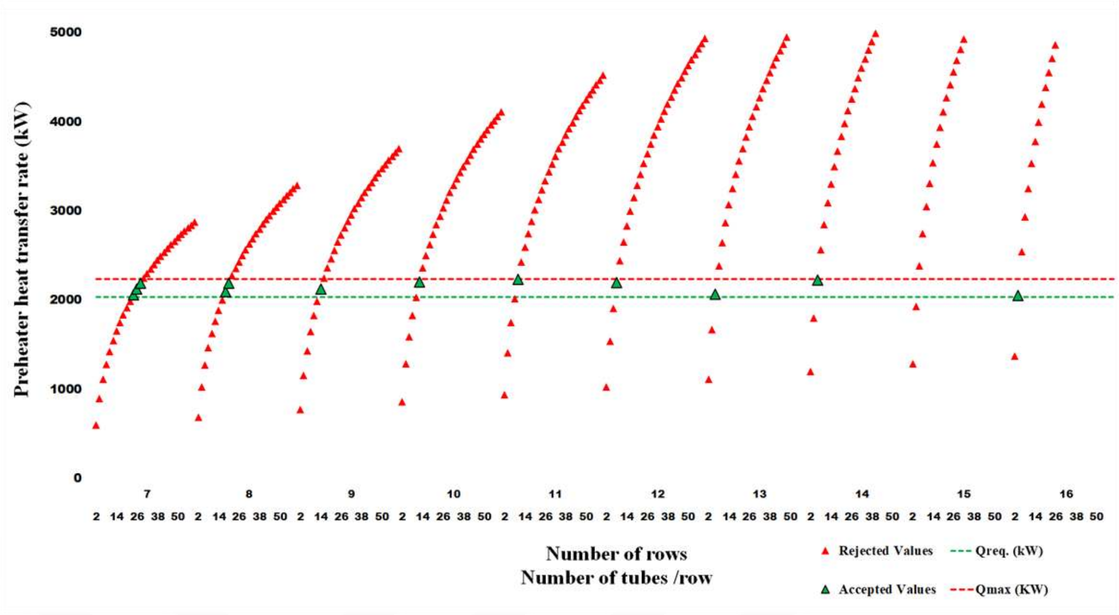

Figure 5.53. Heat transfer rate through the preheater R142b

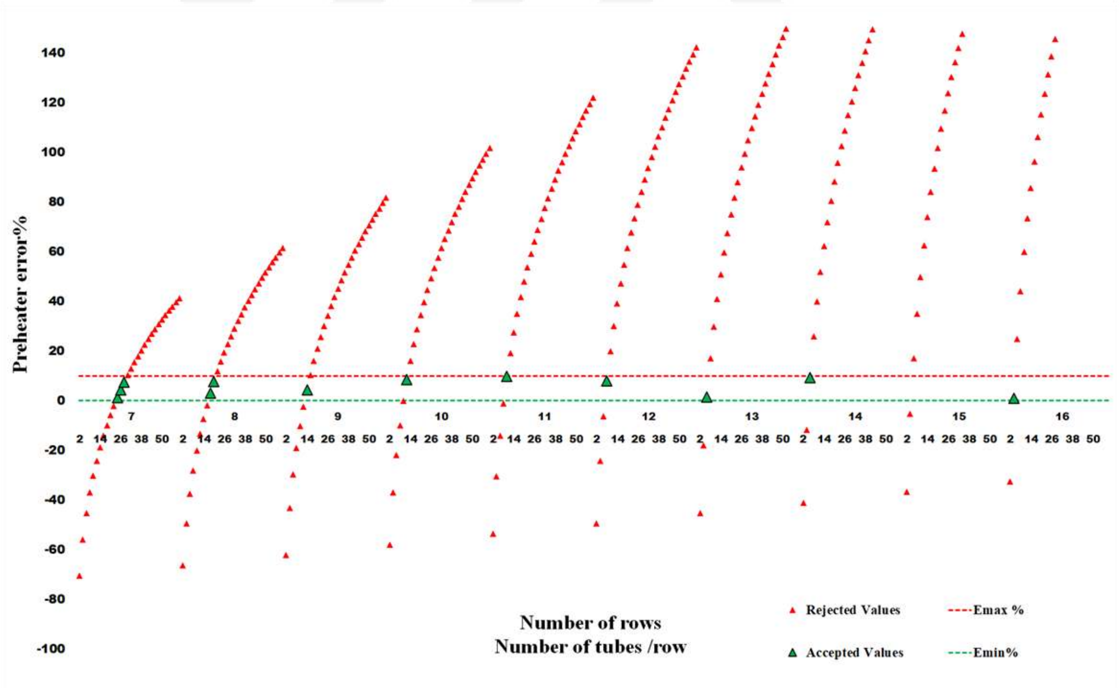

Figure 5.54. Preheater design error % diagram R142b

Figure 5.53 represents the preheater heating duty (kW) accordeing to the total number of tube rows and tubes in one row of each preheater design. The green triangles illustrated in the figure refer to the designs that meet the acceptable values of heating duty that are within the range of two design limitations. These limitations include the upper limit that is represented by a red dashed line, which indicates the maximum permissible preheater heat transfer which is equal to.2240.48 kW, and the lower limit, which is represented by a dashed green line, which corresponds to the minimum required heating rate at 2036.8 kW. On the other hand, the rejected designs that have a heating duty value (kW) outside of the defined range are represented by red triangles. Figure 5.54, illustates the percentage design error, corresponding to the total number of tube rows and tubes in one row for each preheater design. The maximum allowable design error, is set at 10%, which is indicated by a red dashed line. The green triangles correspond to preheater designs that have a design error value of less than 10%, which are placed inside the accepted range. Conversely, the red triangles represent designs with values that exceed the maximum allowable limit or less than zero, indicating unsatisfactory designs. Notably, out of the 600 preheater designs ,only 12 were able to meet this limitation successfully and are represented by green triangles, while the remaining designs were represented by red triangles due to a design error value greater than 10% or less than zero. Overall, this figure insured that all the accepted desings were out of overdesigning or underdesigning.

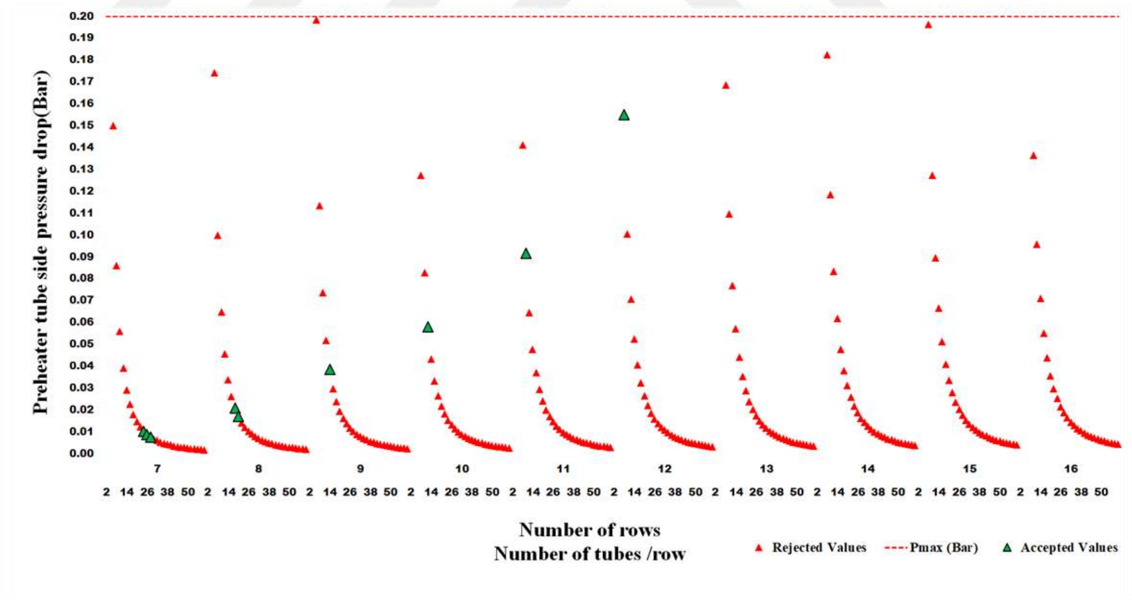

Figure 5.55. Shell side pressure drop through the preheater diagram R142b

Figure 5.55 presents the shell side pressure drop corresponding to the total number of tube rows and the total number of tubes in one row for each preheater design. The red dashed line illustrates the maximum allowable shell side pressure drop of 0.2 bar. The green triangles refer to the designs that have successfully passed all previous tests and have a shell side pressure drop value less than 0.2 bar. On the other hand, the red triangles represent the rejected designs that either have a value exceeding 0.2 bar or failed to pass one of the previous tests. It is noteworthy that only 9 preheater designs out of 600 designs have meeted all the design requirements and successfully have passed all the limitations. Conversely, the remaining designs, although some of them have a shell side pressure drop value less than 0.2 bar they are still rejected as they failed to pass the pervious limitations (heat transfer and design error).

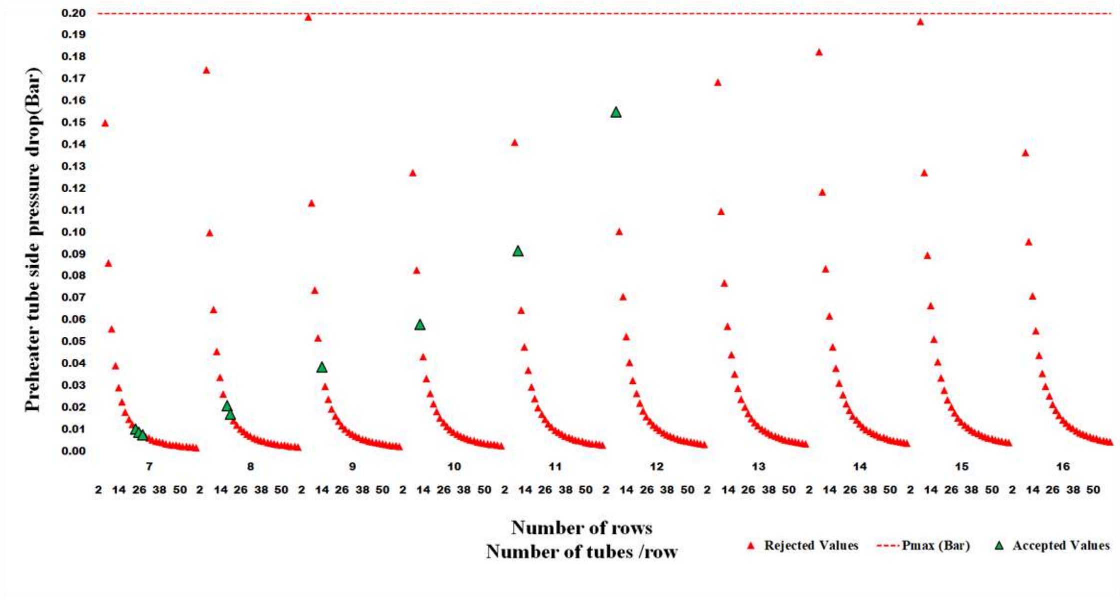

Figure 5.56. Tube side pressure drop through the preheater diagram R142b

Figure 5.56 presents the tube side pressure drop for each preheater design, with respect to the total number of tube rows and the total number of tubes in one row. the red dashed line indicates the maximum allowable tube side pressure drop of 0.2 bar. The green triangles represent the designs that have successfully passed all the previous tests, as well as this limitation, exhibiting a tube side pressure drop value of less than 0.2 bar. Conversely, the red triangles signify the rejected designs that failed to pass one of the pervious tests or have a tube side pressure drop value exceeding the maximum limit. It is noteworthy that only 9 designs, out of the 600 total designs were able to satisfy all the design requirements and constraints, that are represented as green triangles. Although, the red triangle designs, have a tube side pressure drop value less than 0.2 bar, they were rejected due to their inability to fulfill the previous requirements (heating duty and design error.

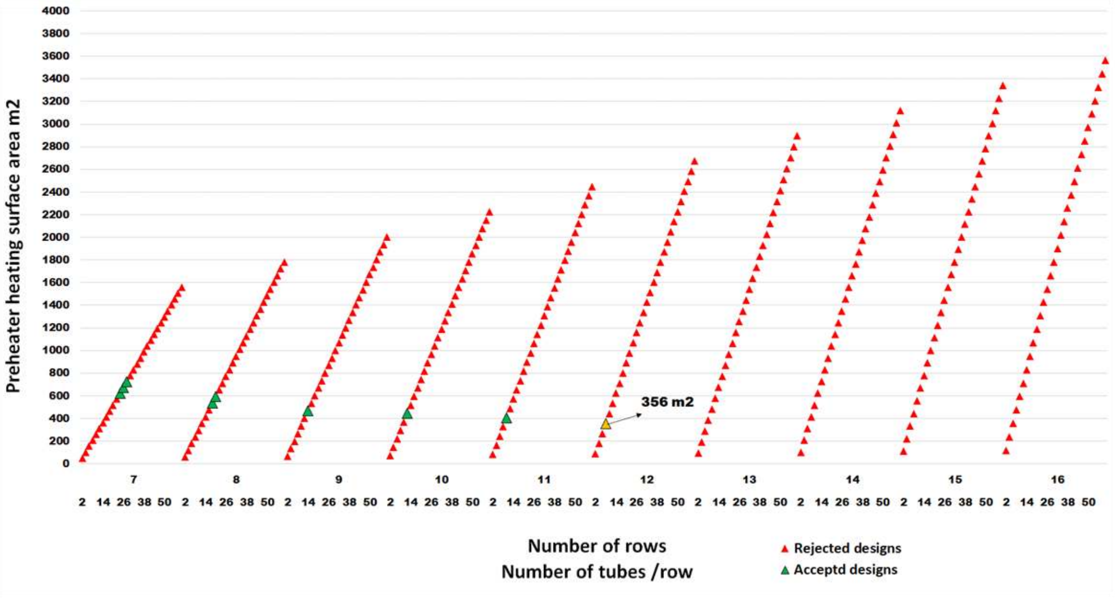

Figure 5.57. Preheater heating surface area diagram R142b

In Figure 5.57, the heating surface area for each preheater design is plotted against the total number of tube rows and the total number of tubes in one row. The green triangles indicate the optimal designs that passed all previous limitations, while the red triangles represent the designs that failed to meet one or more of the previous requirements. It is noteworthy that out of the 600 designs, only 9 satisfied all constraints and are depicted in green, while the remaining designs are rejected. The optimized preheater design, denoted by the yellow triangle, has the smallest heating surface area of 356 m2, corresponding to 8 tubes in one row and 12 tube rows. This design is the most cost-effective option with a minimum investment, while still meeting the required performance. Therefore, it is the preferred choice for the preheater, resulting in significant cost savings in the long run. The results of this optimization process demonstrate the importance of considering both operational costs and efficiency in preheater design, leading to a cost-effective and optimal design.

Table 5.14 records in detail all the preheater final designs parameters including the geometrical and performace ones as it could be used in future studies regarding this field of energy generation.

Table 5.14. Finned tube preheater design result for R142b

NO	$N_{tube/raw}$	N_{raw}	N_{total}	Error	ΔP_t	ΔP_s	A	$\dot{Q}_{est}$	Design Test Result
	#	#	#	%	bar	bar	m^2	kW	accepted/not accepted
1	2	7	14	-70.4745751	1.27098673	0.26946707	51.9774791	601.358228	Not accepted
2	4	7	28	-55.8019867	0.32962073	0.074628	103.954958	900.201745	Not accepted
⋮	⋮	⋮	⋮	⋮	⋮	⋮	⋮	⋮	
12	24	7	168	1.23387807	0.0103276	0.00278197	623.729749	2061.87805	Acceptable design
13	26	7	182	4.42659331	0.00885573	0.00240402	675.707228	2126.90559	Acceptable design
14	28	7	196	7.43309177	0.00768128	0.00210017	727.684707	2188.14036	Acceptable design
15	30	7	210	10.2760552	0.00672879	0.00185202	779.662186	2246.04433	Not accepted
16	32	7	224	12.9741556	0.00594537	0.00164658	831.639666	2300.99781	Not accepted
⋮	⋮	⋮	⋮	⋮	⋮	⋮	⋮	⋮	⋮
37	14	8	112	-7.21829236	0.03380814	0.00745142	415.819833	1889.72872	Not accepted
38	16	8	128	-1.80780673	0.02613187	0.00583569	475.222666	1999.92663	Not accepted
39	18	8	144	3.10952043	0.02082541	0.00470481	534.625499	2100.08015	Acceptable design
40	20	8	160	7.62388959	0.01700121	0.0038808	594.028333	2192.02643	Acceptable design
41	22	8	176	11.8022771	0.01415225	0.00326081	653.431166	2277.12961	Not accepted
42	24	8	192	15.6958606	0.01197161	0.00278197	712.833999	2356.43206	Not accepted
⋮	⋮	⋮	⋮	⋮	⋮	⋮	⋮	⋮	⋮
66	12	9	108	-2.40380134	0.05180767	0.00988315	400.969124	1987.78773	Not accepted
67	14	9	126	4.3794211	0.03846781	0.00745142	467.797312	2125.94481	Acceptable design
68	16	9	144	10.4662174	0.02973037	0.00583569	534.625499	2249.91746	Not accepted
⋮	⋮	⋮	⋮	⋮	⋮	⋮	⋮	⋮	⋮
95	10	10	100	-0.10037895	0.08264748	0.01380812	371.267708	2034.70261	Not accepted
96	12	10	120	8.44022073	0.05808875	0.00988315	445.521249	2208.65303	Acceptable design
97	14	10	140	15.9771346	0.04312748	0.00745142	519.774791	2362.1609	Not accepted
⋮	⋮	⋮	⋮	⋮	⋮	⋮	⋮	⋮	
124	8	11	88	-1.00170049	0.14111247	0.02080384	326.715583	2016.34497	Not accepted
125	10	11	110	9.88958315	0.0915922	0.01380812	408.394479	2238.17287	Acceptable design
⋮	⋮	⋮	⋮	⋮	⋮	⋮	⋮	⋮	
153	6	12	72	-6.24019772	0.27069724	0.03532253	267.31275	1909.65003	Not accepted
154	8	12	96	7.99814492	0.15490674	0.02080384	356.417	2199.64906	**Acceptable design***
155	10	12	120	19.8795453	0.10053692	0.01380812	445.521249	2441.64314	Not accepted
⋮	⋮	⋮	⋮	⋮	⋮	⋮	⋮	⋮	⋮
599	58	26	1508	418.720813	0.00762607	0.00055848	5598.71703	10565.031	Not accepted
600	60	26	1560	424.750969	0.0071466	0.00052516	5791.77624	10687.85	Not accepted

*Minimal Preheater area, ideal choice-lowest cost

** All the preheater design calculations are carried out assuming P2=22bar.

5.4.2.6 Preheater optimization procedure for R600a

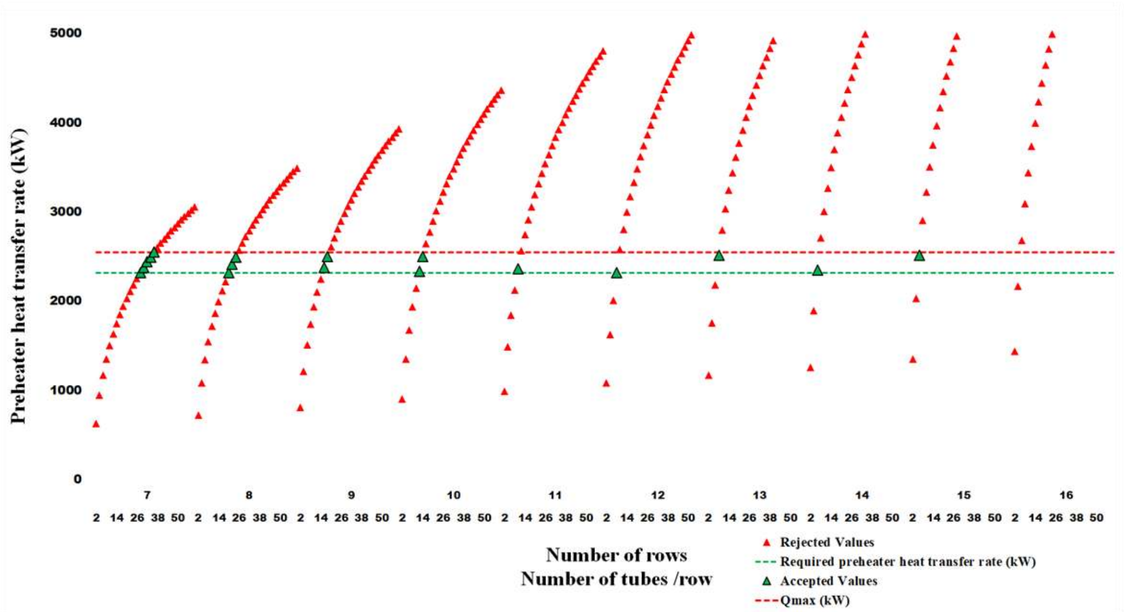

Figure 5.58. Heat transfer rate through the preheater R600a

Figure 5.58 represents the preheater heating duty (kW) accordeing to the total number of tube rows and tubes in one row of each preheater design. The green triangles illustrated in the figure refer to the designs that meet the acceptable values of heating duty that are within the range of two design limitations. These limitations include the upper limit that is represented by a red dashed line, which indicates the maximum permissible preheater heat transfer which is equal to 2551 kW, and the lower limit, which is represented by a dashed green line, which corresponds to the minimum required heating rate at 2319.1 kW. On the other hand, the rejected designs that have a heating duty value (kW) outside of the defined range are represented by red triangles.

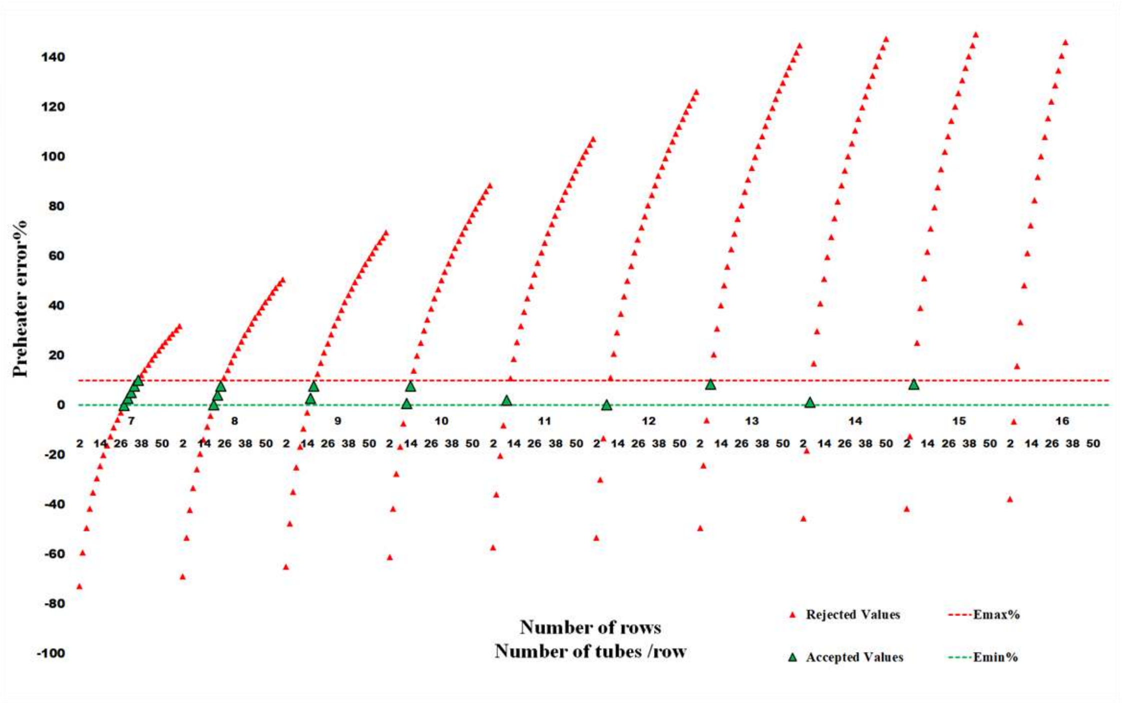

Figure 5.59. Preheater design error % diagram R600a

Figure 5.59, illustates the percentage design error, corresponding to the total number of tube rows and tubes in one row for each preheater design. The maximum allowable design error, is set at 10%, which is indicated by a red dashed line. The green triangles correspond to preheater designs that have a design error value of less than 10%, which are placed inside the accepted range. Conversely, the red triangles represent designs with values that exceed the maximum allowable limit or less than zero, indicating unsatisfactory designs. Notably, out of the 600 preheater designs ,only 17 were able to meet this limitation successfully and are represented by green triangles, while the remaining designs were represented by red triangles due to a design error value greater than 10% or less than zero. Overall, this figure insured that all the accepted desings were out of overdesigning or underdesigning.

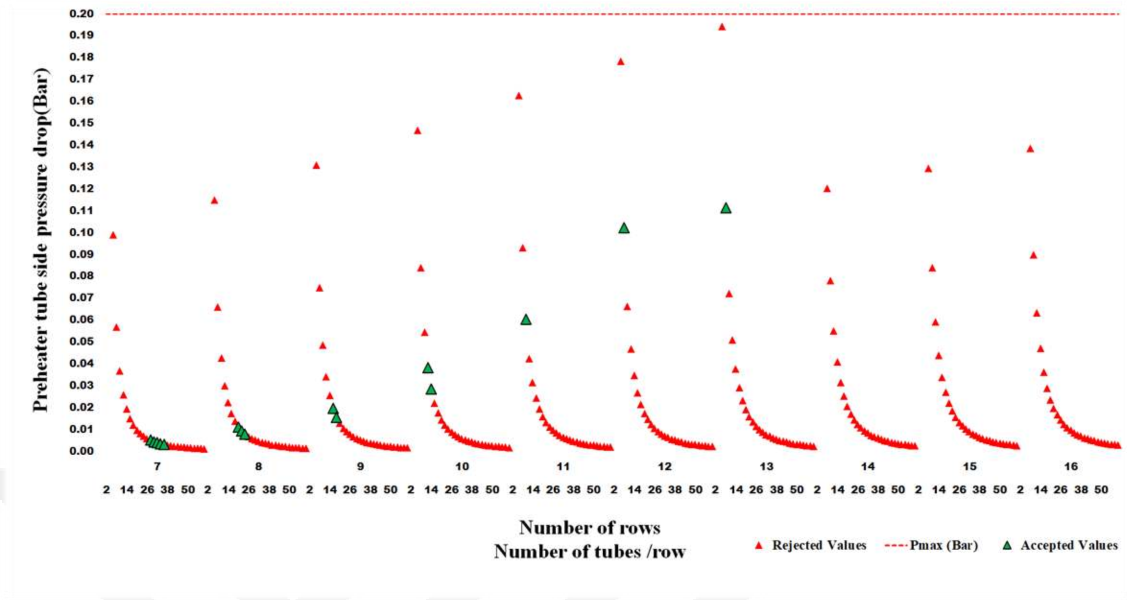

Figure 5.60. Shell side pressure drop through the preheater diagram R600a

Figure 5.60 presents the shell side pressure drop corresponding to the total number of tube rows and the total number of tubes in one row for each preheater design. The red dashed line illustrates the maximum allowable shell side pressure drop of 0.2 bar. The green triangles refer to the designs that have successfully passed all previous tests and have a shell side pressure drop value less than 0.2 bar. On the other hand, the red triangles represent the rejected designs that either have a value exceeding 0.2 bar or failed to pass one of the previous tests. It is noteworthy that only 15 preheater designs out of 600 designs have meeted all the design requirements and successfully have passed all the limitations. Conversely, the remaining designs, although having a shell side pressure drop value less than 0.2 bar they are still rejected as they failed to pass the pervious limitations (heat transfer and design error).

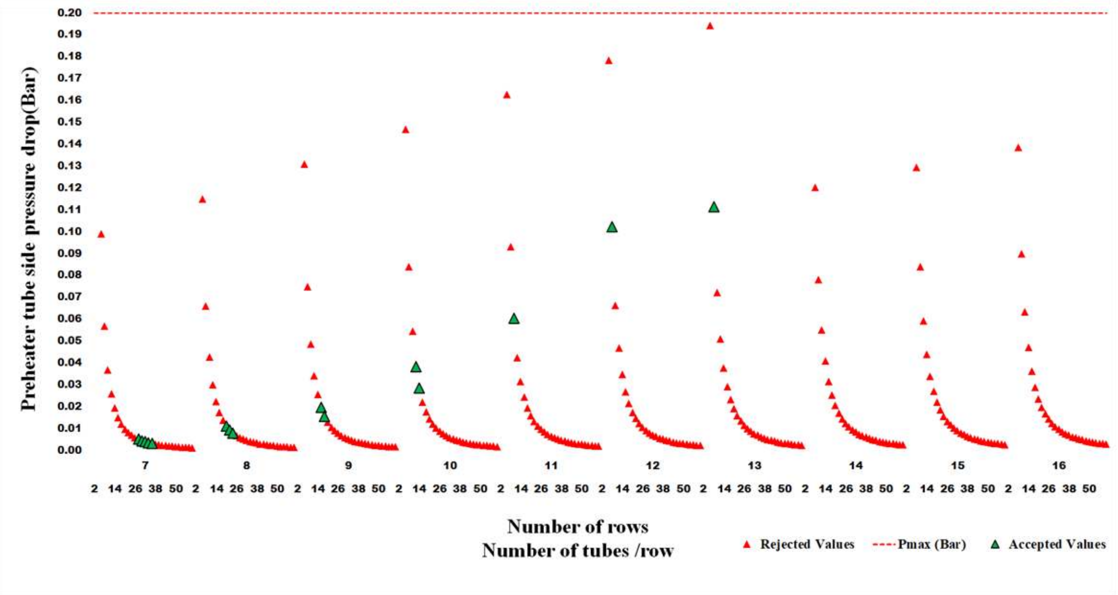

Figure 5.61. Tube side pressure drop through the preheater diagram R600a

Figure 5.61 presents the tube side pressure drop for each preheater design, with respect to the total number of tube rows and the total number of tubes in one row. the red dashed line indicates the maximum allowable tube side pressure drop of 0.2 bar. The green triangles represent the designs that have successfully passed all the previous tests, as well as this limitation, exhibiting a tube side pressure drop value of less than 0.2 bar. Conversely, the red triangles signify the rejected designs that failed to pass one of the pervious tests or have a tube side pressure drop value exceeding the maximum limit. It is noteworthy that only 15 designs, out of the 600 total designs were able to satisfy all the design requirements and constraints, that are represented as green triangles. Although, the red triangle designs, have a tube side pressure drop value less than 0.2 bar, they were rejected due to their inability to fulfill the previous requirements (heating duty and design error.

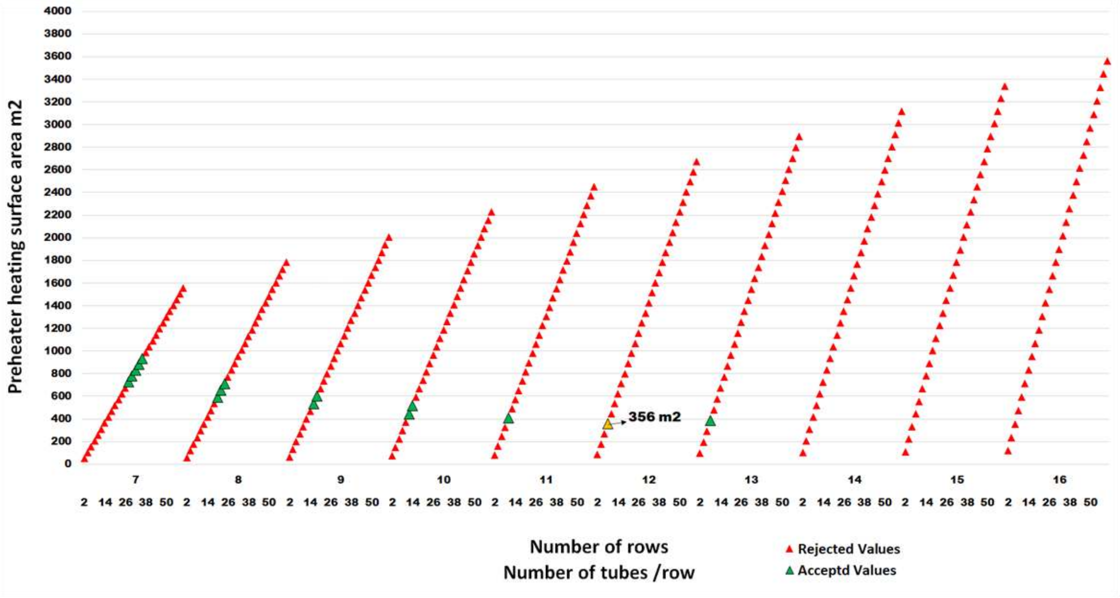

Figure 5.62. Preheater heating surface area diagram R600a

In Figure 5.62, the heating surface area for each preheater design is plotted against the total number of tube rows and the total number of tubes in one row. The green triangles indicate the optimal designs that passed all previous limitations, while the red triangles represent the designs that failed to meet one or more of the previous requirements. It is noteworthy that out of the 600 designs, only 15 satisfied all constraints and are depicted in green, while the remaining designs are rejected. The optimized preheater design, denoted by the yellow triangle, has the smallest heating surface area of 356 m2, corresponding to 8 tubes in one row and 12 tube rows. This design is the most cost-effective option with a minimum investment, while still meeting the required performance. Therefore, it is the preferred choice for the preheater, resulting in significant cost savings in the long run. The results of this optimization process demonstrate the importance of considering both operational costs and efficiency in preheater design, leading to a cost-effective and optimal design.

Table 5.15 records in detail all the preheater final designs parameters including the geometrical and performace ones as it could be used in future studies regarding this field of energy generation.

Table 5.15. Finned tube preheater design result for R600a

NO	$N_{tube/raw}$	N_{raw}	N_{total}	Error	ΔP_t	ΔP_s	A	$\dot{Q}_{est}$	Design Test Result
	#	#	#	%	bar	bar	m^2	kW	accepted/not accepted
1	2	7	14	-72.7688648	0.83664014	0.27354592	51.9774791	631.51546	Not accepted
2	4	7	28	-59.1285087	0.21722614	0.07576441	103.954958	947.84806	Not accepted
⋮	⋮	⋮	⋮	⋮	⋮	⋮	⋮	⋮	⋮
14	28	7	196	0.05524091	0.00508147	0.00213264	727.684707	2320.37449	Acceptable design
15	30	7	210	2.7252186	0.00445203	0.00188067	779.662186	2382.29377	Acceptable design
16	32	7	224	5.25962044	0.00393424	0.00167206	831.639666	2441.06892	Acceptable design
17	34	7	238	7.67297883	0.00350302	0.0014973	883.617145	2497.03695	Acceptable design
18	36	7	252	9.97754687	0.00313999	0.00134935	935.594624	2550.48204	Acceptable design
19	38	7	266	12.1837569	0.0028314	0.00122291	987.572103	2601.64611	Not accepted
⋮	⋮	⋮	⋮	⋮	⋮	⋮	⋮	⋮	⋮
39	18	8	144	-4.11121276	0.01376155	0.00477732	534.625499	2223.75054	Not accepted
40	20	8	160	0.12286946	0.01123695	0.00394065	594.028333	2321.94286	Acceptable design
41	22	8	176	4.0431457	0.0093558	0.00331114	653.431166	2412.85773	Acceptable design
42	24	8	192	7.69727992	0.00791567	0.00282494	712.833999	2497.60052	Acceptable design
43	26	8	208	11.1225842	0.0067881	0.00244117	772.236832	2577.03652	Not accepted
⋮	⋮	⋮	⋮	⋮	⋮	⋮	⋮	⋮	⋮
67	14	9	126	-3.01563447	0.02540355	0.00756603	467.797312	2249.15803	Not accepted
68	16	9	144	2.68838597	0.01963875	0.00592554	534.625499	2381.43959	Acceptable design
69	18	9	162	7.87488564	0.01565307	0.00477732	601.453687	2501.71936	Acceptable design
70	20	9	180	12.6382281	0.01278034	0.00394065	668.281874	2612.18572	Not accepted
⋮	⋮	⋮	⋮	⋮	⋮	⋮	⋮	⋮	⋮
95	10	10	100	-7.29213813	0.054538	0.01401996	371.267708	2149.98191	Not accepted
96	12	10	120	0.70139459	0.0383455	0.01003499	445.521249	2335.3594	Acceptable design
97	14	10	140	7.76040614	0.02847791	0.00756603	519.774791	2499.06447	Acceptable design
98	16	10	160	14.0982066	0.02201357	0.00592554	594.028333	2646.04399	Not accepted
99	18	10	180	19.860984	0.01754459	0.00477732	668.281874	2779.68818	Not accepted
⋮	⋮	⋮	⋮	⋮	⋮	⋮	⋮	⋮	⋮
124	8	11	88	-8.20595871	0.0930722	0.02112245	326.715583	2128.78956	Not accepted
125	10	11	110	1.97864805	0.06043587	0.01401996	408.394479	2364.9801	Acceptable design
126	12	11	132	10.7715341	0.04248844	0.01003499	490.073374	2568.89534	Not accepted
⋮	⋮	⋮	⋮	⋮	⋮	⋮	⋮	⋮	⋮
153	6	12	72	-13.15961	0.17843742	0.03586223	267.31275	2013.90976	Not accepted
154	**8**	**12**	**96**	**0.13895414**	**0.1021641**	**0.02112245**	**356.417**	**2322.31588**	**Acceptable design***
155	10	12	120	11.2494342	0.06633375	0.01401996	445.521249	2579.97829	Not accepted
⋮	⋮	⋮	⋮	⋮	⋮	⋮	⋮	⋮	⋮
183	6	13	78	-5.92291081	0.19433517	0.03586223	289.588812	2181.73557	Not accepted
184	8	13	104	8.48386698	0.11125601	0.02112245	386.118416	2515.84221	Acceptable design
185	10	13	130	20.5202204	0.07223163	0.01401996	482.64802	2794.97649	Not accepted
⋮	⋮	⋮	⋮	⋮	⋮	⋮	⋮	⋮	⋮
599	58	26	1508	384.132568	0.00504791	0.00056715	5598.71703	11227.4865	Not accepted
600	60	26	1560	389.805595	0.00473089	0.00053332	5791.77624	11359.0493	Not accepted

*Minimal Preheater area, ideal choice-lowest cost

** All the preheater design calculations are carried out assuming P2=22bar.

5.4.3 Design optimization procedure for Superheater

Table 5.16. Superheater's fixed properties and parameters

Tube fixed geometries	
Do (mm)	57.15
Din (mm)	53.8
Ltube (mm)	800
Material	Carbon steel
Fin fixed geometries	
Df (mm)	89.6
Lf (mm)	15.8
tf (mm)	0.4
S (mm)	15
Material	Alaminum
Dbend	3 x Do
Tube layout	Staggered (°60)

Nr= (2 – 11) raws & nt=(2-31) tubes per rows

$Nt = Nr\ X\ nt;\ (\mathbf{2x3, 2x4, 2x5 \ldots \ldots \ldots \ldots \ldots \ldots \ldots \ldots \ldots \ldots \ldots. 11x31})$

(300 design) attempted in all calculations for superheater and each design is tested by previous mentioned limitations. This careful approach was taken to ensure that the final design would meet the required performance specifications while also minimizing costs and maximizing efficiency. By evaluating numerous design options, we were able to identify the most effective configuration for the superheater, resulting in an optimal and reliable solution for the project.

5.4.3.1 Superheater optimization procedure for R245fa

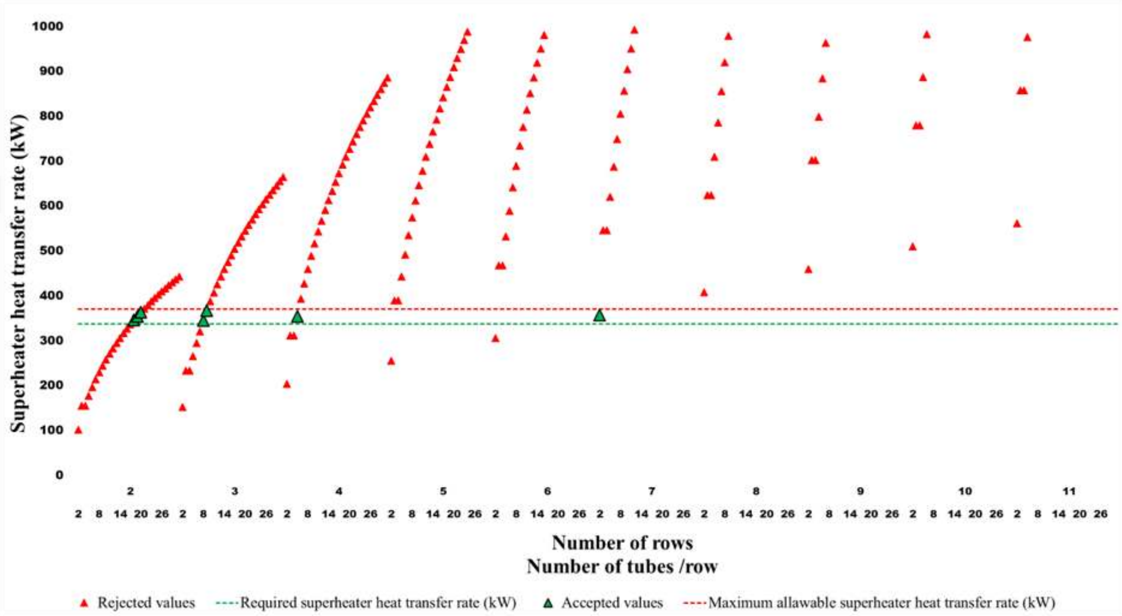

Figure 5.63. Heat transfer rate through the superheater R245fa

Figure 5.63, illustrates the total heat transfer rate of 300 different designs of superheaters as a function of the total number of tube rows and tubes in one row of each design. The green triangles represent the superheater designs that meet required value of the heat transfer that are located between the upper limit and the lower limit. The upper limit, shown as a red dashed line, signifies the maximum permissible superheater heat transfer (kW) at 371, while the lower limit is denoted by a dashed green line, representing the minimum required heating rate (kW) at 338. On the other hand, the red triangles signify the designs that do not meet the established criteria and, consequently, have been rejected. It shown by the figure that only 7 designs have successfully satisfied this range out of 300 superheater designs attempted. This outcome is expected since the heating duty required for superheaters is considerably lower than that of evaporators and preheaters. These results indicate that only a few superheater designs meet the established criteria, that consequently go through other design limitations to select the optimal design among them. horizontal axis represents the number of tubes per row and the total number of tubes rows of each superheater design and each design of them results in a value of heat transfer kW which is indicated in vertical axis.

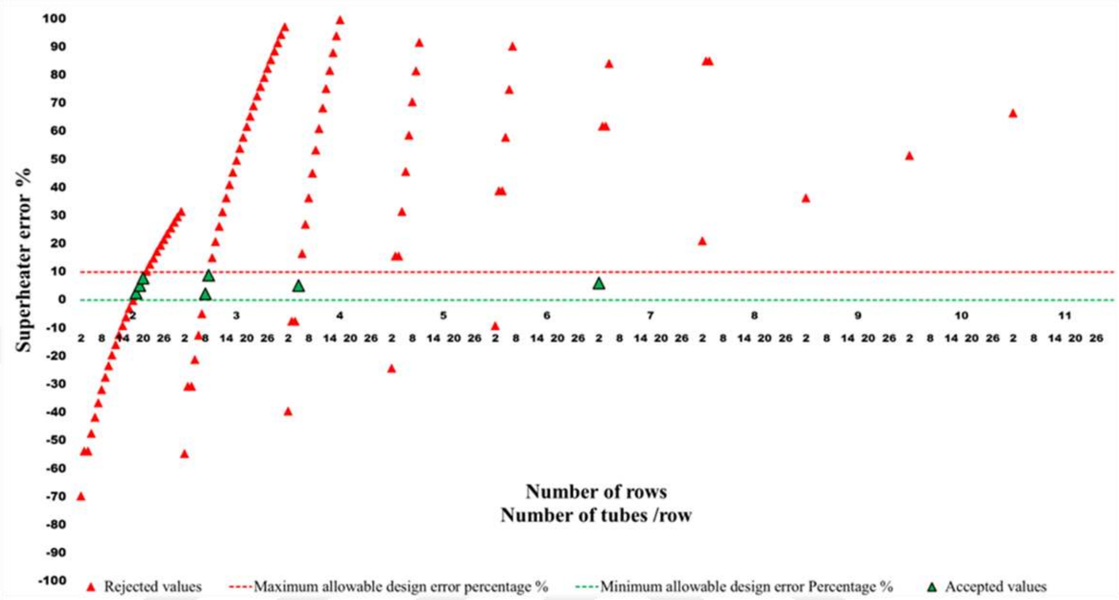

Figure 5.64. Superheater design error% diagram R245fa

Figure 5.64 provides a representation of superheater design error for 300 superheater designs with respect to the total number of tube rows and the total number of tubes in one row of each superheater design. The maximum allowable percentage of the design error for each superheater design is represented as an upper limit of 10% marked by a red dashed line. The successful designs that meet this criterion and have a design error value of less than 10% are denoted by green triangles, while the designs that exceed the upper limit or have negative values are represented by red triangles, indicating their failure to meet the design requirements. It is noteworthy that out of all the attempted superheater designs, only 7 were able to pass this limitation. The findings of this analysis provided superheater designs with an accurate volume that were prevented from being underdesigned or overdesigned and this enable them to go further through other design limitations in order to select the optimal design of them.

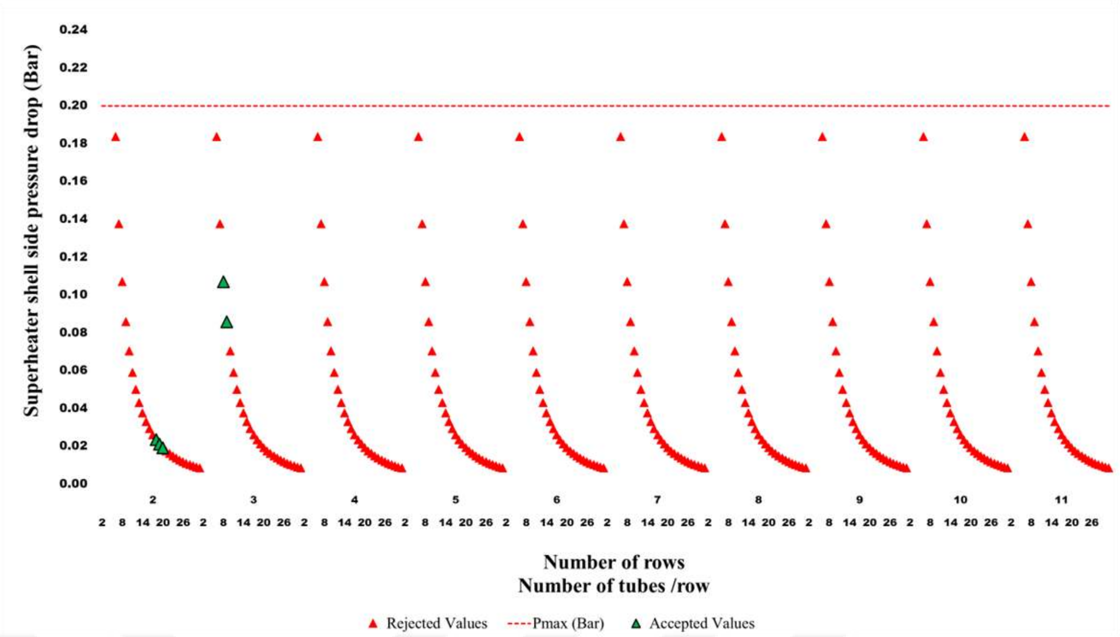

Figure 5.65. Shell side pressure drop through the superheater R245fa

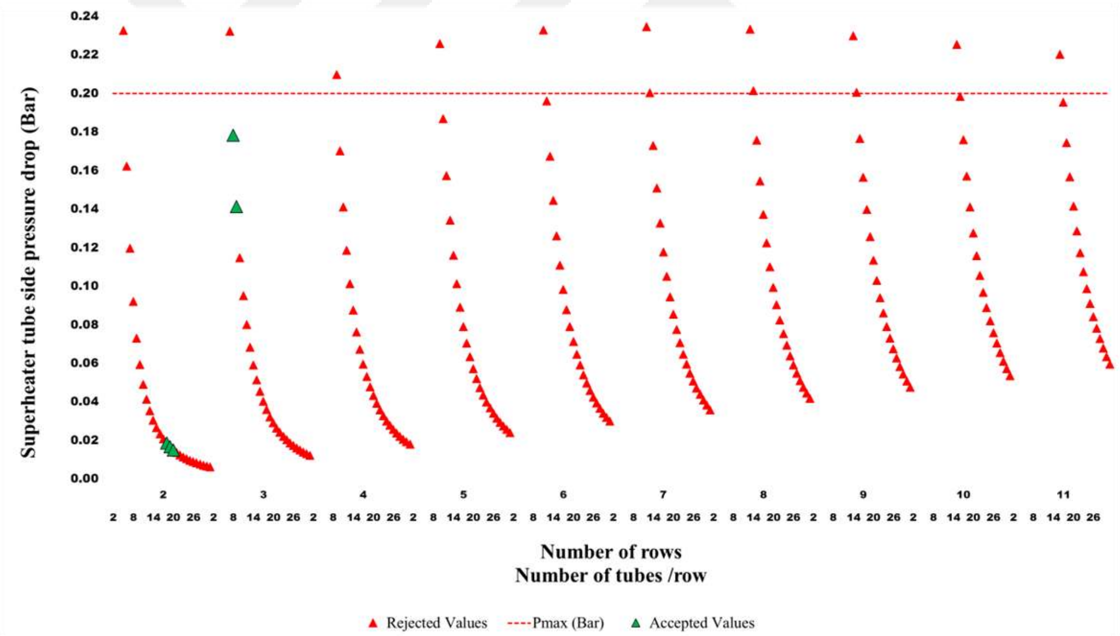

Figure 5.66. Tube side pressure drop through the superheater

Figures 5.65 and 5.66 provide a representation of the superheater's shell side pressure drop, tube side pressure drop,as a function of the total number of tube rows and tubes in one row of each superheater design. The red dashed line, which marks the maximum allowable value of 0.2 bar, serves as a stringent criterion for evaluating each design's suitability. The figure illustrates that out of the 300 attempted designs, only 5 superheater designs were approved to be the ultimate choice, demonstrating outstanding performance that satisfies all previous design limitations and conform with the pressure drop requirement. These accepted designs were represented by green triangles in the figure, while the red triangles depicted the rejected designs that failed to meet the previous limitations, despite some of them had a pressure drop less than 0.2 bar. This emphasizes the critical role of the optimization process in ensuring the creation of an efficient and high-performing superheaters that meet all the essential design requirements.

Efficiency and cost are critical considerations when designing a superheater. The heating surface area of a superheater is a crucial factor that affects its performance and cost. A larger heating surface area can enhance its efficiency by reducing the pressure drop through it as there is a trade off between the surface area and the pressure drop, but it also increases the investment cost. Therefore, finding the optimal heating surface area that meets the pressure drop limitation of 0.2 bar is essential to achieve maximum efficiency while minimizing costs by reducing it. This optimization process provided a balancing between investment cost (minimum heating surface area) and operational expenses (mimimal pressur drop less that 0.2 bar), ensuring that the superheater is designed to the highest standards. A well-designed superheater with an optimized heating surface area can lead to significant cost savings in the long run and investment costs. The following figure shows the corresponding surface area of 300 designs in which the perfect designs that have successfully passed all the suggested design limitation by this paper are repersented in a green color while the other that failed to pass on of the previous mentioned design limitation are pollted in the figure as red triangles. The optimal design what satisfy all the design criteria and has the smallest heating surface area between the accepted design is shown as a yellow triangle.

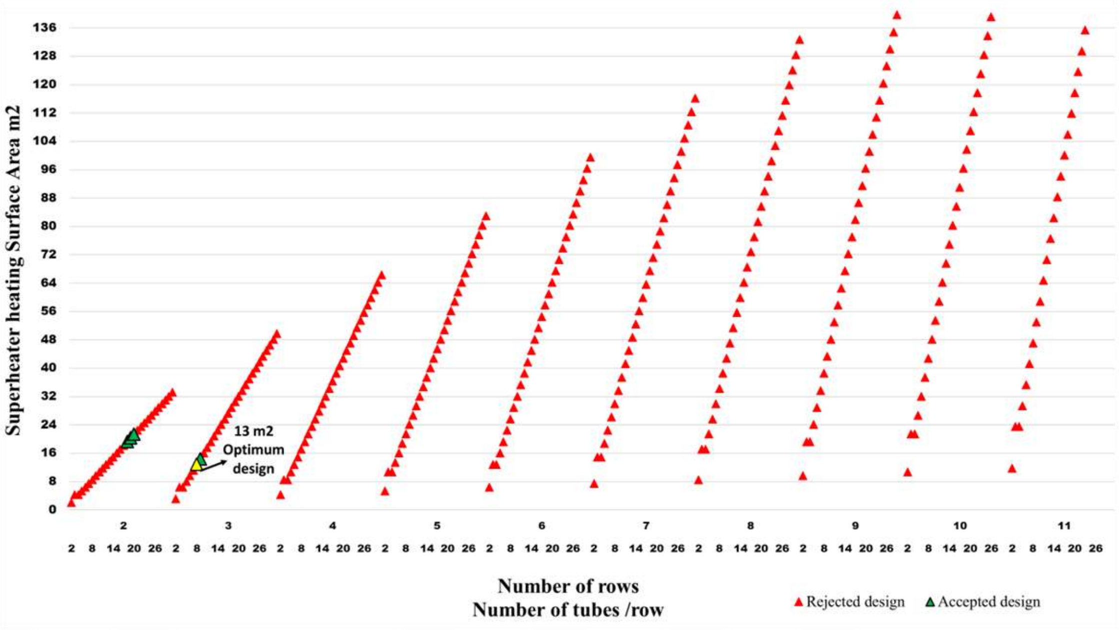

Figure 5.67. Superheater heating surface area diagram R245fa

Figure 5.67, repersents the heating surface areas that correspond to the variables indicated in the x- axis of each superheater design. The superheater designs that have successfully satisfyed all the desing limitations are shown in the figure as green triangles.while the other that were rejected as they falled out the acceptaple range are in a red color. A design between these accepted ones was selected as an optimal design as it had the smallest surface area, in other words, it has a lower material cost than the other's. This optimal desing was shown in the chart as a yellow triangle with a minimal heating surface area of 13 m2, a number of tubes in one row of 8, and a number of tubes rows of 3. The findings from this process indicate that the methodology which was suggested in this study has reached its goels by obtaining a superheater which has a minimal heating surface area while keeping the pressure drop in a low level of less than 0.2 bar.

A table is inserted below which shows in detail all the findings of this process with concering in the accepted superheater designs

Table 5.17. Finned Tube Superheater Design Result R245fa

NO	$N_{tube/raw}$	N_{raw}	N_{total}	Error	ΔP_t	ΔP_s	A	$\dot{Q}_{est}$	Design Test Result
	#	#	#	%	bar	bar	m^2	kW	accepted/not accepted
1	2	2	4	-70	1.42	1.464	2	102.2	Not accepted
⋮	⋮	⋮	⋮	⋮	⋮	⋮	⋮	⋮	⋮
17	18	2	36	3	0.019	0.023	19	346.3	Accepted
18	19	2	38	5	0.017	0.021	20	355.2	Accepted
19	20	2	40	8	0.0152	0.019	21	363.9	Accepted
⋮	⋮	⋮	⋮	⋮	⋮	⋮	⋮	⋮	⋮
36	7	3	21	-5	0.232	0.138	11	321.3	Not accepted
37	**8**	**3**	**24**	**2**	**0.178**	**0.107**	**13**	**345.2**	**Accepted***
38	9	3	27	9	0.141	0.086	14	367.4	Accepted
39	10	3	30	15	0.115	0.07	16	388.2	Not accepted
⋮	⋮	⋮	⋮	⋮	⋮	⋮	⋮	⋮	⋮
293	24	11	264	545	0.099	0.014	141	2176.7	Not accepted
294	25	11	275	557	0.091	0.013	147	2217.4	Not accepted
295	26	11	286	569	0.084	0.012	153	2256.9	Not accepted
296	27	11	297	580	0.078	0.011	159	2295.4	Not accepted
297	28	11	308	591	0.073	0.01	165	2332.9	Not accepted
298	29	11	319	602	0.068	0.01	171	2369.5	Not accepted
299	30	11	330	613	0.064	0.009	177	2405.2	Not accepted
300	31	11	341	623	0.06	0.009	183	2440.1	Not accepted

*Minimal superheater area, ideal choice-lowest cost

** All the superheater design calculations are carried out assuming P2=22bar.

5.4.3.2 Superheater optimization procedure for R600

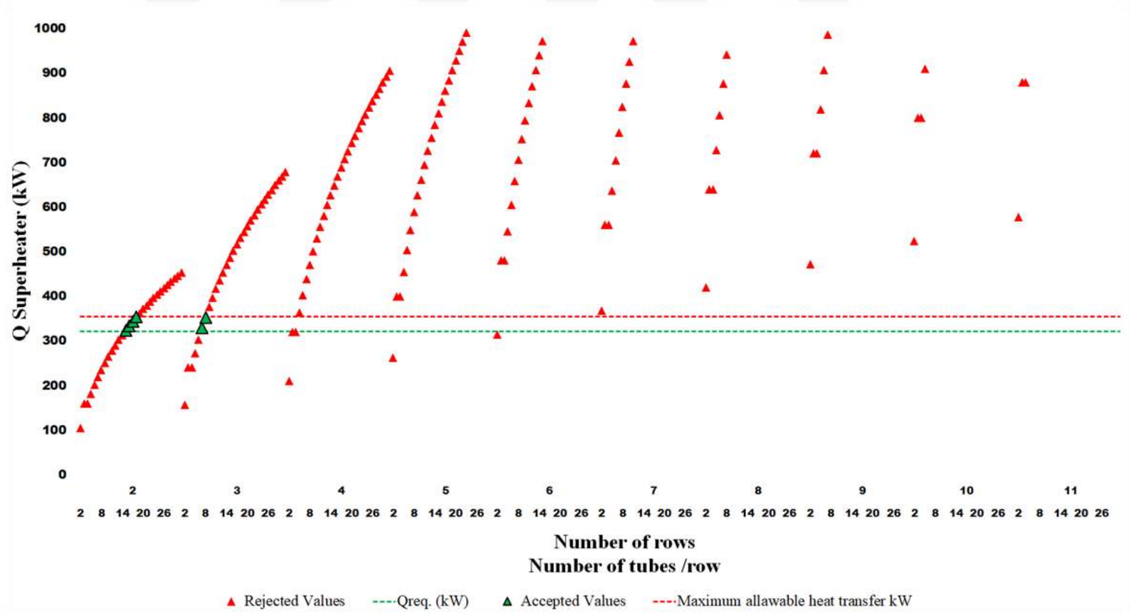

Figure 5.68. Heat transfer rate through the superheater R600

Figure 5.68, shows the total heat transfer rate of 300 different designs of superheaters as a function of the total number of tube rows and tubes in one row of each design. The green triangles represent the superheater designs that meet required value of the heat transfer that are located between the upper limit and the lower limit. The upper limit, shown as a red dashed line, signifies the maximum permissible superheater heat transfer (kW) at 354.56 , while the lower limit is denoted by a dashed green line, representing the minimum required heating rate (kW) at 322.33 On the other hand, the red triangles signify the designs that do not meet the established criteria and, consequently, have been rejected. It shown by the figure that only 6 designs have successfully satisfied this range out of 300 superheater designs attempted. This outcome is expected since the heating duty required for superheaters is considerably lower than that of evaporators and preheaters. These results indicate that only a few superheater designs meet the established criteria, that consequently go through other design limitations to select the optimal design among them. horizontal axis represents the number of tubes per row and the total number of tubes rows of each superheater design and each design of them results in a value of heat transfer kW which is indicated in vertical axis.

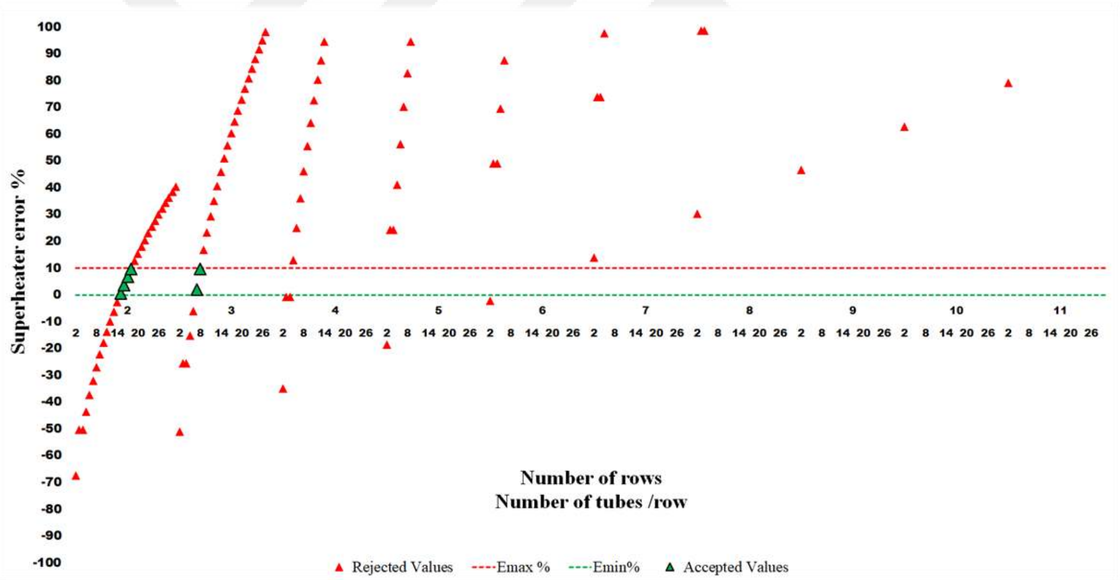

Figure 5.69. Superheater design error% diagram R600

Figure 5.69 provides a representation of superheater design error for 300 superheater designs with respect to the total number of tube rows and the total number of tubes in one row of each superheater design. The maximum allowable percentage of the design error for each superheater design is represented as an upper limit of 10% marked by a red dashed line. The successful designs that meet this criterion and have a design error value of less than 10% are denoted by green triangles, while the designs that exceed the upper limit or have negative values are represented by red triangles, indicating their failure to meet the design requirements. It is noteworthy that out of all the attempted superheater designs, only 6 were able to pass this limitation. The findings of this analysis provided superheater designs with an accurate volume that were prevented from being underdesigned or overdesigned and this enable them to go further through other design limitations in order to select the optimal design of them.

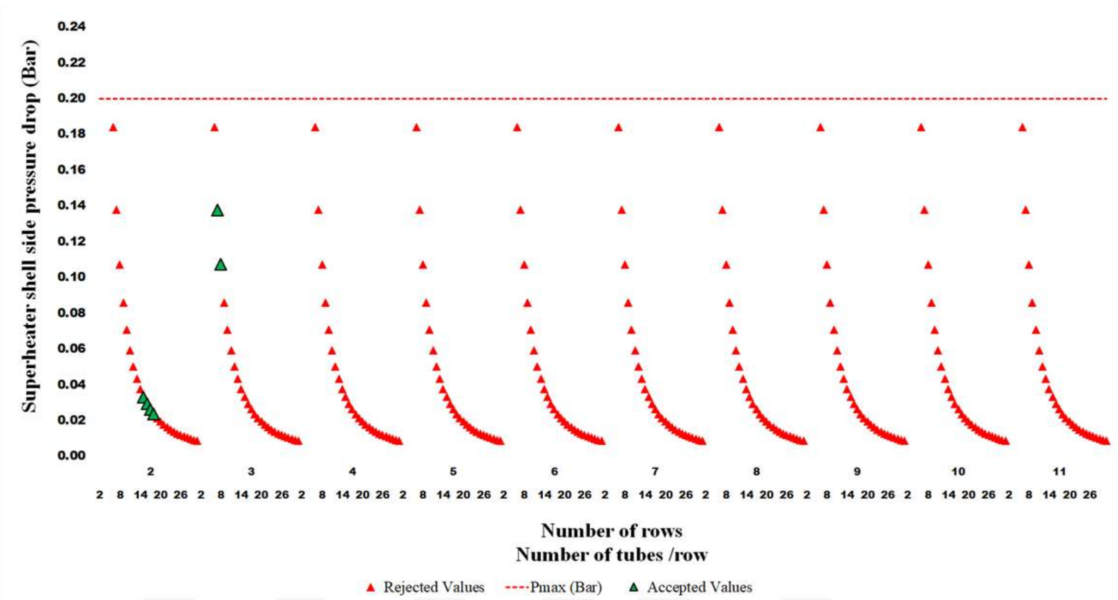

Figure 5.70. Shell side pressure drop through the superheater R600

Figure 5.70 presents the shell side pressure drop for each superheater design as a function of the total number of tube rows and the total number of tubes in one row of each design. A red dashed line indicates the maximum allowable shell side pressure drop of 0.2 bar, which is a crucial factor in ensuring optimal preheater performance. The green triangles represent the designs that have successfully passed all the previous tests, as well as this limitation, exhibiting a shell side pressure drop value of less than 0.2 bar. Conversely, the red triangles are the rejected designs that failed to pass one of the previous limitations or have a tube side pressure drop value exceeding the maximum limit. It is noteworthy that only 6 designs, out of the 300 total designs considered, were able to satisfy all the design requirements and constraints.

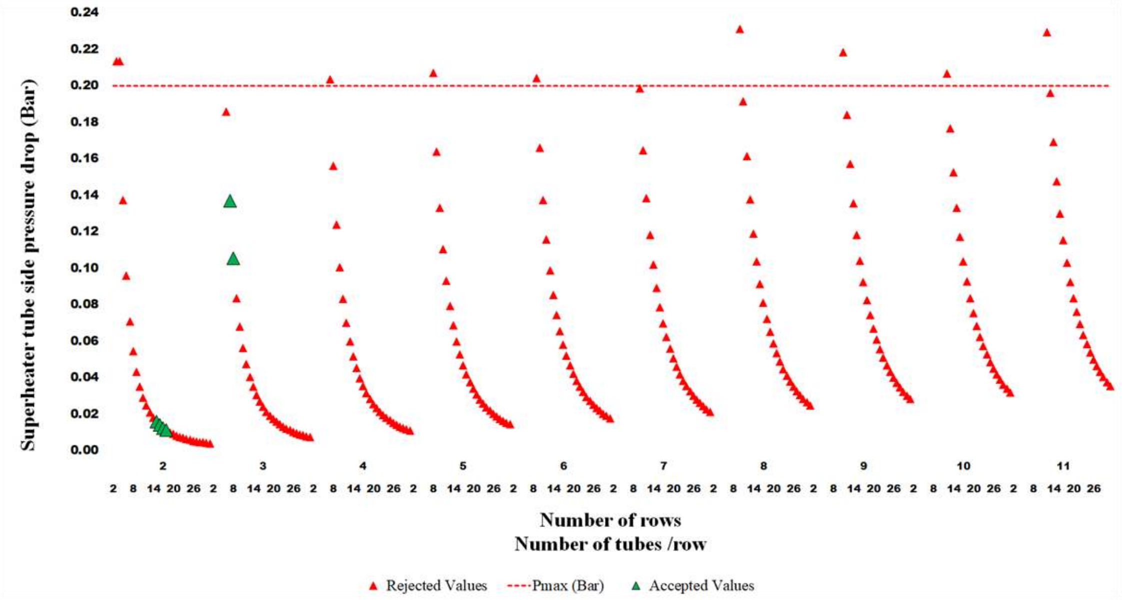

Figure 5.71. Tube side pressure drop through the superheater R600

Figures 5.71 provide a representation of the superheater's tube side pressure drop, as a function of the total number of tube rows and tubes in one row of each superheater design. The red dashed line, which marks the maximum allowable value of 0.2 bar, serves as a stringent criterion for evaluating each design's suitability. The figure illustrates that out of the 300 attempted designs, only 6 superheater designs were approved to be the ultimate choice, demonstrating outstanding performance that satisfies all previous design limitations and conform with the pressure drop requirement. These accepted designs were represented by green triangles in the figure, while the red triangles depicted the rejected designs that failed to meet the previous limitations, despite some of them had a pressure drop less than 0.2 bar. This emphasizes the critical role of the optimization process in ensuring the creation of an efficient and high-performing superheaters that meet all the essential design requirements.

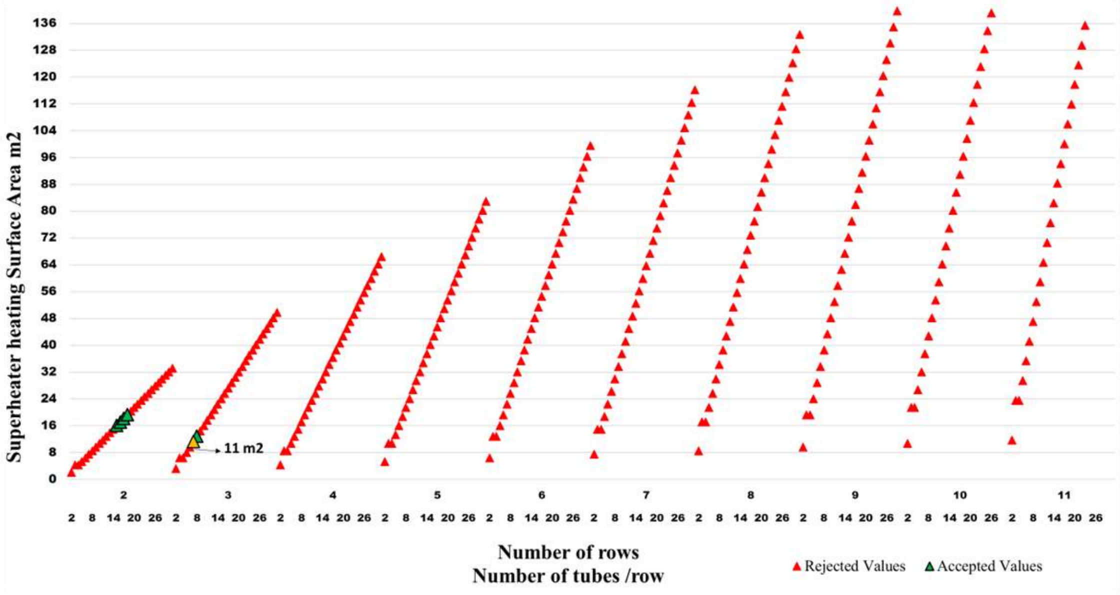

Figure 5.72. Superheater heating surface area diagram R600

Figure 5.72, repersents the heating surface areas that correspond to the variables of each superheater design that are indicated in the x- axis. The superheater designs that have successfully satisfyed all the desing limitations are shown in the figure as green triangles.while the other that were rejected as they falled out the acceptaple range are in a red color. A design between these accepted ones was selected as an optimal design as it had the smallest surface area, in other words, it has a lower material cost than the other's. This optimal desing was shown in the chart as a yellow triangle with a minimal heating surface area of 11 m2, a number of tubes in one row of 7, and a number of tubes rows of 3. The findings from this process indicate that the methodology which was suggested in this study has reached its goels by obtaining a superheater which has a minimal heating surface area while keeping the pressure drop in a low level of less than 0.2 bar.

A table is inserted below which shows in detail all the findings of this process with concering in the accepted superheater designs

Table 5.18. Finned Tube Superheater Design Result R600

NO	$N_{tube/raw}$	N_{raw}	N_{total}	Error	ΔP_t	ΔP_s	A	$\dot{Q}_{est}$	Design Test Result
	#	#	#	%	bar	bar	m^2	kW	accepted/not accepted
1	2	2	4	-67.4393	0.8372	1.4654	2.1415	104.9517	Not accepted
2	4	2	8	-50.3463	0.2131	0.3949	4.2829	160.0470	Not accepted
:	:	:	:	:	:	:	:	:	:
14	15	2	30	0.5794	0.0158	0.0330	16.0609	324.1941	Acceptable design
15	16	2	32	3.7604	0.0139	0.0293	17.1316	334.4473	Acceptable design
16	17	2	34	6.8111	0.0124	0.0262	18.2024	344.2806	Acceptable design
17	18	2	36	9.7433	0.0111	0.0235	19.2731	353.7319	Acceptable design
18	19	2	38	12.5672	0.0100	0.0213	20.3438	362.8341	Not accepted
19	20	2	40	15.2917	0.0090	0.0193	21.4145	371.6159	Not accepted
20	21	2	42	17.9246	0.0082	0.0176	22.4853	380.1023	Not accepted
:	:	:	:	:	:	:	:	:	:
34	5	3	15	-15.3153	0.2664	0.2593	8.0304	272.9611	Not accepted
35	6	3	18	-6.2090	0.1858	0.1840	9.6365	302.3133	Not accepted
36	**7**	**3**	**21**	**2.0498**	**0.1370**	**0.1377**	**11.2426**	**328.9338**	**Acceptable design***
37	8	3	24	9.6298	0.1053	0.1072	12.8487	353.3660	Acceptable design
38	9	3	27	16.6510	0.0834	0.0859	14.4548	375.9973	Not accepted
39	10	3	30	23.2027	0.0678	0.0705	16.0609	397.1149	Not accepted
:	:	:	:	:	:	:	:	:	:
299	30	11	330	661.2945	0.0375	0.0091	176.6699	2453.8544	Not accepted
300	31	11	341	672.2715	0.0352	0.0086	182.5589	2489.2362	Not accepted

*Minimal superheater area, ideal choice-lowest cost

** All the superheater design calculations are carried out assuming P2=22bar.

5.4.3.3 Superheater optimization procedure for R123

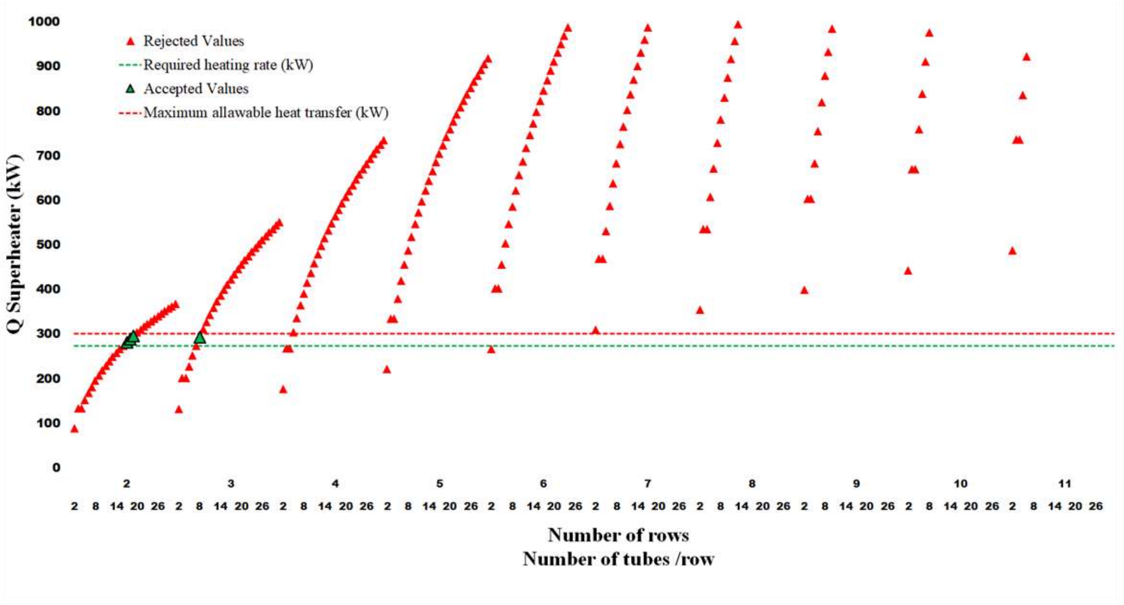

Figure 5.73. Heat transfer rate through the superheater R123

Figure 5.73, illustrates the total heat transfer rate of 300 different designs of superheaters as a function of the total number of tube rows and tubes in one row of each design. The green triangles represent the superheater designs that meet required value of the heat transfer that are located between the upper limit and the lower limit. The upper limit, shown as a red dashed line, signifies the maximum permissible superheater heat transfer (kW) at 302, while the lower limit is denoted by a dashed green line, representing the minimum required heating rate (kW) at 274.56. On the other hand, the red triangles signify the designs that do not meet the established criteria and, consequently, have been rejected. It shown by the figure that only 4 designs have successfully satisfied this range out of 300 superheater designs attempted. This outcome is expected since the heating duty required for superheaters is considerably lower than that of evaporators and preheaters. These results indicate that only a few superheater designs meet the established criteria, that consequently go through other design limitations to select the optimal design among them. horizontal axis represents the number of tubes per row and the total number of tubes rows of each superheater design and each design of them results in a value of heat transfer kW which is indicated in vertical axis.

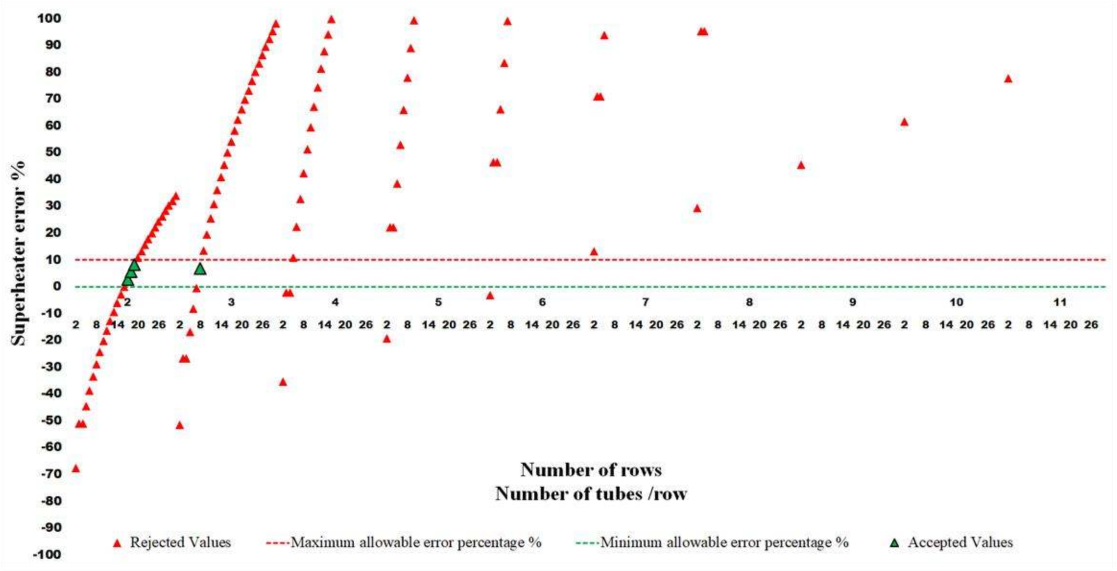

Figure 5.74. Superheater design error% diagram R123

Figure 5.74 provides a representation of superheater design error for 300 superheater designs with respect to the total number of tube rows and the total number of tubes in one row of each superheater design. The maximum allowable percentage of the design error for each superheater design is represented as an upper limit of 10% marked by a red dashed line. The successful designs that meet this criterion and have a design error value of less than 10% are denoted by green triangles, while the designs that exceed the upper limit or have negative values are represented by red triangles, indicating their failure to meet the design requirements. It is noteworthy that out of all the attempted superheater designs, only 4 were able to pass this limitation. The findings of this analysis provided superheater designs with an accurate volume that were prevented from being underdesigned or overdesigned and this enable them to go further through other design limitations in order to select the optimal design of them.

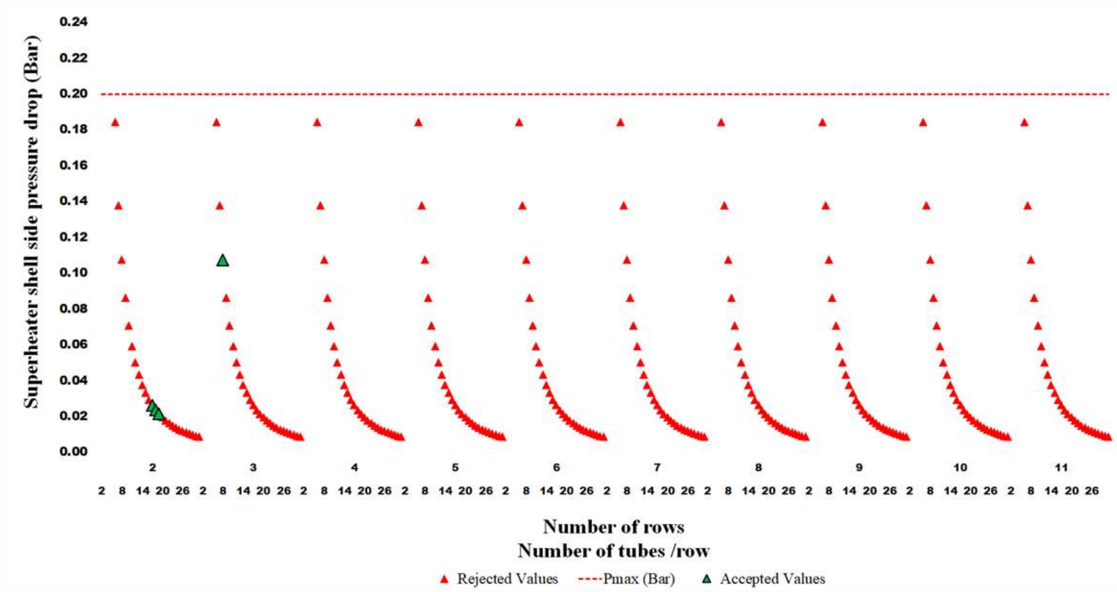

Figure 5.75. Shell side pressure drop through the superheater R123

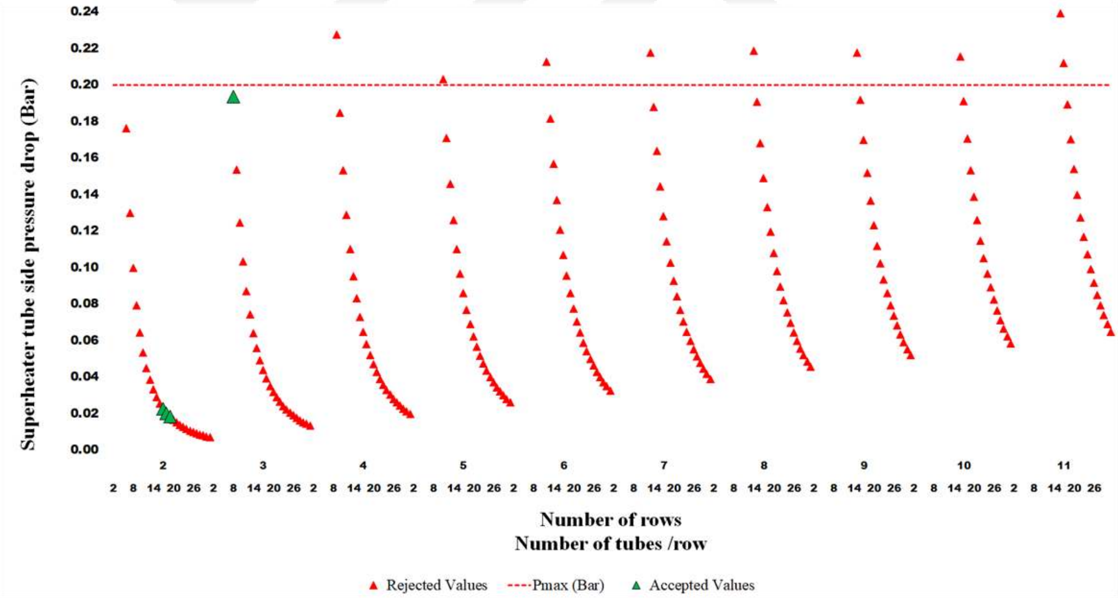

Figure 5.76. Tube side pressure drop through the superheater R123

Figure 5.75 presents the shell side pressure drop for each superheater design as a function of the total number of tube rows and the total number of tubes in one row of each design. A red dashed line indicates the maximum allowable shell side pressure drop of 0.2 bar, which is a crucial factor in ensuring optimal preheater performance. The green triangles represent the designs that have successfully passed all the previous tests, as well as this limitation, exhibiting a shell side pressure drop value of less than

0.2 bar. Conversely, the red triangles are the rejected designs that failed to pass one of the previous limitations or have a tube side pressure drop value exceeding the maximum limit. It is noteworthy that only 4 designs, out of the 300 total designs considered, were able to satisfy all the design requirements and constraints.
Figures 5.76 provide a representation of the superheater's tube side pressure drop, as a function of the total number of tube rows and tubes in one row of each superheater design. The red dashed line, which marks the maximum allowable value of 0.2 bar, serves as a stringent criterion for evaluating each design's suitability. The figure illustrates that out of the 300 attempted designs, only 4 superheater designs were approved to be the ultimate choice, demonstrating outstanding performance that satisfies all previous design limitations and conform with the pressure drop requirement. These accepted designs were represented by green triangles in the figure, while the red triangles depicted the rejected designs that failed to meet the previous limitations, despite some of them had a pressure drop less than 0.2 bar. This emphasizes the critical role of the optimization process in ensuring the creation of an efficient and high-performing superheaters that meet all the essential design requirements.

The following figure shows the corresponding surface area of 300 designs in which the perfect designs that have successfully passed all the suggested design limitation by this paper are repersented in a green color while the other that failed to pass on of the previous mentioned design limitation are pollted in the figure as red triangles. The optimal design what satisfy all the design criteria and has the smallest heating surface area between the accepted design is shown as a yellow triangle.

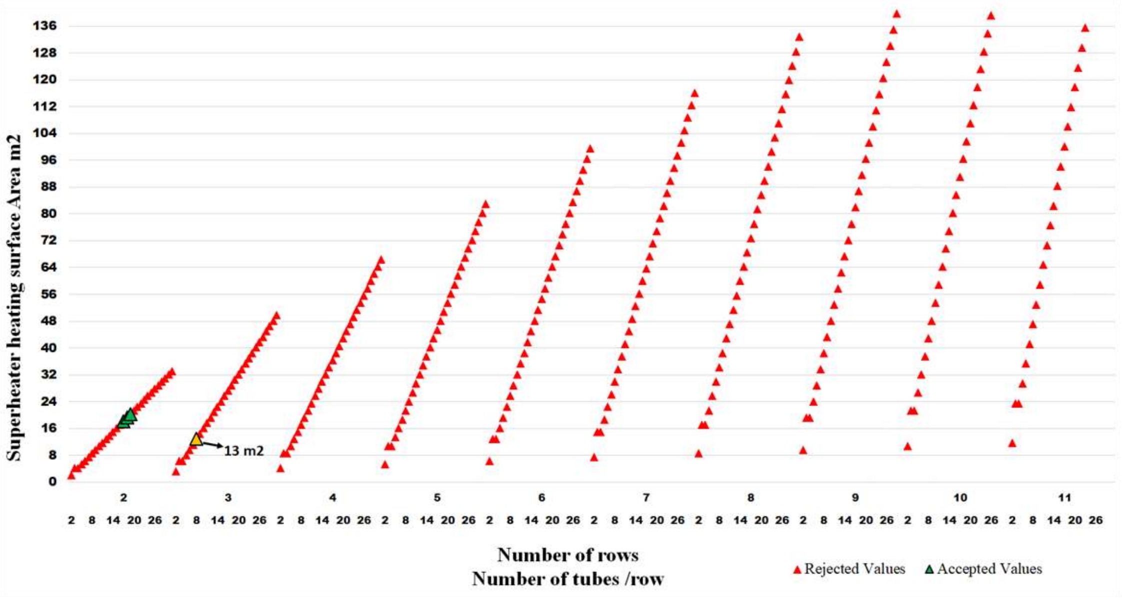

Figure 5.77. Superheater heating surface area diagram R123

Figure 5.77 provides a representation of the heating surface area for each of the 300 superheter designs based on the total number of tube rows and the total number of tubes in one row of each superheater. It is worth noting that only 4 designs satisfy all the previous limitations and can be considered as good superheater designs, and these designs are represented as green triangles in the figure. Conversely, the rejected designs, which failed to pass one or more of the previous tests, are shown as red triangles. The optimum design that is associated with the yellow triangle with the minimum surface area of 13 m2, corresponding to 8 tubes in one row and 3 number of tube rows. This design ensures the lowest possible cost and investment while also maintaining the required performance of ORC, making it the ideal choice for the superheater.

Table 5.19. Finned Tube Superheater Design Result R123

NO	$N_{tube/raw}$	N_{raw}	N_{total}	Error	ΔP_t	ΔP_s	A	$\dot{Q}_{est}$	Design Test Result
	#	#	#	%	bar	bar	m^2	kW	accepted/not accepted
1	2	2	4	-67.699	1.540	1.468	2.141	88.686	Not accepted
2	4	2	8	-51.177	0.392	0.396	4.283	134.048	Not accepted
⋮	⋮	⋮	⋮	⋮	⋮	⋮	⋮	⋮	⋮
15	16	2	32	-0.064	0.026	0.029	17.132	274.383	Not accepted
16	17	2	34	2.777	0.023	0.026	18.202	282.184	Acceptable design
17	18	2	36	5.504	0.020	0.024	19.273	289.672	Acceptable design
18	19	2	38	8.128	0.018	0.021	20.344	296.876	Acceptable design
19	20	2	40	10.657	0.016	0.019	21.415	303.819	Not accepted
⋮	⋮	⋮	⋮	⋮	⋮	⋮	⋮	⋮	⋮
36	7	3	21	-0.460	0.252	0.138	11.243	273.298	Not accepted
37	**8**	**3**	**24**	**6.720**	**0.194**	**0.107**	**12.849**	**293.011**	**Acceptable design***
38	9	3	27	13.353	0.153	0.086	14.455	311.222	Not accepted
⋮	⋮	⋮	⋮	⋮	⋮	⋮	⋮	⋮	⋮
299	30	11	330	626.112	0.069	0.009	176.670	1993.612	Not accepted
300	31	11	341	636.210	0.065	0.009	182.559	2021.338	Not accepted

*Minimal superheater area, ideal choice-lowest cost

** All the superheater design calculations are carried out assuming P2=22bar.

5.4.3.4 Superheater optimization procedure for R236fa

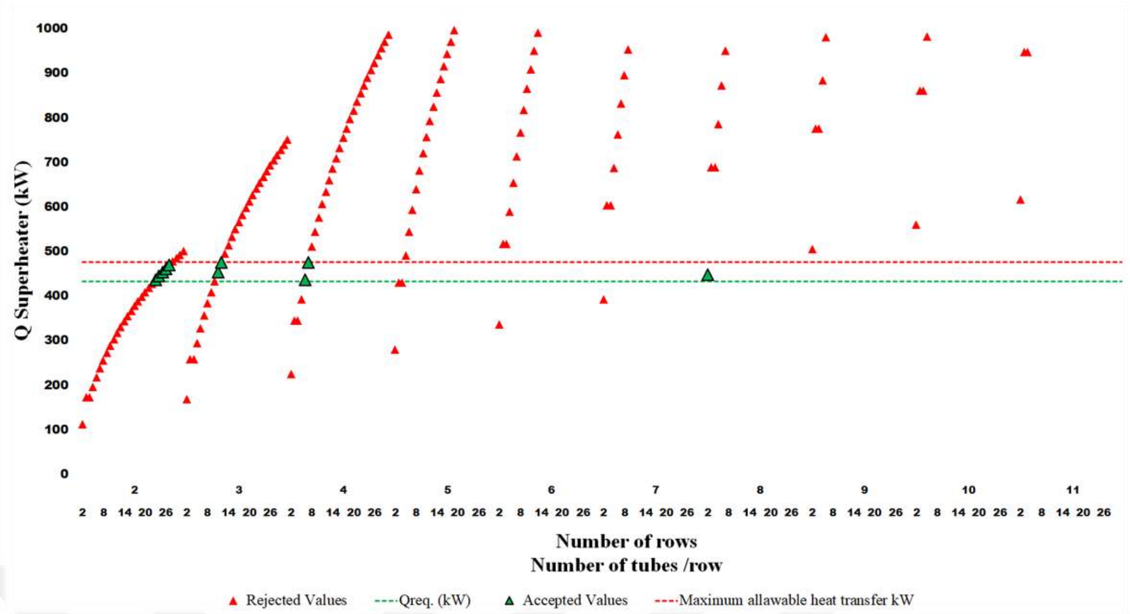

Figure 5.78. Heat transfer rate through the superheater R236fa

Figure 5.78, illustrates the total heat transfer rate of 300 different designs of superheaters as a function of the total number of tube rows and tubes in one row of each design. The green triangles represent the superheater designs that meet required value of the heat transfer that are located between the upper limit and the lower limit. The upper limit, shown as a red dashed line, signifies the maximum permissible superheater heat transfer (kW) at 476.3, while the lower limit is denoted by a dashed green line, representing the minimum required heating rate (kW) at 433. On the other hand, the red triangles signify the designs that do not meet the established criteria and, consequently, have been rejected. It shown by the figure that only 10 designs have successfully satisfied this range out of 300 superheater designs attempted. This outcome is expected since the heating duty required for superheaters is considerably lower than that of evaporators and preheaters. These results indicate that only a few superheater designs meet the established criteria, that consequently go through other design limitations to select the optimal design among them. horizontal axis represents the number of tubes per row and the total number of tubes rows of each superheater design and each design of them results in a value of heat transfer kW which is indicated in vertical axis.

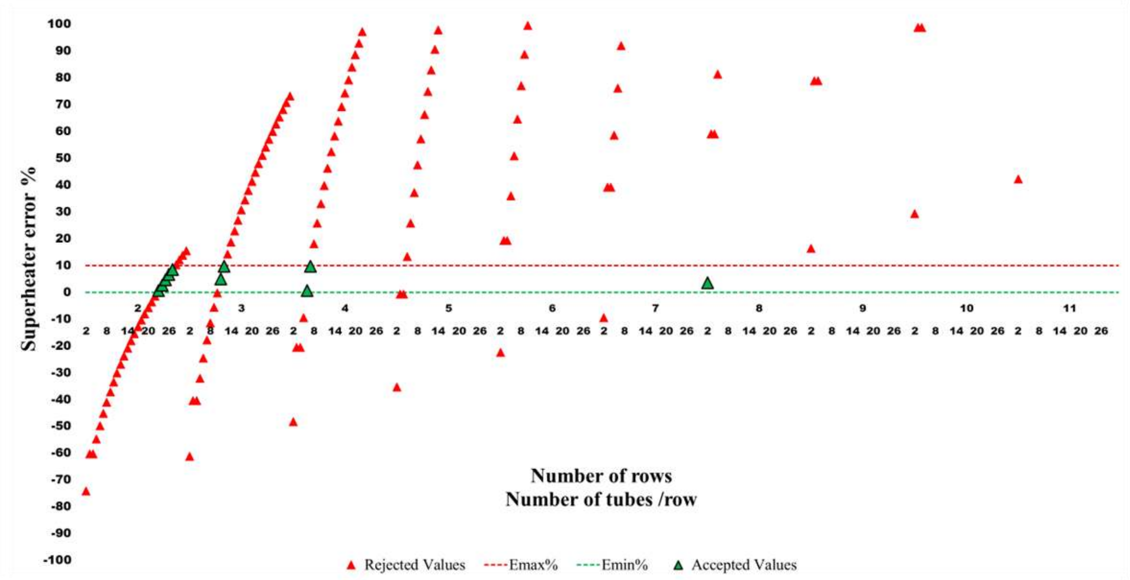

Figure 5.79. Superheater design error% diagram R236fa

Figure 5.79 provides a representation of superheater design error for 300 superheater designs with respect to the total number of tube rows and the total number of tubes in one row of each superheater design. The maximum allowable percentage of the design error for each superheater design is represented as an upper limit of 10% marked by a red dashed line. The successful designs that meet this criterion and have a design error value of less than 10% are denoted by green triangles, while the designs that exceed the upper limit or have negative values are represented by red triangles, indicating their failure to meet the design requirements. It is noteworthy that out of all the attempted superheater designs, only 10 were able to pass this limitation. The findings of this analysis provided superheater designs with an accurate volume that were prevented from being underdesigned or overdesigned and this enable them to go further through other design limitations in order to select the optimal design of them.

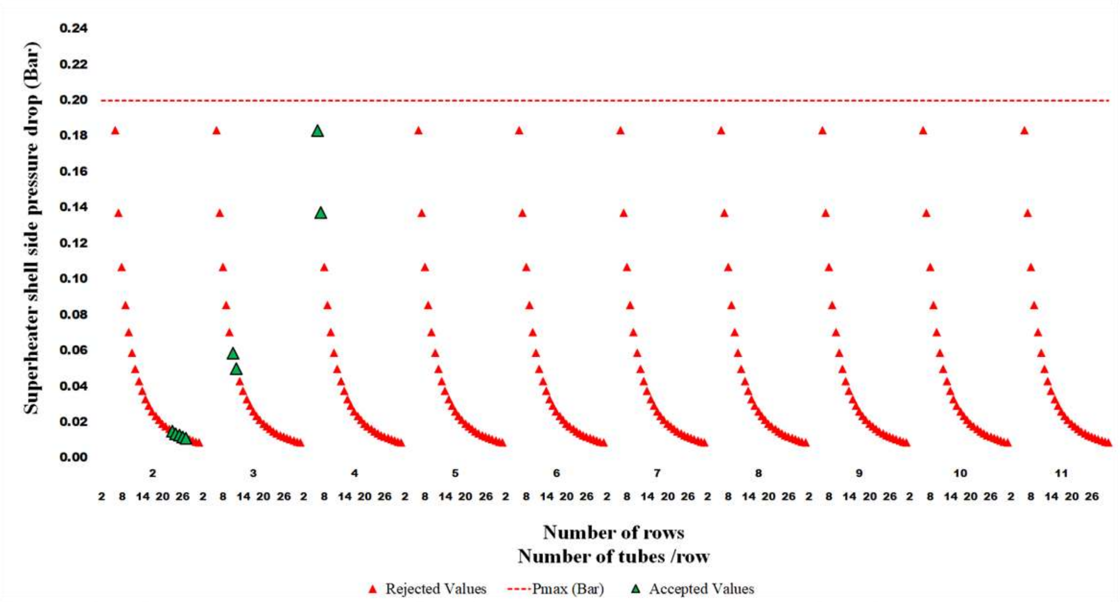

Figure 5.80. Shell side pressure drop through the superheater R236fa

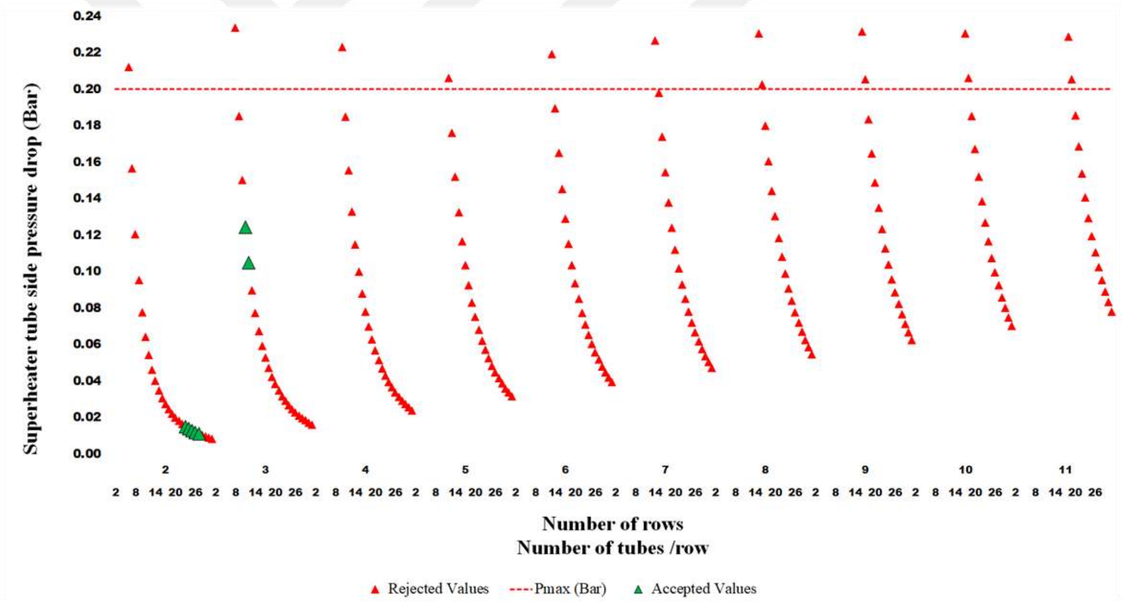

Figure 5.81. Tube side pressure drop through the superheaterR236fa

Figure 5.80 presents the shell side pressure drop for each superheater design as a function of the total number of tube rows and the total number of tubes in one row of each design. A red dashed line indicates the maximum allowable shell side pressure drop of 0.2 bar, which is a crucial factor in ensuring optimal preheater performance. The green triangles represent the designs that have successfully passed all the previous tests, as well as this limitation, exhibiting a shell side pressure drop value of less than 0.2 bar. Conversely, the red triangles are the rejected designs that failed to pass one of the previous limitations or have a tube side pressure drop value exceeding the maximum limit. It is noteworthy that only 9 designs, out of the 300 total designs considered, were able to satisfy all the design requirements and constraints.

Figures 5.81 provide a representation of the superheater's tube side pressure drop, as a function of the total number of tube rows and tubes in one row of each superheater design. The red dashed line, which marks the maximum allowable value of 0.2 bar, serves as a stringent criterion for evaluating each design's suitability. The figure illustrates that out of the 300 attempted designs, only 7 superheater designs were approved to be the ultimate choice, demonstrating outstanding performance that satisfies all previous design limitations and conform with the pressure drop requirement. These accepted designs were represented by green triangles in the figure, while the red triangles depicted the rejected designs that failed to meet the previous limitations, despite some of them had a pressure drop less than 0.2 bar.emphasizes the critical role of the optimization process in ensuring the creation of an efficient and high-performing superheaters that meet all the essential design requirements.

The following figure shows the corresponding surface area of 300 designs in which the perfect designs that have successfully passed all the suggested design limitation by this paper are repersented in a green color while the other that failed to pass on of the previous mentioned design limitation are pollted in the figure as red triangles. The optimal design what satisfy all the design criteria and has the smallest heating surface area between the accepted design is shown as a yellow triangle.

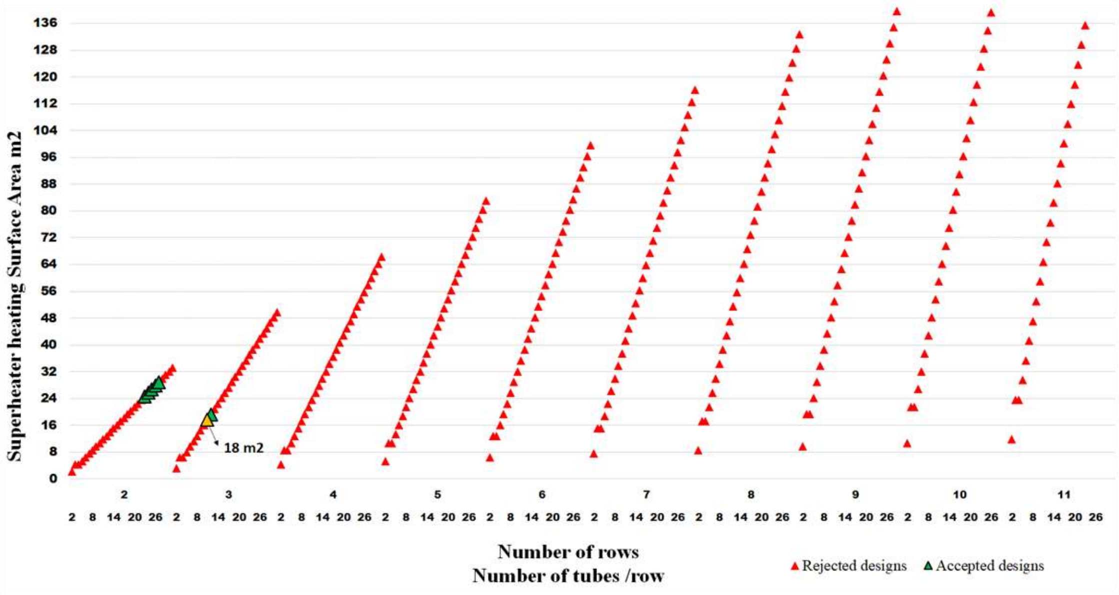

Figure 5.82. Superheater heating surface area diagram R236fa

Figure 5.82 provides a representation of the heating surface area for each of the 300 superheter designs based on the total number of tube rows and the total number of tubes in one row of each superheater. It is worth noting that only 7 designs satisfy all the previous limitations and can be considered as good superheater designs, and these designs are represented as green triangles in the figure. Conversely, the rejected designs, which failed to pass one or more of the previous tests, are shown as red triangles. The optimum design that is associated with the yellow triangle with the minimum surface area of 18 m2, corresponding to 11 tubes in one row and 3 number of tube rows. This design ensures the lowest possible cost and investment while also maintaining the required performance of ORC, making it the ideal choice for the superheater.

A table is inserted below which shows in detail all the findings of this process with concering in the accepted superheater designs

Table 5.20. Finned Tube Superheater Design Result R236fa

NO	$N_{tube/raw}$	N_{raw}	N_{total}	Error	ΔP_t	ΔP_s	A	$\dot{Q}_{est}$	Design Test Result
	#	#	#	%	bar	bar	m^2	kW	accepted/not accepted
1	2	2	4	-74.0955488	1.85978384	1.45951785	2.14145317	112.126231	Not accepted
2	4	2	8	-60.2044881	0.47244132	0.39332999	4.28290634	172.253051	Not accepted
⋮	⋮	⋮	⋮	⋮	⋮	⋮	⋮	⋮	⋮
20	21	2	42	-3.44319937	0.01801875	0.01757079	22.4852583	417.94169	Not accepted
21	22	2	44	-1.29396825	0.01644548	0.01611275	23.5559849	427.244538	Not accepted
22	23	2	46	0.79062217	0.01507091	0.01483314	24.6267114	436.267592	Acceptable design
23	24	2	48	2.81496321	0.01386285	0.0137037	25.697438	445.02986	Acceptable design
24	25	2	50	4.7829919	0.01279536	0.01270157	26.7681646	453.548382	Acceptable design
25	26	2	52	6.69825318	0.0118474	0.01180811	27.8388912	461.838503	Acceptable design
26	27	2	54	8.56395156	0.01100172	0.01100798	28.9096178	469.914093	Acceptable design
27	28	2	56	10.3829944	0.01024407	0.0102885	29.9803444	477.787736	Not accepted
28	29	2	58	12.1580286	0.00956261	0.00963905	31.0510709	485.470891	Not accepted
⋮	⋮	⋮	⋮	⋮	⋮	⋮	⋮	⋮	⋮
39	10	3	30	-0.12642922	0.15032307	0.07025048	16.0608988	432.298177	Not accepted
40	**11**	**3**	**33**	**4.99154533**	**0.12451727**	**0.05876779**	**17.6669886**	**454.451096**	**Acceptable design***
41	12	3	36	9.82855336	0.10485145	0.0499377	19.2730785	475.387864	Acceptable design
42	13	3	39	14.4188421	0.08951884	0.04299552	20.8791684	495.256718	Not accepted
⋮	⋮	⋮	⋮	⋮	⋮	⋮	⋮	⋮	⋮
299	30	11	330	526.403092	0.08323733	0.00905074	176.669886	2711.3571	Not accepted
300	31	11	341	535.720452	0.07801256	0.00851603	182.558883	2751.68686	Not accepted

*Minimal superheater area, ideal choice-lowest cost

** All the superheater design calculations are carried out assuming P2=22bar.

5.4.3.5 Superheater optimization procedure for R142b

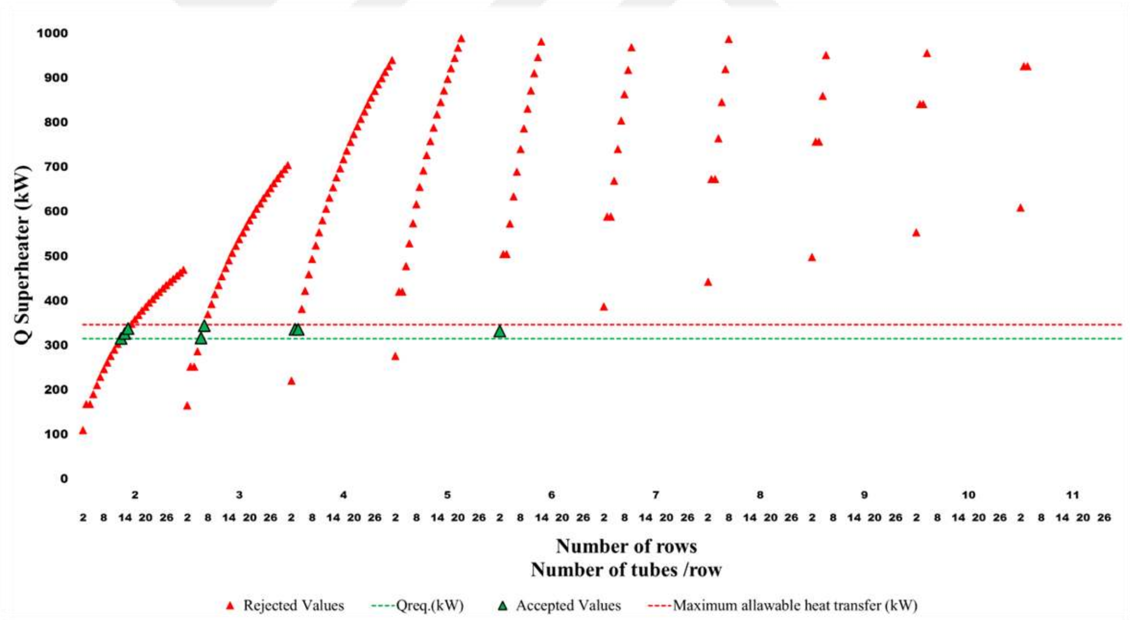

Figure 5.83. Heat transfer rate through the superheater R142b

Figure 5.83, illustrates the total heat transfer rate of 300 different designs of superheaters as a function of the total number of tube rows and tubes in one row of each design. The green triangles represent the superheater designs that meet required value of the heat transfer that are located between the upper limit and the lower limit. The upper limit, shown as a red dashed line, signifies the maximum permissible superheater heat transfer (kW) at 347.16, while the lower limit is denoted by a dashed green line, representing the minimum required heating rate (kW) at 315.6. On the other hand, the red triangles signify the designs that do not meet the established criteria and, consequently, have been rejected. It shown by the figure that only 8 designs have successfully satisfied this range out of 300 superheater designs attempted. This outcome is expected since the heating duty required for superheaters is considerably lower than that of evaporators and preheaters. These results indicate that only a few superheater designs meet the established criteria, that consequently go through other design limitations to select the optimal design among them. horizontal axis represents the number of tubes per row and the total number of tubes rows of each superheater design and each design of them results in a value of heat transfer kW which is indicated in vertical axis.

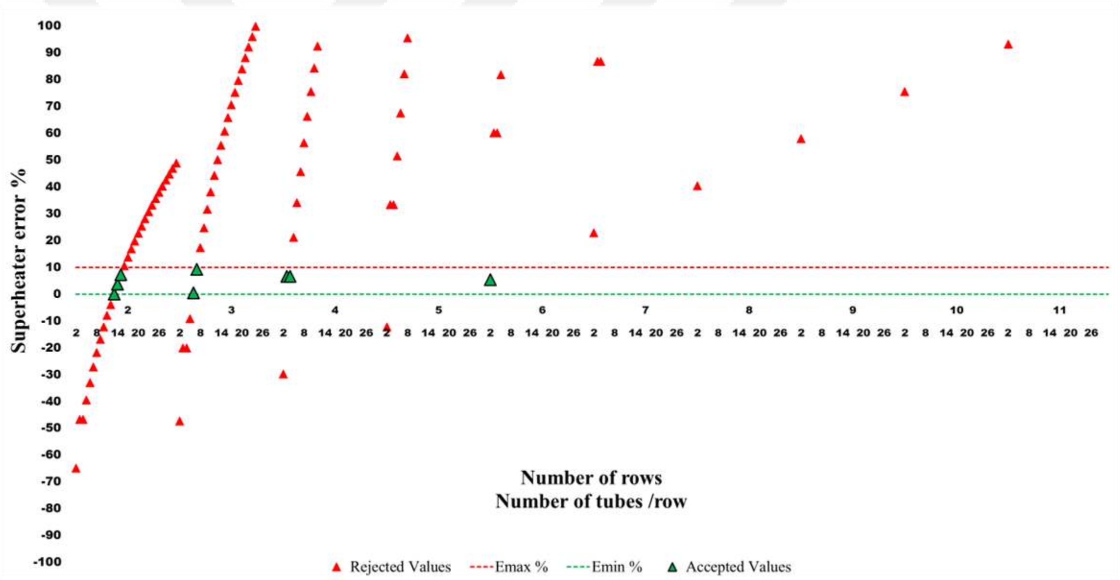

Figure 5.84.Superheater design error% diagram R142b

Figure 5.84 provides a representation of superheater design error for 300 superheater designs with respect to the total number of tube rows and the total number of tubes in one row of each superheater design. The maximum allowable percentage of the design error for each superheater design is represented as an upper limit of 10% marked by a red dashed line. The successful designs that meet this criterion and have a design error value of less than 10% are denoted by green triangles, while the designs that exceed the upper limit or have negative values are represented by red triangles, indicating their failure to meet the design requirements. It is noteworthy that out of all the attempted superheater designs, only 8 were able to pass this limitation. The findings of this analysis provided superheater designs with an accurate volume that were prevented from being underdesigned or overdesigned and this enable them to go further through other design limitations in order to select the optimal design of them.

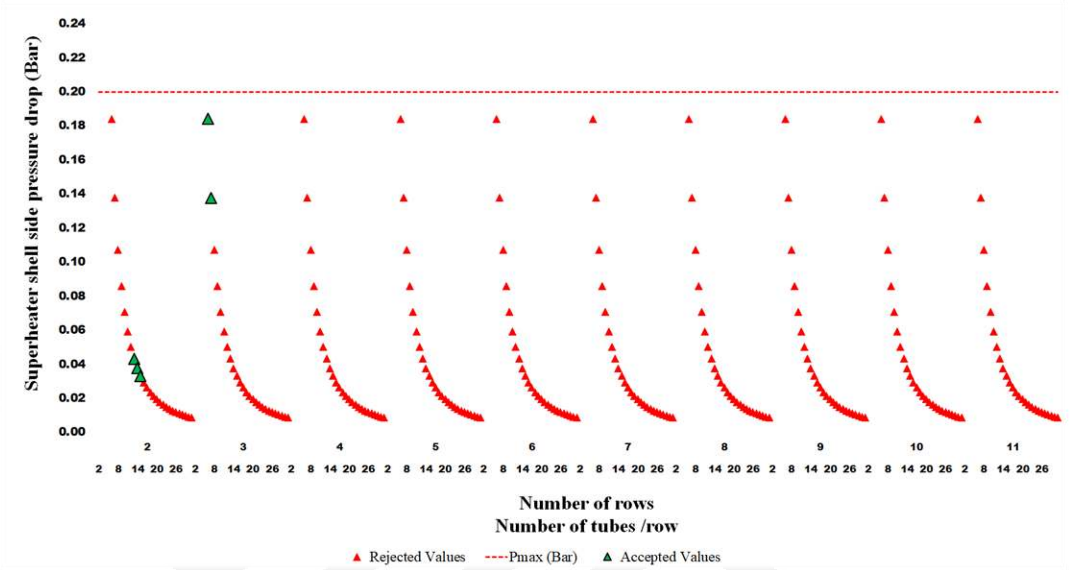

Figure 5.85. Shell side pressure drop through the superheater R142b

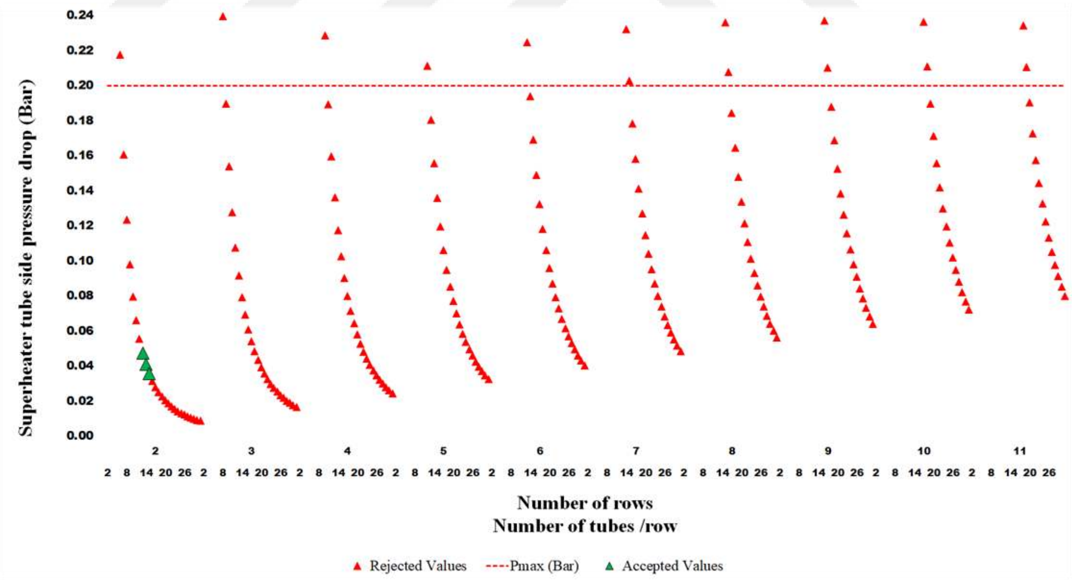

Figure 5.86. Tube side pressure drop through the superheaterR142b

Figure 5.85 presents the shell side pressure drop for each superheater design as a function of the total number of tube rows and the total number of tubes in one row of each design. A red dashed line indicates the maximum allowable shell side pressure drop of 0.2 bar, which is a crucial factor in ensuring optimal preheater performance.

The green triangles represent the designs that have successfully passed all the previous tests, as well as this limitation, exhibiting a shell side pressure drop value of less than 0.2 bar. Conversely, the red triangles are the rejected designs that failed to pass one of the previous limitations or have a tube side pressure drop value exceeding the maximum limit. It is noteworthy that only 5 designs, out of the 300 total designs considered, were able to satisfy all the design requirements and constraints.

Figure 5.86 presents the tube side pressure drop for each superheater design as a function of the total number of tube rows and the total number of tubes in one row of each design. A red dashed line indicates the maximum allowable tube side pressure drop of 0.2 bar, which is a crucial factor in ensuring optimal preheater performance. The green triangles represent the designs that have successfully passed all the previous tests, as well as this limitation, exhibiting a tube side pressure drop value of less than 0.2 bar. Conversely, the red triangles are the rejected designs that failed to pass one of the previous limitations or have a tube side pressure drop value exceeding the maximum limit. It is noteworthy that only 3 designs, out of the 300 total designs considered, were able to satisfy all the design requirements and constraints.
emphasizes the critical role of the optimization process in ensuring the creation of an efficient and high-performing superheaters that meet all the essential design requirements.

The following figure shows the corresponding surface area of 300 designs in which the perfect designs that have successfully passed all the suggested design limitation by this paper are repersented in a green color while the other that failed to pass on of the previous mentioned design limitation are pollted in the figure as red triangles. The optimal design what satisfy all the design criteria and has the smallest heating surface area between the accepted design is shown as a yellow triangle.

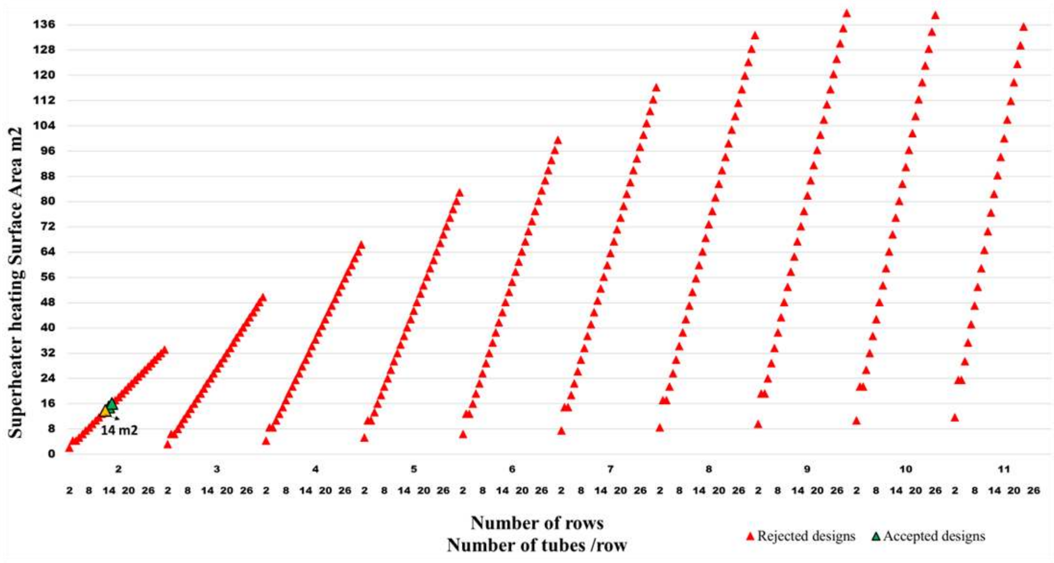

Figure 5.87. Superheater heating surface area diagram R142b

Figure 5.87 provides a representation of the heating surface area for each of the 300 superheter designs based on the total number of tube rows and the total number of tubes in one row of each superheater. It is worth noting that only 3 designs satisfy all the previous limitations and can be considered as good superheater designs, and these designs are represented as green triangles in the figure. Conversely, the rejected designs, which failed to pass one or more of the previous tests, are shown as red triangles. The optimum design that is associated with the yellow triangle with the minimum surface area of 14 m2, corresponding to 13 tubes in one row and 2 number of tube rows. This design ensures the lowest possible cost and investment while also maintaining the required performance of ORC, making it the ideal choice for the superheater.

A table is inserted below which shows in detail all the findings of this process with concering in the accepted superheater designs

Table 5.21. Finned Tube Superheater Design Result R142b

NO	$N_{tube/raw}$	N_{raw}	N_{total}	Error	ΔP_t	ΔP_s	A	$\dot{Q}_{est}$	Design Test Result
	#	#	#	%	bar	bar	m^2	kW	accepted/not accepted
1	2	2	4	-64.8519666	1.90500452	1.46573242	2.14145317	110.931683	Not accepted
2	4	2	8	-46.5951813	0.48419044	0.3950155	4.28290634	168.5524293	Not accepted
:	:	:	:	:	:	:	:	:	:
11	12	2	24	-3.73590494	0.0555514	0.05015387	12.848719	303.8217798	Not accepted
12	**13**	**2**	**26**	**0.12842631**	**0.04745941**	**0.04318178**	**13.9194456**	**316.0181028**	**Acceptable design***
13	14	2	28	3.80072996	0.04102391	0.03759693	14.9901722	327.6083622	Acceptable design
14	15	2	30	7.30186218	0.03582082	0.03305117	16.0608988	338.6583827	Acceptable design
15	16	2	32	10.6493018	0.03155374	0.02929961	17.1316253	349.2233296	Not accepted
:	:	:	:	:	:	:	:	:	:
299	30	11	330	708.544161	0.08528151	0.00909024	176.669886	2551.868648	Not accepted
300	31	11	341	720.029598	0.07993046	0.00855321	182.558883	2588.118155	Not accepted

*Minimal superheater area, ideal choice-lowest cost

** All the superheater design calculations are carried out assuming P2=22bar.

5.4.3.6 Superheater optimizatiom procedure R600a

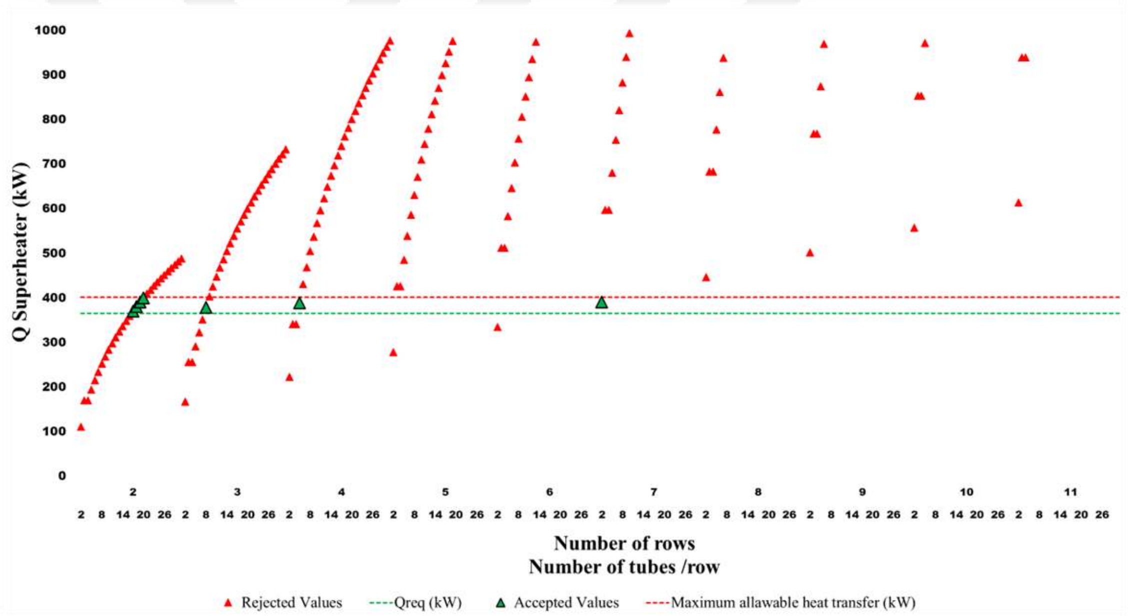

Figure 5.88. Heat transfer rate through the superheater R600a

Figure 5.88, illustrates the total heat transfer rate of 300 different designs of superheaters as a function of the total number of tube rows and tubes in one row of each design. The green triangles represent the superheater designs that meet required value of the heat transfer that are located between the upper limit and the lower limit. The upper limit, shown as a red dashed line, signifies the maximum permissible superheater heat transfer (kW) at 402.33, while the lower limit is denoted by a dashed green line, representing the minimum required heating rate (kW) at 365.76. On the other hand, the red triangles signify the designs that do not meet the established criteria and, consequently, have been rejected. It shown by the figure that only 7 designs have successfully satisfied this range out of 300 superheater designs attempted. This outcome is expected since the heating duty required for superheaters is considerably lower than that of evaporators and preheaters. These results indicate that only a few superheater designs meet the established criteria, that consequently go through other design limitations to select the optimal design among them. horizontal axis represents the number of tubes per row and the total number of tubes rows of each superheater design and each design of them results in a value of heat transfer kW which is indicated in vertical axis.

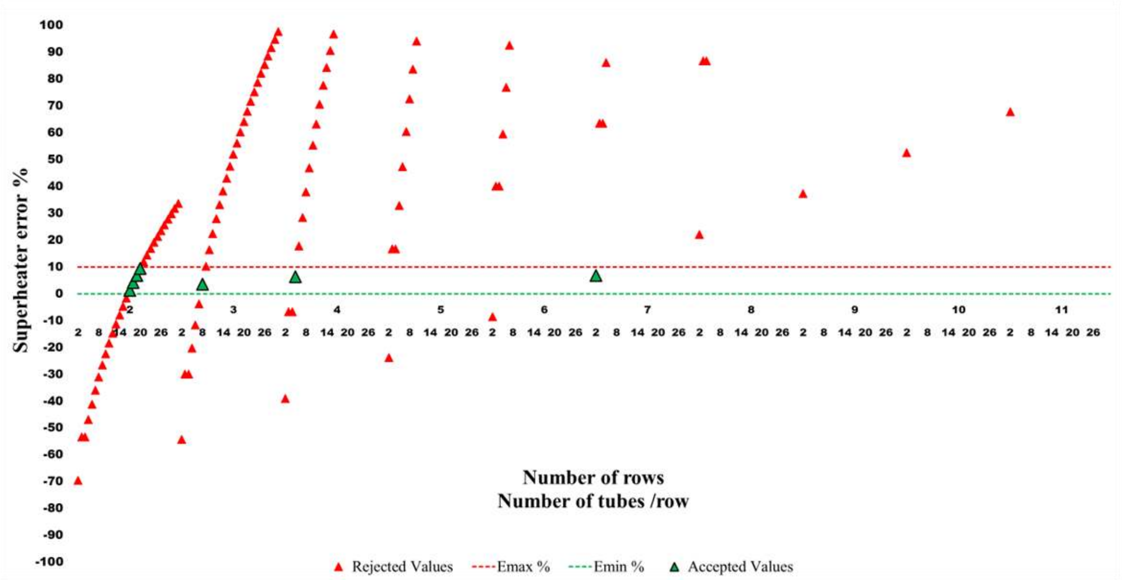

Figure 5.89. Superheater design error% diagram R600a

Figure 5.89 provides a representation of superheater design error for 300 superheater designs with respect to the total number of tube rows and the total number of tubes in one row of each superheater design. The maximum allowable percentage of the design error for each superheater design is represented as an upper limit of 10% marked by a red dashed line. The successful designs that meet this criterion and have a design error value of less than 10% are denoted by green triangles, while the designs that exceed the upper limit or have negative values are represented by red triangles, indicating their failure to meet the design requirements. It is noteworthy that out of all the attempted superheater designs, only 7 were able to pass this limitation. The findings of this analysis provided superheater designs with an accurate volume that were prevented from being underdesigned or overdesigned and this enable them to go further through other design limitations in order to select the optimal design of them.

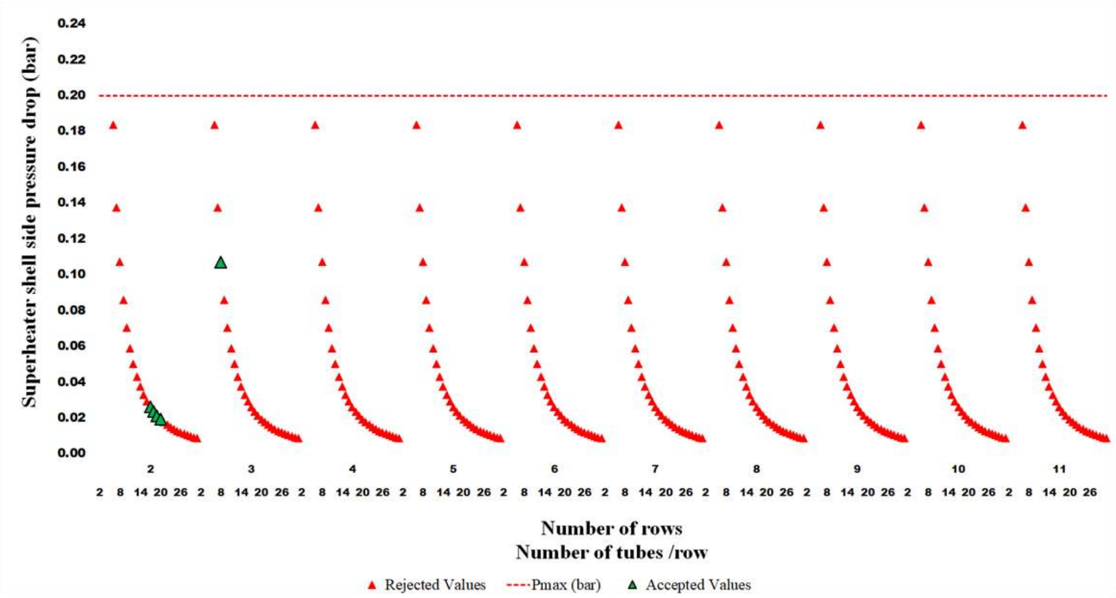

Figure 5.90. Shell side pressure drop through the superheater R600a

Figure 5.90 presents the shell side pressure drop for each superheater design as a function of the total number of tube rows and the total number of tubes in one row of each design. A red dashed line indicates the maximum allowable shell side pressure drop of 0.2 bar, which is a crucial factor in ensuring optimal preheater performance. The green triangles represent the designs that have successfully passed all the previous tests, as well as this limitation, exhibiting a shell side pressure drop value of less than 0.2 bar. Conversely, the red triangles are the rejected designs that failed to pass one of the previous limitations or have a shell side pressure drop value exceeding the maximum limit. It is noteworthy that only 5 designs, out of the 300 total designs considered, were able to satisfy all the design requirements and constraints.

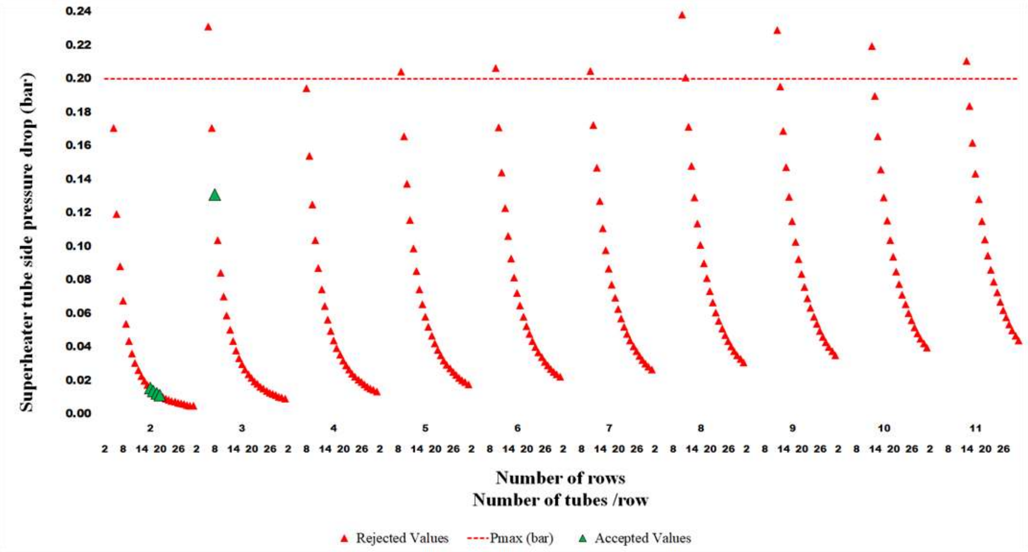

Figure 5.91. Tube side pressure drop through the superheater R600a

Figures 5.91 provide a representation of the superheater's tube side pressure drop, as a function of the total number of tube rows and tubes in one row of each superheater design. The red dashed line, which marks the maximum allowable value of 0.2 bar, serves as a stringent criterion for evaluating each design's suitability. The figure illustrates that out of the 300 attempted designs, only 5 superheater designs were approved to be the ultimate choice, demonstrating outstanding performance that satisfies all previous design limitations and conform with the pressure drop requirement. These accepted designs were represented by green triangles in the figure, while the red triangles depicted the rejected designs that failed to meet the previous limitations, despite some of them had a pressure drop less than 0.2 bar. emphasizes the critical role of the optimization process in ensuring the creation of an efficient and high-performing superheaters that meet all the essential design requirements.

The following figure shows the corresponding surface area of 300 designs in which the perfect designs that have successfully passed all the suggested design limitation by this paper are repersented in a green color while the other that failed to pass on of the previous mentioned design limitation are pollted in the figure as red triangles. The optimal design what satisfy all the design criteria and has the smallest heating surface area between the accepted design is shown as a yellow triangle.

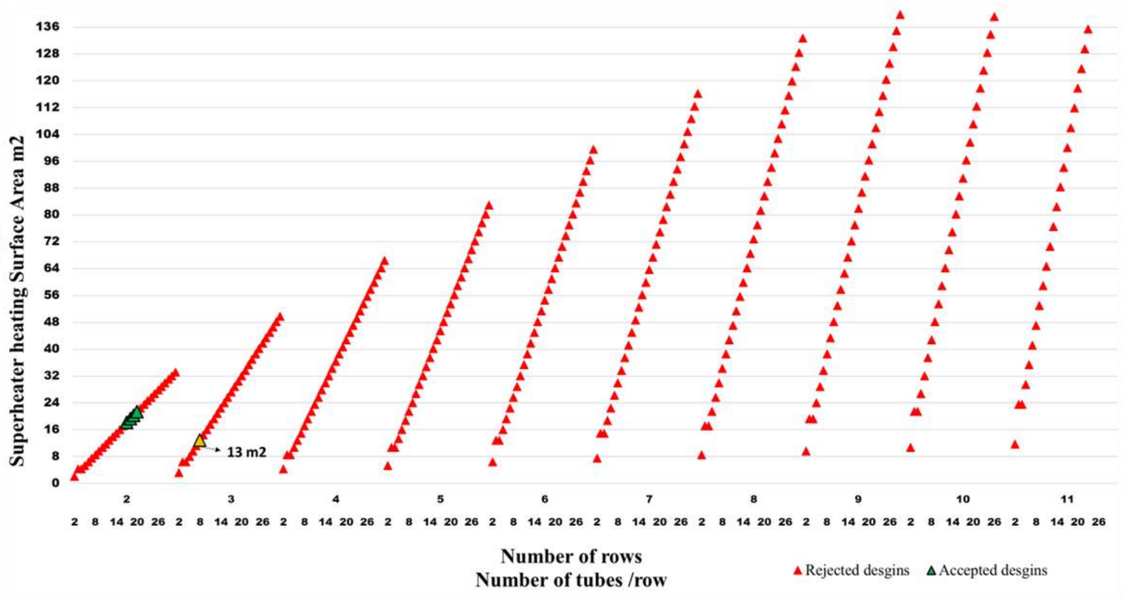

Figure 5.92. Superheater heating surface area diagram R600a

Figure 5.92 represents the heating surface area for each of the 300 superheter designs as a function of the total number of tube rows and the total number of tubes in one row of each superheater. It is seen from the chart that only 5 designs have conformed with all the previous limitations . These designs are represented as green triangles in the figure. While, the rejected designs, which failed to pass one or more of the previous limitations, are shown in red color. The optimum design is indicated in the figure as a yellow triangle with minimal surface area of 13 m2, corresponding to 8 tubes in one row and 3 number of tube rows. This design ensures the lowest possible cost and investment while also maintaining the required performance of ORC, making it the ideal choice for the superheater.

Table 5.22. Finned Tube Superheater Design Result R600a

NO	$N_{tube/raw}$	N_{raw}	N_{total}	Error	ΔP_t	ΔP_s	A	$\dot{Q}_{est}$	Design Test Result
	#	#	#	%	bar	bar	m^2	kW	accepted/not accepted
1	2	2	4	-69.449779	1.04137955	1.46307485	2.14145317	111.739884	Not accepted
2	4	2	8	-53.2551344	0.26496643	0.39429471	4.28290634	170.973096	Not accepted
⋮	⋮	⋮	⋮	⋮	⋮	⋮	⋮	⋮	⋮
14	15	2	30	-4.58796208	0.0196509	0.03299013	16.0608988	348.977183	Not accepted
15	16	2	32	-1.53148907	0.01731239	0.02924546	17.1316253	360.156478	Not accepted
16	17	2	34	1.40132536	0.01537028	0.02611741	18.2023519	370.883482	Acceptable design
17	18	2	36	4.22161463	0.01373955	0.02347641	19.2730785	381.198916	Acceptable design
18	19	2	38	6.93900147	0.01235686	0.02122541	20.3438051	391.137977	Acceptable design
19	20	2	40	9.56186637	0.0111742	0.01929049	21.4145317	400.731315	Acceptable design
⋮	⋮	⋮	⋮	⋮	⋮	⋮	⋮	⋮	⋮
35	6	3	18	-11.5083839	0.23113663	0.18370624	9.63653926	323.665185	Not accepted
36	7	3	21	-3.63176903	0.17043329	0.1374968	11.2426291	352.474536	Not accepted
37	**8**	**3**	**24**	**3.60627627**	**0.13091328**	**0.10700761**	**12.848719**	**378.948267**	**Acceptable design***
38	9	3	27	10.3180043	0.10374352	0.0857969	14.4548089	403.496951	Not accepted
⋮	⋮	⋮	⋮	⋮	⋮	⋮	⋮	⋮	⋮
298	29	11	319	614.412045	0.04987097	0.00966313	170.78089	2613.01936	Not accepted
299	30	11	330	625.267894	0.04664132	0.00907335	176.669886	2652.7255	Not accepted
300	31	11	341	635.873659	0.04371697	0.00853731	182.558883	2691.51694	Not accepted

*Minimal superheater area, ideal choice-lowest cost

** All the superheater design calculations are carried out assuming P2=22bar.

CHAPTER 6
ORC PERFORMANCE ANALYSIS FOR REAL CASE

6.1 Recorded values of ORC (real case)

In the following section, we endeavor to undertake a comprehensive and rigorous performance analysis and calculation of Organic Rankine Cycle (ORC) system, which is built upon the foundation of the pressure drop resulting from the optimal design of the heat exchanger units represented in **Chapter 5**. Our primary objective is to delve into how the performance of the ORC system is influenced by the pressure drop. The significance of this study is paramount since it provides invaluable insights into the optimal design and operation of ORC systems, which are gaining increased popularity in diverse industrial applications. The research findings have the potential to revolutionize the overall efficiency and sustainability of energy conversion processes, which is integral to the realization of a cleaner and more sustainable energy future.

The following table shows the optimization results that were obtained in the previous chapter based on pumping pressure equal to 22 bar with the use of R245fa, R123, R600, R236fa, R124b, and R600a.

Table 6.1. Recorded optimum designs

Refrigerant, name	Equipment	Heating surface area m^2	Refrigerant side pressure drops bar
R245fa	Condenser	240	0.095
	Preheater	445.521	0.162
	Evaporator	205	0.100
	Superheater	12.849	0.173
R123	Condenser	233	0.160
	Preheater	631.155	0.131
	Evaporator	238	0.119
	Superheater	12.849	0.194
R600	Condenser	317	0.024
	Preheater	356.417	0.180
	Evaporator	205	0.062
	Superheater	11.243	0.137
R236fa	Condenser	402	0.037
	Preheater	445.521	0.134
	Evaporator	186	0.053
	Superheater	17.667	0.125
R142b	Condenser	451	0.151

	Preheater	356.417	0.153
	Evaporator	312	0.058
	Superheater	13.919	0.047
R600a	Condenser	380	0.018
	Preheater	356.417	0.102
	Evaporator	178	0.14
	Superheater	12.849	0.131

Table 6.2. Optimum design's geometrical parameters HExU

Refrigerant, name	H.T. Us	A	Nr	nt	N	L
R245fa	Unit	m2	#	#	#	m
	Preheater	445.521	8	15	120	2
	Evaporator	205	8	7	56	2
	Superheater	12.849	8	3	24	0.8
R123	Unit	m2	#	#	#	m
	Preheater	631.155	10	17	170	2
	Evaporator	238	8	8	64	2
	Superheater	12.849	8	3	24	0.8
R600	Unit	m2	#	#	#	m
	Preheater	356.417	6	16	96	2
	Evaporator	205	8	7	56	2
	Superheater	11.243	7	3	21	0.8
R236fa	Unit	m2	#	#	#	m
	Preheater	445.521	10	12	120	2
	Evaporator	186	10	5	50	2
	Superheater	17.667	11	3	33	0.8
R142b	Unit	m2	#	#	#	m
	Preheater	356.417	8	12	96	2
	Evaporator	312	12	7	84	2
	Superheater	13.919	13	2	26	0.8
R600a	Unit	m2	#	#	#	m
	Preheater	356.417	8	12	96	2
	Evaporator	178	6	8	48	2
	Superheater	12.849	8	3	24	0.8

Table 6.3. Optimum design's geometrical parameters of Condensers

Refrigerant, name	H.T. Us	A m^2	L m	NT #	Ntp
R245fa	Condenser	240	6	502	6
R123	Condenser	233	6	844	6
R600	Condenser	317	5.5	724	8
R236fa	Condenser	402	6	840	8
R142b	Condenser	451	6	942	8
R600a	Condenser	380	6	794	8

Table 6.4. The flow parameters for ORC (Real case)

State	Fluid	Pressure bar	Temperature °C	Enthalpy kJ/kg	Mass flow kg/s
1	R245fa	2.905	44.561	259.26	20.9821
2	R245fa	22	45.616	261.11	20.9821
3	R245fa	21.838	126.23	384.27	20.9821
4	R245fa	21.738	125.99	487.49	20.9821
5	R245fa	21.565	135.99	503.75	20.9821
6	R245fa	3	73.747	467.15	20.9821
7	Water	1	20.00	84.01	69.57095
8	Water	1	35.00	146.70	69.57095
9	Exhaust gas	1	375	784.3018	21.80
10	Exhaust gas	1	360.2477	768.6531	21.80
11	Exhaust gas	1	265.4602	669.3061	21.80
12	Exhaust gas	1	150	550.7663	21.80
1	R600	3.48	36.981	289.19	10.67
2	R600	22.00	38.201	293.32	10.67
3	R600	21.82	119.21	524.65	10.67
4	R600	21.76	119.05	739.95	10.67
5	R600	21.62	129.05	770.54	10.67
6	R600	3.50	66.415	694.46	10.67
7	Water	1	20.00	84.01	68.96
8	Water	1	35.00	146.70	68.96

9	Exhaust gas	1	375	784.3018	21.80
10	Exhaust gas	1	360.8862	769.3294	21.80
11	Exhaust gas	1	260.3134	663.9686	21.80
12	Exhaust gas	1	150	550.7663	21.80
1	R123	1.84	45.404	246.23	22.54
2	R123	22.00	46.575	248.01	22.54
3	R123	21.87	152.37	370.34	22.54
4	R123	21.75	152.06	461.57	22.54
5	R123	21.56	162.06	473.9	22.54
6	R123	2.00	78.674	433.3	22.54
7	Water	1	20.00	84.01	67.25
8	Water	1	35.00	146.70	67.25
9	Exhaust gas	1	375	784.3018	21.80
10	Exhaust gas	1	362.989	771.557	21.80
11	Exhaust gas	1	273.0984	677.2378	21.80
12	Exhaust gas	1	150	550.7663	21.80
1	R236fa	3.84	35.762	243.88	27.06
2	R236fa	22.00	36.948	245.59	27.06
3	R236fa	21.87	105.9	342.72	27.06
4	R236fa	21.75	105.63	417.63	27.06
5	R236fa	21.56	115.63	433.74	27.06
6	R236fa	4.00	63.528	408.24	27.06
7	Water	1	20.00	84.01	70.94
8	Water	1	35.00	146.70	70.94
9	Exhaust gas	1	375	784.3018	21.80
10	Exhaust gas	1	356.1459	764.3113	21.80
11	Exhaust gas	1	267.4037	671.3231	21.80
12	Exhaust gas	1	150	550.7663	21.80
1	R142b	4.85	37.303	248.52	21.38
2	R142b	22.00	38.507	250.5	21.38
3	R142b	21.85	102.7	346.05	21.38

4	R142b	21.79	102.56	473.88	21.38
5	R142b	21.74	112.56	488.58	21.38
6	R142b	5.00	51.414	455.47	21.38
7	Water	1	20.00	84.01	70.58
8	Water	1	35.00	146.70	70.58
9	Exhaust gas	1	375	784.3018	21.80
10	Exhaust gas	1	361.4055	769.8794	21.80
11	Exhaust gas	1	241.4808	644.4842	21.80
12	Exhaust gas	1	150	550.7663	21.80
1	R600a	4.98	37.578	290.15	12.21
2	R600a	22.00	38.876	294.12	12.21
3	R600a	21.90	105.3	483.34	12.21
4	R600a	21.76	104.95	680.66	12.21
5	R600a	21.63	114.95	710.95	12.21
6	R600a	5.00	62.595	652.72	12.21
7	Water	1	20.00	84.01	70.63
8	Water	1	35.00	146.70	70.63
9	Exhaust gas	1	375	784.3018	21.8
10	Exhaust gas	1	359.0033	767.3355	21.8
11	Exhaust gas	1	253.3766	656.7833	21.8
12	Exhaust gas	1	150	550.7663	21.8

Table 6.5. ORC thermodynamic analysis results (Real case)

Ref.	$\dot{Q}_{pre}$ kW	$\dot{Q}_{evap}$ kW	$\dot{Q}_{sup}$ kW	$\dot{W}_{pump}$ kW	$\dot{W}_{tur}$ kW	$\dot{W}_{net}$ kW	$\eta_{th,ORC}$ %	$\eta_{ex,ORC}$ %
R245fa	2582	2169	341	39	768	729	14%	32%
R600	2468	2297	326	44	812	768	15%	34%
R123	2757	2056	278	40	915	875	17%	39%
R236fa	2611	2042	437	46	696	650	13%	29%
R142b	2043	2734	314	42	708	666	13%	29%
R600a	2311	2410	370	48	711	663	13%	29%

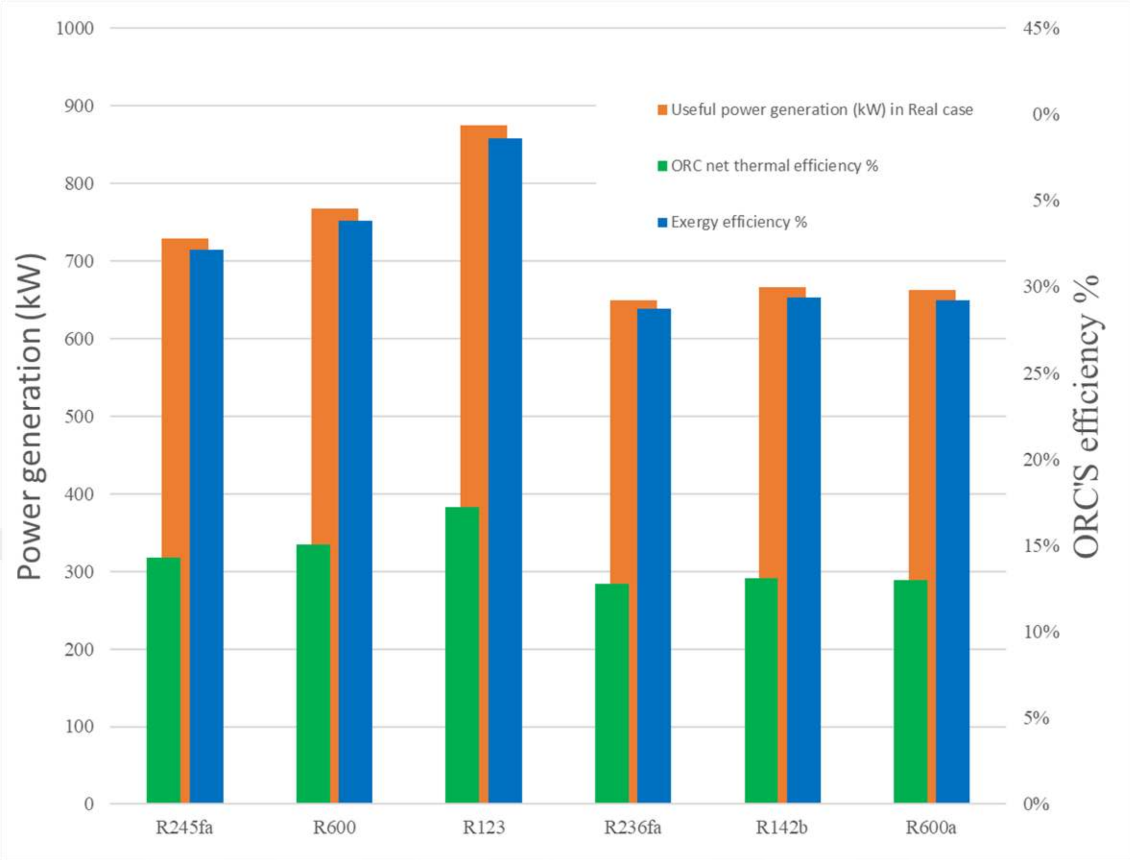

Figure 6.1. Performance analysis of ORC (Real case)

Based on a real case where the pressure drop across the heat transfer units is considered, the values presented in Figure 6.1 demonstrate that R123 is the top performer in the Organic Rankine Cycle (ORC), surpassing other fluids such as R600, R245fa, R142b, R600a, and R236fa.

By comparing between the ideal and real case performance analysis of ORC the following table is created as:

Table 6.6. HExUs heat transfer rate for ideal and real case

Ref.	Case	$\dot{Q}_{pre}$ kW	$\dot{Q}_{evap}$ kW	$\dot{Q}_{sup}$ kW
R245fa	Ideal	2585.3	2168.26	337.46
	Real	2581.65	2168.57	340.852
R600	Ideal	2480.76	2287.98	322.33
	Real	2467.81	2296.87	326.399
R123	Ideal	2740.79	2075.73	274.56
	Real	2757	2056	277.8
R236fa	Ideal	2623	2036	433
	Real	2611	2042	437.4
R142b	Ideal	2036.8	2738.71	315.6
	Real	2043	2734	314.4
R600a	Ideal	2319.1	2406.22	365.76
	Real	2311	2410	369.9

Table 6.7. ORC performance for ideal and real case

Ref.	Case	$\dot{W}_{pump}$ kW	$\dot{W}_{tur}$ kW	$\dot{W}_{net}$ kW	$\eta_{th,ORC}$ %	$\eta_{ex,ORC}$ %
R245fa	Ideal	39.07	778.36	739.28	14.52%	32.61%
	Real	38.9826	768	728.967	14.32%	32.15%
R600	Ideal	44.13	818.57	774.43	15.21%	34.16%
	Real	44.1187	811.654	767.535	15.08%	33.85%
R123	Ideal	40.61	932	891.39	17.51%	39.32%
	Real	40.2	915	874.8	17.20%	38.60%
R236fa	Ideal	47	702	655.87	12.88%	28.93%
	Real	46.47	696.2	649.7	12.80%	28.70%
R142b	Ideal	42.4	717.1	674.771	13.25%	29.76%
	Real	42.38	708.1	665.7	13.10%	29.40%
R600a	Ideal	48.48	718.25	669.77	13.16%	29.54%
	Real	48.48	711.2	662.7	13.00%	29.20%

Table 6.8. The performance ratio between real and ideal case

Refrigerant	**R245fa**	**R123**	**R600**	**R236fa**	**R142b**	**R600a**
Wnet,ideal (kW)	739	891	774	656	675	670
Wnet,Real (kW)	729	875	768	650	666	663
Wnet,Real / Wnet, ideal	98.6%	98.1%	99.1%	99.06%	98.66%	98.94%

CHAPTER 7
CONCLUSİON

This thesis presents a comprehensive and simple approach to optimizing the design of heat transfer units in an Organic Rankine Cycle (ORC) system. The ORC system was operated using six different refrigerants, namely R245fa, R600, R123, R236fa, R142b, and R600a, selected for their appropriate properties. The optimization process involved evaluating each heat exchanger unit considering multiple design limitations to achieve maximum efficiency and minimum cost.

The study provides insights into the design of finned tube heat exchangers for the preheater, evaporator, and superheater, as well as shell and tube condensers. The optimized designs for each heat exchanger unit offer a balance between surface area and pressure drop, resulting in an efficient, cost-effective, and sustainable ORC system.

To summarize the procedure, constant working conditions were defined, including the exhaust gas inlet and outlet temperature and mass flow rate. Then, the ORC system was defined, and its schematic was drawn, including four types of heat exchanges (preheater, evaporator, and superheater), turbine, and pump. Thermodynamic calculations based on the ideal case were performed to determine the ideal power generation and heating duties required by each heat exchanger unit. This information was used to determine the required size for each component to perform the required duty.

The design and optimization process for each heat exchanger component was shown in detail, and the best designs were selected as optimum designs that balanced between pressure drop and minimum heat surface area. Lastly, the study checked how the optimum designs found affect the overall performance of the ORC compared to the ideal case to confirm that these components conform with the required results.

In conclusion, This study have reached the following results :

1. This study has reached the optimum designs that balance between minimal heat transfer surface area and low value of pressure drop.
2. ORC system experiences power losses of less than 2% when using the recorded optimal designs. This is an excellent result, indicating that the design and optimization methodology developed in this study has successfully reached cost-effective and high-performing designs that can serve as a foundation for future research

REFERENCES

Reference list

[1] Vélez, F., Segovia, J. J., Martín, M. C., Antolín, G., Chejne, F., & Quijano, A. (2012). A technical, economical and market review of organic Rankine cycles for the conversion of low-grade heat for power generation. Renewable and Sustainable Energy Reviews, 16(6), 4175-4189.

[2] Andersen, W. C., & Bruno, T. J. (2005). Rapid screening of fluids for chemical stability in organic Rankine cycle applications. Industrial & Engineering Chemistry Research, 44(15), 5560-5566.

[3] Su, Y., Shen, W., Chien, I. L., & Ren, J. (2019). Multi-objective optimization of organic Rankine cycle system for the waste heat recovery in the heat pump assisted reactive dividing wall column. Energy Conversion and Management, 199, 112041.

[4] Su, Y., Chien, I. L., Jin, S., Yan, C., & Shen, W. (2019). Investigation of an energy-saving double-thermally coupled extractive distillation for separating ternary system benzene/toluene/cyclohexane. Energy, 186, 115756.

[5] Pethurajan, V., Sivan, S., & Joy, G. C. (2018). Issues, comparisons, turbine selections and applications–An overview in organic Rankine cycle. Energy conversion and management, 166, 474-488.

[6] Xu, W., Deng, S., Zhao, L., Su, W., Zhang, Y., Li, S., & Ma, M. (2018). How to quantitatively describe the role of the pure working fluids in subcritical organic Rankine cycle: A limitation on efficiency. Energy conversion and management, 172, 316-327.

[7] Bao, J., & Zhao, L. (2013). A review of working fluid and expander selections for organic Rankine cycle. Renewable and sustainable energy reviews, 24, 325-342.

[8] Kasaeian, A. B., & Daviran, S. (2013). Performance analysis of solar combined ejector-vapor compression cycle using environmental friendly refrigerants. IIUM Engineering Journal, 14(1).

[9] Messineo, A., & Panno, D. (2012). Performance evaluation of cascade refrigeration systems using different refrigerants. International Journal of Air-Conditioning and Refrigeration, 20(03), 1250010.

[10] Aghahosseini, S., & Dincer, I. (2013). Comparative performance analysis of low-temperature Organic Rankine Cycle (ORC) using pure and zeotropic working fluids. Applied Thermal Engineering, 54(1), 35–42.

[11] Eyerer, S., Wieland, C., Vandersickel, A., & Spliethoff, H. (2016). Experimental study of an ORC (Organic Rankine Cycle) and analysis of R1233zd-E as a drop-in replacement for R245fa for low temperature heat utilization. Energy, 103, 660–671.

[12] ÖZDEMİR, E., & KILIÇ, M. (2017). Energy and exergy analysis of an organic Rankine Cycle Using different working Fluids from Waste Heat Recovery. International Journal of Environmental Trends (IJENT), 1(1), 32-45.

[13] BADEMLİOĞLU, A., CANBOLAT, A., Yamankaradeniz, N., & KAYNAKLI, Ö. (2019). A Parametric Analysis of the Performance of Organic Rankine Cycle with Heat Recovery Exchanger and Its Statistical Evaluation. Isı Bilimi ve Tekniği Dergisi, 39(2), 121-135.

[14] Kaynakli, O., Bademlioglu, A. H., Yamankaradeniz, N., & Yamankaradeniz, R. (2017). Thermodynamic analysis of the Organic Rankine Cycle and the effect of refrigerant selection on cycle performance. International Journal of Energy Applications and Technologies, 4(3), 101-108.

[15] Hossin, K., Mahkamov, K., & Belgasim, B. (2020). Thermodynamic Analysis and Sizing of a Small Scale Solar ThermalPower System Based on Organic Rankine Cycle. Journal of Sustainable Development of Energy, Water and Environment Systems, 8(3), 493-506.

[16] Arabkoohsar, A., & Nami, H. (2019). Thermodynamic and economic analyses of a hybrid waste-driven CHP–ORC plant with exhaust heat recovery. Energy Conversion and Management, 187, 512–522.

[17] Usman, M., Imran, M., Yang, Y., Lee, D. H., & Park, B. S. (2017). Thermo-economic comparison of air-cooled and cooling tower based Organic Rankine Cycle (ORC) with R245fa and R1233zde as candidate working fluids for different geographical climate conditions. Energy, 123, 353–366.

[18] Shawabkeh, R. (2015). Steps for design of Heat Exchanger. King Fahd University of Petroleum & Minerals.

[19] Towler, G., & Sinnott, R. (2021). Chemical engineering design: principles, practice and economics of plant and process design. Butterworth-Heinemann.

[20] Incropera, F. P., DeWitt, D. P., Bergman, T. L., & Lavine, A. S. (1996). Fundamentals of heat and mass transfer (Vol. 6, pp. 408-409). New York: Wiley.

[21] Kakac, S., Liu, H., & Pramuanjaroenkij, A. (2020). Heat exchangers: selection, rating, and thermal design. CRC press.

[22] Maalouf, Samer; BouLawz Ksayer, Elias; and Clodic, Denis, "ORC Finned - Tube Evaporator Design and System Performance Optimization" (2012). International Refrigeration and Air Conditioning Conference. Paper 1275.

[23] Mon, M. S., & Gross, U. (2004). Numerical study of fin-spacing effects in annular-finned tube heat exchangers. International Journal of Heat and Mass Transfer, 47(8–9), 1953–1964.

[24] Kaya, A., Lazova, M., & De Paepe, M. (2015). Design and rating of an evaporator for waste heat recovery organic rankine cycles using SES36. In 3rd International Seminar on ORC Power Systems (ASME ORC 2015).

[25] Kandlikar, S. G. (1990). A General Correlation for Saturated Two-Phase Flow Boiling Heat Transfer Inside Horizontal and Vertical Tubes.

[26] Fenko, Anna, "Evaluation of two-phase evaporation pressure drop correlations for low refrigerant mass flux." (2015). Electronic Theses and Dissertations. Paper 2292.

[27] Li, X., Song, J., Yu, G., Liang, Y., Tian, H., Shu, G., & Markides, C. N. (2019). Organic Rankine cycle systems for engine waste-heat recovery: Heat exchanger design in space-constrained applications. Energy Conversion and Management, 199.

[28] Huang, X., Lu, P., Luo, X., Chen, J., Yang, Z., Liang, Y., Wang, C., & Chen, Y. (2020). Synthesis and simultaneous MINLP optimization of heat exchanger network, steam Rankine cycle, and organic Rankine cycle. Energy, 195.

[29] Imran, M., Usman, M., Park, B. S., Kim, H. J., & Lee, D. H. (2015). Multi-objective optimization of evaporator of organic Rankine cycle (ORC) for low temperature geothermal heat source. Applied Thermal Engineering, 80, 1–9.

[30] Walraven, D., Laenen, B., & D'Haeseleer, W. (2014). Comparison of shell-and-tube with plate heat exchangers for the use in low-temperature organic Rankine cycles. Energy Conversion and Management, 87, 227–237.

[31] Luo, J., Lu, P., Chen, K., Luo, X., Chen, J., Liang, Y., Yang, Z., & Chen, Y. (2023). Experimental and simulation investigation on the heat exchangers in an ORC under various heat source/sink conditions. Energy, 264.

[32] Blondel, Q., Tauveron, N., Lhermet, G., & Caney, N. (2023). Zeotropic mixtures study in plate heat exchangers and ORC systems. Applied Thermal Engineering, 219.

[33] Jankowski, M. (2022). A new indicator for minimizing size of an ORC power plant based on heat exchanger and turbine design parameters. Applied Thermal Engineering, 201.

[34] Ceglia, F., Marrasso, E., Roselli, C., & Sasso, M. (2021). Effect of layout and working fluid on heat transfer of polymeric shell and tube heat exchangers for small size geothermal ORC via 1-D numerical analysis. Geothermics, 95.

[35] Nikolaisen, M., & Andresen, T. (2021). System impact of heat exchanger pressure loss in ORCs for smelter off-gas waste heat recovery. Energy, 215.

[36] Jin, Y., Gao, N., & Wang, T. (2020). Influence of heat exchanger pinch point on the control strategy of Organic Rankine cycle (ORC). Energy, 207.

[37] Chatzopoulou, M. A., Lecompte, S., Paepe, M. De, & Markides, C. N. (2019). Off-design optimisation of organic Rankine cycle (ORC) engines with different heat exchangers and volumetric expanders in waste heat recovery applications. Applied Energy, 253.

[38] Wei, F., Senchuang, G., & Zhonghe, H. (2019). Economic analysis of Organic Rankine Cycle (ORC) and Organic Rankine Cycle with internal heat exchanger (IORC) based on industrial waste heat source constraint. Energy Procedia, 158, 2403–2408.

[39] Huang, X., Zhang, J., & Haglind, F. (2023). Experimental analysis of high temperature flow boiling of zeotropic mixture R134a/R245fa in a plate heat exchanger. Applied Thermal Engineering, 220.

[40] Wang, Z., Xu, Z., Luo, L., Xia, X., Li, X., He, J., & Chen, Y. (2023). Experimental investigation of condensation heat transfer of zeotropic

refrigerant/oil mixtures in plate heat exchanger. International Journal of Thermal Sciences, 185.

[41] Kücük, H. (2023). The effect of minichannels on the overall heat transfer coefficient and pressure drop of a shell and tube heat exchanger: Experimental performance comparison. International Journal of Thermal Sciences, 188.

[42] Wu, Y., Rong, J., Wang, D., Zhao, X., Meng, L., Arıcı, M., Liu, C., Yang, R., & Li, D. (2023). Synergistic enhancement of heat transfer and thermal storage characteristics of shell and tube heat exchanger with hybrid nanoparticles for solar energy utilization. Journal of Cleaner Production, 387.

[43] Krishna, A. B., Jin, K., Ayyaswamy, P. S., Catton, I., & Fisher, T. S. (2023). Technoeconomic optimization of superalloy supercritical CO2 microtube shell-and-tube-heat exchangers. Applied Thermal Engineering, 220.

[44] Ghazanfari, V., Imani, M., Shadman, M. M., Amini, Y., & Zahakifar, F. (2023). Numerical study on the thermal performance of the shell and tube heat exchanger using twisted tubes and Al2O3 nanoparticles. Progress in Nuclear Energy, 155, 104526.

[45] Dong, X., Zhang, S., Liu, L., & Zhang, Y. (2023). Experimental thermal study of solar salt and subcritical pressure water in a shell and tube heat exchanger. International Journal of Thermal Sciences, 186.

[46] Fetuga, I. A., Olakoyejo, O. T., Abolarin, S. M., Gbegudu, J. K., Onwuegbusi, A., & Adelaja, A. O. (2023). Numerical analysis of thermal performance of waste heat recovery shell and tube heat exchangers on counter-flow with different tube configurations. Alexandria Engineering Journal, 64, 859–875.

[47] Fadaei, M., Izadi, M., Assareh, E., & Ershadi, A. (2023). Conjugated non-Newtonian phase change process in a shell and tube heat exchanger: A parametric-geometric analysis. Applied Thermal Engineering, 220.

[48] Lokhande, A. A., Waghole, D. R., & Dayane, S. A. (2023). Heat transfer augmentation in shell and tube heat exchangers using copper oxide nanofluid with modified geometry: A numerical investigation. Materials Today: Proceedings, 72, 1240–1245.

[49] Venkata Rao, R., & Majethia, M. (2022). Design optimization of shell-and-tube heat exchanger using Rao algorithms and their variants. Thermal Science and Engineering Progress, 36.

[50] Caputo, A. C., Federici, A., Pelagagge, P. M., & Salini, P. (2022). On the selection of design methodology for shell-and-tube heat exchangers optimization problems. Thermal Science and Engineering Progress, 34.

[51] Yılmaz, M. S., Ünverdi, M., Kücük, H., Akcakale, N., & Halıcı, F. (2022). Enhancement of heat transfer in shell and tube heat exchanger using mini-channels and nanofluids: An experimental study. International Journal of Thermal Sciences, 179.

[52] Maghsoudali, Y., Rastegarkoutenaei, A., Sahami, M., & Bandpy, M. G. (2022). Investigation of the effect of using the finned tubes on the performance of shell and tube heat exchanger by 3D modeling. Journal of Energy Storage, 56.

[53] Daneshparvar, M. R., & Beigzadeh, R. (2022). Multi-objective optimization of helical baffles in the shell-and-tube heat exchanger by computational fluid dynamics and genetic algorithm. Energy Reports, 8, 11064–11077.

[54] Khatoon, B., Kumar Choudhary, V., Kumar, R., Siraj Alam, M., Pandey, S. K., Singh, R., & Naresh, R. (2022). Enhancement of heat transfer rate in shell & tube heat exchanger using CuO/Al2O3-water based nanofluids. Materials Today: Proceedings.

[55] Modi, J. P., Raja, B. D., & Patel, V. K. (2022). Thermo-ecological optimization of shell and tube heat exchanger. Materials Today: Proceedings.

[56] Kumar Raushan, A., Yadav, R., Mohan, R., & Goga, G. (2023). CFD analysis of different finned tube heat exchanger designs using a non newtonian fluid. Materials Today: Proceedings.

[57] Guo, S., Cheng, K. X., & Lee, P. S. (2023). Numerical study of the cold finned-tube bundle heat exchanger under natural convection for a novel passive displacement cooling system. Building and Environment, 233.

[58] Erdinc, M. T. (2023). Computational thermal-hydraulic analysis and geometric optimization of elliptic and circular wavy fin and tube heat exchangers. International Communications in Heat and Mass Transfer, 140.

[59] Zhang, T., Chen, L., & Wang, J. (2023). Multi-objective optimization of elliptical tube fin heat exchangers based on neural networks and genetic algorithm. Energy, 269.

[60] Feng, Y., Xu, R., Cao, Y., Wu, X., Liang, C., & Zhang, L. (2023). Optimization of H-type finned tube heat exchangers with combinations of longitudinal vortex generator, dimples/protrusions and grooves by Taguchi method. International Communications in Heat and Mass Transfer, 143.

[61] Zhao, B., Bi, H., Wang, H., & Zhou, Y. (2022). Experimental and numerical investigation on frosting of finned-tube heat exchanger considering droplet impingement. Applied Thermal Engineering, 216.

[62] Herbinger, F., & Groulx, D. (2022). Experimental comparative analysis of finned-tube PCM-heat exchangers' performance. Applied Thermal Engineering, 211.

[63] Gungor, S. (2023). Experimental comparison on energy consumption and heat transfer performance of corrugated H-type and L-type brazed plate heat exchangers. International Communications in Heat and Mass Transfer, 144.

[64] Wang, D., Zhang, H., Wang, G., Yuan, H., & Peng, X. (2023). Experimental and numerical study on the heat transfer and flow characteristics of convex plate heat exchanger based on multi-objective optimization. International Journal of Heat and Mass Transfer, 202.

[65] Ham, J., Lee, G., KWon, O., Bae, K., & Cho, H. (2023). Numerical study on the flow maldistribution characteristics of a plate heat exchanger. Applied Thermal Engineering, 224.

[66] Mikhaeil, M., Nowak, S., Palomba, V., Frazzica, A., Gaderer, M., & Dawoud, B. (2023). Experimental and analytical investigation of applying an asymmetric plate heat exchanger as an evaporator in a thermally driven adsorption appliance. Applied Thermal Engineering, 228, 120525.

[67] Ham, J., Yong, J., KWon, O., Bae, K., & Cho, H. (2023). Experimental investigation on heat transfer and pressure drop of brazed plate heat exchanger using LiBr solution. Applied Thermal Engineering, 225.

[68] Çuhadaroğlu, B., & Hacisalihoğlu, M. S. (2022). An experimental study on the performance of water-based CuO nanofluids in a plate heat exchanger. International Communications in Heat and Mass Transfer, 137.

[69] Aboul Khail, A., & Erişen, A. (2022). Heat transfer and performance enhancement investigation of novel plate heat exchanger. Thermal Science and Engineering Progress, 34.

[70] Yu, J., Qiu, H., Jiao, Y., Tian, Y., Meng, Y., Wang, W., Min, H., & Li, X. (2022). Numerical prediction of heat transfer performance of plate heat exchanger based on experimental data assimilation to calibrate turbulence model constants. Thermal Science and Engineering Progress, 34.

[71] Tamkhade, P. K., Lande, R. D., Gurav, R. B., & Lele, M. M. (2023). Investigations on tube in tube metal foam heat exchanger. Materials Today: Proceedings, 72, 951–957.

[72] Liu, P., Wang, R., Liu, S., & Bao, Z. (2023). Experimental study on the thermal-hydraulic performance of a tube-in-tube helical coil air–fuel heat exchanger for an aero-engine. Energy, 267.

[73] Zhao, B., Zhang, T., Tan, J., Zhao, Y., Xue, R., Tan, H., Wu, S., Zhai, Y., & Dang, H. (2022). Design and optimization of the four-stage recuperative coiled tube-in-tube heat exchanger for a 1.8 K hybrid cryocooler. Cryogenics, 126.

[74] Liu, H., Katsura, T., & Nagano, K. (2022). An inverter-driven heat pump with a multi-tubular tube-in-tube heat exchanger for domestic hot water supply. Journal of Building Engineering, 54.

[75] Liu, P., Han, H., & Bao, Z. (2022). Multi-objective optimization of fuel–air tube-in-tube helical coil heat exchangers for cooled cooling air system applied in aeroengines. Aerospace Science and Technology, 130, 107933.

[76] Cao, Y., Ayed, H., Anqi, A. E., Tutunchian, O., Dizaji, H. S., & Pourhedayat, S. (2021). Helical tube-in-tube heat exchanger with corrugated inner tube and corrugated outer tube; experimental and numerical study. International Journal of Thermal Sciences, 170.

[77] Zhang, X., Zhao, M., Liu, L., Huan, C., Zhao, Y., Qi, C., & Song, K. I. I. L. (2020). Numerical simulation on heat storage performance of backfill body based on tube-in-tube heat exchanger. Construction and Building Materials, 265.

[78] Aghahosseini, S., & Dincer, I. (2013). Comparative performance analysis of low-temperature Organic Rankine Cycle (ORC) using pure and zeotropic working fluids. Applied Thermal Engineering, 54(1), 35–42.

[79] Eyerer, S., Wieland, C., Vandersickel, A., & Spliethoff, H. (2016). Experimental study of an ORC (Organic Rankine Cycle) and analysis of R1233zd-E as a drop-in replacement for R245fa for low temperature heat utilization. Energy, 103, 660–671.

[80] M., & García-Rodríguez, L. (2007). Preliminary assessment of solar organic Rankine cycles for driving a desalination system. Desalination, 216(1-3), 252-275.

CURRICULUM VITAE

Ad / SOYAD: Abdulraaouf OKASH

EDUCATION

Master's Degree in Mechanical Engineering (3.44 out of 4) 09/2020-08/2023
Gaziantep University
Honor graduate

Bachelor's Degree in Civil Engineering (3.33 out of 4) 09/2018-06/2021
Gaziantep University
Honor graduate

Bachelor's Degree in Mechanical Engineering (3.44 out of 4) 09/2015-06/2020
Gaziantep University
Honor graduate